AD

TECHNICAL REPORT ECOM-00394

HIGH VOLTAGE BREAKDOWN STUDY

FINAL REPORT

16 November 1964 through 15 November 1969

Prepared by:

ION PHYSICS CORPORATION

BURLINGTON, MASSACHUSETTS

June 1970

DISTRIBUTION STATEMENT

This document has been approved for public release and sale; its distribution is unlimited

ECOM

UNITED STATES ARMY ELECTRONICS COMMAND · FORT MONMOUTH, N.J. 07703

DDC

SEP 17 1970

C

219

HIGH VOLTAGE BREAKDOWN STUDY

16 November 1964 through 15 November 1969

Final Report

Contract No. DA-28-043-AMC-00394(E)
AMC Task No. 00.21.243.40.00

Prepared for:

U. S. ARMY ELECTRONICS COMMAND
FORT MONMOUTH, NEW JERSEY

Sponsored by:

ADVANCED RESEARCH PROJECTS AGENCY
ARPA Order No. 517

Prepared by:

M. J. Mulcahy, P. C. Bolin, W. R. Bell, A. S. Denholm,
F. J. McCoy, G. K. Simcox, M. M. Thayer,
F. Y. Tse and A. Watson

ION PHYSICS CORPORATION
BURLINGTON, MASSACHUSETTS

DISTRIBUTION STATEMENT

This document has been approved for public
release and sale; its distribution is unlimited.

TABLE OF CONTENTS

TABLE OF CONTENTS (Continued)

TABLE OF CONTENTS (Continued)

TABLE OF CONTENTS (Continued)

LIST OF ILLUSTRATIONS

LIST OF ILLUSTRATIONS (Continued)

LIST OF ILLUSTRATIONS (Continued)

LIST OF ILLUSTRATIONS (Continued)

LIST OF ILLUSTRATIONS (Continued)

LIST OF TABLES

LIST OF TABLES (Continued)

SECTION 1
REVIEW OF THE CONTRACT

On 16 November 1964, Ion Physics Corporation was awarded
Contract DA-28-043-AMC-00394(E) entitled High Voltage Breakdown Study.
The objective of this was to determine and study the factors influencing high volt-
age vacuum breakdown under conditions pertinent to high power tube operation
in the range of 100 to 300 kV. The Contract called for a statistically designed
controlled experiment. Factorial design was chosen because it provided a
powerful tool for the analysis of the results and enabled information to be de-
rived from a minimum number of experiments on both the effects of the individ-
ual factors and on the degree of interaction among factors.

The Contract started on 16 November 1964 and was scheduled to run
until 15 November 1969. This report summarizes the program. A general
introduction is followed by a description of the apparatus, an introduction to the
factors important in vacuum breakdown, a discussion of the technique of factorial
design and the following sequence of experiments:

I   Preliminary Experiment

II   Pilot Experiment

III   Block of Eight Experiment

IV   Block of Thirty-Two Experiment

V   Energy Conditioning Study

VI   Barium Contamination Experiment

SECTION 2
GENERAL INTRODUCTION

2.1   Introduction

There is a need for very high voltage vacuum tubes for certain high power radar systems. Unfortunately, serious problems are experienced in operating tubes reliably at the required voltage, which can be as high as 300 kV or more. For example, klystrons of the modulated anode type, where direct voltage has to be supported, are particularly prone to breakdown within the vacuum envelope. There seems to be little information on the precise nature of the problem. This is partly because usual method of packaging high power tubes and the radiation they produce makes difficult the visual observation of the discharge. Deductions about the problem appear to be essentially of the "post mortem" nature; i. e., from breakdown damage. However, it is clear that both vacuum gap breakdown and internal insulator flashover can occur. THE program has been directed to the study and solution of the problem of breakdown within high power tubes to 300 kV. During the course of THE study, visits to and discussions with tube manufacturers have confirmed the complexity and practical consequences of THE problem of vacuum gap breakdown and insulator flashover, and puncture.

The available literature on vacuum breakdown was, at program outset and still is, confusing, sometimes contradictory, and mostly related to voltages and environments which are not particularly relevant to the problem of breakdown in very high voltage tubes. It was therefore important that the program should start without preconceived notions, which could be wrong, and through scientifically designed experiments and sufficient sustained effort arrive at the truly significant factors in vacuum breakdown; and hence, better high voltage tubes. Although preconceived but unproven ideas should not influence the conduct of the program, it was essential that in designing the experiments no factors which might be important should be omitted. Hence, there was a need for the investigator to combine an objective perspective with a detailed knowledge of those variables known to be critical to the phenomenon.

The factors which could be important had to be determined, and a decision made on those which would be varied in the designed experiment. The others were maintained constant. The greater the number of conclusive tests which could be accomplished within a given effort and time, and the more control over the experimental parameters, the more powerful the program. This in turn, leads to a discussion of the design of the test vehicle, the technique of factorial and statistical design, the selection of factors and the sequence of the experiments.

2.2   300 kV Test Apparatus

In order to simulate high power vacuum tube conditions the apparatus has to satisfy the following requirements. The vacuum test chamber should evacuate to 10^{-9} torr and be free of organic contamination. Further, it is required to bake to 400°C either the chamber and contents, or the electrodes alone. Within the chamb r a voltage up to 300 kV is specified for application across the electrode gap, which should be variable up to about 5 cm for a range of geometries. In some experiments a magnetic field of 500 gauss is required either perpendicular or parallel to the electric field vector. Finally, a range of energy levels up to 7000 J are desired together with the facility of crowbarring in the latter case at variable times after initiation of a vacuum breakdown. Facilities should be provided for monitoring voltage, prebreakdown current, total and partial pressures, voltage collapse waveforms, breakdown current pulse, optical and X-ray output. The apparatus designed to meet these requirements is described in Section 3.

2.3   Factors Influencing Vacuum Breakdown

In any experimental program it is important to be aware of all the parameters which may be significant. If one strongly significant parameter is omitted, i.e., not controlled, the results will exhibit a large random scatter or error and the significance, reliability and level of confidence of the trends and conclusions will be, accordingly, reduced. To minimize this possibility,

both theory and previous experimental work were examined so that all factors would be controlled. The factors selected for study are discussed in Section 4.

2.4   Factorial and Statistical Design

Two methods of approach usually exist for investigating a physical system. The fundamental processes affecting the behavior of the system may be studied or a more empirical approach may be adopted and the effects of various changes in the system studied directly. The latter method is indicated when the underlying physical mechanisms are little understood and practical results are of primary importance. In this case, the principles of Factorial Design[1] can be used to optimize experimental design. This provides a powerful tool for the analysis of the results and enables information to be derived from a minimum number of experiments both on the effects of the individual factors and on the degree of interaction among factors. It is discussed in Section 5.

2.5   Sequence of Experiments

Six major experimental blocks have been completed which investigated via factorial design the factors of electrode materials, electrode processing, surface finish, electrode geometry, electrode and system bakeout, electrode size, energy conditioning, transverse magnetic field, gas exposure, and barium contamination. The allocation of these factors to experimental blocks and the levels of each factor are given in Table 2-1. Also given are the major details of experimental conditions and the variables of prime interest during each block. In addition, common factors such as electrode spacing and low energy conditioning were investigated in all blocks. The results of each block were used in designing the succeeding block.

2-3

Table 2-1. Sequence of Experiments - High Voltage Breakdown Study

I	II	III	IV	V	VI
Preliminary Experiment	Pilot Experiment	Block of Eight	Block of Thirty-Two	Energy Conditioning Study	Barium Contamination Study

Uniform Field
Stainless Steel
 	
To 160 kV
Prebreakdown Phenomena
  Field Emission
  Microdischarges
  X-Radiation
  Visible Radiation
  Pressure Surge
Conditioning Techniques
  Sparking
  Gas Evolution
 	
(Performed with Existing Apparatus while 300 kV Apparatus was Constructed)
	To 300 kV
	Factors
	Anode Material
	  Ti-7Al-4Mo
	  OFHC Cu
	Cathode Material
	  Ti-7Al-4Mo
	  OFHC Cu
	Anode Finish
	  Fine
	  Coarse
	Cathode Finish
	  Fine
	  Coarse
	Anode Geometry
	  Bruce Profile
	  Sphere
	Cathode Geometry
	  Bruce Profile
	  Sphere
	Bakeout
	  Complete System
	  Electrodes Only
		To 300 kV Uniform Field
		Factors
		Anode Processing
		  Vacuum Firing
		  Hydrogen Firing
		Cathode Processing
		  Vacuum Firing
		  Hydrogen Firing
		Electrode Size
		  4 Inch Diameter
		  1.28 Inch Diameter
		Transverse Magnetic Field
		  to 500 Gauss
			To 300 kV
			2 Inch Diameter
			Spherical Cathode
			Factors
			Anode Material
			  OFHC Cu
			  Aluminum
			Cathode Material
			  OFHC Cu
			  Aluminum
			Electrode Processing
			  Vacuum Firing
			  Hydrogen Firing
			Anode Size
			  4 Inch Diameter
			  1.28 Inch Diameter
			Anode Shape
			  Bruce Profile
			  Sphere
			Transverse Magnetic Field
			  0 to 400 Gauss
			Energy Storage
			  100 to 6750 Joules
			Gas Exposure
			Conditioning
			Time to Voltage Collapse
				To 300 kV
				Initial Gap = 0.75 cm
				Uniform Field
				Factors
				High Impedance
				Conditioning
				  With
				  Without
				Cathode Material
				  Ti-7Al-4Mo
				  Nickel
				Electrode Size
				  4 Inch Diameter
				  1.28 Inch Diameter
				Anode OFHC Copper
				Also tests with:
				  Aluminum, Ti-7Al-4Mo
				  Nickel, Stainless Steel
				  Lead, Molybdenum
				  Tungsten
				Energy Conditioning
				Level
				  Series Resistance from 25 Ohms to 30 kilohms
				  Energy Storage from 50 J to 6750 J with 0.15 µF Capacitor Bank
				Prebreakdown Current
				Breakdown Voltage Collapse and Current Pulse
					To 300 kV
					Initial Gap = 0.75 cm
					Uniform Field
					Factors
					Electrode Material
					  Ti-7Al-4Mo
					  Nickel
					  OFHC Cu
					  304 Stainless Steel
					Barium Contamination
					Level
					  Without
					  Cathode Only
					  Anode Only
					  Both Electrodes
					Energy Conditioning
					Prebreakdown Current

SECTION 3

300 kV TEST APPARATUS AND EXPERIMENTAL PROCEDURES

3.1   Introduction

The apparatus and techniques developed to carry out controlled vacuum breakdown experiments up to 300 kV are completely described in this section. However, where considerable evolution has occurred, only the final design is given. For the most part such changes did not modify experimental conditions but were necessary to eliminate persistant failure or malfunction. Thus, this section serves to establish the basic experimental conditions.

3.2   Vacuum Chamber and System

The test vehicle is shown in Figure 3-1. The vacuum chamber was made by welding two spun hemispherical sections of 304 stainless steel, 36 inches in diameter by 1-1/8 inches thick. This thickness eliminates the need for welded flanges at the ports. The chamber is equipped with three 16 inch diameter ports, one at the top for the electrode support and adjustment mechanism, another at the bottom for the bakeable feedthrough bushing and the third at the side for access and electrode changes. There is also a 10 inch port for the pumping system and 6 inch ports are available for optical and X-ray detectors, a mass spectrometer, cryo pump and controlled leak valve. Gold or copper O-ring seals are used throughout.

An automated mantle heating system is used for chamber bakeout. It is shown in Figure 3-2 and consists of two hemispherical sections of asbestos blanket fabricated to fit the vacuum chamber. The heaters are built in and an automatic controller-recorder brings the chamber up to 375°C in 2 hours, and continuously records the temperature using thermocouples located at the viewport. The temperature is maintained at the pre-set value to within 5°C, using automated switches. Safety devices are incorporated which shut off the power if the thermocouple should break, if the ion pump pressure should rise over
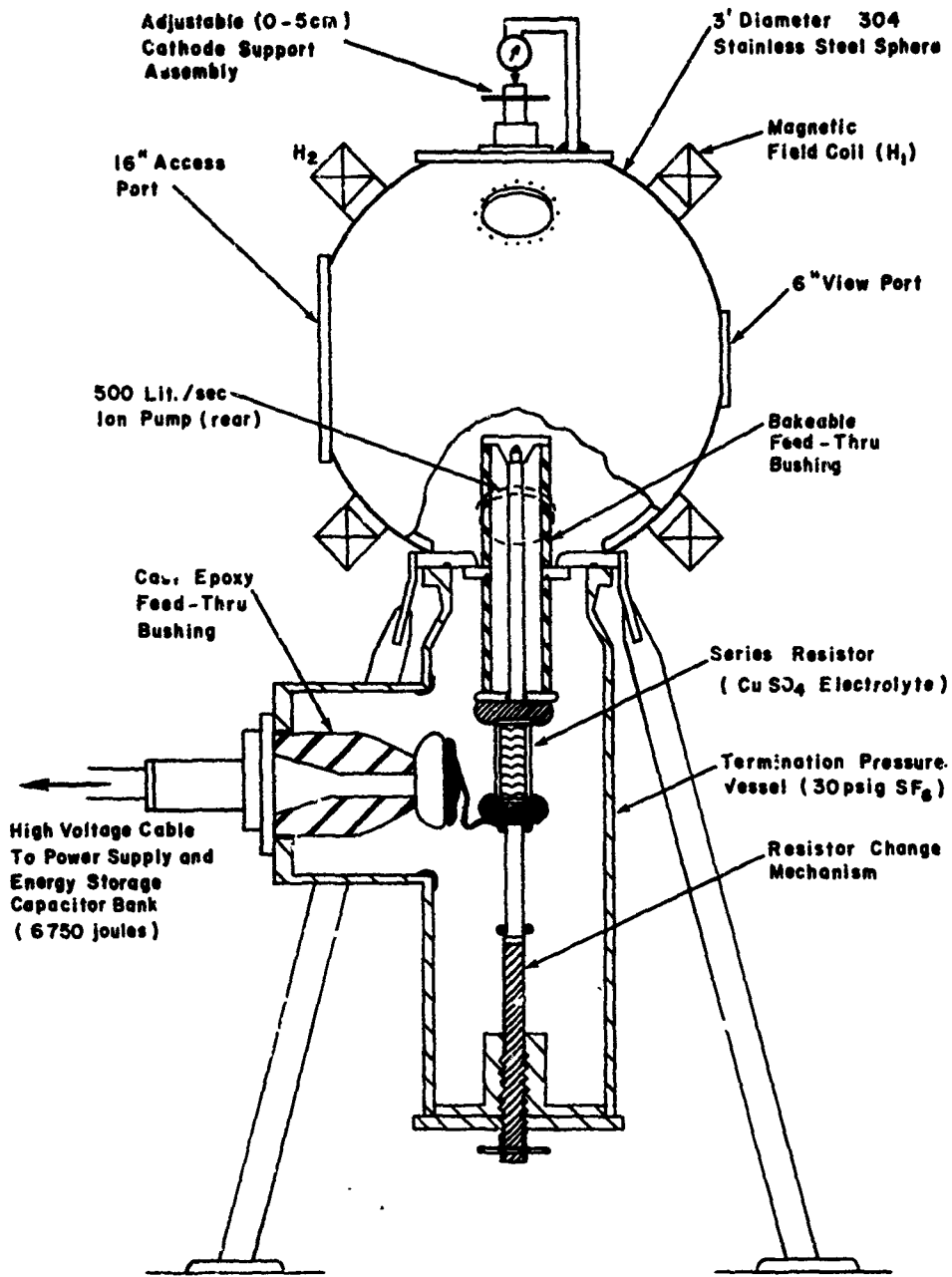
Figure 3-1 Vacuum Chamber System for 300 kV dc Testing

1-4252
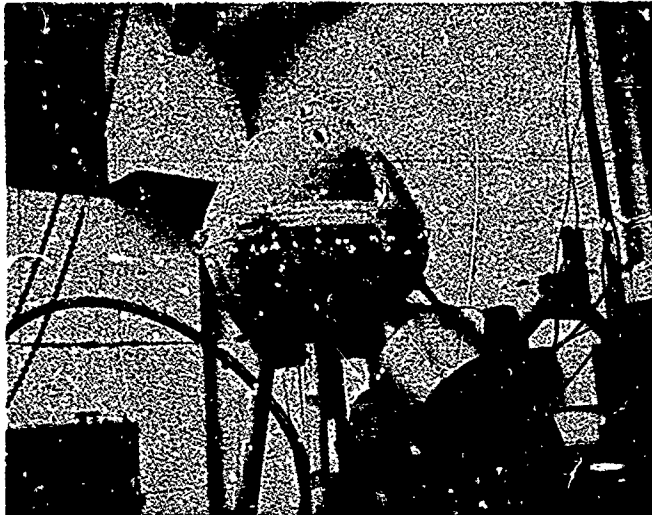
Figure 3-2. Asbestos Blanket Baking
Oven Installed on Chamber

2-638

1×10^{-5} torr, or if the current to either of the two halves of the baking mantle changes by more than 15%.

The electrode heating system is similarly controlled and safeguarded with the temperature maintained at 450°C. The IPC designed heater is welded into the electrode support structures as shown in Figure 3-3, and thus, makes direct contact with the electrodes while at the same time all thermocouple and heater leads are removed from the vacuum envelope.

The oil-free pumping system is shown in Figure 3-4. The roughing system consists of one Varian Gasp pump and two Varian Sorption pumps which are isolated from the main chamber by means of a Varian 1-1/2 inch bakeable right angle valve. The Gasp pump is a gas operated venturi type pump with a base pressure capability of 125 torr. The Sorption pumps are a molecular sieve type pump which require liquid N_2 to activate and have a base pressure capability of 1×10^{-6} torr.

The main pumping system consists of one General Electric 500 L/S triode ion pump with a base pressure capability of 10^{-12} torr. Additional pressure readings are taken using two Aero-Vac RGA heads mounted one in the pumping throat and the other in the main chamber. Before system bakeout the pressure is in the high 10^{-8} torr region, while afterwards the high 10^{-9} torr regime is achieved in the chamber.

3.3   Electrical Circuit

The original power supply was a Van de Graaff generator which was current limited to 200 μA. Heavy prebreakdown currents made necessary its replacement with a 2 mA, 300 kV Universal Voltronics dc supply. This supply is connected to the anode electrode via high voltage coaxial cable and a pressurized feedthrough bushing. Also incorporated into the system are an energy storage capacitor bank, a fast high pressure crowbar, and resistor change mechanisms. A schematic of the overall system is given in Figure 3-5.

The design of the feedthrough bushing is shown in Figure 3-6 and has been described in detail in the Quarterly Progress Reports. It consists of
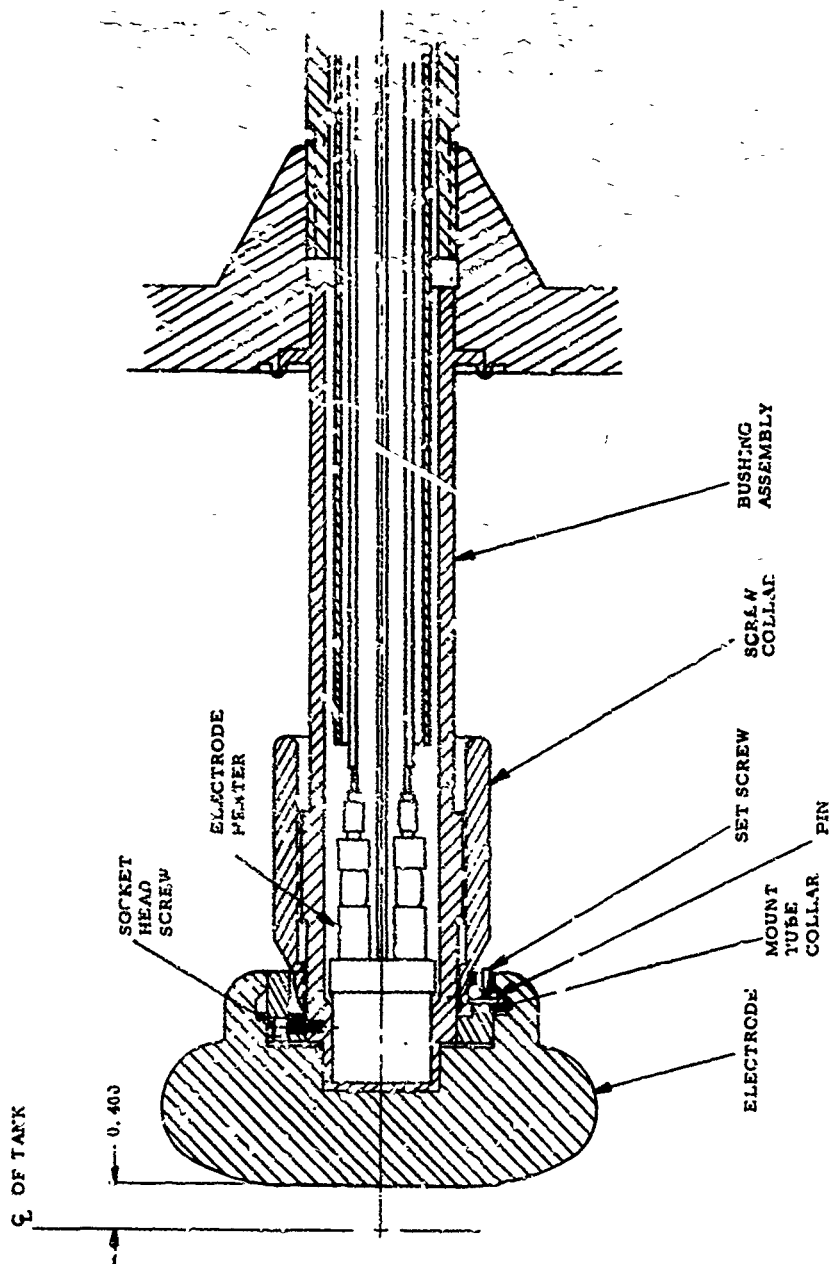
Figure 3-3. Modified Bottom Electrode Support with Quick Disconnect Mechanism

1-2263
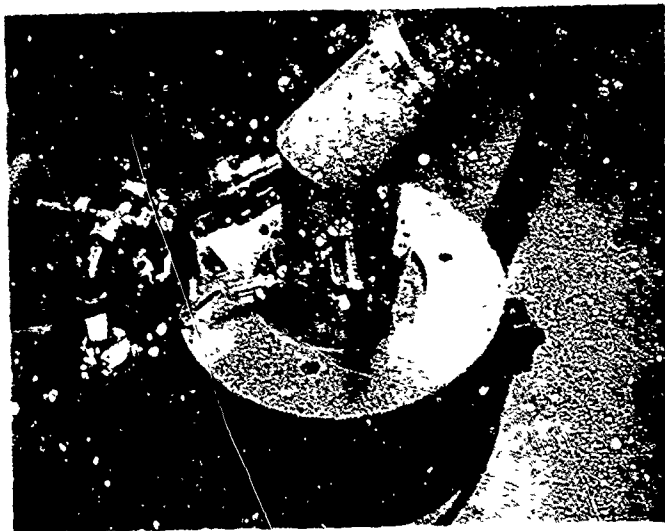
Figure 3-4. Modified Pumping System
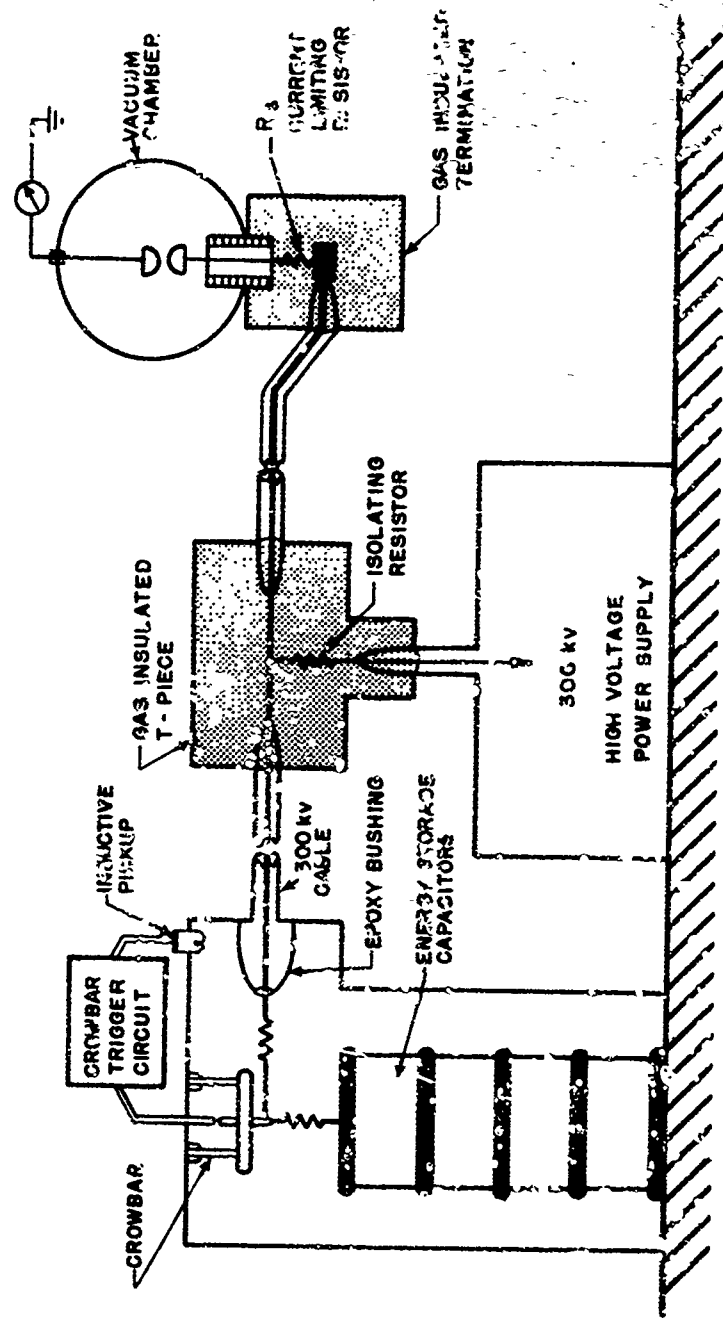
Figure 3-5. Outline of 300 kV Vacuum Breakdown Apparatus

VACUUM CHAMBER

R₃ CURRENT LIMITING RESISTOR

GAS INSULATED TERMINATION

GAS INSULATED T-PIECE

ISOLATING RESISTOR

300 kV HIGH VOLTAGE POWER SUPPLY

INDUCTIVE PICKUP

300 kV CABLE

EPOXY BUSHING

ENERGY STORAGE CAPACITORS

CROWBAR TRIGGER CIRCUIT

CROWBAR

1-2907a
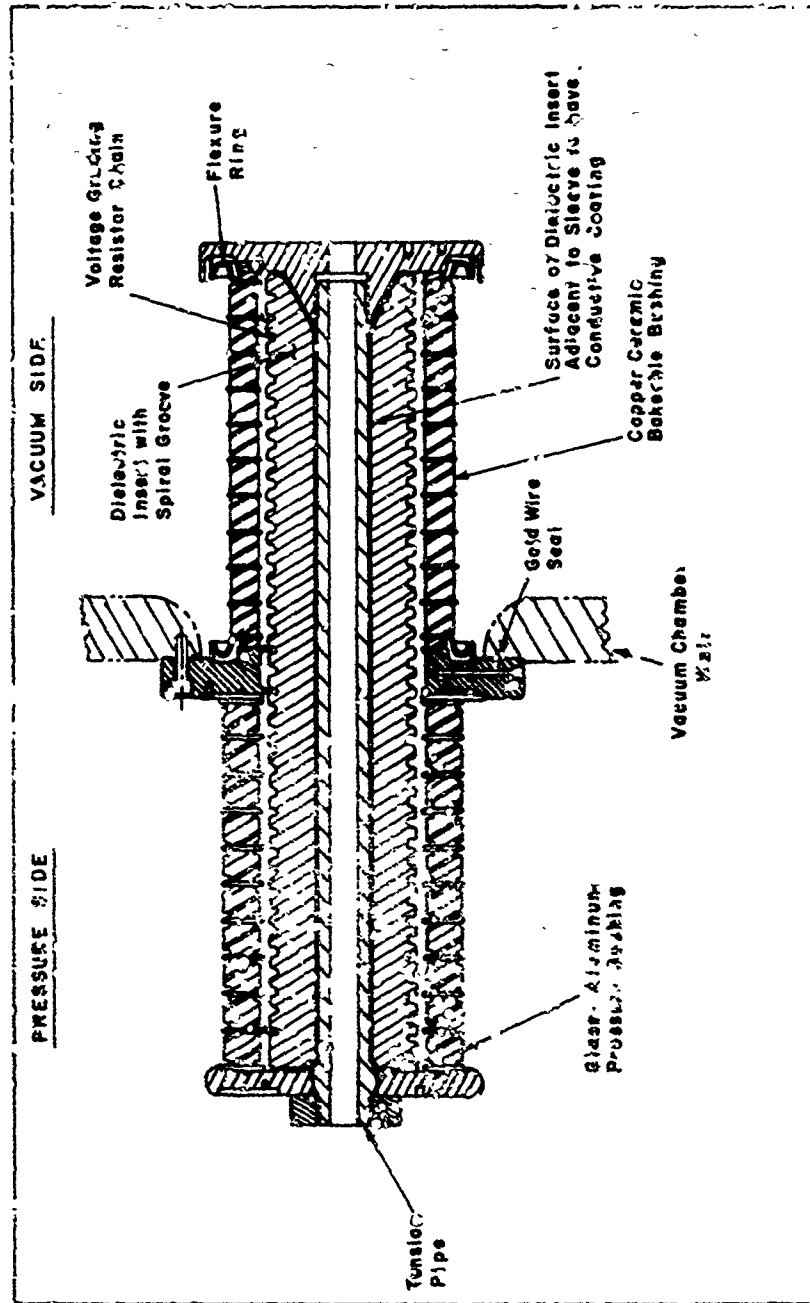
Figure 3-6. Feedthrough Bushing

VACUUM SIDE

PRESSURE SIDE

Voltage Grading Resistor Chain

Flexure Ring

Surface of Dielectric Insert Adjacent to Sleeve to have Conductive Coating

Dielectric Insert with Spiral Groove

Copper Ceramic Bakeable Brazing

Gold Wire Seal

Vacuum Chamber Wall

Glass-Aluminum Pressure Bushing

Tungsten Pipe

1-1275a

a bakeable ceramic-copper column which extends into the vacuum chamber and an unbakeable glass-aluminum column located in the bottom pressure tank. The ceramic column is brazed via a Monel alloy 404 flexure ring to a stainless steel flange and the latter makes a gold O-ring seal at the bottom port. The two columns are held together using a stainless steel tension rod which also carries the heater and thermocouple leads for the high voltage electrode. The bushing is pressurized to 45 psia SF_6 and voltage grading is effected using a solid dielectric insert (lucite) with a spiral groove along which are wound two strings of 100 megohm resistors, one for each column. This insert also provides axial insulation at the ground plane.

The 7000 joule energy storage unit consists of four 80 kV, 0.6 μF cylindrical Tobe Deutschmann capacitors, 20 inches high and 13 inches in diameter. They are stacked vertically as shown in Figure 3-5 with grading resistors housed axially inside each unit in a vessel pressurized to 2 atmospheres of SF_6. It is connected to the vacuum gap and the 300 kV power supply via high voltage cable and a gas insulated T-piece. The energy storage vessel also incorporates an IPC built high pressure gas crowbar (see Figure 3-7) which is triggered by breakdown of the vacuum gap. The static breakdown voltage of the crowbar can be varied by changing either its electrode gap setting or its gas pressure. The crowbar, when triggered, diverts energy from the capacitor bank to ground, thus limiting in a controlled fashion the energy reaching the vacuum gap. Diversion times of less than 500 ns are routinely achieved.

Current limiting resistors employ $CuSO_4$ electrolyte in order to handle the significant energies involved when energy storage is used. Mechanical adjustments are provided to make possible rapid removal or change of resistors.

3.4   Magnetic Field

The requirement of producing a magnetic field of 500 gauss in any selected direction relative to the electrode geometry was achieved using two water-cooled concentric coils (Figure 3-8) which could be dropped over the chamber for test and removed during system bakeout. The dimensions are as follows:
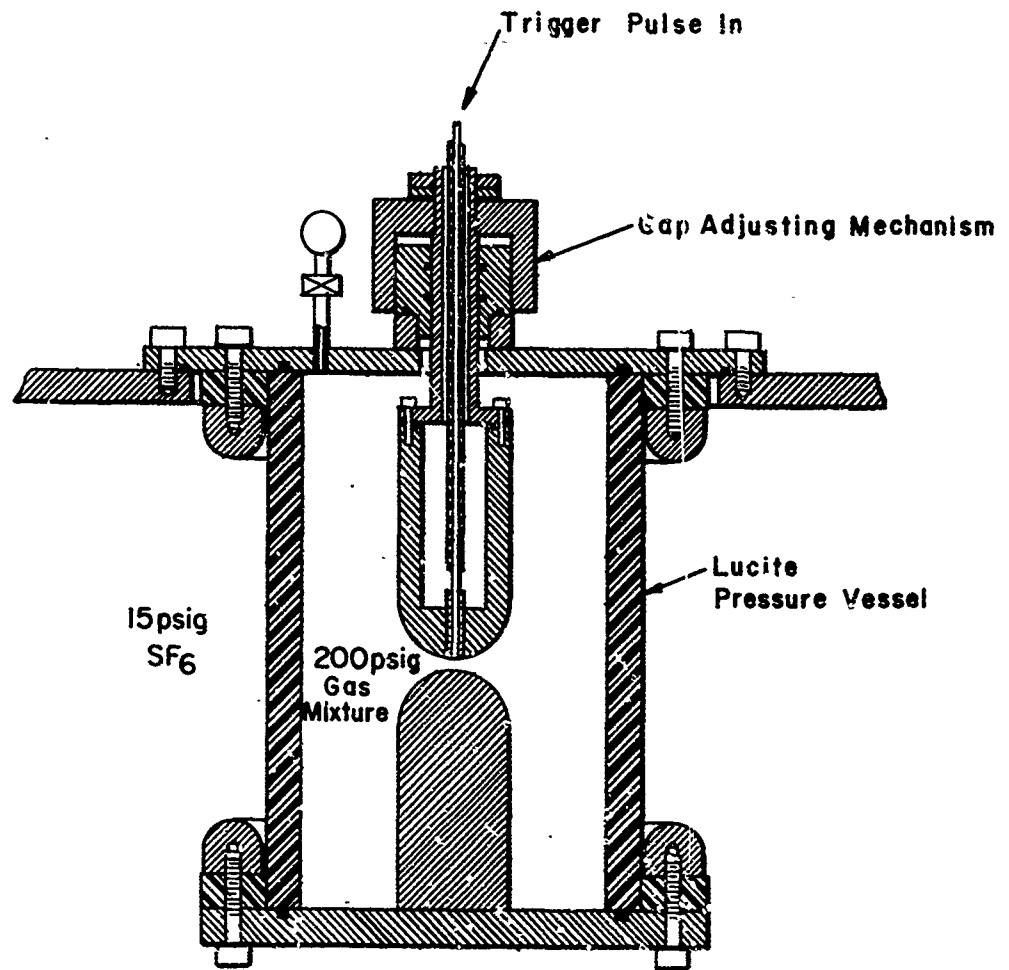
Figure 3-7. Variable Gap Pressurized Crowbar

1-2580A

Figure 3-8. 300 kv System with Magnets
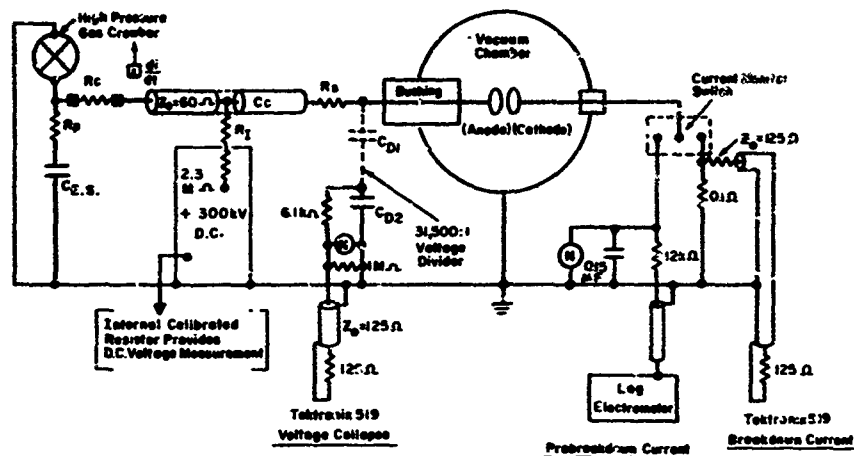
Figure 3-9. Schematic of Electrical Test and
Instrumentation Circuits

R_s = Series Resistance

R_c = Crowbarring Resistance (20 ohm)
(Removeable)

R_p = Protective Resistance (4 ohm)

$C_{E.S.}$ = Energy Storage Capacitance
(0. 15 μf)

C_{D1} = Voltage Divider Capacitance
(1. 9 pF)

C_{D2} = Voltage Divider Capacitance
(1200 pF)

R_I = Power Supply Isolation Resistance
(2. 3 Mohm)

C_c = Cable Capacitance (~900 pF)

1-3556a

3-12

Coil	Mean Radius	Copper Weight	Approximate Power
Inner	56.00 cm	430 lb	12.5 kW
Outer	67.44 cm	610 lb	17.0 kW

A solid state rectifier set provides up to 300 amperes dc to each coil and is automatically controlled to maintain a set magnetic field level independent of fluctuations in supply voltage.

While any orientation of the magnetic field relative to the electric field in the gap is possible with this system, it has been found that only a transverse magnetic field is useful in a practical sense. Tests with a parallel magnetic field encountered a severly limited maximum voltage due to discharges and gas evolution along the bushing surfaces.

3.5   Instrumentation

The monitoring instrumentation enables the following to be continuously measured and recorded during the complete voltage application cycle:

- gap voltage - calibrated resistors in the power supply
- breakdown voltage waveform - 31,500 :1 capacitive voltage divider, Tektronix 519 oscilloscope
- breakdown current waveform - 0.1 or 0.3 ohm resistive monitor of low inductance construction, Tektronix 519
- electrode gap current - Keithley 14A logarithmic electrometer -10^{12} to 10^{-4} amperes
- total power supply current - power supply meters
- total chamber and pump pressure - ion gauges and pumping current
- partial chamber pressure of H_2, O_2 or N_2 - mass spectrometer
- total X-radiation - sodium iodide crystals with photomultipliers

- collimated X-radiation from the gap - collimated with aluminum blocks
- total visible radiation - photomultipliers

Figure 3-9 gives the details of the electrical instrumentation.

3.6 Electrode Processing

In order to obtain repeatable results it was found necessary to control electrode gas content by an extended pre-firing at high temperature in either vacuum or hydrogen. Firing is carried out in Linberg heavy duty furnaces capable of 1200°C operation. Inconel retorts and contamination free ion pumping systems provide a clean environment. The firing system is shown in Figure 3-10. Figure 3-11 gives the setup for hydrogen firing.

Electrodes are ultrasonically cleaned with solvents before firing and are allowed to cool to ambient before being removed from the retorts and installed in the vacuum chamber via dry nitrogen environment transfer chambers. Special quick-disconnect assemblies minimize handling which is done with lint-free cotton gloves.

3.7 Barium Contamination Device

In order to study the effects of barium contamination as would exist in vacuum tubes using barium oxide thermionic cathodes it was necessary to position a heated cathode assembly in the vacuum chamber so as to deposit barium in a controlled way. This was achieved using a rod and bellows assembly as shown in Figure 3-12. The internally heated cathode (from Machlett Laboratories) can be moved into the vacuum gap and withdrawn beyond the loading port surface, a distance of about 18 inches.

3.8 Dielectric Envelope

The influence of dielectric surfaces near the vacuum gap was studied using a glass envelope 8 inches in diameter by 10 inches long by 1/4 inch thick.

Figure 3-10. Double Furnace Arrangement for
Vacuum or Hydrogen Firing

2-804
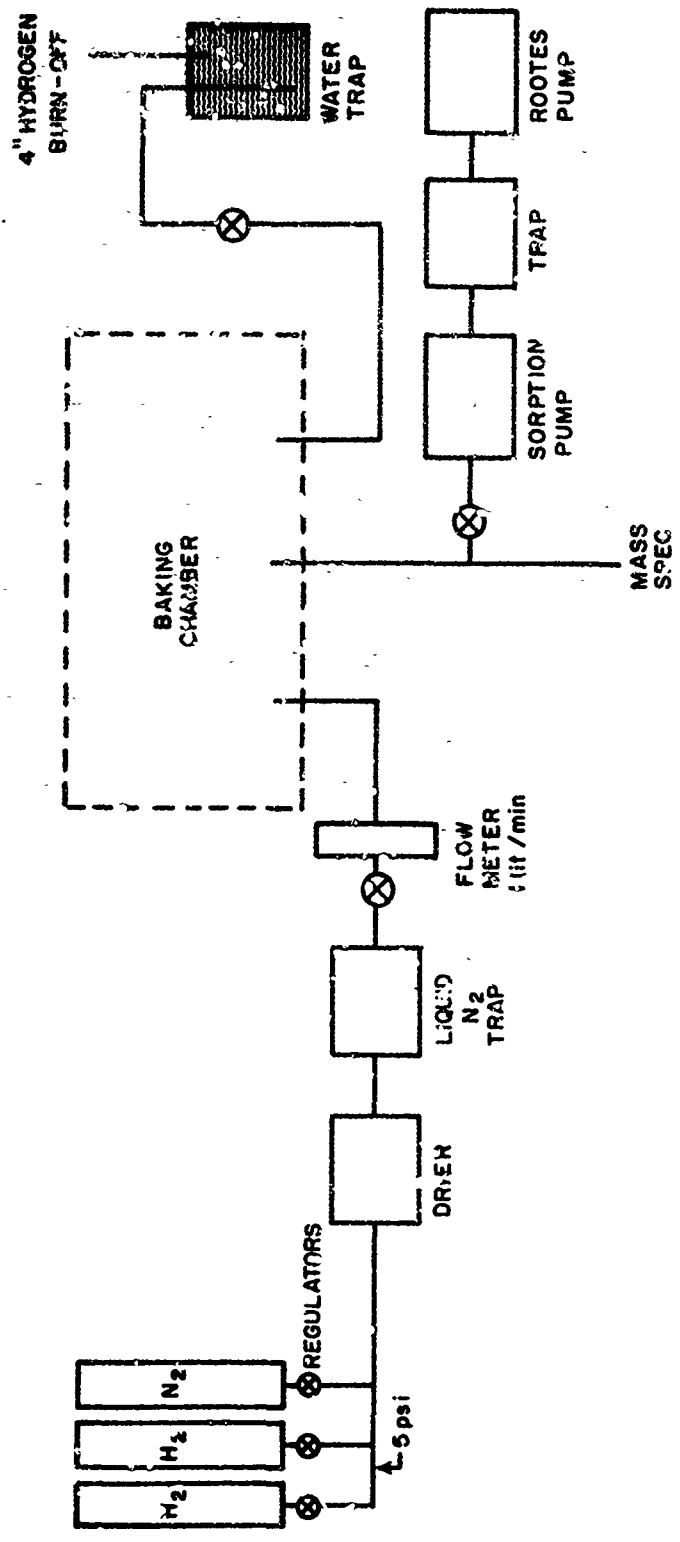
Figure 3-11. Hydrogen Firing System
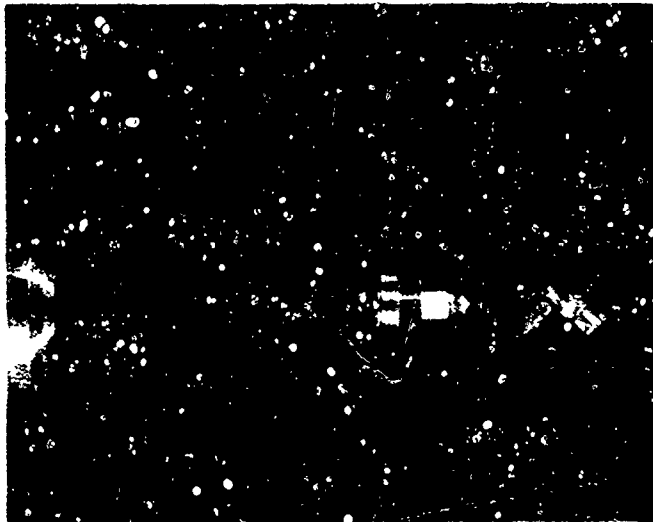
Figure 3-12. Mechanism for Introducing Barium
Contamination Source into Vacuum Gap

2-1315

The complete assembly which rests on the anode support is shown in Figure 3-13. The envelope can be used either before or after initial bakeout.

3.9   Electrode Geometry

Throughout the experimental program, Bruce Profile electrodes were used when a uniform electric field was desired. These follow a design experimentally investigated by Bruce. The basic outline is shown in Figure 3-14a. The diameter of the central flat portion is usually less than the maximum gap separation and all regions are made to blend smoothly with each other. The back portion is finished with gradual contours to avoid excessive field enhancement. A typical electrode outline showing the mounting arrangement is given in Figure 3-14b.

3.10   Experimental Procedure

Early in the program it was found that apparently minor details of experimental procedure were important. Indeed, even the duration and position of quiescent periods in the test sequence could influence the breakdown voltage. Accordingly, a rigidly specified schedule was adopted. A weekly cycle proved both convenient and efficient and was as follows:

Thursday: Install electrodes in chamber, pump down overnight.

Friday: Bake at 400°C for six hours.

Saturday and Sunday: Allow chamber to cool for > 48 hours.

Monday: Connect power supply, day 1 test sequence.

Tuesday: Day 2 test sequence.

Wednesday: Day 3 test sequence.

Thursday: Day 4 test sequence (1/2 day), prepare chamber for
next treatment.
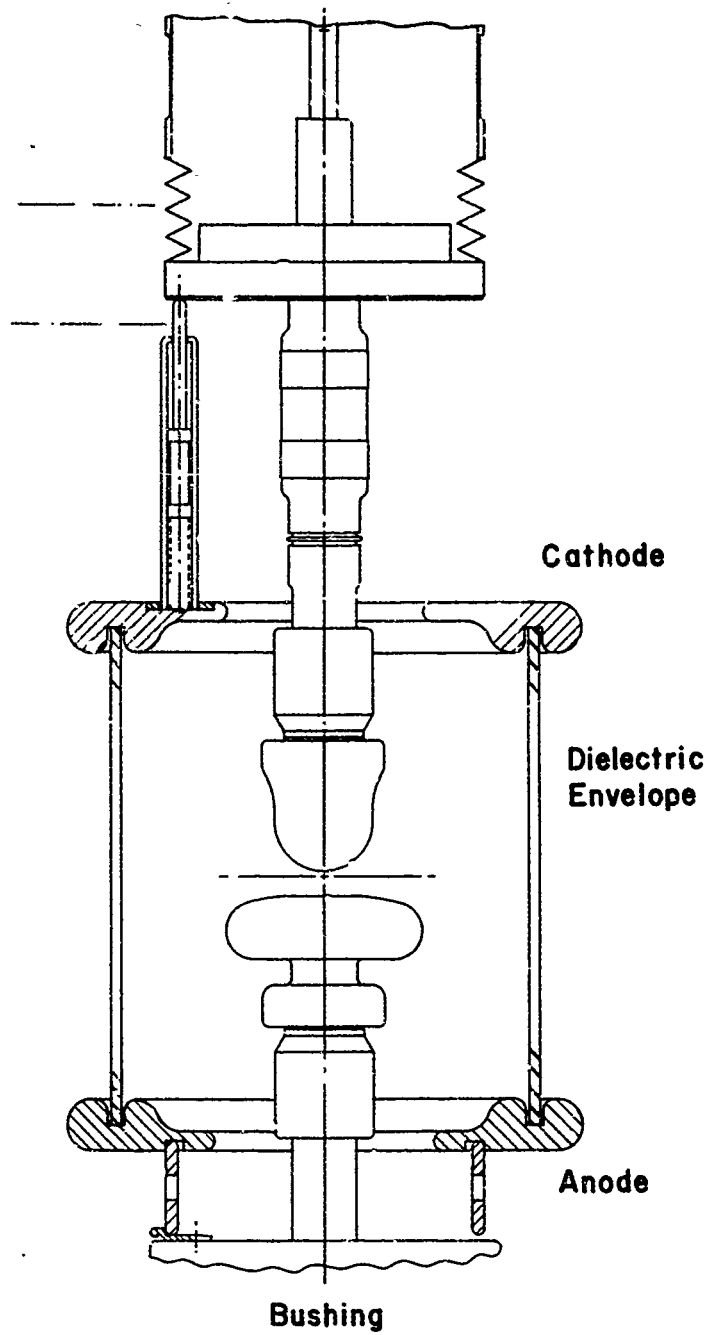
Figure 3-13 Dielectric Envelope Assembly

1-2545

Flat

$$XY = CO \sin \left(\frac{BX}{BO} \cdot \frac{\pi}{2} \right)$$
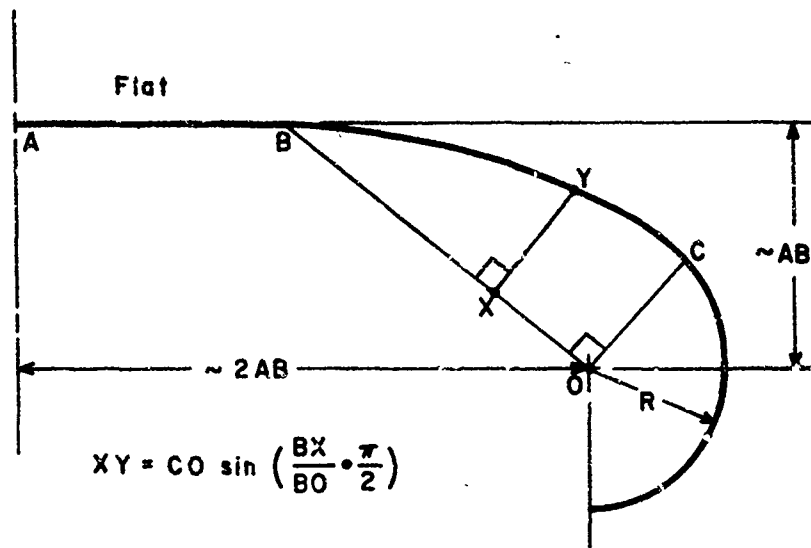
(a) Specifications for Bruce Profile

Position of Electrode Heater

Quick-Disconnect Mount
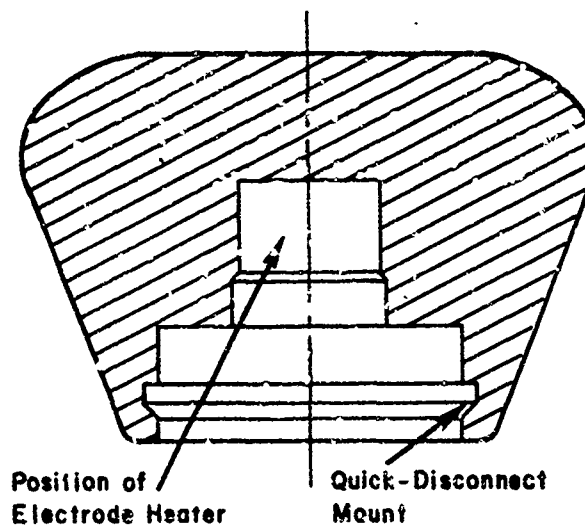
(b) Typical Uniform Field Electorde

Figure 3-14. Bruce Profile Electrode Geometry for Uniform Field

1-4253

SECTION 4

FACTORS INFLUENCING VACUUM BREAKDOWN

4.1   Introduction

To insure repeatable experimental results it is necessary to have all contributing factors under control. Thus, at the onset of the program both theory and experimental work were examined to determine what factors should be controlled and what factors might prove most interesting. This section discusses theory and prior experimental work as a background to the factors that were ultimately studied.

4.2   Theories of Vacuum Breakdown

Present theories of vacuum breakdown may be classified as particle exchange, electron beam, or clump mechanisms. While the electron beam theory has considerable experimental support in the small gap regime (< 1 mm), no single theory has been proven capable of accounting for all the phenomena observed at the larger gaps and higher voltages which are of interest to this study. Thus, theoretical insight into important factors was, and is, at best extremely limited. Since excellent reviews of the major theories are available,[1-3] they will not be discussed here.

4.3   Environmental Factors

4.3.1   Residual Gas

The residual gas can influence the breakdown voltage of a gap through adsorption on the electrode surfaces, interelectrode collisions and ionization, and positive ion sputtering of cathode protrusions. If an electrode surface is initially completely desorbed of all gas, a monolayer of nitrogen would be absorbed in eight hours at 7.5×10^{-10} torr and a monolayer of water vapor at 4×10^{-10} torr. The present limitations at very high voltage (e.g., 300 kV) are

4-1

believed related to surface "contamination" effects, but as far as is known no tests at very high voltage have been conducted in the truly "clean surface" pressure regime to determine what improvements could be obtained. However, to maintain a completely desorbed surface would require pressures of many orders of magnitude below that mentioned above, which does not seem practical for present engineering purposes.

At the other end of the pressure range ($\sim 10^{-4}$ torr) collision processes in the gap and sputtering of the cathode surface can be important, and it has been demonstrated[4] that in the range above 200 kV, operation at 10^{-4} torr can give a 100% improvement in attainable voltage compared with operations at 10^{-6} torr. It is only the last few years that experiments at the University of Illinois,[5] and independently at Ion Physics Corporation,[6] showed that with small vacuum gaps (~ 1 mm) performance at 10^{-4} torr is better than at 10^{-6} torr, which is contrary to earlier opinion.

It is important that the nature of the residuals should be known through the use of mass spectrometer techniques, and, where needed, controlled, pure gases should be used. This is also a partial check that satisfactory electrode cleaning processes are being followed. There is a considerable body of evidence[7, 8] which shows that a significant partial pressure of organic vapor is undesirable in very high voltage vacuum equipment. The initial investigation should be at pressures of around 10^{-8} torr in a clean environment.

4.3.2 Temperature

The effect of electrode temperature on vacuum breakdown has not been studied extensively, but it appears from experiments by Slivkov[9] that there is no deterioration in vacuum insulation properties up to about 800 C (for nickel). Recent studies at the Naval Research Laboratories by Little and Whitney[10] appear to confirm this, although Maitland's[11] information does not. It seems that temperature as a parameter should not be investigated until late in the program, if then, and that initially the experiments should be at room temperature.

4.3.5   Envelope

The discussion of the envelope effect is included in the environment group because there has been some evidence[12] that the presence of glass can influence gap performance. Certainly the presence of a closely confining envelope could influence the field in a gap, particularly if a geometry such as a sphere to plane was being used - and it could also be a source of contamination or ions. The diameter of the envelope is a parameter which could be important to gap performance.

The dielectric envelope has to withstand the total voltage and this poses a breakdown problem which may be separate from that of the gap. The factors which are important to the insulating properties of the dielectric envelope[13] are the end conditions, the length, the material and, possibly, the diameter - probably in that order of importance. Conditions at the negative end are particularly important, because intense fields can produce a copious supply of electrons from the metal termination.

So-called "corona shields" can also be utilized to reduce the electric field at the ends of the envelope, but these will be most effective, and perhaps unnecessary, or even undesirable, when proper attention is paid to end conditions.

The materials which should be examined are ceramic (alumina) and glass. These could be either glazed or unglazed. A typical tube glass or alumina should be chosen for the initial experiments. If it is found that the presence of the envelope material has a weakening effect on the vacuum gap, or if the envelope itself is electrically weak, decisions can be made later to examine either other materials or a graded structure.

It is thought important to the lucid conduct of the program to be able to test gaps without the presence of the envelope and vice versa. Further, when both gap and envelope are together they should be arranged to permit the separate monitoring of the prebreakdown current associated with each, and the equipment should be provided with an indicator to show which has broken down when the test is taken to the limit.

4.3.4 Magnetic Field

It is known that the presence of a magnetic field can change the maximum electric field which can be supported by a vacuum gap. For example, Pivovar et al[14] have used a magnetic field parallel to the electrode surfaces in studies up to 170 kV to remove the electron component of prebreakdown conduction and hence to raise the breakdown voltage. Also, the interaction of the magnetic and electric fields in crossed field particle separators is known to be a problem. The difficulties are believed to exist in the fringing fields rather than within the gap. Separators at Brookhaven National Laboratory are now operating at 500 kV across a 4-inch gap at a pressure of about 10^{-4} torr with one spark every 5 to 6 hours.[15] The magnetic field is 200 to 300 gauss and must be applied _after_ the electric field. In the event of a spark, the magnetic field has to be interrupted to re-establish the electric field, and it is expected that operation at fields higher than 300 gauss will cause difficulties.

4.3.5 Contamination

The sensitivity of spark gaps to dust particles is well known, and the vacuum gap is particularly so. In early experiments, breakdown voltage was raised by 50% just by improved methods of installing dust-free electrodes.

Organic contamination is known to be deleterious to vacuum insulation.[8] Such contamination can be from processing of electrodes before installation, oil vapor in the atmosphere, or from sources inside the vacuum system. The vacuum system should be designed to be free of organic contamination, and to confirm this a continuous check should be made of the residuals using a mass spectrometer. The elimination of dust particles and organic contamination introduced to the system on the electrode surfaces is best accomplished using a clean bench processing system coupled to the vacuum chamber.

It is possible using the above methods to eliminate contamination which is not necessarily present in the average high power electron device.

There is also the possible contaminant BaO which originates at thermionic cathodes, and the presence of BaO has been shown to adversely affect vacuum insulation in a study at small gaps by Brodie.[16]

4.3.6   Oxide Films

A film of oxide forms almost instantly on most, if not all, freshly prepared metal surfaces. The film continues to grow with time after preparation, and it is reasonable to assume that the thickness of this film should be important to vacuum insulation. Indeed, the controlled growth of micron-thick alumina films on aluminum cathodes (by anodization) has been used by CERN[17] to increase stress levels in large electrostatic particle separators by a factor of two. Jedynak[18] has shown similar increases in performance for sputtered metal oxide and flouride films.

Oxide growth is a possible parameter which has not been sufficiently appreciated, and it may account for some of the conflicting data obtained from past experiments. It is important to the proposed program to determine if oxide growth between preparation and installation of electrodes is important, and to design subsequent experiments according to the results obtained.

4.4   Fields and Geometry

4.4.1   Electrostatic Field, Macroscopic

The significance of electric field to breakdown in high vacuum is well known, if not well defined. At small gaps, less than a few millimeters, breakdown takes place approximately at a constant gradient ($\rightarrow$ 100 kV/mm) after suitable conditioning. At larger gaps, a large body of evidence supports for uniform field electrodes a relationship:[4, 19]

$$V_s = Cd^{1/2}$$

Where V_s is the breakdown voltage, d is the gap spacing and C a constant. This relationship holds for the range of greatest interest here, but the support data is from tests subject to contaminating influences which should not exist in ultra-high vacuum. Cranberg[19] derived the above expression from:

$$V_s E_b = \text{Constant}$$

where E_s is the field at an electrode surface on which a "clump" originates. However, experiments at voltages up to 1.7 MV[20] using sphere to plane geometry did not confirm this expression, nor did they confirm a criterion $V_s E_c E_a^{2/3} = \text{Constant}$, developed by Slivkov.[21] The relationship $E_s = \text{Constant}$ was found to be more representative of experimental data.

The macroscopic field at the electrode surface is obviously determined by the electrode geometry and, to a lesser extent, by the proximity of shields. Further information is required on macroscopic field effects for the design of high voltage equipment, particularly in the relatively clean environment of high power electron devices, and this is a good area for investigation during the program.

4.4.2   Electrostatic Field, Microscopic

The field as determined by gross geometry is intensified by the presence of asperities or roughness of the electrode surface. The microscopic field is difficult to control, but a first step is through surface finish. It has been stated that surface finish has been determined to be an unimportant parameter, which is surprising considering the mechanisms postulated for vacuum breakdown. However, recent experiments[22] with perhaps other parameters under better control than previous investigators have shown it can be important. In other experiments[23] to examine the effect of residual gas pressures on breakdown, much greater field enhancement factors have been measured. This effect has been attributed to the growth of sharp whiskers on the electrode surface. These intensifications can be calculated from the Fowler-Nordheim equation when the current, voltage and gap are known.

Electrolytic, mechanical and chemical techniques are available for application to electrode surfaces and the first two seem most attractive. Electropolishing has not compared well with other methods, probably because it influences another important parameter (surface hardness - later). Hadden[24] failed to improve the breakdown strength of copper electrodes by electropolishing. However, both mechanical and electropolished surfaces might be compared at the large gaps and low gradients used in tubes.

4.4.3   Area Effect

It has been known for some time by those acquainted with vacuum insulation problems that increasing the area of a stressed surface reduced the stress which could be supported. However, it was not until recently that quantitative information on this effect was obtained to assist in the design of vacuum insulated electrostatic generators, which are large area devices. Figure 4-1 shows a plot of early data indicating the severity of the problem at a 1 mm gap.

Area effects have been studied in other dielectrics such as oil and capacitor insulation. It can be expected that breakdown mechanisms depending on randomly distributed weak spots will have values for their occurrence which decrease with area. Statistically this is covered by the theory of extreme values[25] which has been applied successfully to the reduced breakdown voltage with an increase in area in liquid and solid dielectrics.[26] Statistical influences alone do not seem to account for the severity of the effect in vacuum, and other factors such as the difficulty in surface preparation of large surfaces and the limited gap pumping speed (at 1 mm) may also be important.

At the higher voltages of particular relevance to the proposed program, there is no specific data on the area effect as exists for 1 mm gaps, although experience indicates that increasing surface area makes conditioning to high voltage more difficult. Where possible during the program electrode surface area should be kept constant, and in the studies of various electrode geometries the possible significance of differences in area should be borne in mind.
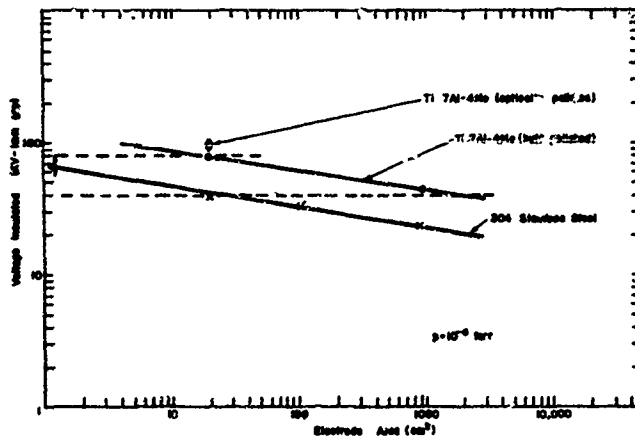
Figure 4-1. Electrode Area Effect

4.5 Electrode Materials and Surface Properties

In "low-voltage" experiments, correlation has been found between vacuum breakdown voltage and metallurgical state of the electrodes as regards surface finish, particle content, surface hardness and grain size. Surface finish has been treated in the earlier discussion of the microscopic electric field. The importance of selecting the best alloy and metallurgical condition is illustrated by reference to Table 4-1, which shows results from tests with various alloys of the stainless steel family.

The following properties are included to indicate what may be important parameters, and where the existing evidence requires substantiation.

4.5.1 Particle Content

Tests and microscopic examination of electrodes have shown that many breakdowns occur at sites of non-metallic inclusions. These inclusions are oxides, silicides, carbides, etc, introduced during processing of the metal, or precipitates which are compounds of alloying constituents introduced to improve strength properties. When alloys were tested which depend upon phase transformation of the crystal structure for their strength properties and which were relatively free of impurities and precipitates, high fields could be insulated (up to 115 kV/mm with Ti-7Al-4Mo alloy).

4.5.2 Grain Size

Using 304 stainless steel electrodes it has been found that 80 kV could be insulated across a 1 mm gap when the average grain size was ~ 500 grains/mm^2, which compares with 40 kV with 62 grains/mm^2.

4.5.3 Hardness

When the surface of electrodes of 304 stainless steel are hardened by cold working, tests have shown that the same fields (80 kV/mm) can be insulated without breakdown as when the electrodes are annealed. However, in the former case, the gap currents are normally 1 to 2 orders of magnitude

Table 4-1. Insulation Strength at 1 mm
Gap for Several Metals

Metal	Strength (kV/mm)
304 Stainless Steel	60
Udimet A	55
Nickel, Inconel-718	50
303 Stainless Steel	44
Inconel	44
Inconel-X, Molybdenum	40
Haynes-25	30
Udimet-41	28
Hastelloy B	15
Multimet	10

lower at maximum voltage. Germain[27] has suggested that hardness is an important parameter at the high voltages of interest here, and has attributed poor experience with electropolishing to the relatively soft surface this polishing technique produces.

4.5.4 Physical Properties

Several attempts have been made to match vacuum breakdown performance with one or more of the physical properties of the electrode material. Rosanova and Granovskii,[28] for example, suggest that electric "strength" of the gap increases with the tensile strength of the anode material. Other properties which could be important include work function, secondary emission coefficients, electrical conductivity, sputtering coefficient, density, thermal conductivity, specific heat, and boiling point. One could add others such as susceptibility to whisker growth, which would require a program on its own to determine.

It seems likely that experiments in the past did not demonstrate a convincing correlation between performance and some physical properties because the parameters were not adequately controlled. The extensive effort and the precise control of parameters which are expended under the present program should permit such a correlation.

4.6 Electrical Circuitry and Energy

At the present time, very high voltage vacuum equipment requires a conditioning process involving low energy discharges to reach the desired operating range, and during operation is likely to break down occasionally. During operation high power electron devices are supplied from energetic sources, and the discharge energy through them at breakdown is limited by crowbarring devices.[29] These facts make it desirable to determine the effect on subsequent performance of discharging different energies through a vacuum insulated gap ; but there is more than energy involved. A fast discharge (high current) will probably produce a different result from a slow discharge, and if the circuitry is suitable voltage reversal can take place, which some

evidence[30] suggests may lead to deterioration of gap performance. Voltage reversals are known to occur in klystrons at breakdown.

If the supply across a vacuum gap at breakdown is simply a charged capacitor with some series resistance, and the first fraction of a microsecond is disregarded, the discharge current follows the usual exponential law and chops at a few tenths of an ampere.[31] This is so for small gaps ($\sim$ 1 mm) and probably also holds for large gaps when complete breakdown takes place. If the series resistance (R_s) is so large that V/R_s is less than the chopping current, a series of suppressed breakdowns occurs.[31] These circuitry effects need more investigation at the high voltages of the present study.

It is obviously desirable to examine energy effects during the program. At the lower end of the energy range, it is difficult to get much less than 10 joules at discharge because of the intrinsic capacitance of the electrode system, and 7000 joules has been suggested as a suitable value for the high energy range. Thought should also be given to the significance of series inductance and resistance which will determine the spark, or arc current, and whether or not polarity reversal will occur. Furthermore, for particular practical situations there is sometimes an acceptable or tolerable sparking rate at the operating voltage level of the system. This is usually represented as a number of faults, breakdowns or "kickouts" per hour and as long as the fault occurs during the "dead time" of the tube cycle, the overall operation of the system may be negligibly impaired. Thus, as related to the present work, long term withstand tests will be of especial interest for application to a field where reliable operating performance is required over extended time periods.

4.7   Experimental Factors

On the basis of the preceding considerations a listing of factors has been made and is given in Table 4-2. Factors are classified as flexible if they can be varied at will during experimentation, and as inflexible if they must be fixed prior to application of voltage and cannot subsequently be altered during the experiment.

It is expected that if these factors are adequately fixed, then the fundamental physical mechanisms will be under sufficient control. It is interesting that few of these factors subject to experimental manipulation are directly involved as parameters in theories of vacuum breakdown. Thus, there is need of care in drawing conclusions as to the basic mechanisms from the measured variations in characteristics caused by changes in the levels of the experimental factors.

Table 4-2. Experimental Factors

Inflexible Factors	Flexible Factors (May Be Varied During Testing)

Electrodes - Cathode and/or Anode
 	
    Material
    Surface Finish
    Final Processing
    Bakeout
 	
Geometry
 	
    Shape
    Size (Area)
 	
Vacuum Chamber
 	
    Material - Metal or Dielectric
    Chamber Geometry - Size
    Bakeout
	Environment
	
	    Residual Gas Pressure and Species
	    Contaminant
	    Magnetic Field
	    Radiation
	
	External Circuit
	
	    Impedance
	    Available Energy and/or Current
	    Voltage Application Rate
	
	Electrode Temperature
	
	Electrode Spacing
	
	Conditioning - Electrical Stress
	
	    History of the Electrodes

SECTION 5

FACTORIAL AND STATISTICAL DESIGN

5.1   Factorial Design

Two methods of approach usually exist for investigating a physical system. The fundamental processes affecting the behavior of the system may be studied, or a more empirical approach may be adopted and the effects of various changes in the system studied directly. The latter method is indicated when the underlying physical mechanisms are little understood and practical results are of primary importance. In this case, the principles of Factorial Design [1] can be used to optimize experimental design. This provides a powerful tool for the analysis of the results and enables information to be derived from a minimum number of experiments both on the effects of the individual factors and on the degree of interaction among factors.

A simple example will most effectively describe Factorial Design. Consider a system whose performance is a function of three factors, A, B and C. All other factors which may be important are to be held constant. In the simplest case, it is decided that two levels of each factor will be explored. Factorial design then directs that the optimum set of experiments (or "treatments") is that consisting of the eight (2^3) unique combinations of the three factors at two levels each. Thus, using as an example the "Block of Eight" experiment, the following program is defined:

| | Levels* | |
Factors	High	Low
A - Anode Processing	Vacuum Firing	Hydrogen Firing
B - Cathode Processing	Vacuum Firing	Hydrogen Firing
C - Electrode Size	Large	Small

* Designation of "high" and "low" is completely arbitrary

Treatments (or Experimental Combinations)

Code*

Code			
(1)	Small	- Hydrogen Fired Anode	- Hydrogen Fired Cathode
a	Small	- Vacuum Fired Anode	- Hydrogen Fired Cathode
b	Small	- Hydrogen Fired Anode	- Vacuum Fired Cathode
ab	Small	- Vacuum Fired Anode	- Vacuum Fired Cathode
c	Large	- Hydrogen Fired Anode	- Hydrogen Fired Cathode
ac	Large	- Vacuum Fired Anode	- Hydrogen Fired Cathode
bc	Large	- Hydrogen Fired Anode	- Vacuum Fired Cathode
abc	Large	- Vacuum Fired Anode	- Vacuum Fired Cathode

* If the factor is at its "high" level, a lower case letter is included in the name; if a factor is at its "low" level, the letter is omitted.

Each treatment is tested (in this case for breakdown voltage), and the results used to obtain estimates of:

Mean: Average breakdown voltage.

Main Effect: For each factor, this is computed by subtracting the average breakdown voltage of the four treatments with the factor at its low level from the average breakdown voltage of the four treatments with the factor at its "high" level.

Thus, a main effect is the average change in breakdown voltage when a factor is varied from its low to high level. The average is taken over a range of other factors. Another way of viewing a main effect is as the average of the four possible comparisons between individual treatments. In the case of factor A, these comparisons are:

(1) (a-(1)) - Effect of A when B and C are at their low level.

(2) (ab-b) - Effect of A when B is high and C is low.

(3) (ac-c) - Effect of A when B is low and C is high.

(4) (abc-bc) - Effect of A when B and C are high.

5-2

It is evident that each treatment will be used once and only once in each computation of a main effect.

Interaction: This is defined as the dependence of the effect of one factor upon the level of another factor. Note that in the comparisons above, two are made with B at its high level ((2) and (4)) and two are made with B at its low level ((1) and (3)). The average difference between these estimates of A is termed the interaction AB. This is symmetrical in that if the effect of A depends upon the level of B, the effect of B will also depend upon the level of A. An interaction among three factors (ABC) is similar in meaning but of more difficult interpretation.

The computation of main effects and interactions can be carried out by detailed application of the definitions which have been given. However, it is convenient to utilize a standard table which assigns to each treatment a positive or negative sign for the computation of each effect or interaction. This is given in Table 5-1 for a five factor two level full factorial experiment. It is derived by noting that for the main effects A, B, and C, treatments with the corresponding factor at its low level are entered negative. Thus the sum of each column gives the difference between the high and low levels of the treatments. This sum is then divided by 16 in the case of a five factor experiment so that the result will indicate the average effect of a factor. The signs of the interaction columns are derived by multiplying together the signs of the component effect columns. Thus the signs for the interaction AB are obtained by multiplying the sign for A by the sign for B. It is simple to verify that the result satisfies the definition given earlier in this section. Again the sum is divided by 16 so that it represents an average.

This method of computation of factorial results is often referred to as Yates Algorithm. Yates[2] has also developed several algorithms suitable for hand calculation in which each step is automatically checked for errors.

5-3

With the easy availability of time-shared computers the table of signs described above can be used directly to generate programs to carry out the basic factorial analysis.

When it is desirable to study many factors at two levels each, but not economically feasible to carry out the number of experiments necessary for a full factorial design, a partial or fractional factorial design can be used. This was the case in the Pilot Experiment, described in Section 7, for which seven factors had been chosen as most interesting on the basis of prior knowledge. A full factorial experiment would have required 128 treatments (2^7), which, because each treatment took approximately a week to complete. would have been prohibitively expensive. Thus, a one quarter fractional factorial design was chosen in which all the main effects and most first order interactions could be computed without confounding, in 32 treatments. That is, the estimate of each main effect could be made without confusing (confounding) it with an effect due to some other change in experimental conditions.

More complex factorial designs are possible, for example a factor may be studied at three or more levels. Factorial design can even be applied to the determination of optimum conditions in situations where the underlying mechanisms are so complicated that an empirical approach is necessary. However, for the purposes of this program the two level, full factorial design has proven most appropriate.

5.2   Statistical Design

The estimates obtained from a factorial analysis contain both real effects and error. Even in a null experiment where all the estimates are a result of error, the largest estimate has an expected value of several times the average value of an estimate. For a 32 run experiment the expected value of this ratio is 2.4. Thus, in order to minimize the number of effects or interactions which are incorrectly judged significant, it is essential to employ statistical techniques. If an estimate of the repeatability (or error) of the result of each treatment is available either from prior experience or sufficient

repetition of single treatments, standard tests of significance can readily be applied. In this experimental program, such information was not available and a technique of half-normal plots as developed by Daniel[3] has been used.

In an experiment in which there are no real effects, the estimates are distributed about the average in a Gaussian pattern if it is assumed that the error is normal. Since the signs based upon high and low levels are arbitrary, only the absolute magnitudes are important in terms of statistical significance. This corresponds to folding the normal distribution at its middle and adding the probabilities of the left to those of the right. Thus, the distribution of the absolute values of the estimates is obtained.

This distribution is appropriately termed the "half-normal distribution" and is available in either tabular or convenient graphical form. Graph paper is scaled so that normally distributed estimates (due entirely to error) will fall on a straight line. In a factorial experiment, when the higher order interactions are negligible, their estimates are due to error. These, when plotted on half-normal paper, will fall on a straight line whose slope is proportional to the magnitude of error. However, any real effects will influence the results in a systematic rather than random way and their estimates will depart from the line. In addition the ranking of the absolute values of the estimates will consistently place a real effect near the top because the sign of a real effect is fixed while the error terms will vary in sign. Such tests of significance were indispensible in the Pilot Experiment (see Section 7.3).

When most of the estimates of a factorial experiment (both main effects and interactions) are related to real effects, it is difficult to generate a true error line. Also systematic errors may be present which influence the half-normal plot. These, and methods of detection, have been discussed by Daniel[3].

Table 5-1. Table of Signs for Computation of Factorial Main Effects and Interactions (From Davies[1])

Estimates of Main Effects and Interactions

EFFECT	T	A	B	AB	C	AC	BC	ABC	D	AD	BD	ABD	CD	ACD	BCD	ABCD	E	AE	BE	ABE	CE	ACE	BCE	ABCE	DE	ADE	BDE	ABDE	CDE	ACDE	BCDE	ABCDE
(1)	+	−	−	+	−	+	+	−	−	+	+	−	+	−	−	+	−	+	+	−	+	−	−	+	+	−	−	+	−	+	+	−
a	+	+	−	−	−	−	+	+	−	−	+	+	+	+	−	−	−	−	+	+	+	+	−	−	+	+	−	−	−	−	+	+
b	+	−	+	−	−	+	−	+	−	+	−	+	+	−	+	−	−	+	−	+	+	−	+	−	+	−	+	−	−	+	−	+
ab	+	+	+	+	−	−	−	−	−	−	−	−	+	+	+	+	−	−	−	−	+	+	+	+	+	+	+	+	−	−	−	−
c	+	−	−	+	+	−	−	+	−	+	+	−	−	+	+	−	−	+	+	−	−	+	+	−	+	−	−	+	+	−	−	+
ac	+	+	−	−	+	+	−	−	−	−	+	+	−	−	+	+	−	−	+	+	−	−	+	+	+	+	−	−	+	+	−	−
bc	+	−	+	−	+	−	+	−	−	+	−	+	−	+	−	+	−	+	−	+	−	+	−	+	+	−	+	−	+	−	+	−
abc	+	+	+	+	+	+	+	+	−	−	−	−	−	−	−	−	−	−	−	−	−	−	−	−	+	+	+	+	+	+	+	+
d	+	−	−	+	−	+	+	−	+	−	−	+	−	+	+	−	−	+	+	−	+	−	−	+	−	+	+	−	+	−	−	+
ad	+	+	−	−	−	−	+	+	+	+	−	−	−	−	+	+	−	−	+	+	+	+	−	−	−	−	+	+	+	+	−	−
bd	+	−	+	−	−	+	−	+	+	−	+	−	−	+	−	+	−	+	−	+	+	−	+	−	−	+	−	+	+	−	+	−
abd	+	+	+	+	−	−	−	−	+	+	+	+	−	−	−	−	−	−	−	−	+	+	+	+	−	−	−	−	+	+	+	+
cd	+	−	−	+	+	−	−	+	+	−	−	+	+	−	−	+	−	+	+	−	−	+	+	−	−	+	+	−	−	+	+	−
acd	+	+	−	−	+	+	−	−	+	+	−	−	+	+	−	−	−	−	+	+	−	−	+	+	−	−	+	+	−	−	+	+
bcd	+	−	+	−	+	−	+	−	+	−	+	−	+	−	+	−	−	+	−	+	−	+	−	+	−	+	−	+	−	+	−	+
abcd	+	+	+	+	+	+	+	+	+	+	+	+	+	+	+	+	−	−	−	−	−	−	−	−	−	−	−	−	−	−	−	−
e	+	−	−	+	−	+	+	−	−	+	+	−	+	−	−	+	+	−	−	+	−	+	+	−	−	+	+	−	+	−	−	+
ae	+	+	−	−	−	−	+	+	−	−	+	+	+	+	−	−	+	+	−	−	−	−	+	+	−	−	+	+	+	+	−	−
be	+	−	+	−	−	+	−	+	−	+	−	+	+	−	+	−	+	−	+	−	−	+	−	+	−	+	−	+	+	−	+	−
abe	+	+	+	+	−	−	−	−	−	−	−	−	+	+	+	+	+	+	+	+	−	−	−	−	−	−	−	−	+	+	+	+
ce	+	−	−	+	+	−	−	+	−	+	+	−	−	+	+	−	+	−	−	+	+	−	−	+	−	+	+	−	−	+	+	−
ace	+	+	−	−	+	+	−	−	−	−	+	+	−	−	+	+	+	+	−	−	+	+	−	−	−	−	+	+	−	−	+	+
bce	+	−	+	−	+	−	+	−	−	+	−	+	−	+	−	+	+	−	+	−	+	−	+	−	−	+	−	+	−	+	−	+
abce	+	+	+	+	+	+	+	+	−	−	−	−	−	−	−	−	+	+	+	+	+	+	+	+	−	−	−	−	−	−	−	−
de	+	−	−	+	−	+	+	−	+	−	−	+	−	+	+	−	+	−	−	+	+	−	−	+	+	−	−	+	−	+	+	−
ade	+	+	−	−	−	−	+	+	+	+	−	−	−	−	+	+	+	+	−	−	−	−	+	+	+	+	−	−	−	−	+	+
bde	+	−	+	−	−	+	−	+	+	−	+	−	−	+	−	+	+	−	+	−	+	−	+	−	+	−	+	−	−	+	−	+
abde	+	+	+	+	−	−	−	−	+	+	+	+	−	−	−	−	+	+	+	+	−	−	−	−	+	+	+	+	−	−	−	−
cde	+	−	−	+	+	−	−	+	+	−	−	+	+	−	−	+	+	−	−	+	−	+	+	−	+	−	−	+	+	−	−	+
acde	+	+	−	−	+	+	−	−	+	+	−	−	+	+	−	−	+	+	−	−	+	+	−	−	+	+	−	−	+	+	−	−
bcde	+	−	+	−	+	−	+	−	+	−	+	−	+	−	+	−	+	−	+	−	+	−	+	−	+	−	+	−	+	−	+	−
abcde	+	+	+	+	+	+	+	+	+	+	+	+	+	+	+	+	+	+	+	+	+	+	+	+	+	+	+	+	+	+	+	+

Column grouping: T, A, B, AB → 2^2; C, AC, BC, ABC → 2^3; D, AD, BD, ABD, CD, ACD, BCD, ABCD → 2^4; E, AE, BE, ABE, CE, ACE, BCE, ABCE, DE, ADE, BDE, ABDE, CDE, ACDE, BCDE, ABCDE → 2^5.

Row labels under TREATMENT COMBINATIONS.

↑ Enter Treatments in Standard Order

↑ Each column gives a sign to each treatment the sum is then the estimate of the main effect or interaction.

SECTION 6

PRELIMINARY EXPERIMENT

6. 1   Introduction

A characteristic of electrode gaps in vacuum is that there exists no unique breakdown voltage but only a band of possible values attainable after many prior sparks have passed during an initial "conditioning" procedure. The literature to date is confused about the significance of this procedure and of the role of electrode materials, shapes and finish in determining breakdown voltage. It is pertinent to question whether shape and finish, which are disturbed after sparking, can be preserved by a different choice of procedure for voltage application, leaving them available for the experimenter to vary at will.

It should be theoretically possible to monitor enough physical variables during voltage application to describe adequately the processes leading up to gap failure. Recognition of an incipient breakdown without damaging the electrodes would permit repetitive testing under similar conditions, being particularly useful with low impedance power supplies.

The present investigation was directed towards developing a conditioning procedure involving minimal sparking and to search for a criterion for incipient breakdown.

One shape only of large area, unbaked, metallurgically polished stainless steel electrodes was used throughout. During stepwise voltage application the variables monitored were gap current, light output, partial pressure of hydrogen or nitrogen, and X-radiation. The processes accompanying the approach to gap failure were monitored to see if they varied slowly enough to provide a reliable indication, prior to breakdown, of the breakdown level.

6. 2   Objective

The objective of the experiment was threefold:

(1)   To determine if there was a unique non-destructive criterion for breakdown which could be used to predict the breakdown voltage of vacuum gaps.

(2) To develop the instrumentation of the major experimental program, instrumentation which would enable the vacuum gap to be completely described prior to and during breakdown.

(3) To develop and optimize standard procedures for preparation, installation and voltage conditioning of the electrodes.

6.3   Apparatus

Hollow domes of 304 stainless steel serving as approximately uniform field electrodes, 8 inches in diameter, were centrally positioned at fixed gaps of up to 1 cm within the 3foot wide stainless steel vacuum chamber at the ends of two 250 kV bushings, as previously described by Britton[1] (Figure 6-1). Organic contamination was eliminated by using gold gaskets throughout, and pumping down to 6×10^{-7} torr with a mercury diffusion pump and liquid nitrogen cold trap. The mass spectrometer ion source, protruding inside from the wall, was screened from the large applied field within the chamber which otherwise perturbed it. Outside of the 3/4 inch thick glass monitoring port were two thallium activated NaI scintillators viewing, respectively, either the whole electorde region or only the interelectrode space through a collimator made from two narrowly separated parallel aluminum slabs. Visible radiation from this port was reflected sideways by a plane mirror to a photomultiplier to separate it from accompanying X-radiation, thus avoiding damage to the photocathode.

The high voltage power supply was a 160 kV, 1.5 ma transformer rectifier source. External resistors of 400 kilohm and 15 megohm were used to vary the effective output impedance.

The electrodes were hand ground initially with wet silicon carbide paper of successively finer grade, followed by finer grinding on a variable speed wheel. This was continued with silk using a succession of fine grades of alumina powder and was completed with a wash and wipedown with gamal cloth.
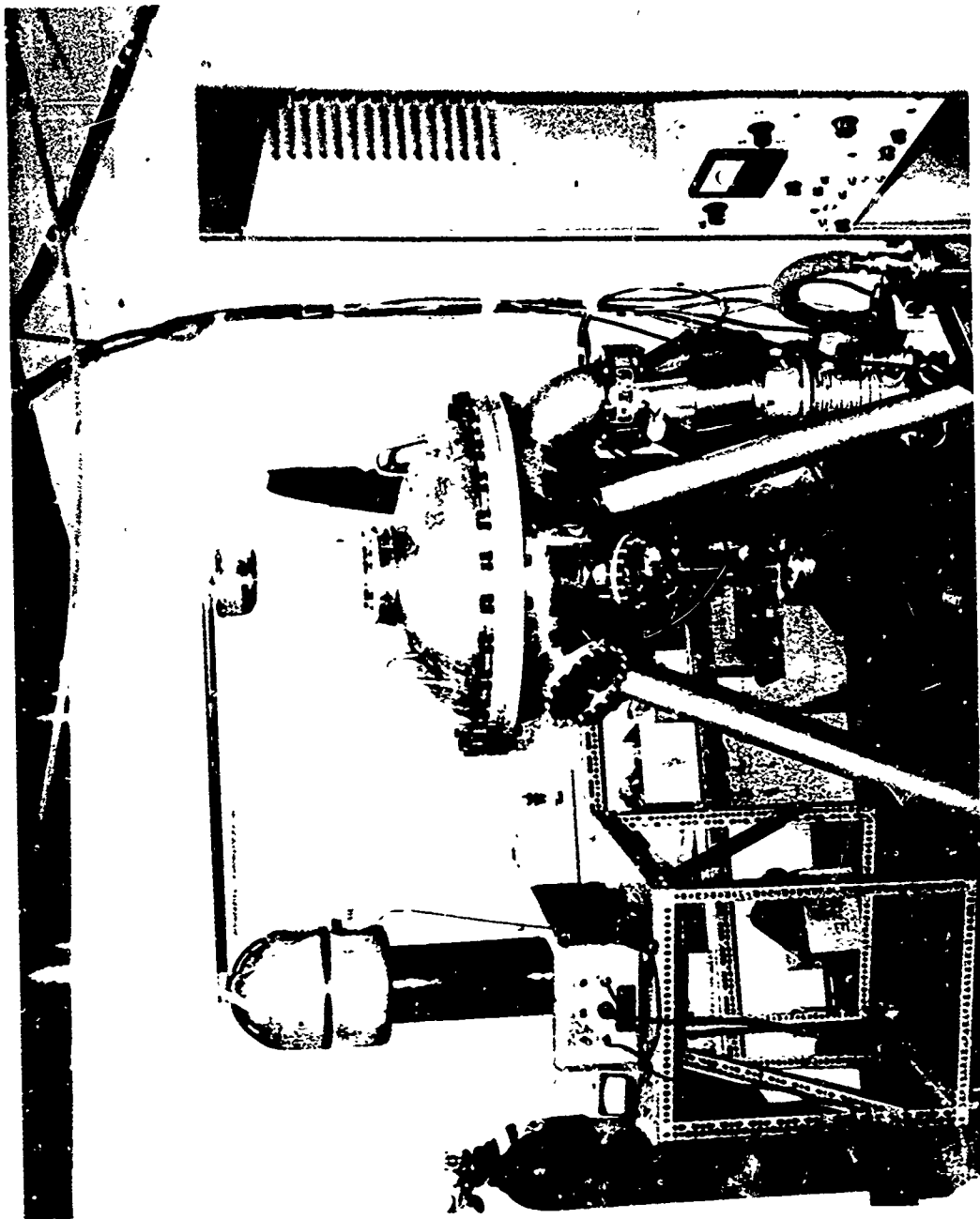
Figure 6-1. High Voltage, High Vacuum Experimental Facility Employing Two 250 kV Bushings

6.4   Electrode Conditioning

Starting with fresh unconditioned electrodes, the voltage was increased in steps of 2, 5 or 10 kV, depending on the gap setting and the voltage, while at the same time monitoring the N_2 or H_2 partial pressure peak on the mass spectrometer. It was found, by observing the current pulse shapes and the associated partial pressure rises, that a threshold voltage existed for the appearance of microdischarges. A plot of initial threshold voltage versus gap separation is shown in Figure 6-2. This is in good agreement with a similar plot of Arnal. [2] Microdischarges appeared as groups of apparently damped oscillatory waveforms similar to those described by Mansfield et al[3] and associated with X-radiation pulses modulated in frequency according to the pressure rise (Figure 6-3).

During the course of the   investigation, no pressure increases were observed until the microdischarge threshold voltage was reached, and above this the magnitude increased with the height of the voltage steps. Frequent breakdowns occurred when the pressure increases were large and it was found that these could be reduced in number, if not eliminated, by using smaller voltage steps. Occasionally, large pressure increases did occur, in which case the voltage was reduced or switched off before breakdown could take place.

From these observations, a conditioning procedure was evolved for unbaked but clean polished electrode surfaces. Initially, the voltage was increased incrementally every two minutes until a pressure rise was observed, and then allowed to decay to zero. The height of the voltage steps was limited to a level at which breakdowns were unlikely to occur during the gas surge and the step-wise voltage increase was continued until surface roughening took place (to be described later).

The conditioning apparently involves the controlled removal of gas from the electrodes.

Comparison in Figure 6-4 of the breakdown voltages measured with the new technique and with spark conditioning clearly shows improvement in the breakdown voltage and its deterioration as a function of number of sparks.

6-4
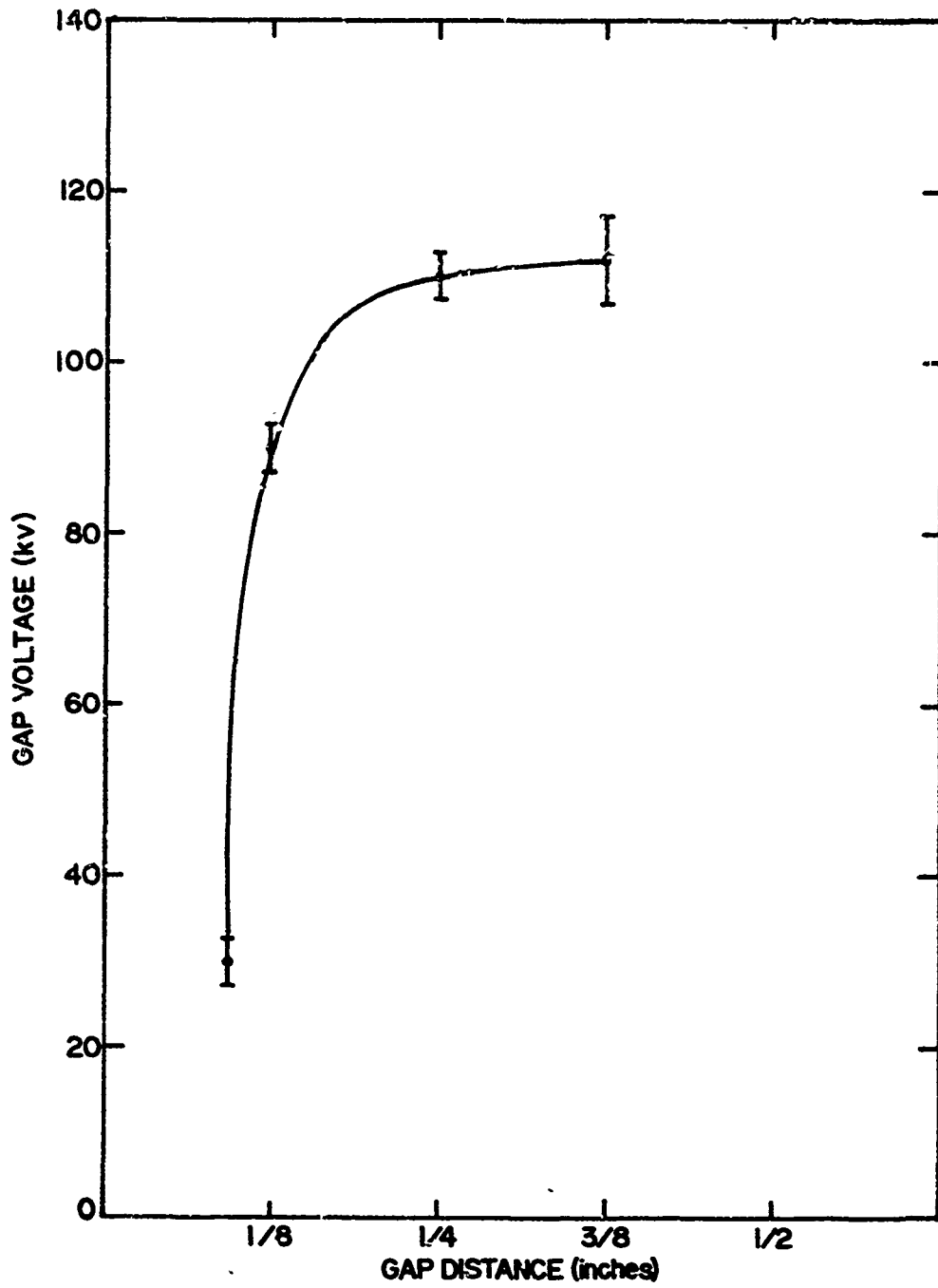
Figure 6-2. Variation of Microdischarge Threshold
Voltage as a Function of Gap Distance

1-1153a

6-5
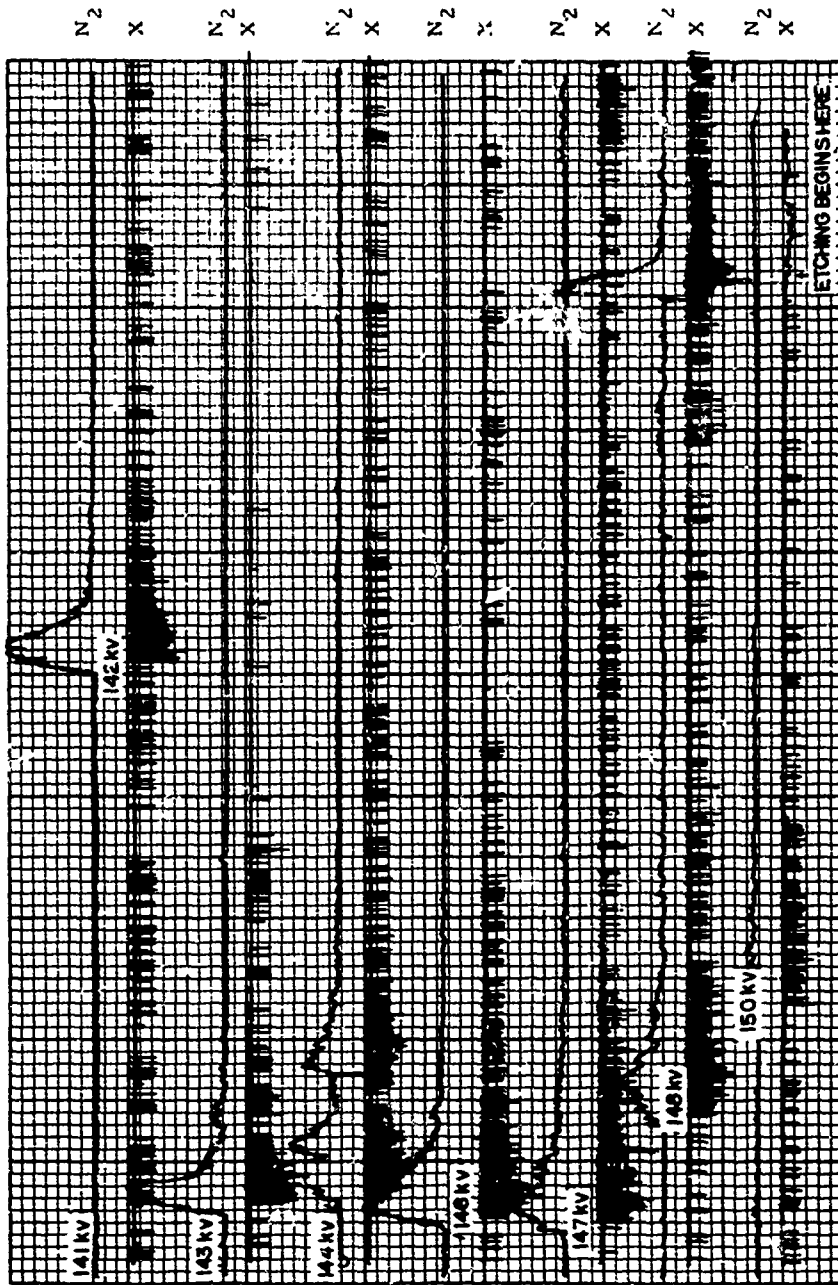
Figure 6-3. Simultaneous Recording of N_2 Partial Pressure and X-Ray Output

1-1266
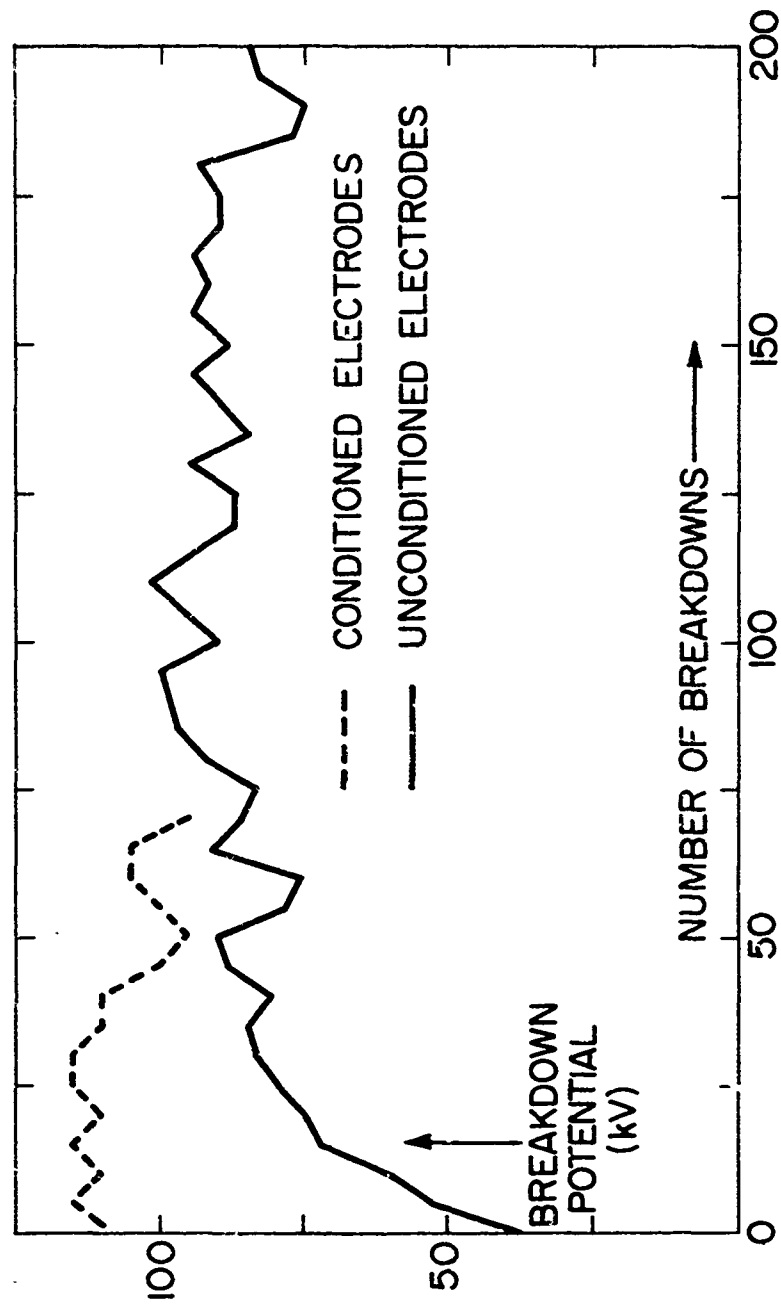
Figure 6-4. Comparison of Breakdown Sequence Diagrams for Electrodes
Conditioned by Sparking and by Present Technique
(Gap = 2.5 mr, Pressure = 5×10^{-7} torr)

2-1340

6.5 Monitoring Techniques

Pulse height histograms drawn from scintillator signal oscillograms of microdischarge activity showed that during the pressure surge there were two peaks in the photon energy spectrum (Figure 6-5) but after its decay the lower energy peak disappeared. Microdischarge current, although initiated by an ion exchange mechanism, was shown by Mansfield[3] and Pivovar and Gordienko[4] to be mostly electrons. The anode presents a thick absorbing X-ray target to these, most of which assume the whole applied potential but during the pressure surge, interelectrode gas intervenes as an additional thin target, intercepting some electrons to generate the lower photon energy peak.

When high voltages were reached with the new conditioning procedure, a steady X-radiation level grew due to cold cathode Fowler-Nordheim emission from sites of enhanced field strength just as Pivovar and Gordienko[4] have observed and attributed to surface etching. At still higher voltages the level rose while microdischarges abated, permitting an accurate measurement of the steady X-ray level as a function of voltage. Typical recordings are shown in Figure 6-6.

In thick targets, electrons generate X-radiation intensity U_x proportionally to the square of the applied voltage, V. [5] Hence relative changes in electron current can be derived from corresponding X-radiation densities and this technique has been used throughout the present investigation. Electrons emitted according to the Fowler-Nordheim law thus produce X-radiation according to:

$$U_x = AK \frac{\beta^2 V^4}{d^2} \exp \left(-\left(\frac{Bd}{\beta V} \right) \right) \qquad (6-1)$$

where:

B, K = constants

A = emitting area
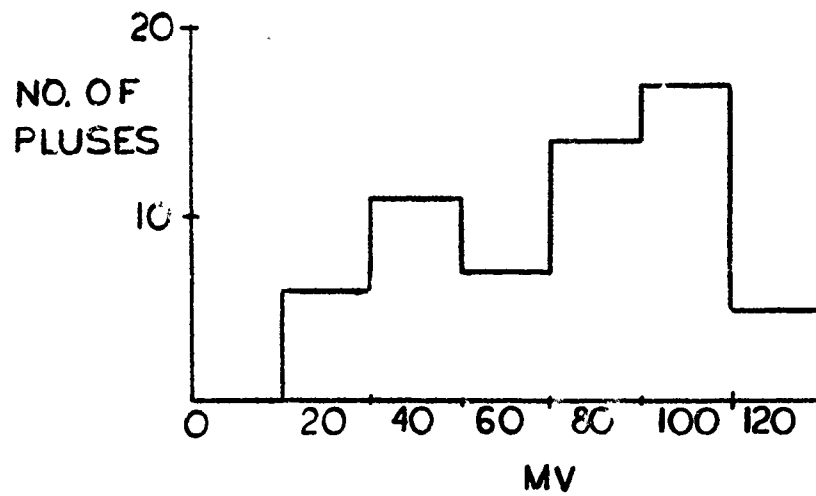
a. First test
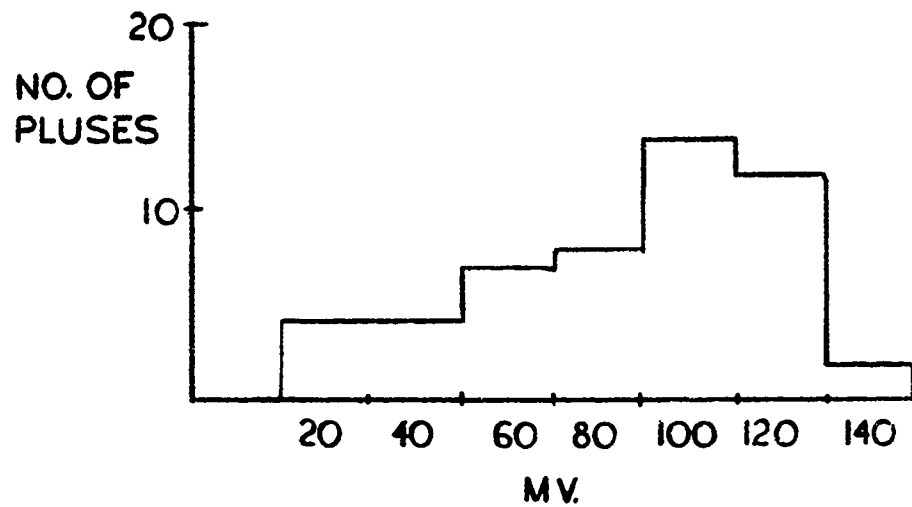
b. Second test

Figure 6-5. Experimentally Determined Pulse Height
Spectra of X-Rays During Conditioning

1-1265
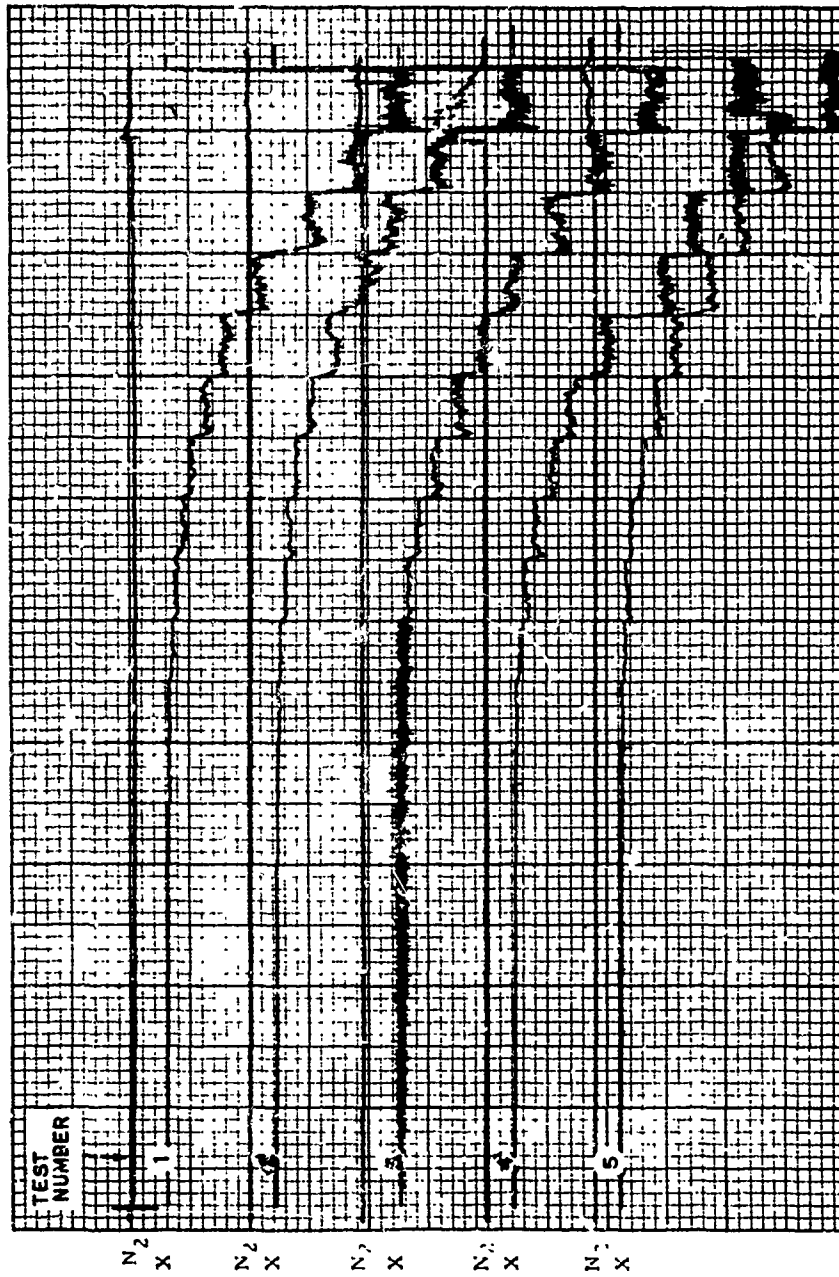
Figure 6-6. Typical Recording of X-Radiation from Etched Surface as the Voltage is Increased in Steps

1-1267

$$d = \text{gap separation}$$

$$\beta = \text{field enhancement factor}$$

A plot of $\log (U_x/V^4)$ as a function of V^{-1} should thus be linear.

Without measured work functions, these plots yield ouly relative values of field enhancement factor and emitting area but their present value is in signifying changes in these parameters taking place as breakdown is approached. While linear plots occurred in this investigation, the commoner non-linear variety (Figure 6-7) evidenced cathode surface changes as the voltage increased. Repetitively raising and lowering the voltage in increments without sparking failed to yield reproducible results (Figure 6-8). When extended to the breakdown limit, this procedure failed to show any correlation between the penultimate field enhancement factor and breakdown voltage (Figure 6-9).

Emission parameters, being derived from the slope of the Fowler-Nordheim plot, require readings at several voltage levels for their measurement. When they are time dependent, the parameter changes should be small during the interval between voltage increments to permit approximate measurement. As breakdown approached, the changes grew faster and rendered their measurement impossible. Changes in field enhancement factor and emitting area were occurring at constant voltage.

Gas or vapor evolution rate just prior to breakdown then suggested itself as a potentially significant parameter with which to describe the approaching breakdown since the accompanying X-ray emission is readily detectable in the case of microdischarges. Radiation density U_{xc} from the inter-electrode space is proportional to the product of gas density, n_g, electron current I_e and the Bremsstrahlung cross section σ_B. (38)

U_{xc} was accordingly monitored by directing at the interelectrode space a collimator made from two narrowly separated aluminum slabs between which photons passed to a scintillator. The current was simultaneously monitored and the relative gas density was derived from:
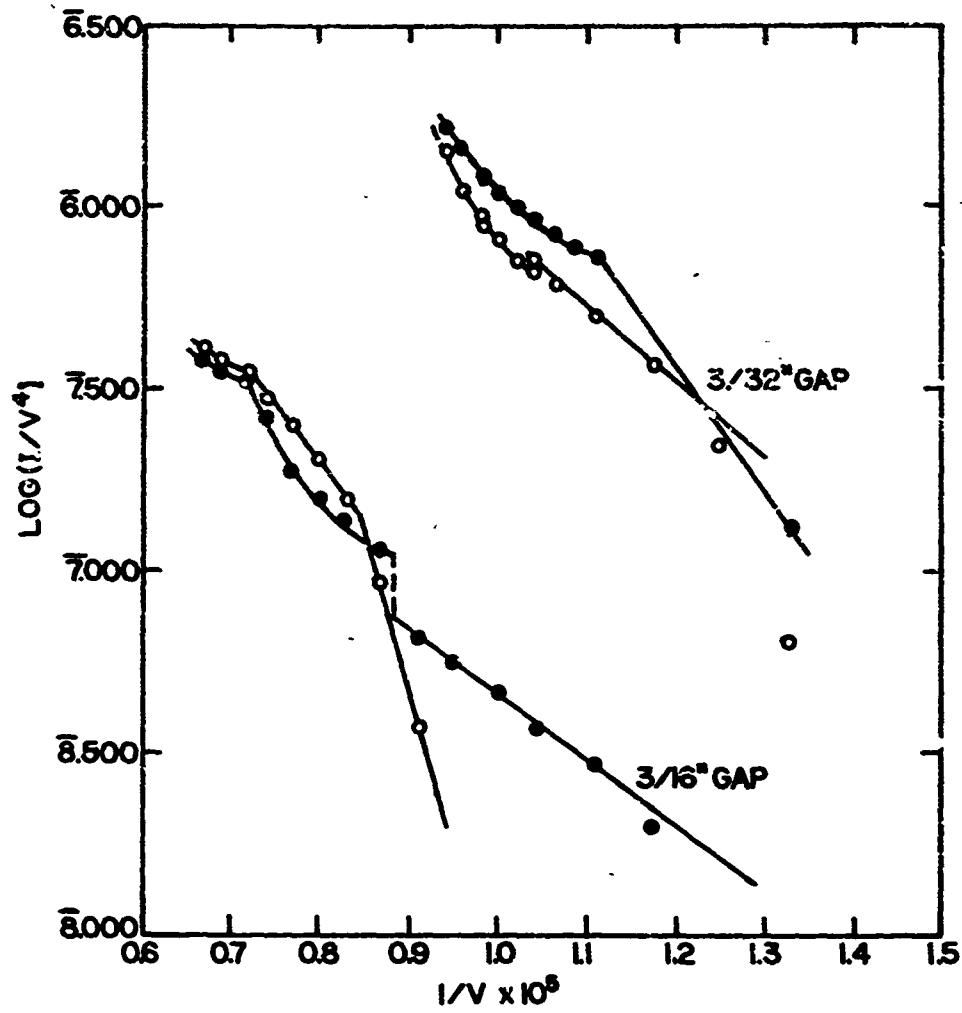
Figure 6-7. Equivalent Fowler-Nordheim Plots of X-Ray
Output Showing Result of Variation in Field
Enhancement Factor and Effective Emitting Surface Area

1-1270
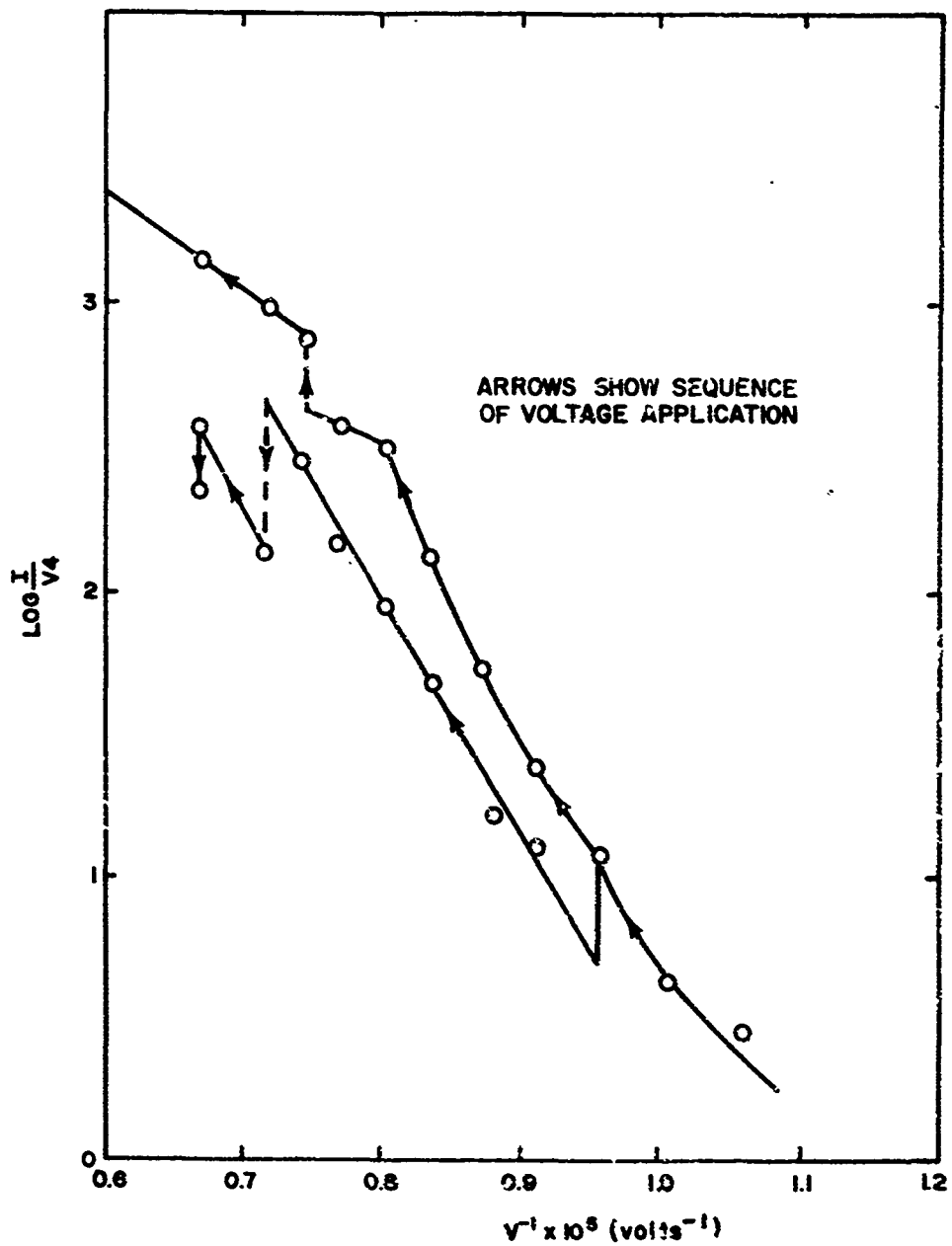
Figure 6-8. Fowler-Nordheim Plots for Two Consecutive
Voltage Applications Without Breakdown

1-1697
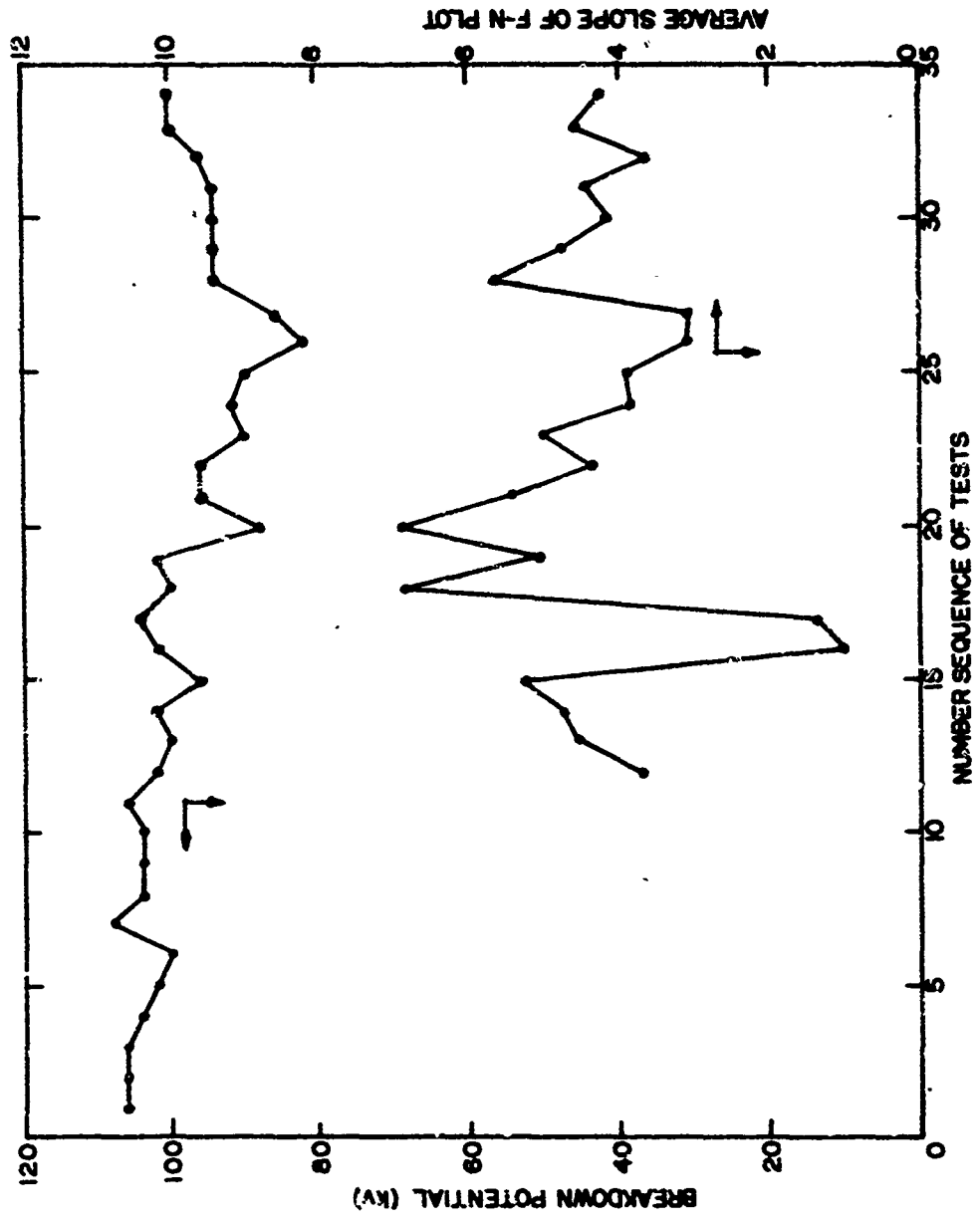
Figure 6-9. Sequence Diagrams of Breakdown Voltages with the Corresponding Average Enhancement Factors

1-1273

$$n_g = \frac{U_{xc}}{I_e \sigma_B} \qquad (6\text{-}2)$$

$$\sigma_B = \frac{8}{3\pi} \cdot \frac{1}{137} \cdot Z^2 \cdot \frac{c^2}{v^2} \doteq KZ^2 v^{-1} \qquad (6\text{-}3)$$

where K = constant. Hence:

$$n_g = \frac{U_{xc} V}{KI_e Z^2} \qquad (6\text{-}4)$$

A typical recording appears in Figure 6-10.

The right-hand side of Equation (6-4) was evaluated experimentally and is plotted in Figure 6-11 as a function of voltage up to breakdown. Surprisingly, the gas density appears to decrease but it must be noted that the average value of σ_B can decrease if the interelectrode gas is progressively diluted with hydrogen. Evidence of this was gathered from hydrogen partial pressure records from the mass spectrometer which show surges as breakdown is approached. It thus appears that hydrogen gas accumulated in the gap.

Thus the quantity measured by this technique is:

$$n_g \overline{Z^2} = n_m Z^2 + n_H \qquad (6\text{-}5)$$

where n_m and n_H are the atomic densities of the metal and hydrogen, respectively. As the voltage increases, these increase also by evaporation from the anode and an increase in n_g must be observed. However, n_g will multiply itself by sputtering and its capability to do this decreases as the sputtering yield and the factor g fall notably when the relative hydrogen concentration is greater. Thus this experimental result must be taken as evidence of the significance of sputtering.
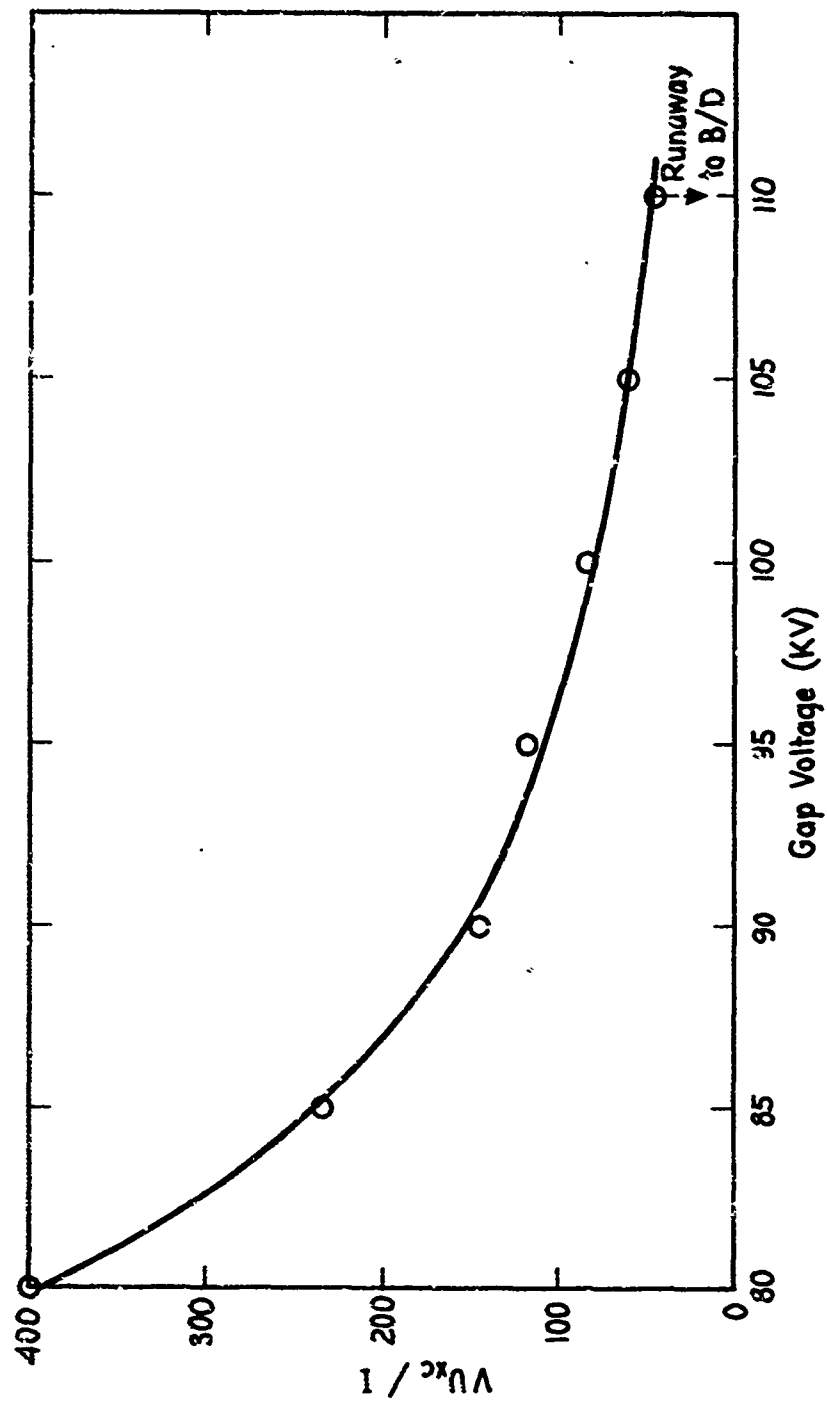
Figure 6-11. Variation of Effective Interelectrode Gas Density
Calculated from Experimental Results
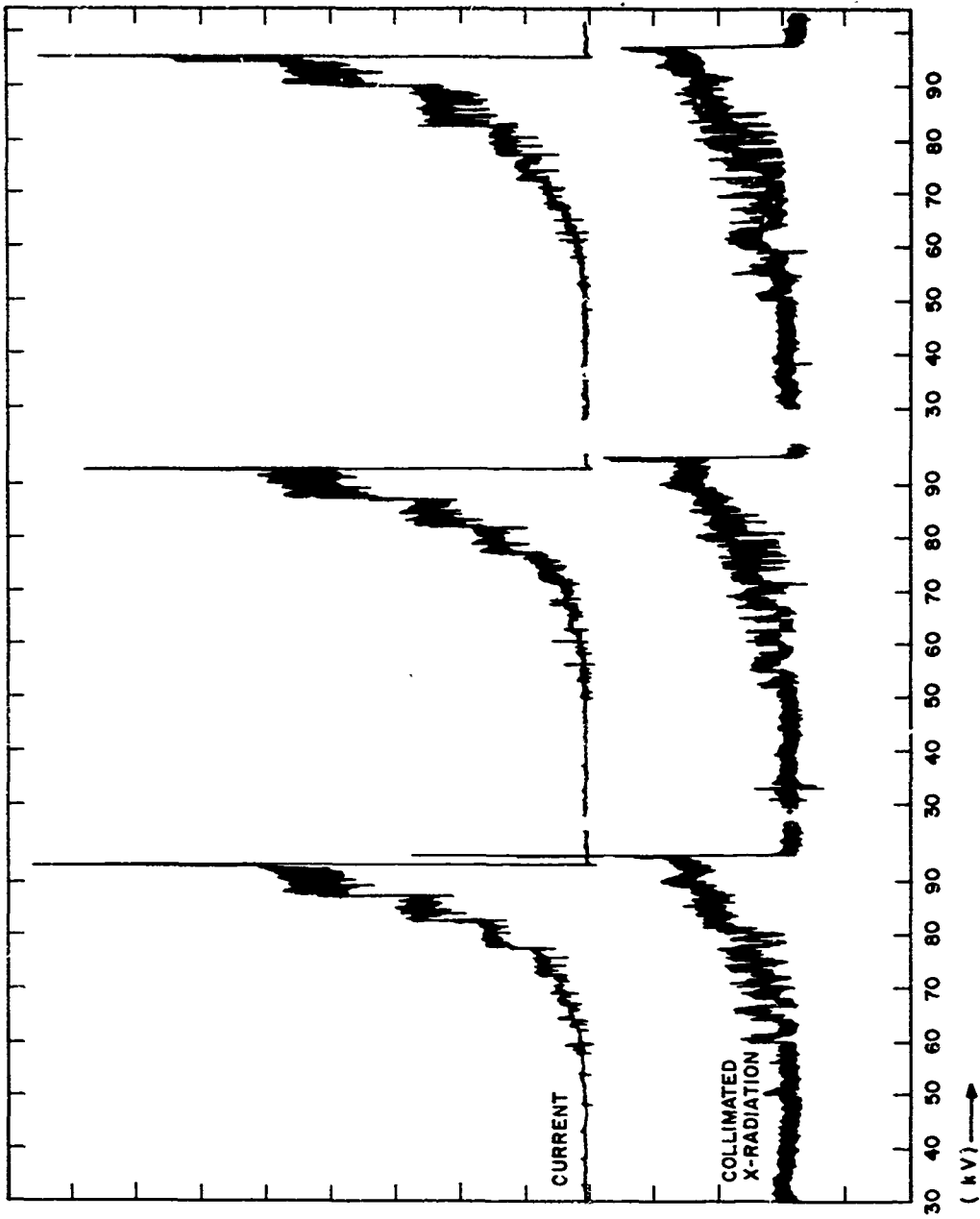
Figure 6-10. Current and Collimated X-Radiation as a Function of Voltage for Three Consecutive Step Tests

1-1391

Light intensity was monitored under these conditions as it increased stepwise with voltage together with X-ray intensity (Figure 6-12). At higher voltages, both X-radiation and light output rose at constant voltage as well as the light output per unit current. Since the light growth occurs during the gas evolution phase, it seems most likely due to gas luminescence. Transition radiation would also appear, but it cannot explain the increase in light output per unit current which would have to remain fixed at constant voltage.

This gradual increase at constant voltage of all of the measured parameters, total and collimated X-radiation, hydrogen partial pressure and light output, was found to increase steadily during the last few voltage increments of 1 kV or less prior to breakdown. The phenomenon has been termed "runaway".

Reduction of the voltage by up to 10% was found to be insufficient to arrest this regenerative process which may take many seconds to complete (see Figure 6-13), the apparent fall in X-ray level is due to scintillator saturation). Breakdown voltages were very reproducible when voltage was applied in 5, 10 or 25 second intervals, but a conditioning effect took place. Experiments with 2.5 mm and 5 mm gaps established that the breakdown voltage varies approximately as the square root of the gap separation.

6.6   Conclusions

From this work, it appears that only under restricted conditions is there a nondestructive criterion for incipient breakdown of vacuum gaps. Nonetheless, the techniques developed and enumerated below are of value in permitting the vacuum gap to be completely described prior to and during breakdown. Thus, current or total X-radiation monitoring each give information on the state of the cathode surface and on microdischarge activity. Collimated X-radiation gives the total residual gas or vapor pressure in the gap with a rapid response time and is complemented by mass spectrometry which yields only chamber pressure but can resolve gas constituents. A steady uncontrolled runaway is indicated by the total and collimated X-radiation measurements under restricted conditiond. Visible radiation intensity monitoring indicates

6-18
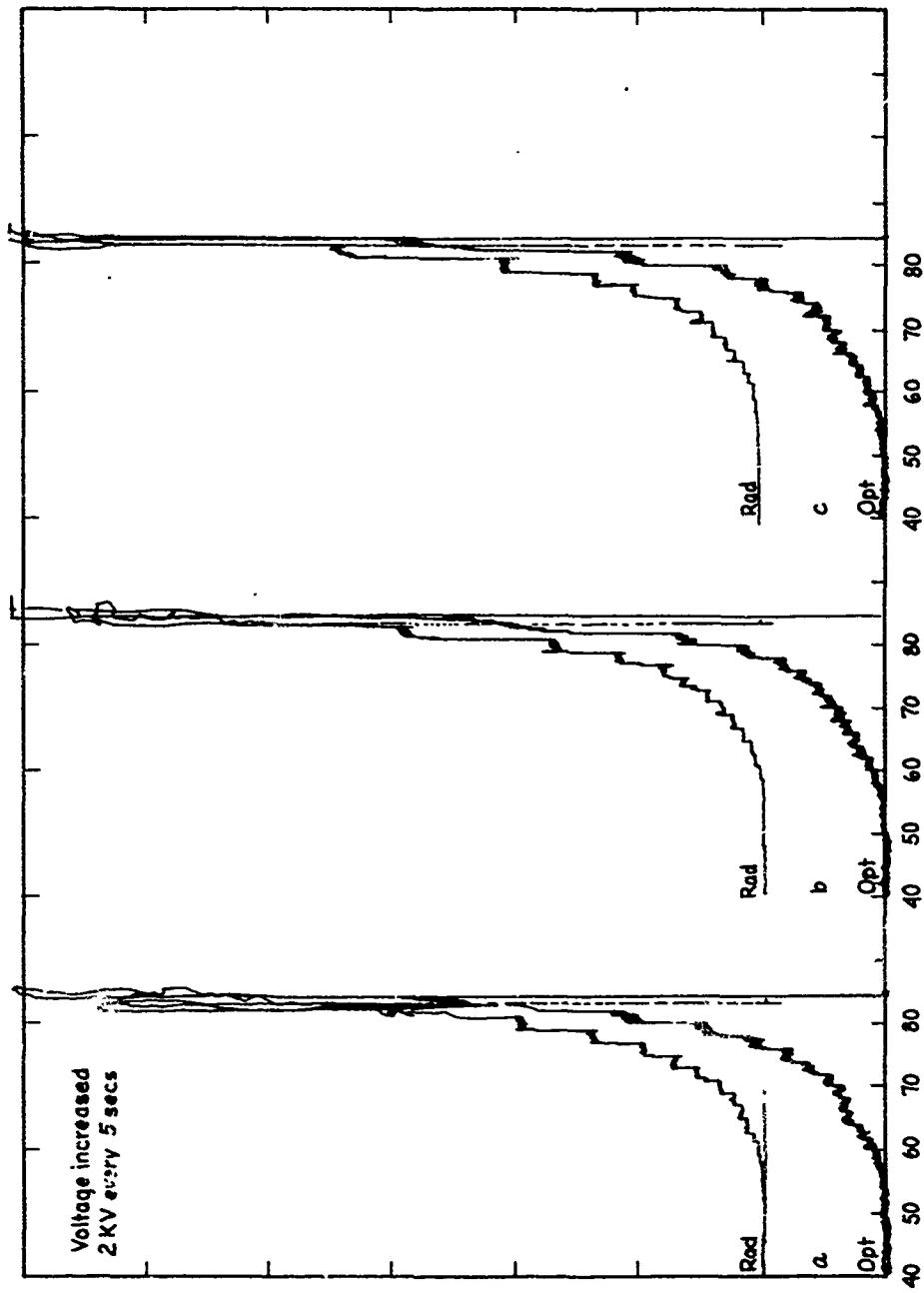
Figure 6-12. Typical Recordings of Visible and X-Radiation (2.5 mm Gap)

1-1385
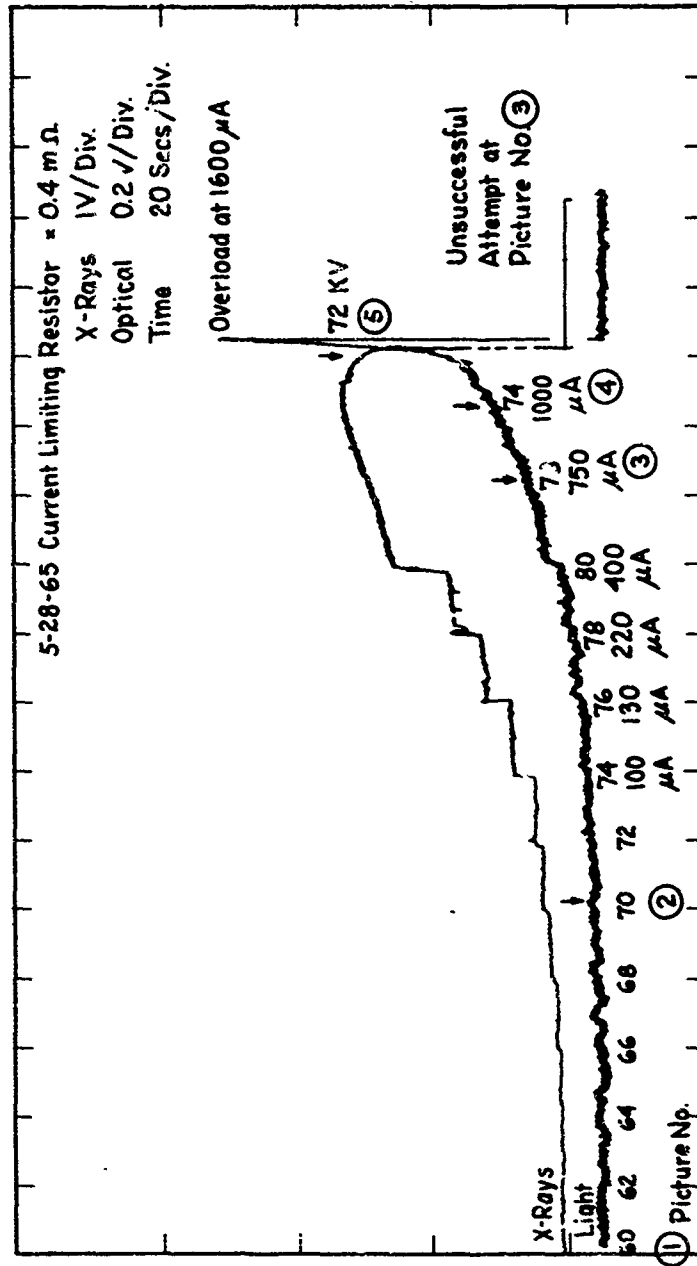
Figure 6-13. Visible and X-Ray Recording Demonstrating Runaway

1-1388

the kind of thermal balance at the anode under electron bombardment and is a sensitive means of studying the gradual runaway of field enhancement to breakdown. Oscillographic monitoring of current pulses yields data on microdischarges and on runaway phenomena preceding breakdown. Mass spectrometry yields total chamber pressure with resolution of the individual components and thus identifies the gases released and their partial pressures during voltage application. Additionally procedures were developed for fabrication and cleaning of electrodes and a transfer of the electrodes in a controlled environment to the vacuum test. In conclusion, the preliminary program was successful in yielding data from which the steps leading up to breakdown were identified. Prebreakdown phenomena associated only with unbaked electrodes were studied, and the principal conclusions derived from this program could be summarized as follows.

(1) A conditioning technique has been developed which does not involve sparking and consequent electrode damage. The technique has been compared with the more conventional spark conditioning method and the decrease in gap strength by sparking has been measured.

(2) Microdischarge phenomena have been studied and the results largely verify the work of previous investigators. In addition, an associated rise in the partial pressures of residual gases has been studied.

(3) Microdischarge activity has been shown to lead to field enhancement at the cathode and Fowler-Nordheim field emission occurs from a variety of sites. Discontinuities in current changes as a function of voltage are believed to be due to the disappearance of some sites.

(4) X-rays are produced by microdischarges and by field emitted electrons. Photons can be generated in the gas or vapor released into the interelectrode space as well

6-21

as from the anode as a target. The X-rays produced
by field emission yield equivalent Fowler-Nordheim
plots.

(5)   At high potentials the enhancement factor grows at con-
      stant voltage and can run away to breakdown. Small
      reductions of voltage will only delay the breakdown after
      growth has proceeded.

(6)   Visible radiation from the gap is consistent with a model
      comprising anode hot spots which are cooled by conduc-
      tive heat transfer. The anode temperature rises rapidly
      during runaway and there is no evidence of boiling for
      the gap separations studied. Intensity variation is not
      fully understood over the whole range.

(7)   Collimated X-radiation monitoring and mass apectrom-
      etry show that there are both pulsed and continuous
      changes in interelectrode gas density prior to break-
      down. The gas appears to be hydrogen which probably
      diffuses out from the anode when it is heated sufficiently
      by electron bombardment.

(8)   Gap failure can occur under two separate circumstances.

      (a)   When gas pressure rise due to microdischarges
            becomes too great.
      (b)   After surface etching and the runaway of the field
            enhancement factor.

      In case (b) the buildup of hydrogen density in the gap may
      also be the cause of breakdown since it seems to be
      always associated with it. A mechanism can be con-
      ceived in which the electron beam current runaway leads
      to hydrogen diffusion into the gap.

Baked out electrodes would presumably not be subject so much to this effect but totally vacuum melted metal electrodes would be much less so. Hence the known high vacuum breakdown strength of electrodes fabricated from titanium (which is refined by vacuum melting) may be explained in this way.

(9) The breakdown voltages at runaway are consistent and the conditioned breakdown voltages appear to be approximately proportional to the square root of the gap separation.

SECTION 7
SEVEN FACTOR PILOT EXPERIMENT

7. 1   Introduction

In applying factorial design to experiments on vacuum breakdown it was decided to conduct initially a two level, seven factor pilot experiment. This experiment should show that all factors are under adequate control and provide information on the effect of varying the most likely factors and in particular on the importance of system bakeout. A one-fourth fractional factorial design involving 32 runs or treatments was chosen. From this the importance of all factors and most two factor interactions can be determined.

The main objectives of the experiment were to:

(1)   Compare complete system versus electrode only bakeout both as to breakdown voltage and reproducibility of breakdown level.

(2)   Determine the effect of surface finish, viz, how much improvement in withstand voltage is attained by highly polishing electrodes.

(3)   Compare electrode materials: other programs carried out by IFC indicated the potential improtance of Ti-7 Al 4Mo as an electrode material for vacuum insulation. This is compared with a common electrode material such as copper.

(4)   Commission and troubleshoot the 300 kV apparatus.

(5)   Gain familiarity with running a large scale factorially designed experiment.

(6)   Optimize procedures for this experiment to maintain control over the relevant parameters for the complete duration of the test.

(7)   Further clarify and understand the mechanism of vacuum
        breakdown.

7.2   Experimental Design

The factorial design as given in Table 7-1 investigates seven factors
which were chosen after consideration of field emission dependent processes,
clump mechanisms, and microdischarge effects. These factors were judged to
be the most likely ones of importance and would, at two levels each, require
2^7 or 128 treatments for a full factorial investigation. To reduce the number of
treatments a one fourth fractional factorial design was used which gives inde-
pendent and balanced estimates of all the main effects and of all of the two
factor interactions except AB, CE, AC, BE, AE and BC. Thus the bakeout
factor D is estimated without confounding with any main effect or any two factor
interaction. Complete specification of each of the 32 individual experiments or
treatments is given in Table 7-1. The order of experimentation (see Table 7-1)
was randomized to minimize any "historical" error.

Experimental procedures were developed for electrode preparation,
installation, bakeout and testing so that the levels of the factors would be stan-
dardized and any other pertinent parameters would be held invariant. Essential
details of procedure and test sequence are given in Table 7-1.

7.3   Breakdown Voltage

Typical variation of breakdown voltage with gap and conditioning is
given for a single treatment in Figure 7-1. An orderly change with gap and
conditioning is indicated with an approximately square root dependence on gap.
A complete tabulation of breakdown voltage is given in Table 7-2.

Factorial analysis was carried out according to Yates Algorithm
on a time-sharing computer for the gaps at which complete data was available.
The initial results showed a consistent ranking of certain factors. However,
because of the high apparent error indicated by the half normal plots, as in
Figure 7-2, there was doubt as to which were most significant.

Table 7-1. Experimental Design - Pilot Experiment

	Factor	High Level	Low Level
A	Anode Material	OFHC Copper	Ti - 7 Al - 4 Mo
B	Cathode Geometry	Bruce Profile	Sphere
C	Cathode Material	OFHC Copper	Ti - 7 Al - 4 Mo
D	Bakeout	Electrode Bakeout Only	Complete System Bakeout
E	Anode Geometry	Bruce Profile	Sphere
F	Anode Finish	0. 05 Micron Polish (Fine)	600 Grit SiC (Coarse)
G	Cathode Finish	0. 05 Micron Polish (Fine)	600 Grit SiC (Coarse)

Bakeout: Chamber 8 hours at 375°C; Electrodes 12 hours at 425°C

Electrodes: 3 inch diameter, cleaned with water, methyl alcohol, acetone, and trichloro-ethylene.

Pressure: Low 10^{-7} torr to mid 10^{-8} torr for Electrode only bakeout, Low 10^{-8} torr for complete system bakeout.

Voltage Application: 10 kV steps every 2 minutes from well below breakdown.

Variables Monitored: Voltage: Gap Current (Prebreakdown); Total and Collimated X-Radiation Optical Radiation, Total and Partial Pressures

Test Sequence:

Initial Series: 3 breakdowns at 1. 0 cm gap, then 1 breakdown at 1. 5. 2. 0, 2. 5, 3. 0 and 0. 50 cm gaps.

Rapid Conditioning: At 1. 0 cm repeated sparking until the breakdown voltage is increased by ~ 30 %.

Final Series: 1 Breakdown at 1. 0, 1. 5, 2. 0, 3. 5, 3. 0 and 0. 50 cm gaps

Specification and Order of Treatments:

Factor	C	G	E	D	A	F	E
Treatment	Cathode Material	Cathode Finish	Cathode Geometry	Bakeout	Anode Material	Anode Finish	
bdefg	Ti	Fine	Bruce	Electrode	Ti	Fine	Bruce
abdf	Ti	Coarse	Bruce	Electrode	Cu	Fine	Sphere
ig	Ti	Fine	Sphere	System	Ti	Fine	Sphere
adcfg	Ti	Fine	Sphere	Electrode	Cu	Fine	Bruce
bcd	Cu	Coarse	Bruce	Electrode	Ti	Coarse	Sphere
ade	Ti	Coarse	Sphere	Electrode	Cu	Coarse	Bruce
ab	Ti	Coarse	Bruce	System	Cu	Coarse	Sphere
beg	Ti	Fine	Bruce	System	Ti	Coarse	Bruce
bef	Ti	Coarse	Bruce	System	Ti	Fine	Bruce
acf	Cu	Coarse	Sphere	System	Cu	Fine	Sphere
abcdeg	Cu	Fine	Bruce	Electrode	Cu	Coarse	Bruce
cu	Cu	Coarse	Sphere	System	Ti	Coarse	Bruce
abfg	Ti	Fine	Bruce	System	Cu	Fine	Sphere
bcf	Cu	Coarse	Bruce	System	Ti	Fine	Sphere
abdg	Ti	Fine	Bruce	Electrode	Cu	Coarse	Sphere
cdeg	Cu	Fine	Sphere	Electrode	Ti	Coarse	Bruce
bde	Ti	Coarse	Bruce	Electrode	Ti	Coarse	Bruce
dg	Ti	Fine	Sphere	Electrode	Ti	Coarse	Sphere
acd	Cu	Coarse	Sphere	Electrode	Cu	Coarse	Sphere
abce	Cu	Coarse	Bruce	System	Cu	Coarse	Bruce
aeg	Ti	Fine	Sphere	System	Cu	Coarse	Bruce
abcfg	Cu	Fine	Bruce	System	Cu	Fine	Bruce
bcdfg	Cu	Fine	Bruce	Electrode	Ti	Fine	Sphere
acg	Cu	Fine	Sphere	System	Cu	Coarse	Sphere
aef	Ti	Coarse	Sphere	System	Cu	Fine	Bruce
(1)	Ti	Coarse	Sphere	System	Ti	Coarse	Sphere
cdef	Cu	Coarse	Sphere	Electrode	Ti	Fine	Bruce
acdfg	Cu	Fine	Sphere	Electrode	Cu	Fine	Sphere
abcdef	Cu	Coarse	Bruce	Electrode	Cu	Fine	Bruce
cefg	Cu	Fine	Sphere	System	Ti	Fine	Bruce
df	Ti	Coarse	Sphere	Electrode	Ti	Fine	Sphere
bcg	Cu	Fine	Bruce	System	Ti	Coarse	Sphere
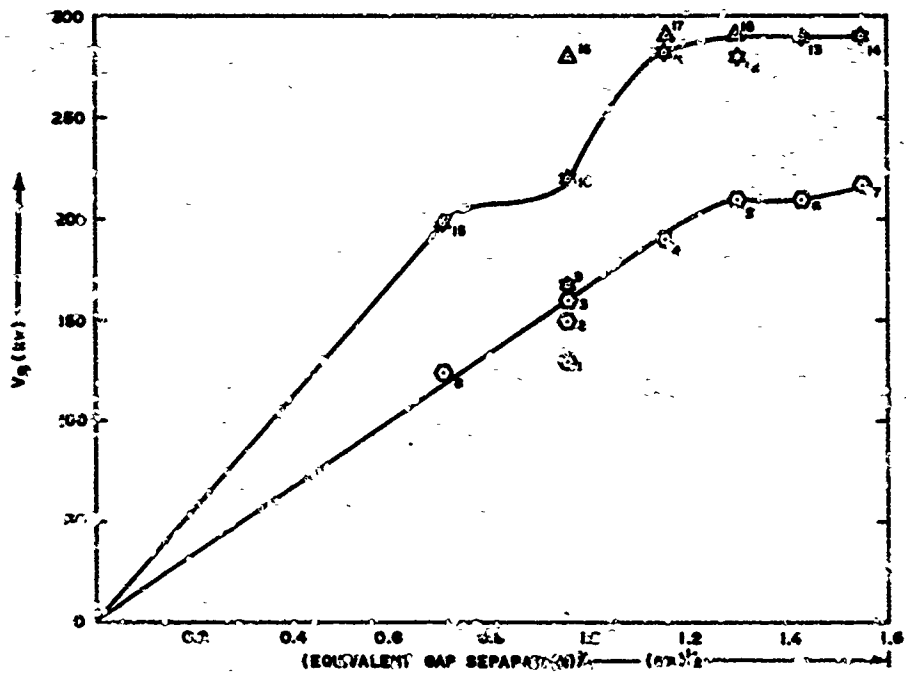
Figure 7-1. Sequence of Breakdowns for Treatment 'acg'
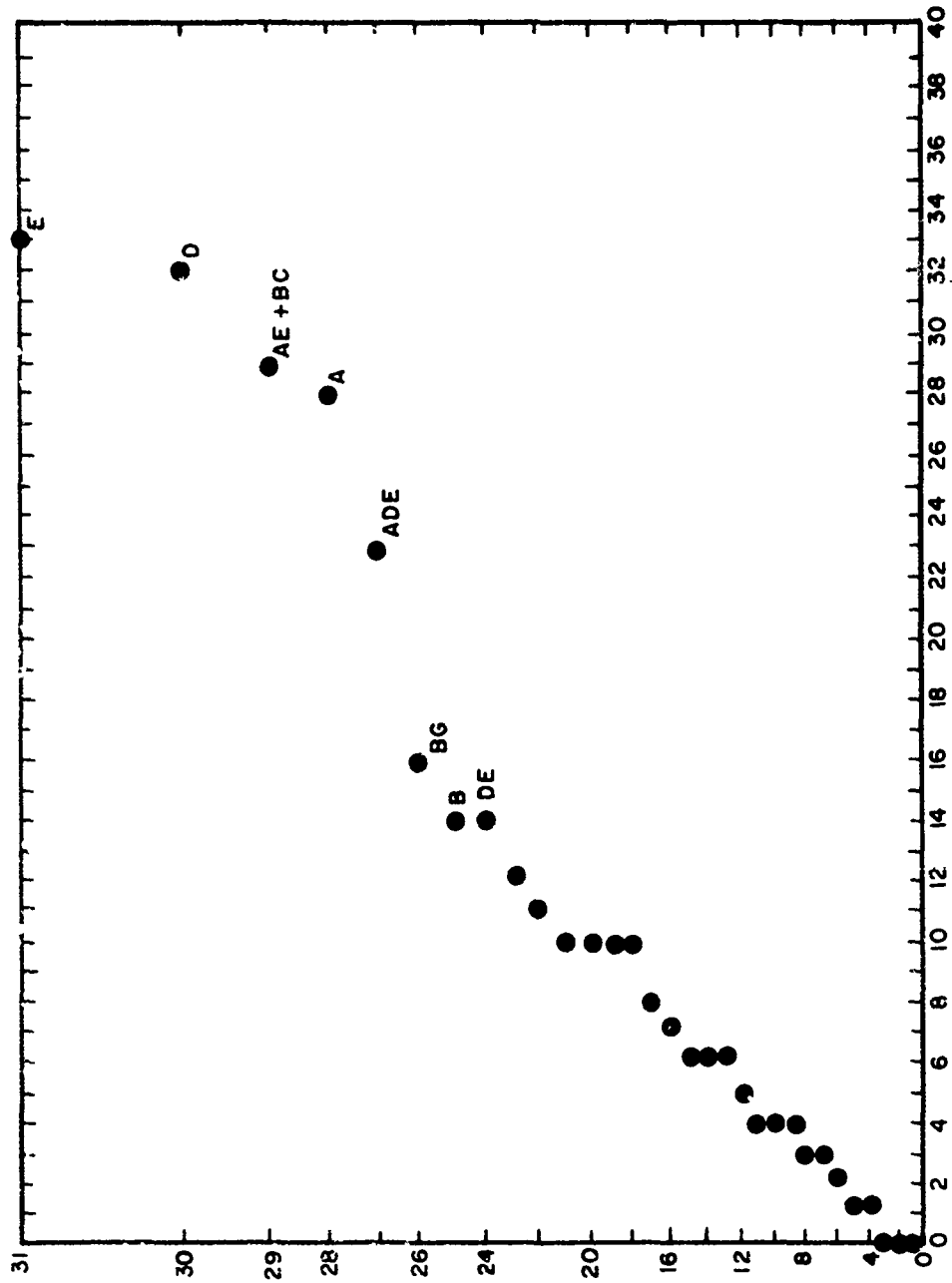
Figure 7-2. Half Normal Plot for 2.0 cm Conditioned Gap

Table 7-2. Breakdown Voltage for Pilot Experiment

Breakdown Order	Initial Series							Final Series (After Conditioning at 1.0 cm)					
Gap (cm)	0.50	1.0		1.5	2.0	2.5	3.0	0.50	1.0	1.5	2.0	2.5	3.0
Treatment	8	1	3	4	5	6	7	25	10	11	12	13	14
bdefg	130	130	150	170	178	220	240	>134	222	242	240	256	257
abdf	120	119	115	177	187	190	200	120	195	235	240	234	228
fg	149	140	172	199	270	260	290	180	286	280	280	>300	>300
adefg	109	120	160	177	190	200	191	>96	>160	190	210	221	220
bcd	124	110	130	150	160	160	160	126	186	210	240	250	220
ade	110	160	170	187	190	210	268	110	179	180	200	200	220
ab	106	169	200	230	217	212	196	>105	>222	280	309	320	>320
beg	74	150	150	210	240	290	300	>116	230	280	290	>320	>320
bef	100	116	160	148	220	250	250	120	170	220	270	260	260
acf	120	130	198	172	230	230	280	190	120	290	310	310	>320
abcdeg	130	150	160	177	188	201	205	120	202	223	229	230	241
ce	120	123	185	210	228	230	260	127	240	260	270	290	280
abfg	190	113	170	210	230	260	280	158	210	250	300		
bef	120	108	194	220	240	240	275	150	234	246	240	233	280
abdg	106	110	150	187	207	220	235	>139	199	220	200	260	220
cdeg	120	130	153	210	230	230	250	130	222	247	220	220	239
bde	80	120	138	156	165	160	170	140	210	210	211	238	226
dg	110	130	180	175	195	205	216	140	256	257	255	237	200
acd	135	175	180	203	210	220	225	144	208	240	241	190	>240
abce	60	80	116	120	148	160	170	90	164	160	185	250	228
aeg	99	100	168	210	220	240	256	>120	242	200	210	207	290
abcefg	65	85	110	120	120	130	133	90	178	190	190	280	260
bcdfg	140	180	170	183	202	215	228	150	247	250	237	290	300
acg	123	129	160	190	210	210	229	199	220	282	280	220	280
aeg	130	89	170	200	229	230	247	>114	200	250	290	310	290
(1)	130	144	220	231	256	280	280	176	250	277	286	310	300
cdef	134	137	150	165	160	186	200	131	230	287	220	300	280
acdfg	148	179	195	210	209	220	192		230	287	220	227	227
abcdef	100	130	140	149	157	161	166	98	>180	>180	220	160	170
cefg	107	100	146	170	210	260	287	>187	180	160	160	280	280
df	120	146	160	180	238	239	247	170	260	259	270	281	282
bcg	110	140	169	170	180	217	230	117	220	260	270	306	280

In order to obtain smoothed measurements of the breakdown voltage which would allow more accurate estimates of the effects of the factors under study a breakdown law of the form:

$$V_B = Kd^{1/2}$$

was assumed and average values of the slope K were calculated from the conditioned results at 1.0, 1.5 and 2.0 cm. This manipulation was successful in that deviations from linearity appeared in a half-normal plot of the factorial estimates as given in Figure 7-3.

Based on this technique and consistency in rank the following conclusions may be drawn:

(1)   The most significant factors are anode material A, anode shape E, cathode shape B, bakeout D, and the interaction AE + BC.

(2)   Complete system bakeout gives higher breakdown voltages than electrode only bakeout.

(3)   Spherical geometry for either anode or cathode or both gives higher breakdown voltages than Bruce profile geometry (plane).

(4)   Cathode material is important for unconditioned gaps and anode material for conditioned gaps, in both cases Ti-7Al-4Mo gives higher breakdown voltages than OFHC copper.

7.4   Prebreakdown Phenomena

Prebreakdown current was measured at each voltage step up to breakdown. In general, the logarithm of the current as a function of voltage indicated both deviations from the simple Fowler-Nordheim law and a dependence upon the amount of conditioning.
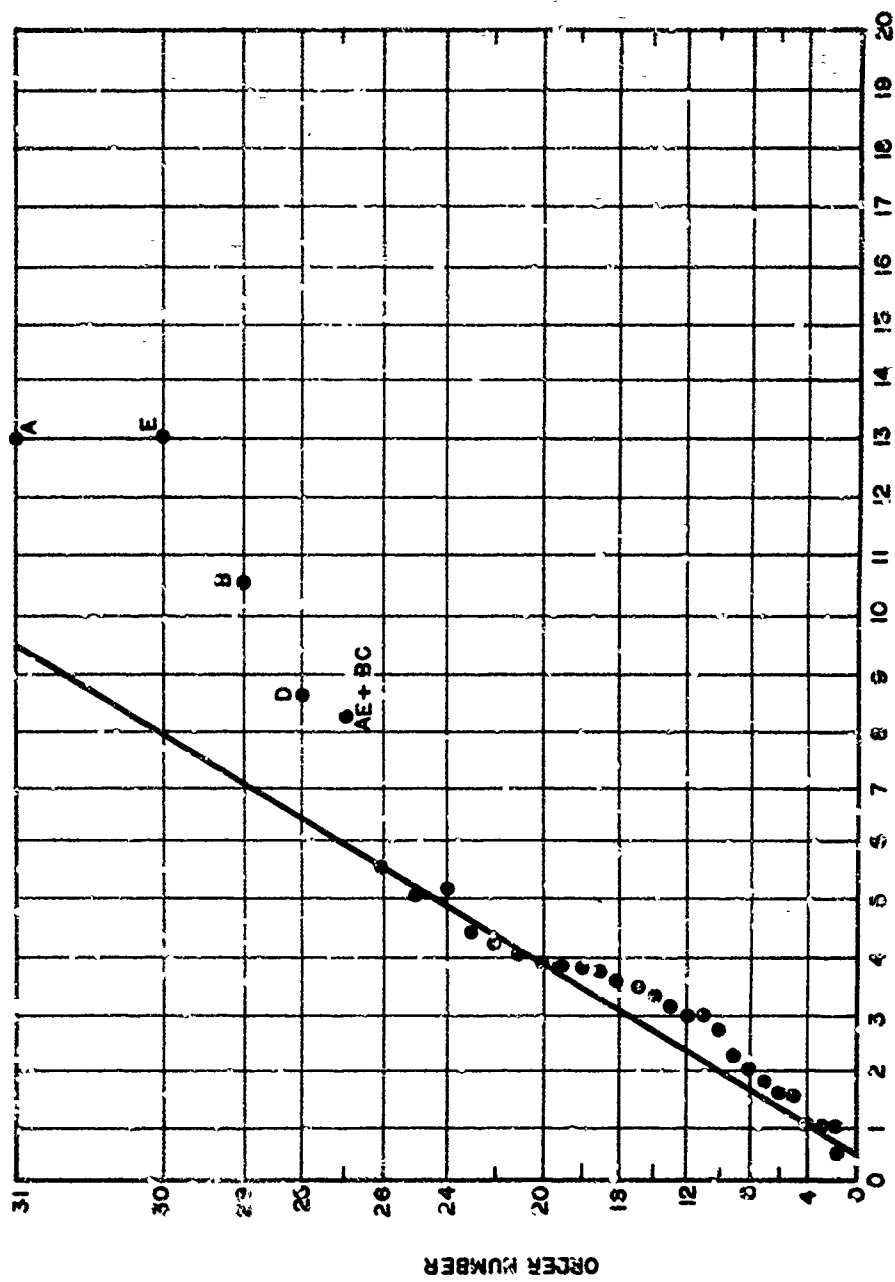
Figure 7-3. Half-Normal Plot of Smoothed Results - Conditioned Electrodes

1-2011

During the early stages of the program certain treatments (later repeated for factorial consistency) were tested for breakdown voltage by ignoring "isolated" breakdowns at a certain gap and raising the voltage until breakdowns appeared in rapid succession. Using this technique, it was found that breakdown voltage increased quite accurately with the square root of the gap. At the same time the logarithm of the last measurable prebreakdown current decreased according to the square root of the gap. Figure 7-4 for uniform field electrodes shows this effect. In this case, if the Fowler-Nordheim law is assumed:

$$I = A \left(\beta \frac{V}{d}\right)^2 \exp \left(- \frac{Bd}{\beta V}\right)$$

and if the breakdown voltage obeys a square root law:

$$V_B = Kd^{1/2}$$

Then it follows that:

$$\log I = \log A + 2 \log \left\{\frac{\beta^2 K^2}{d}\right\} - \frac{Bd^{1/2}}{\beta d}$$

Thus, log I at breakdown decreases linearly with $d^{1/2}$ provided that the second term can be neglected, the emitting area A is constant, and that B (governed by the electron tunneling probability) is constant.

For spherical electrodes similar behavior was found, except that corrections had to be applied to d so that cathode field strength would still be given by $E = V/d$. Thus, Figure 7-5 employing an equivalent gap separation demonstrates a good fit to square root dependence. Consequently, it appears that breakdown voltage is influenced by cathode curvature through the effect of this upon prebreakdown current.
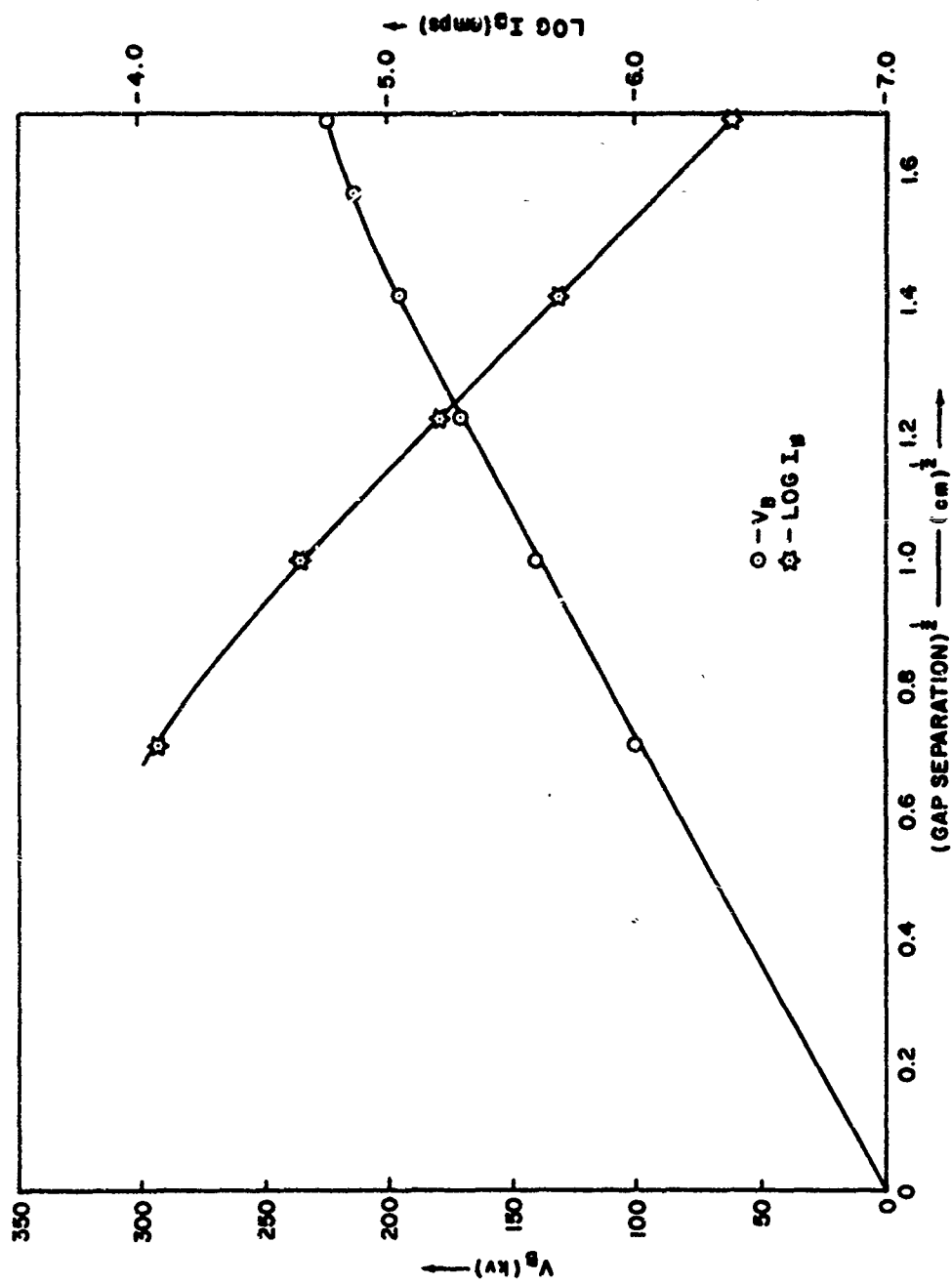
Figure 7-4. The Square Root Law for Treatment abcdeg
(Cu-Bruce-Cu Bruce)

1-1636
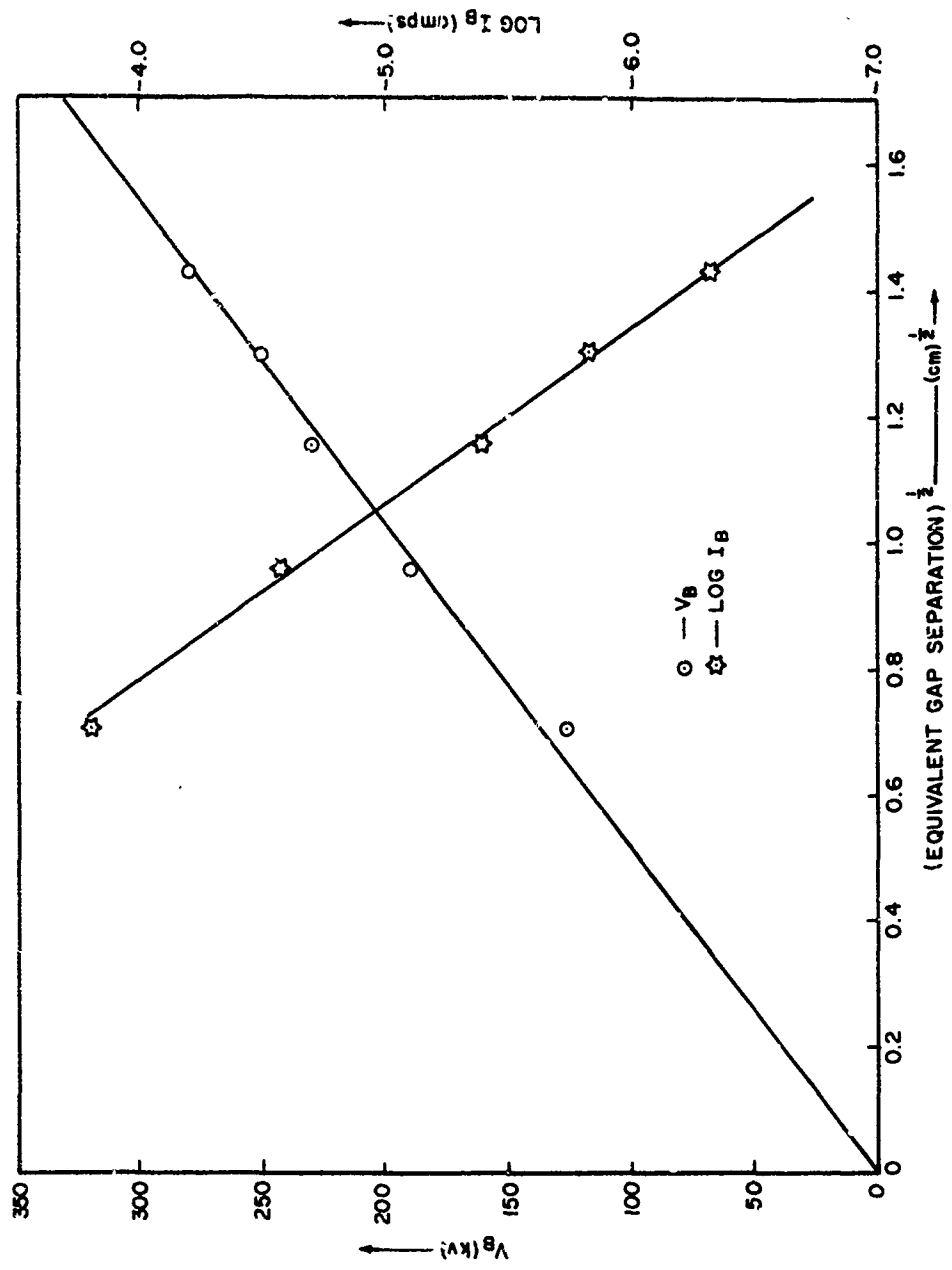
Figure 7-5. The Square Root Law for Treatment acf
(Cu-Sphere-Cu Sphere)

1-1637

It is to be emphasized that the above behavior was explored with repeated breakdowns at each gap setting. With the sequence specified for the factorial experiment it was necessary to repeat the gap cycle several times to get even an approximate fit to the square root relationship between gap and the final prebreakdown current and breakdown voltage.

7.5   Effect of Breakdown on Electrode Surfaces

After testing, each set of electrodes was microscopically examined and interesting details photographed. While the range of gaps used renders interpretation of typical dimensions difficult, there are features of general nature worth noting.

The most spectacular result of attack, shown in Figure 7-6, is the deposit of anode material on the cathode surface. This apparently, is caused by a breakdown which ejects a surface layer of anode material previously rendered molten by a localized cathode beam. The ejected material splatters onto the relatively cold cathode surface and solidifies almost instantaneously but not before it spreads out into a shallow crater formation. The centers of many of these splatters show varying degrees of structure. Splatters are normally seen when the anode is copper but rarely seen when it is the titanium alloy. Even when seen, the titanium splatters are very small.

Attendant with the more severe splatter deposits is a definite vacuum evaporated coating of the anode material. This coating has been noticed only when copper was the anode material. It occurs near the center of the most heavily splattered area on the cathode and is easily removed by abrading with a sharp metal instrument. Significant evaporation indicates that the copper surface reaches a temperature of approximately 1273°C. [1] The comparable temperature for titanium is 1546°C at which point the vapor pressure reaches 10 microns of mercury.

Both copper anodes and titanium alloy anodes are severely attacked as seen by the dark area in Figure 7-7 and the convoluted surface in Figure 7-8 for the respective materials. It is most likely that the splatters are expelled from areas such as these.
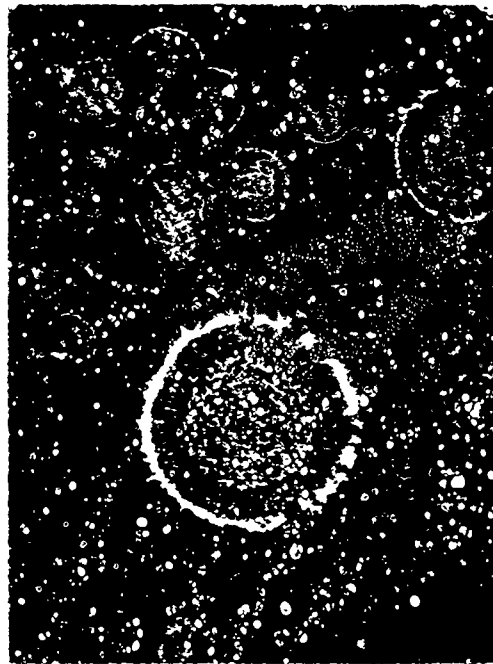
Figure 7-6. Copper Splatters on Titanium Alloy Cathode
Magnification: 500 X

2-513

Figure 7-7. Severe Attack on Copper Anode
Magnification: 50 X
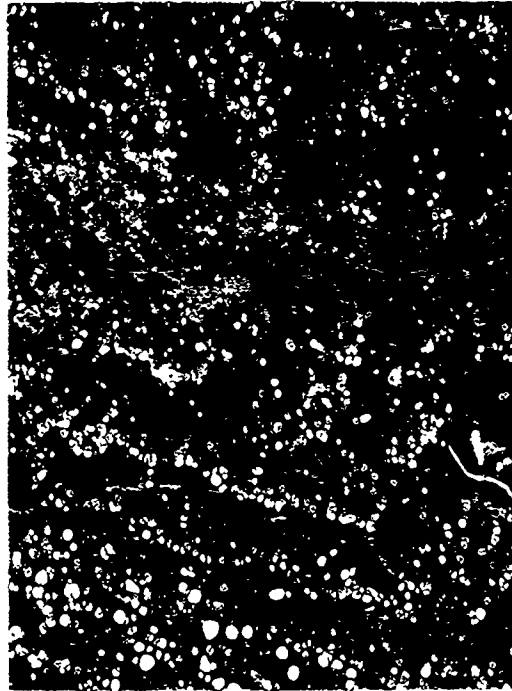
Figure 7-8. Severe Attack on Titanium Alloy Anode
Magnification: 150 X

2-517

Anode attack grades down to microstructural delineation in the form of grain boundaries for copper and revelation of the alpha-beta structure of the titanium alloy as shown in Figure 7-9 for the fine surface finish. Light attack on the coarse finish takes the form of smoothened abrasive marks.

7.6   Conclusions

The trends appearing in the factorial analysis add to and confirm the theory[2] of vacuum breakdown which was developed during this study. Prebreakdown current measurements and observation of gas released prior to breakdown further support the hypothesis that a beam of field emitted electrons heats up the anode to a temperature at which gas is evolved copiously into the gap. The gas accumulates on the beam axis at an average density depending on both the electrode geometry and gap separation. Ionization by the primary beam then leads to an unstable condition producing breakdown. The total ionization depends on the product of gas density along the beam and gap separation in a manner depending on the field distribution.

In consequence of this, the factors expected to be of significance would be anode material, bakeout, shape of both electrodes, and gap separation, all of which figure prominently in the results of this pilot experiment.

An interesting point is that anode material appears as a prominent single factor for conditioned electrodes, but appears only as an interaction with bakeout for the unconditioned case. Conditioning is pictured in the present theory to be the process of removal of gas from the surface layers on the anode with the consequent establishment of a density gradient which then governs the rate of gas evolution. The precise gradient will depend on the diffusion coefficient of the anode material, hence its appearance as a factor in this case. Before conditioning, however, the density of sorbed gas at the surface will be the main factor which is more a function of bakeout.

Electrode geometry and gap separation effect the pumping conductance, electric field distribution and ionization efficiency simultaneously. In the next experiment, this ambiguity is expected to be removed by studying uniform field electrodes only, thus removing the electrode shape as a factor.

Figure 7-9. Alpha-Beta Microstructure Revealed by
Electron Bombardment
Magnification: 200 X

2-519

In a practical sense the highest breakdown voltages are obtained with curved (spherical) rather than plane (Bruce profile) electrodes. Ti-7Al-4Mo has been shown to be superior to OFHC copper, with anode material being more important. Bakeout of the entire system gives higher breakdown voltages than electrode only bakeout. Electrode surface finish did not emerge as a significant factor, leading to the conclusion that 600 grit finish is adequate.

7.7   Recommendations

- Electrode Material

  The titanium alloy Ti-7Al-4Mo is a very promising electrode material. Both it and other materials of the same family are recommended for tube electrodes.

- Electrode Finish

  Six hundred grit finish is good enough for electrodes in vacuum environments. A higher polish appears to buy no significant improvement in the way of increased voltage hold-off and merely adds to the time and cost factors in tube production.

- Electrode Geometry

  If the choice is available spherical or similarly curved electrode geometries should be used, rather than plane uniform field.

- System Bakeout

  For reliability, less scatter and higher withstand voltages it is desireable to bake out the complete system. Time and temperature of the bakeout may be chosen to suit specific needs but 400 °C for six hours appears reasonable and may be used as a general guide. A separate study in a high temperature chamber would establish more clearly the guidelines for recommended bakeout cycles.

7-18

SECTION 8
BLOCK OF EIGHT EXPERIMENT

8.1   Introduction

Statistical analysis of the pilot experiment indicated that, consistently throughout the conditioning history of a pair of electrode, the decisive factors in determining breakdown voltage were anode material, electrode shapes, and bakeout. High apparent error in the pilot experiment indicated that a factor was not under full control. This appeared most likely to be the gas content of the electrodes, in ·greement with a theoretical model in which evolution of hydrogen just prior to breakdown plays a significant role. Observation of pressure surges with a mass spectrograph in both the preliminary and pilot experiment further supported this theory. It would appear that hydrogen is evolved by electron beam heating of the anode, releasing gas which accumulates in the gap and ionizes at a rate dependent on the gap distance, electrode geometry and applied voltage.

Thus, the next experiment, called the Block of Eight, was designed with the primary objective being to check the role that evolution of hydrogen from the electrodes plays in determining the breakdown voltage. This was accomplished by controlling the hydrogen level in cathode or anode at one of two levels by prefiring in either hydrogen or vacuum at 900°C for 6 hours. OFHC copper was chosen as a material typical of high voltage vacuum tubes. Uniform field geometry (Bruce profile) and two sizes of electrodes provided a simple variation in pumping conductance which would influence accumulation of gas in the gap. The basic design and an outline of experimental procedure appears in Table 8-1. The entire system was baked at 400°C prior to testing, this further assured control of gas level.

The test sequence first explored a series of gaps in two conditioning cycles, then the effect of a 250 gauss transverse magnetic field was investigated over a series of gaps, and finally the effect of various levels of transverse magnetic field at several gaps was explored.

Table 8-1. Experimental Design - Block of Eight

		High Level	Low Level
Factors	A Anode Processing	Vacuum Firing	Hydrogen Firing
	B Cathode Processing	Vacuum Firing	Hydrogen Firing
	C Electrode Size	4 inch diameter	1.28 inch diameter

Electrode Material: Certified OFHC Copper.

Firing: 900°C for 6 hours

Electrode Geometry: Bruce Profile - Uniform Field

Surface Finish: 600 Grit Silicon Carbide Paper

Bakeout: Entire System at 400°C for 6 hours.

Voltage Application: 10 kV steps every 2 minutes from well below breakdown.

Variables Monitored: Voltage, Prebreakdown Current, Breakdown Voltage Collapse and Current Pulse, Pressure.

Test Sequence:

Initial Series: 3 Breakdowns at 1.0 cm, then 1 breakdown each at 1.25, 1.50, 1.75, 2.0, 2.25, 2.50, 2.75, 3.0, 0.75, 0.50, 0.25, 1.0, 1.25, 1.50, 1.75, 2.0, 2.25, 2.50, 2.75, 3.0, 0.75, 0.50, 0.25, 1.0 cm for a total of 27 breakdowns

Magnetic Field Series: Breakdowns Without, With, and Without 250 gauss Transverse Magnetic Field at gaps of 1.0, 1.5, 2.0, 2.5, 3.0, 0.50 cm.

Magnetic Field at 4 Levels: Gaps of from 1.0 to 3.0 cm with Transverse Magnetic Field Levels from 0 to 250 guass.

Specification of Treatments

	Anode Processing	Cathode Processing	Electrode Size	Date Tested
1	H_2	H_2	1.28 inch	3/27/67
a	Vacuum	H_2	1.28 inch	5/9/67
b	H_2	Vacuum	1.28 inch	5/6/67
ab	Vacuum	Vacuum	1.28 inch	4/24/67
c	H_2	H_2	4 inches	3/30/67
ac	Vacuum	H_2	4 inches	5/3/67
bc	H_2	Vacuum	4 inches	6/20/67
abc	Vacuum	Vacuum	4 inches	5/15/67

8.2   Breakdown Voltage

Breakdown voltage was found to depend on gap conditioning, anode gas level, cathode gas level, electrode size, and transverse magnetic field in a complex manner with many significant interactions. For example, the effect of electrode gas content is strongly dependent on electrode size. For this reason only a detailed reporting of results can accurately describe the experiment.

Tables 8-2 and 8-3 give the breakdown voltages for each treatment for the major conditioning sequences. These results, when subjected to standard factorial analysis according to Yates' Algorithm, yield the estimates of the mean, main effects, and interactions as given in Tables 8-4 and 8-5. Further detail is provided by Table 8-6 which gives the comparisons between treatments which are physically appropriate.

The major conclusions from this data and factorial analysis are:

(1)   Gap: Breakdown voltage varies approximately as the square root of the gap distance for gaps greater than 0.75 cm. While single treatments may not follow this exactly, the overall average breakdown voltage (u) fits very well as shown in Figure 8-1.

(2)   Conditioning: Breakdown voltage increases considerably as a result of the twelve breakdowns intervening between two breakdowns at a certain gap. This beneficial conditioning is more rapid at first than later as shown by the decreasing slope of the curves of Figure 8-1. For the prime gap of 1.0 cm the overall average conditioning effect of 26 breakdowns was 231% (61 kV to 139 kV).

(3)   Transverse Magnetic Field: The usual effect of applying a 250 gauss transverse magnetic field at gaps greater than 0.75 cm was to lower the breakdown voltage. Figure 8-2 uses the overall average breakdown voltage with and without the transverse magnetic field and

Table 8-2. Breakdown Voltage (kV) – Initial Series – Block of Eight

Gap (cm)

Treatment	1.0	1.0	1.0	1.25	1.25	1.5	1.5	1.75	1.75	2.0	2.0	2.25	2.25	2.5	2.5	2.75	2.75	3.0	3.0	0.75	0.75	0.50	0.50	0.25	0.25	1.0
Sequence	1	3	15	4	16	5	17	6	18	7	19	8	20	9	21	10	22	11	23	12	24	13	25	14	26	27
(1)	100	120	158	130	160	139	174	241	200	167	200	189	220	180	230	190	240	190	250	120	120	100	107	45	39	168
a	80	90	160	90	160	109	170	135	170	150	180	166	187	170	200	180	216	160	206	90	119	83	100	49	44	160
b	64	80	155	100	170	131	180	130	190	180	190	170	210	190	220	200	200	216	200	115	145	90	127	61	60	160
ab	56	50	110	70	128	77	120	70	120	80	120	80	130	90	140	99	140	110	160	70	80	57	80	80	-	130
c	50	69	110	80	120	90	120	100	125	105	130	110	140	110	130	120	140	140	140	100	100	85	85	85	37	110
ac	67	70	100	79	130	90	147	100	130	130	130	127	140	130	160	114	180	150	150	67	90	39	69	69	25	140
bc	50	80	100	87	90	89	90	89	110	150	150	100	120	110	120	120	120	120	120	76	90	63	80	80	51	130
abc	20	70	130	80	140	100	133	100	150	90	159	120	160	120	150	143	179	140	140	29	107	90	90	90	38	140

Table 8-3. Breakdown Voltage (kV) With and Without 250 Gauss Transverse Magnetic Field – Block of Eight

Treatment	Gap (cm)																	
	1.0			1.5			2.0			2.5			3.0			0.5		
	w/o	w	w/o	w/o	w	w/o	w/o	w	w/o	w/o	w	w/o	w/o	w	w/o	w/o	w	w/o
(1)	152	140	160	190	200	200	220	217	200	230	230	250	270	240	260	98	100	100
c	90	100	110	120	130	130	130	127	130	149	150	130	150	150	140	79	97	100
ab	130	90	100	107	100	100	150	100	150	169	110	150	150	110	160	90	80	90
ac	129	70	100	140	88	150	170	80	160	170	90	179	200	90	140	86	74	85
b	115	120	170	191	150	199	220	160	220	230	180	240	245	180	240	95	130	130
a	150	130	160	160	130	140	170	160	190	210	170	200	190	170	200	95	99	110
abc	140	120	140	160	119	130	160	130	170	180	150	160	180	150	150	78	99	100
bc	90	90	95	120	120	118	140	120	130	140	130	130	150	150	170	78	110	110

Table 8-4. Estimates of Effects and Interactions of Factors
Initial Series of the Block of Eight

	Gap (cm)																						
	1.0			1.25		1.50		1.75		2.0		2.25		2.50		2.75		3.0		.50		.75	
Sequence	1	3	15	4	16	5	17	6	18	7	19	8	20	9	21	10	22	11	23	13	25	12	24
Factor																							
μ	61	79	128	90	137	103	142	108	149	119	151	132	163	138	169	143	171	155	171	76	93	84	106
A	-10	-17	-6	-20	5	-18	2	-14	-14	-26	-8	-17	-18	-20	-13	-18	-9	-29	-14	-17	-15	-39	-15
B	-27	-17	-8	-11	-11	-3	-22	-22	-14	-23	-18	-28	-17	-20	-23	-16	-47	-11	-37	-2	4	-22	-2
AB	-9	-3	-2	1	-1	-7	-10	-11	-4	-20	2	-18	-2	-25	-13	-10	-17	-19	4	14	-4	-8	-9
C	-28	-13	-36	-16	-35	-22	-39	-22	-41	-41	-43	-35	-47	-40	-58	-28	-57	-29	-67	-13	-23	-30	-19
AC	4	13	16	16	26	24	34	19	36	23	37	35	38	35	43	17	23	39	29	6	12	-1	18
BC	3	23	18	15	7	12	0	16	16	16	17	20	17	15	13	40	11	1	15	16	4	-9	5
ABC	-15	-3	22	-4	21	9	18	16	19	12	27	20	22	20	17	15	1	19	22	22	17	-2	23

(Values given are in kV and refer to breakdown voltage)

8-6

Table 8-5 Estimates of Effects by Yates Algorithm for
Conditioned Gaps With ("yes") and Without ("no") 250 Gauss Transverse
Magnetic Field – Field of Flight

Gap (cm)

Effect or Interaction	0.50			1.00			1.50			2.00			2.50			3.00		
	no	yes	no	no	yes	no	no	yes	no	no	yes	no	no	yes	no	no	yes	no
μ	87	99	102	126	108	129	149	130	146	169	137	170	185	151	180	192	155	183
A	0	-21	-16	28	-10	-9	-14	-41	-32	-3	-39	-15	-5	-43	-15	-24	-50	-40
B	-4	12	13	-14	-5	-6	-8	-15	-18	-3	-19	-5	-10	-18	-20	-21	-15	-5
AB	-2	-9	-9	5	10	4	-9	15	-12	-13	14	-10	-6	18	-15	-9	15	-10
C	-14	-7	-6	-27	-25	-36	-27	-31	-28	-43	-45	-40	-50	-43	-60	-44	-40	-65
AC	4	4	4	17	10	26	44	19	48	38	20	45	34	-23	55	64	20	30
BC	0	7	1	19	25	19	10	25	2	8	40	5	11	38	10	11	45	25
ABC	-1	15	11	1	20	31	19	5	8	18	15	0	15	23	5	-1	15	0

Table 8-6. Factorial Comparisons - Conditioned Breakdown Voltages
Without Magnetic Field - Block of Eight

	Factor	Comparisons	Gap (cm)									Final
			1.0	1.25	1.5	1.75	2.0	2.25	2.5	0.75	0.5	1.0
Individual Comparisons Made for Computing Main Effects of the Factors	A Anode Processing	a-1	2	9	-4	-30	-20	-33	-30	-1	-7	-8
		ab-b	-45	-45	-60	-70	-30	-80	-80	-65	-42	-30
		ac-c	-10	20	57	5	0	0	0	-14	-16	50
		abc-bc	30	56	43	40	59	40	30	17	10	40
	B Cathode Processing	b-1	-3	18	6	-30	-10	-10	-10	25	20	-8
		ab-a	-50	-32	-50	-50	-20	-57	-60	-39	-20	-30
		bc-c	-20	-30	-30	-15	-30	-20	-10	-10	-5	-10
		abc-ac	30	10	-14	20	49	20	-10	17	21	0
	C Electrode Size	c-1	-48	-40	-54	-75	-70	-80	-100	-26	-22	-38
		ac-a	-80	-30	-23	-40	-50	-47	-40	-29	-31	-20
(Note: Reversal of Area Effect)		bc-b	-55	-80	-90	-80	-90	-90	-100	-55	-47	-60
		abc-ab	20	12	13	30	39	30	10	27	10	10
Additional Physically Meaningful Comparisons		ab-1	-48	-32	-54	-80	-90	-90	-100	-40	-27	-38
		abc-c	20	20	13	25	39	20	20	-7	5	20
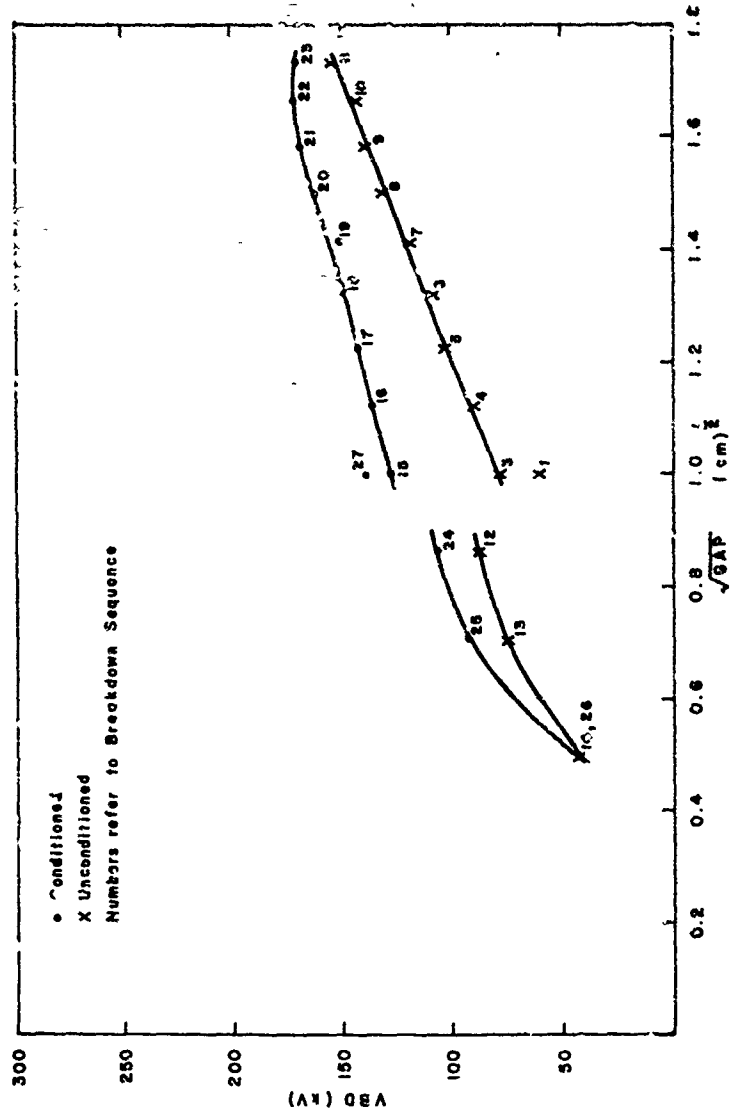
Figure 8-1. Breakdown Voltage vs $\sqrt{Gap}$ - Initial Series - Block of Eight

1-4081

Figure 8-2. Breakdown Voltage with and without 250 Gauss Transverse
Magnetic Field vs $\sqrt{Gap}$ - Block of Eight

1-4082

demonstrates that the square root dependence upon gap remains even with the magnetic field. An investigation was also made into the breakdown voltage as a function of transverse magnetic field strength from 0 to 250 gauss. Measurements were made arbitrarily at 2.0 and 3.0 cm gaps so the results are arbitrarily confounded somewhat with gap. However, the percentage change in breakdown voltage was calculated and on the average it was found that breakdown voltage increased slightly up to 100 amps of magnetizing current (approximately 85 gauss) and decreased above that level as shown in Figure 8-3.

(4) Anode Gas Content: The average effect of vacuum firing of the anode was to lower breakdown voltage as shown by the generally negative main effect A in Tables 8-4 and 8-5.

(5) Cathode Gas Content: The average effect of vacuum firing of the cathode was also to lower breakdown voltage as shown by the generally negative main effect B in Tables 8-4 and 8-5.

(6) Electrode Size: This factor was the most significant in the factorial analysis and in general the larger electrodes had lower breakdown voltages as shown by the negative main effect C in Tables 8-4 and 8-5.

(7) Factorial Interactions: The high level of the interactions AC, BC, and ABC implies that the main effects just discussed must be more carefully examined. For example the positive interaction AC indicates that electrode size and anode gas content cannot be considered independently. In this case the comparison of Table 8-6 for conditioned breakdown voltages without magnetic

8-11
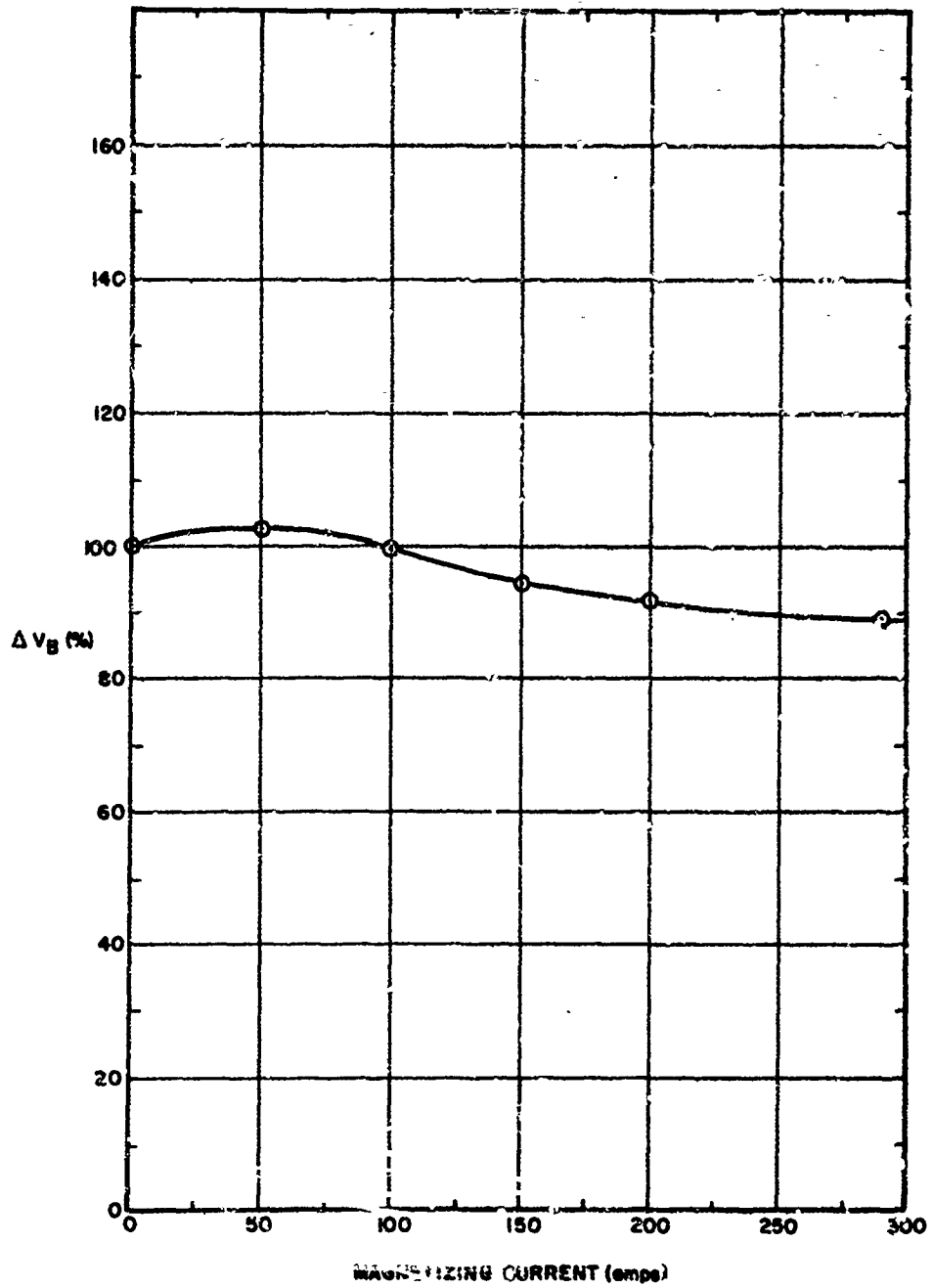
Figure 8-3. Average Percentage Change in Breakdown Voltage
at Large Gaps as a Function of Transverse Magnetic
Field Strength

1-2407a

field provide the information that when the electrodes are large and the cathode is vacuum fired, then vacuum firing of the anode raises the breakdown voltage (see line 4 of Table 8-6). When the physically meaningful comparison is made between electrodes with anode and cathode fired similarly, it is found that hydrogen firing is better for small electrodes while vacuum firing is better for large electrodes (see last two lines of Table 8-6). The electrode size factor is further complicated by the observation that in one case, when both electrodes were vacuum fired, the large electrodes had higher breakdown voltages than the small electrodes (see Note: Reversal of Area Effect, Table 8-6).

This apparent complexity of effects and interactions in vacuum breakdown demonstrates the importance of full factorial design which does not overlook interactions. However, in practical terms a more straightforward interpretation is desirable, and at least for this experiment, can be found in the theoretical motivation which stressed gas accumulation and ionization in the gap. Thus, if the eight treatments are ranked in breakdown voltage level for the larger gaps (> 0.75 cm) it is consistently found that the following grouping occurs:

Treatment	Last B/D at 1.0 cm in Initial Series	Common Features
1	168 kV	small electrodes, one or both hydrogen fired
b	160 kV	
a	160 kV	
abc	140 kV	large electrodes, anode or both vacuum fired, and small vacuum fired
ac	140 kV	
ab	130 kV	
c	110 kV	large electrodes, anode or both hydrogen fired
bc	100 kV	

It would seem that gas contributed by either the cathode or anode for small electrodes results in the highest breakdown voltage, that with increasing size vacuum firing of the anode becomes important and that for large electrodes hydrogen firing of the anode results in the lowest breakdown voltage. The theory would be expected to predict some critical level of gas concentration at which a maximum breakdown voltage is obtained.

In summary the factorial conclusion would be that adding gas (hydrogen firing) is beneficial for small electrodes, is detrimental for large electrodes, with anode gas content being more decisive than cathode gas content.

8.3   Prebreakdown Current

Prebreakdown current exhibited in general an exponential dependence upon voltage typical of field emission. The details of most interest in this experiment are the effects of transverse magnetic field of up to 250 gauss on prebreakdown currents. It has been found that the last measured current prior to breakdown is often a useful indication of emission characteristics and is referred to as I_{BD} - the ultimate prebreakdown current or current at breakdown.

The variation of prebreakdown current with magnetic field level as a function of voltage is given in Figure 8-4. It can be seen that as the transverse magnetic field increases the prebreakdown current typically decreases. This effect has been explained by Watson[1] as being due to a Hall effect in emitting protrusions on the cathode surface.

The ultimate prebreakdown current, I_{BD}, as a function of the square root of the gap goes through a minimum in the gap range from 1.5 to 2.0 cm. This is shown in Figure 8.5 for averaged current levels with, without, and again with a 250 gauss transverse magnetic field. Again this effect can be explained by the Hall effect. A more extensive description of these effects is contained in an addendum[1] to this report.
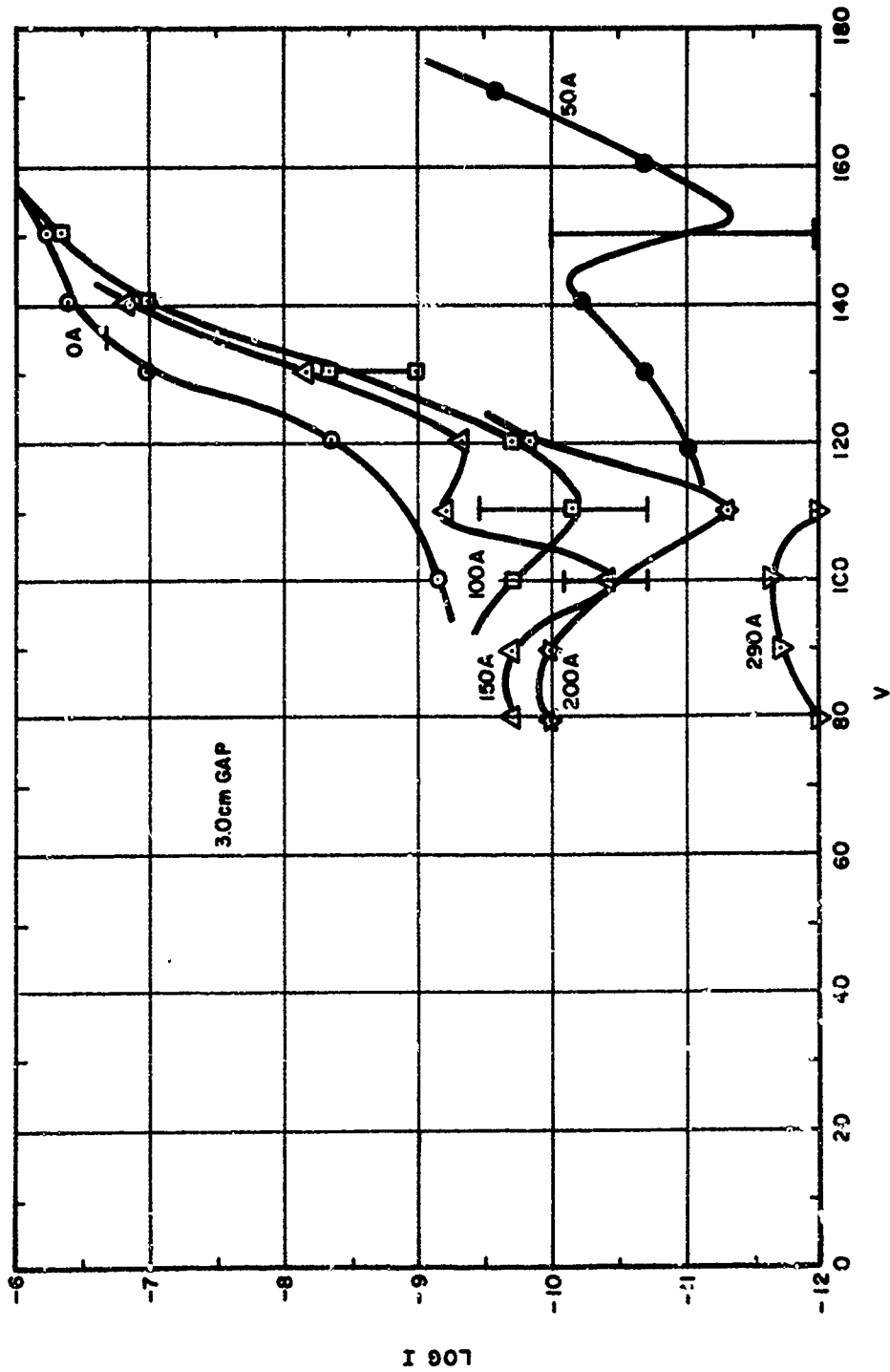
Figure 8-4. V~I Characteristics for Different Magnetic Field Strengths

1-2431
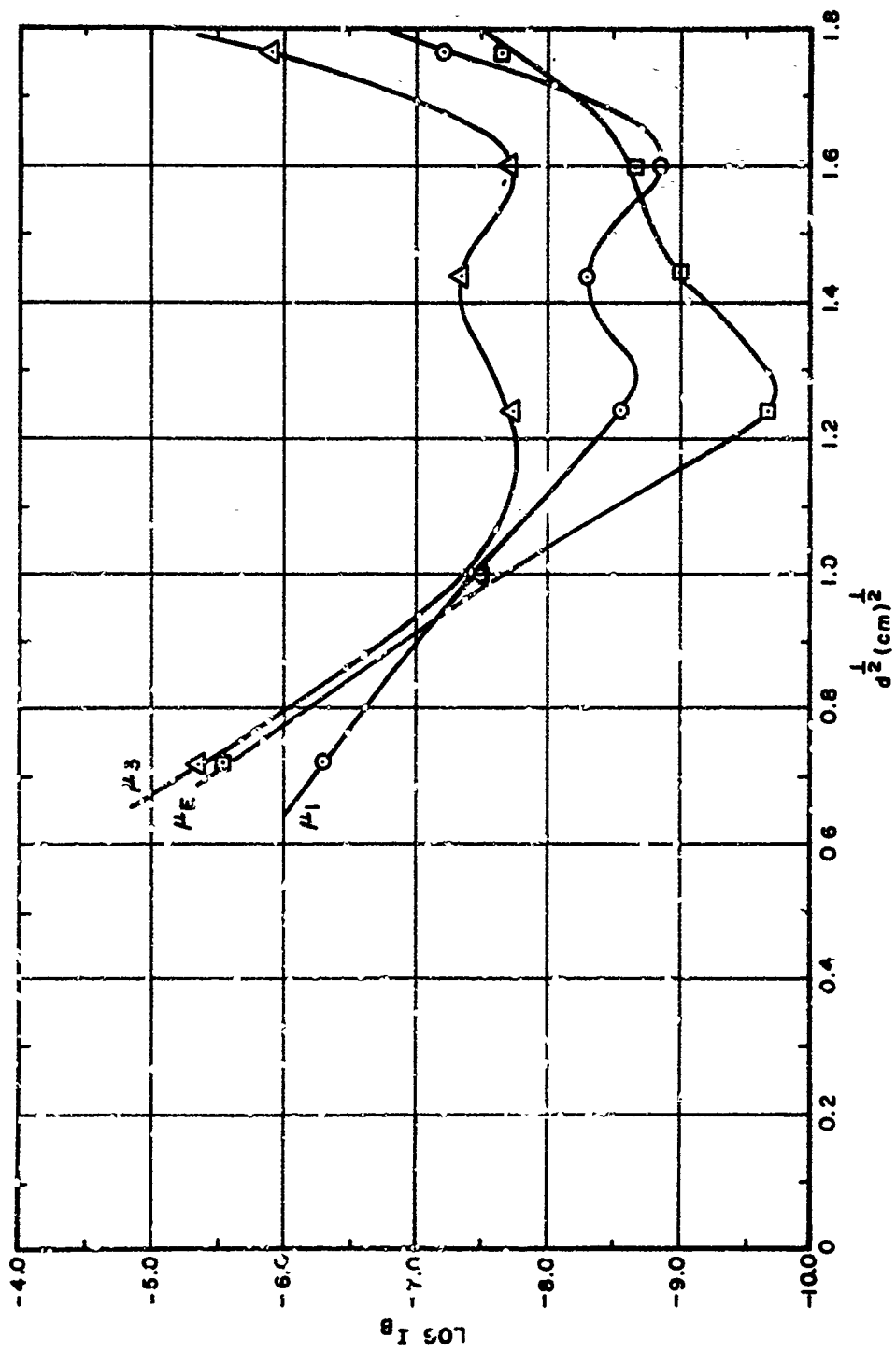
Figure 8-5. The μ Effect on Current

1-2415

8.4   Voltage Collapse

For five of the eight treatments the collapse of gap voltage upon breakdown was observed with the capacitive voltage divider during the early stages of testing (up to 25 breakdowns). Time to collapse is defined as the time interval between scope triggering (indicating a rapid fluctuation in voltage of several kilovolts) and collapse of gap voltage to near zero. The results are shown in Figure 8-6 where it is seen that for gaps up to 1.5 cm the mean collapse time increases almost linearly with gap $(300 \times 10^{-9}$ s/cm) while for 2 to 3 cm gaps the mean time is approximately 550 ns.

In the majority of waveforms, the gap voltage tended to collapse partially (20 to 30%) and then recover before proceeding to total collapse. During the total collapse some oscillation on the decaying voltage was usually observed. In the few cases where corresponding current waveforms were recorded, the voltage waveform oscillations coincided with current oscillations. At a given gap, the waveforms were seldom reproducible suggesting variations of gap impedance as being the main cause of oscillations rather than the external circuit. The frequency of these oscillations decreased with increasing gap from 45 to 15 MHz.

The peak current recorded was normally several hundred amperes, in reasonable agreement with the value calculated from voltage and source impedance (160 ohms). However, it was frequently not as high as expected, leading to the conclusion that the initial phase of the arc (during which substantial voltage is still across the gap) is of fairly high impedance (>100 ohms).

8.5   Conclusions

Gas content has been shown to be an influential factor whose effect depends upon electrode size. Thus, small electrodes (1.28 inch diameter) benefited from hydrogen firing while large electrodes (4 inch diameter) have lower breakdown voltages when hydrogen fired. Gas content of either electrode was important, with anode gas content having the greatest effect. Similarly area (or size) is a decisive factor with small electrodes usually having higher breakdown voltages than large electrodes.
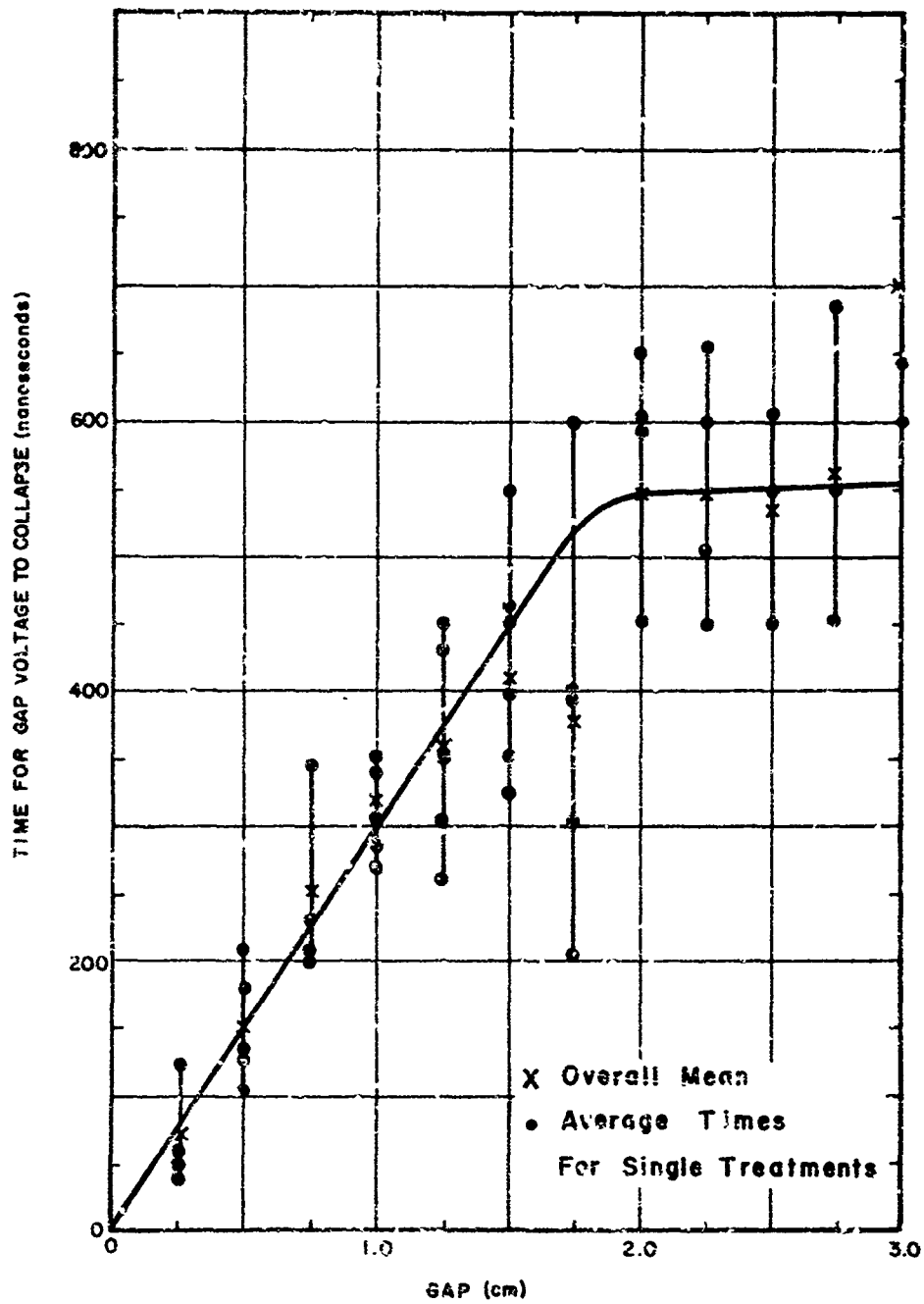
Figure 8-6. Collapse of Gap Voltage
Block of Eight Experiment

1-2444

The variation of breakdown voltage with gap follows a square root law above about 0. 75 cm. A weak transverse magnetic field of 250 gauss lowers the breakdown voltage for gaps larger than 0. 75 cm and raises breakdown voltage for smaller gaps. Prebreakdown current was found to be profoundly affected by the transverse magnetic field level and possible explanation of this based on the Hall effect is contained in an addendum [1] to this report.

Voltage collapse time was found to vary linearly with gap up to approximately 1. 5 cm, beyond which it was constant at ~ 550 ns. The average rate was 300×10^{-9} s/cm.

These observations, and results of the preceding two experiments have been used by Watson as the experimental basis for a comprehensive theory of vacuum breakdown. Instability in the growth of interelectrode space charge is seen as the initiating mechanism and results from the heating of anode spots by field emission electron beams. This heating leads to gas evolution which contributes an ionic space charge which in turn enhances the emitted beam. A complete description of this theory is contained in an addendum [2] to this report.

SECTION 9
BLOCK OF THIRTY-TWO EXPERIMENT

9.1   Introduction

The Block of Eight Experiment demonstrated the important influence of electrode pretreatment and size on breakdown voltage. These effects were attributed to different gas sorptions for hydrogen or vacuum firing. The significant interaction between anode gas content and electrode size was theoretically related to the pumping conductance of plane parallel electrodes. To investigate these and the effects of conditioning in more detail, and to extend the uniform field, single material (copper) scope of the Block of Eight Experiment, a Factorial Experiment consisting of 32 treatments and 8 replications was designed.

The basic experimental design, procedures and conditions are given in Table 9-1. The test sequence specifies about 90 breakdowns over a three or four day period. Performance over a range of gaps, with and without a transverse magnetic field, before and after gas exposure, and with energy storage was explored.

9.2   Breakdown Voltage

A complete tabulation of breakdown voltages is contained in an addendum to this report. For the purposes of this review the optimum conditioned and average breakdown voltage levels are of most interest and are given in Tables 9-2 and 9-3. The grouping of results according to level of factor E (anode shape) follows the experimental order since the factorial design was divided into two blocks of 16 treatments. Each block studied the same four factors (A, B, C and D) at two levels each for the different levels of the fifth factor (E). This was done so that analysis could begin when the overall experiment was half completed.

While many different factorial analyses were carried out at various stages of the analysis, it seems worthwhile here to include only the final

Table 9-1. Experimental Design - Block of Thirty-Two

			High Level	Low Level
Factors	A	Anode Material	Copper (OFHC)	Aluminum (1100)
	B	Cathode Material	Copper (OFHC)	Aluminum (1100)
	C	Electrode Processing	Vacuum Firing	Hydrogen Firing
	D	Anode Size	4 inch diameter	1.28 inch diameter
	E	Anode Shape	Bruce Profile	Sphere

Firing: 900°C for 6 hours for copper; 600°C for 6 hours for aluminum

Cathode Geometry: 2 Inch Diameter Sphere

Surface Finish: 600 Grit Silicon Carbide Paper

Bakeout: Chamber at 375°C for 6 hours; Electrodes at 400°C for 8 hours.

Voltage Application: 10 kV Steps every minute from well below breakdown

Variables Monitored: Voltage, Prebreakdown Current, Breakdown Voltage Collapse, Pressure

Test Sequence:

    Initial Series (Day 1): 3 Breakdowns at 1.0 cm gap, then 1 breakdown at 1.5, 2.0, 3.0, 0.25, 0.50, 0.75, 1.0, 1.5, 2.0, 3.0, 0.25, 0.50, 0.75, 1.0, 1.9, 2.0 cm for a total of 19 Breakdowns

    Magnetic Field Series (Day 2): 2 Conditioning Breakdowns at 1.0 cm, then sequence of 6 breakdowns each (0, 100, 200, 300, 400, 0, gauss) at gaps of 1.0, 2.0, 0.25, 0.50, 0.75, 1.5 cm

    Exposure Tests: For Bruce Profile Anodes exposure was to $20\% O_2$ - $80\% N_2$ at 10^{-6} torr for 1 minute; for Spherical Anodes, exposure was to Air, N_2 or O_2 At Atmospheric Pressure.

    Energy Conditioning Tests: Preliminary Tests with Energy Storage Capacitor Bank (6750 Joules at 300 kV)

Bushing Conditioning: At ~ 5 cm Electrode Gap, Preceeded each Day's Testing.

Specification of Treatments:

Treatment	Anode Material	Cathode Material	Electrode Processing	Anode Size (Inches)	Anode Shape	Date Tested	Date Replicated
(1)	Al	Al	H_2	1.28	Sphere	10/14/68	
a	Cu	Al	H_2	1.28	Sphere	9/23/68	
b	Al	Cu	H_2	1.28	Sphere	9/11/68	
ab(R)	Cu	Cu	H_2	1.28	Sphere	11/25/68	7/29/68
c	Al	Al	Vac	1.28	Sphere	10/7/68	
ac	Cu	Al	Vac	1.28	Sphere	9/3/68	
bc	Al	Cu	Vac	1.28	Sphere	11/11/68	
abc	Cu	Cu	Vac	1.28	Sphere	8/5/68	
d	Al	Al	H_2	4	Sphere	8/26/68	9/16/68
ad	Cu	Al	H_2	4	Sphere	10/21/68	
bd	Al	Cu	H_2	4	Sphere	10/28/68	
abd	Cu	Cu	H_2	4	Sphere	8/12/68	
cd(R)	Al	Al	Vac	4	Sphere	12/9/68	9/3/68
acd(R)	Cu	Al	Vac	4	Sphere	11/18/68	12/4/68
bcd	Al	Cu	Vac	4	Sphere	11/?/68	
abcd	Cu	Cu	Vac	4	Sphere	8/19/68	
e	Al	Al	H_2	1.28	Bruce	2/26/68	6/24/68
ae	Cu	Al	H_2	1.28	Bruce	4/22/68	
be	Al	Cu	H_2	1.28	Bruce	3/26/68	
abe	Cu	Cu	H_2	1.28	Bruce	2/5/68	7/22/68
ce	Al	Al	Vac	1.28	Bruce	4/8/68	
ace	Cu	Al	Vac	1.28	Bruce	3/18/68	6/10/68
bce	Al	Cu	Vac	1.28	Bruce	6/3/68	
abce	Cu	Cu	Vac	1.28	Bruce	3/4/68	
de	Al	Al	H_2	4	Bruce	3/11/68	7/1/68
ade	Cu	Al	H_2	4	Bruce	4/29/68	
bde	Al	Cu	H_2	4	Bruce	5/21/68	
abde	Cu	Cu	H_2	4	Bruce	2/12/68	
cde	Al	Al	Vac	4	Bruce	4/15/68	
acde	Cu	Al	Vac	4	Bruce	5/6/68	
bcde	Al	Cu	Vac	4	Bruce	5/27/68	
abcde	Cu	Cu	Vac	4	Bruce	2/19/68	

Table 9-2.   Optimum and Average Breakdown Voltages Treatments with Spherical Anodes

Treatment	Optimum Conditioned Breakdown Voltages on First and Second Day						Average Breakdown Voltage Without Magnetic Field on First and Second Day						Average Breakdown Voltage With 100 to 400 Gauss Magnetic Field on Second Day					
Gap (cm)	0.25	0.50	0.75	1.0	1.5	2.0	0.25	0.50	0.75	1.0	1.5	2.0	0.25	0.50	0.75	1.0	1.5	2.0
(1)	100	160	210	230	290	>300	59	117	162	204	245	281	71	132	167	205	235	290
a	130	200	260	280	>300	>300	75	152	212	244	257	300	99	171	132	225	272	298
b	45	98	134	180	240	290	31	86	113	166	219	271	40	90	123	168	223	272
ab(R)	140	220	280	>300	>300	>300	90	148	235	278	278	290	93	177	237	244	269	291
c	55	110	140	190	240	280	43	94	118	169	215	256	50	97	138	180	219	252
ac	60	130	160	220	246	295	40	100	144	171	215	253	54	114	156	176	334	256
bc	83	150	210	260	280	290	60	126	163	209	241	263	77	135	186	202	245	270
abc	66	128	168	210	276	>300	35	94	129	174	245	284	41	95	143	158	(230)	275
d	64	139	180	230	260	300	42	101	157	203	235	292	50	120	166	192	250	272
ad	90	170	180	250	280	300	47	104	157	181	225	249	45	118	172	177	270	247
bd	70	127	188	240	290	300	54	104	163	269	264	306	54	110	155	193	242	260
abd	120	188	248	290	>300	>300	70	140	227	253	283	310	96	181	215	214	285	291
cd(R)	70	130	200	240	270	290	48	101	58	190	247	280	55	117	174	192	203	212
acd(R)	57	120	160	210	280	300	49	100	129	180	234	270	52	103	141	179	232	222
bcd	80	150	210	250	280	>300	59	125	173	219	252	289	69	122	177	192	213	220
abcd	77	170	240	289	>300	>300	39	110	164	215	252	280	48	134	199	135	285	282

Table 9-3. Optimum and Averaged Breakdown Voltages for Treatments with Bruce Profile Anodes

Treatment	Optimum Conditioned Breakdown Voltages				Average of Eight Uniformly Distributed Breakdowns				Average of Six Breakdowns With 100 to 400 Gauss Transverse Magnetic Field				
	Gap (cm)												
	0.25	0.50	1.0	1.5	0.25	0.50	1.0	1.5	0.25	0.50	1.0	1.5	2.0
e (R)	95	115	202	260	47	98	180	238	47	94	153	245	265
ae	85	165	220	270	66	139	209	260	66	160	165	265	285
be	50	105	197	240	49	98	190	235	56	105	163	179	228
abe (R)	100	190	260	300	82	151	243	285	95	132	228	292	>300 (315)
ce	97	157	250	280	77	139	224	268	79	139	205	280	285
ace (R)	85	160	230	283	63	136	206	272	68	135	190	275	294
bce	85	140	230	280	61	118	196	252	57	126	198	230	250
abce	120	195	260	295	83	156	202	257	87	168	203	269	285
de	55	105	195	255	46	98	164	234	46	98	174	225	242
ade	60	130	225	270	46	117	205	252	43	116	175	210	230
bde	84	140	235	255	75	126	213	234	75	129	215	240	255
abde	140	200	280	285	113	181	235	249	133	198	232	270	290
cde	57	125	210	280	48	113	196	255	55	113	198	235	245
acde	90	160	210	255	73	146	203	245	74	145	182	320	238
bcde	70	143	215	267	59	125	191	254	63	133	170	230	230
abcde	95	190	250	260	70	147	207	234	70	155	198	265	290

overall analysis according to Yates'Algorithm. This (see Table 9-4) contains the most accurate estimates and all essential information. Table 9-5 gives the factorial results obtained when both electrodes were of the same material.

The factorial estimates are seen to be consistent across a range of gap, degree of conditioning and magnetic field level. Thus, interaction of the factorial factors with these parameters can be considered negligible to a first approximation. The effect of conditioning on the factorial estimates is considered further in Section 9.3.

The factors and interactions of most significance are A, B, and AC. A and B, anode and cathode material respectively, are positive indicating that copper yields higher breakdown voltages than aluminum. The interaction AC relates anode material to electrode processing and detailed examination of the results indicates that usually hydrogen firing was better for copper while vacuum firing was better for aluminum (as the negative sign of AC would suggest).

The other main effects C, D and E; electrode processing, anode size and anode shape, do not appear significant based on statistical estimates obtained with half-normal plots. However, their signs, if constant across gap, may fairly be taken as indicative of the direction of their effect. Thus on the average, a negative C would suggest that hydrogen firing is preferable, but the significant interaction AC has indicated that this depends upon material. The negative D would suggest that small anodes give higher breakdown voltages but there is little consistency across gap with this effect. Similarly E suggests that spherical anodes yield higher breakdown voltages but little consistency with gap is evident.

In a practical sense the factorial estimates would suggest that small, spherical, hydrogen fired copper electrodes would give the highest breakdown voltages while large, Bruce profile, hydrogen fired aluminum electrodes would give the lowest breakdown voltages. These specifications correspond to treatments "ab" and "de" respectively. Examination of the optimum breakdown voltages of these treatments for the prime gap of 1.0 cm reveals that treatment "ab" at > 300 kV did indeed have the highest breakdown voltage and that treatment "de" at 195 kV had the lowest breakdown voltage.

9-5

Table 9-4. Yate's Analysis with Optimum and Averaged Breakdown Voltage
Block of Thirty-two

Effects and Interactions	Optimum Conditioned Breakdown Voltages Gap (cm)				Average of Uniformly Distributed Breakdown Voltages Without Magnetic Field Gap (cm)				Average Breakdown Voltage with 100-400 Gauss Magnetic Field Gap (cm)				
	0.25	0.50	1.0	1.5	0.25	0.50	1.0	1.5	0.25	0.50	1.0	1.5	2.0
μ	82	150	235	276	59	122	203	248	65	130	191	244	263
A	24	38	27	18	11	23	17	0	13	28	9	28	21
B	13	16	22	10	11	12	16	7	12	13	12		10
AB	11	14	15	11	6	6	8	6	7	3	11	17	20
C	-8	-5	-6	-3	-5	-3	-13	-4	-6	-6	-7	-6	-24
AC	-18	-21	-23	-14	-11	-17	-21	-14	-15	-18	-16	-8	1
BC	0	6	2	4	-7	-3	-7	-3	-9	3	-10	2	4
ABC	-8	-8	-6	-5	-8	-9	-8	-5	-11	-8	-9	-3	-2
D	-4	-1	5	0	-1	-2	0	-2	-3	1	0	-5	-3
AD	-2	-5	-3	-5	-2	-4	-6	-10	-2	-1	-5	-3	2
BD	10	13	12	3	8	5	10	3	11	14	4	17	15
ABD	-2	-1	3	-3	-2	-1	-1	-2	2	9	0	2	7
CD	-2	5	-2	3	0	2	6	3	0	0	-2	-6	-4
ACD	6	9	10	4	6	7	12	3	3	6	12	14	11
BCD	-11	-4	-4	-9	-9	-7	-3	-4	-10	-12	-5	0	-1
ABCD	0	4	13	8	-3	-2	-5	2	-5	-5	6	7	4
E	1	1	-13	-10	13	16	0	6	7	8	-1	1	-1
AE	3	6	-2	-6	5	9	1	0	6	6	3	-2	-7
BE	6	6	0	-7	4	2	-5	-10	7	4	7	-3	-3
ABE	2	2	2	0	2	3	-4	-4	6	-2	5	11	5
CE	17	20	11	11	6	12	12	10	5	17	12	16	5
ACE	10	11	9	-1	5	7	5	-1	6	8	4	-3	-5
BCE	-9	-13	-12	-6	-4	-7	-11	-3	-10	-5	-11	-9	-10
ABCE	4	8	9	1	5	7	12	0	4	11	8	-1	0
DE	1	-2	-9	-10	1	4	-4	-11	3	2	5	-12	0
ADE	4	2	6	-3	3	4	7	0	2	3	0	-18	-7
BDE	1	1	0	-5	1	1	-2	-4	0	2	-3	9	4
ABDE	0	-3	-9	0	0	-2	-5	-2	-3	-5	-1	-8	4
CDE	-13	-9	-15	-12	-8	-5	-9	-5	-7	-9	-13	-1	0
ACDE	0	0	-6	-8	-1	-3	-5	-3	-2	-3	-2	-1	0
BCDE	-1	-3	1	6	0	-1	3	11	1	-2	0	-2	1
ABCDE	-9	-9	-11	-3	-5	-7	-1	0	-5	-13	0	0	3

Table 9-5. Yate's Analysis with Optimum and Averaged Breakdown Voltages of Sub-Block with Same Metals for Anode and Cathode - Block-of-32

Effect	Optimum Conditioned Breakdown Voltages — Gap in cm				Average of Uniformly Distributed Breakdown Voltages Without Magnetic Field — Gap in cm				Average of Breakdown Voltages with 100-400 Gauss Magnetic Field — Gap in cm				
	0.25	0.50	1.0	1.5	0.25	0.50	1.0	1.5	0.25	0.50	1.0	1.5	2.0
μ	88	157	243	281	62	125	208	251	69	134	196	253	271
X	38	55	50	28	22	36	34	18	26	41	21	34	29
C	-17	-14	-12	-7	-14	-12	-22	-9	-18	-14	-16	-10	-17
XC	-18	-14	-20	-8	-19	-20	-29	-17	-24	-19	-26	-6	4
D	-6	-3	9	-2	-4	-3	-1	-5	1	10	0	-2	-14
XD	8	7	8	-1	6	5	4	-6	9	13	0	13	8
CD	-2	9	10	12	-4	0	1	6	-6	-4	4	0	2
XCD	-5	5	6	-3	-2	0	9	-2	-6	-6	7	14	10
E	3	4	-10	-6	16	20	-4	2	13	6	4	13	1
XE	9	13	-2	-20	10	11	-3	-10	13	10	11	-6	4
CE	21	28	20	15	11	19	24	11	10	28	21	14	13
XCE	1	-2	-2	-7	1	0	-6	-6	-3	2	-7	-12	-14
DE	0	-5	-13	-8	1	1	-10	-13	0	-3	3	-20	-2
XDE	5	4	6	7	5	6	5	-4	2	5	-3	-4	2
CDE	-23	-19	-26	-13	-14	-16	-10	-5	-13	-22	-13	-1	2
XCDE	0	-3	-5	0	-1	-4	-2	7	-1	-5	-3	-3	3

X - Electrode Material - Aluminum to Copper
C - Electrode Treatment - Hydrogen to Vacuum Firing
D - Anode Size - 1.28 to 4-Inch Diameter
E - Anode Shape - Bruce Profile to Sphere

Relation of these factorial estimates to theoretical models is extremely complicated and will not be attempted here. It is, however, interesting to note, that the most significant interaction was that of anode material with electrode processing which supports both the Pilot Experiment and the Block of Eight in their conclusion that anode gas content is a decisive factor.

9.3   Conditioning, Reproducibility and Factorial Estimates

Meaningful analysis of a factorial experiment requires that an accurate, reproducible measure of performance be obtained for each treatment. This is usually achieved by careful experimental control and by repeating each treatment one or several times to determine the magnitude of error and to obtain a valid measure for performance. Economic considerations often limit the number of replications and in addition, other complicating factors may also be present. In particular, vacuum breakdown has an inherent ambiguity due to the phenomena of conditioning. No matter how carefully and thoroughly a set of electrodes is prepared, its vacuum insulation performance depends not only on the factorial influences and easily specified conditions such as gap and magnetic field, but also on its electrical stress history. Breakdown and prebreakdown phenomena can strongly influence subsequent breakdown performance.

Typical conditioning behavior for this experiment is given in Figure 9-1, which contains representative conditioning curves for the prime gap of 1.0 cm. Most treatments follow the trend of treatment "cde" which rises in approximately five breakdowns (at the 1.0 cm gap, additional breakdowns at other gaps will have occurred) to a plateau which is then rather flat. There is no discernable pattern among the factors which would allow prediction of the type of conditioning curve.

The simplest and most direct factorial analysis assumes that each breakdown voltage is a valid measure of the performance of the electrodes under the specified conditions. These values can be used in Yates' Algorithm to compute an unbiased estimate of all main effects and interactions. In such a computation for main effects each treatment is compared with one other treatment; for example, one component of the estimate of effect of cathode material

9-8
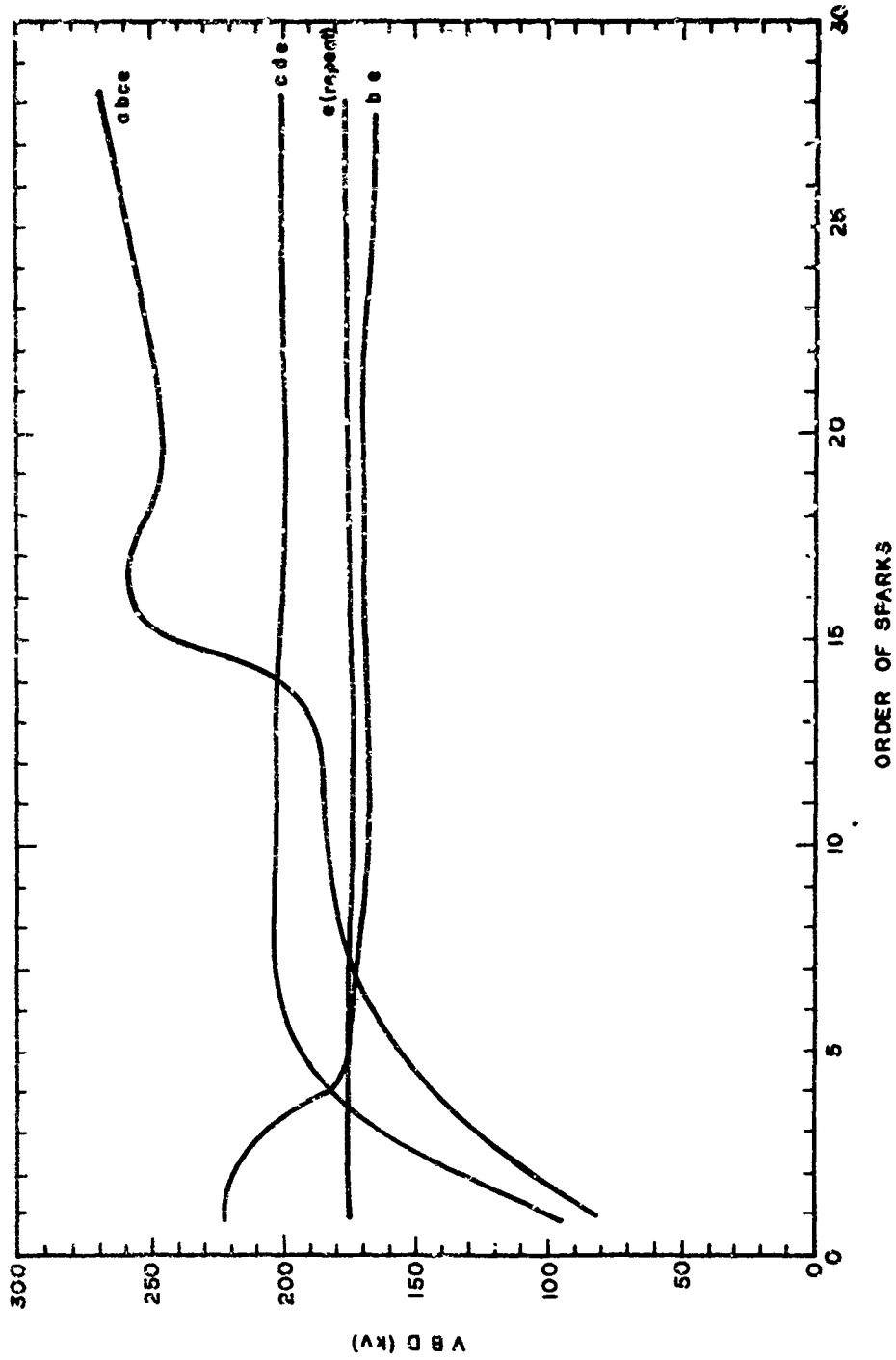
Figure 9-1. Various Types of Conditioning Curves - 1.0 cm Cap

1-3035

is obtained by subtracting the breakdown voltages of treatment ade from those of treatment abde. Figure 9-2 illustrates this comparison at the prime gap of 1.0 cm. As can be seen the result of such a comparison is clear; a 2-inch spherical copper cathode gives higher breakdown voltages than similar aluminum cathode when the anode is a 4-inch diameter Bruce profile copper electrode and when both electrodes are hydrogen fired and baked. This factorial component is not strongly dependent upon conditioning, magnetic field, or exposure. The shape of the conditioning curves are very much alike, only the levels differ.

That such curves are reproducible is evident in Figures 9-3 and 9-4 which compare replications of two treatments with the original treatments. While individual points may differ somewhat the overall trends are closely related.

Such a point-by-point computation of factorial estimates did not yield satisfactory results when applied to the Block of Thirty-Two Experiment. The apparent error was high. main effects small and variable, and high order interactions large. Either experimental control was insufficient (which the reproducibility as shown in Figures 9-3 and 9-4 denies) or the point-by-point comparison which appears valid in Figure 9-2 is not always reliable.

This second possibility turned out to be the case. Due to conditioning, any point-by-point comparison is subject to variations of both immediate and long-term nature. The immediate variation due to conditioning is evident in Figure 9-2. Breakdowns 1 and 3 show no effect of changing cathode material while breakdowns 2 and 4 show a + 20% effect. The long-term variation is shown in Figure 9-5 which graphically illustrates the comparison (at 1.0 cm) of treatment abce and ace (R), giving another component of the factorial estimate of the effect of cathode material. Here the first 10 breakdowns imply that aluminum is better than copper, the next five show little effect, and the rest confirm the initial finding of Figure 9-2 that copper is better than aluminum. This changeover is due to the slow, but steady conditioning for treatment abce which rises rather smoothly from 80 kV to 280 kV. As a consequence
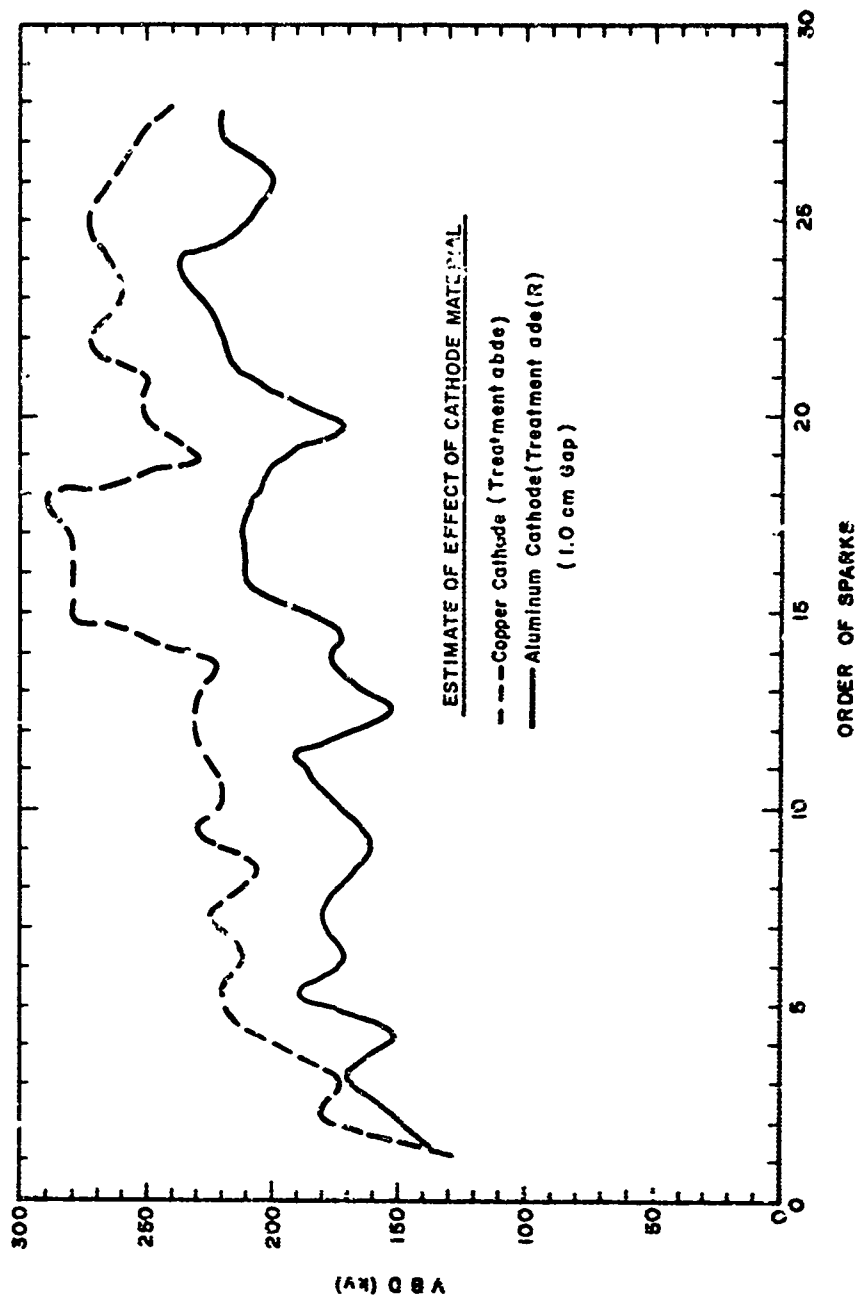
Figure 9-2. Comparison for Factorial Estimate of Effect of Cathode Material

1-3395

9-11
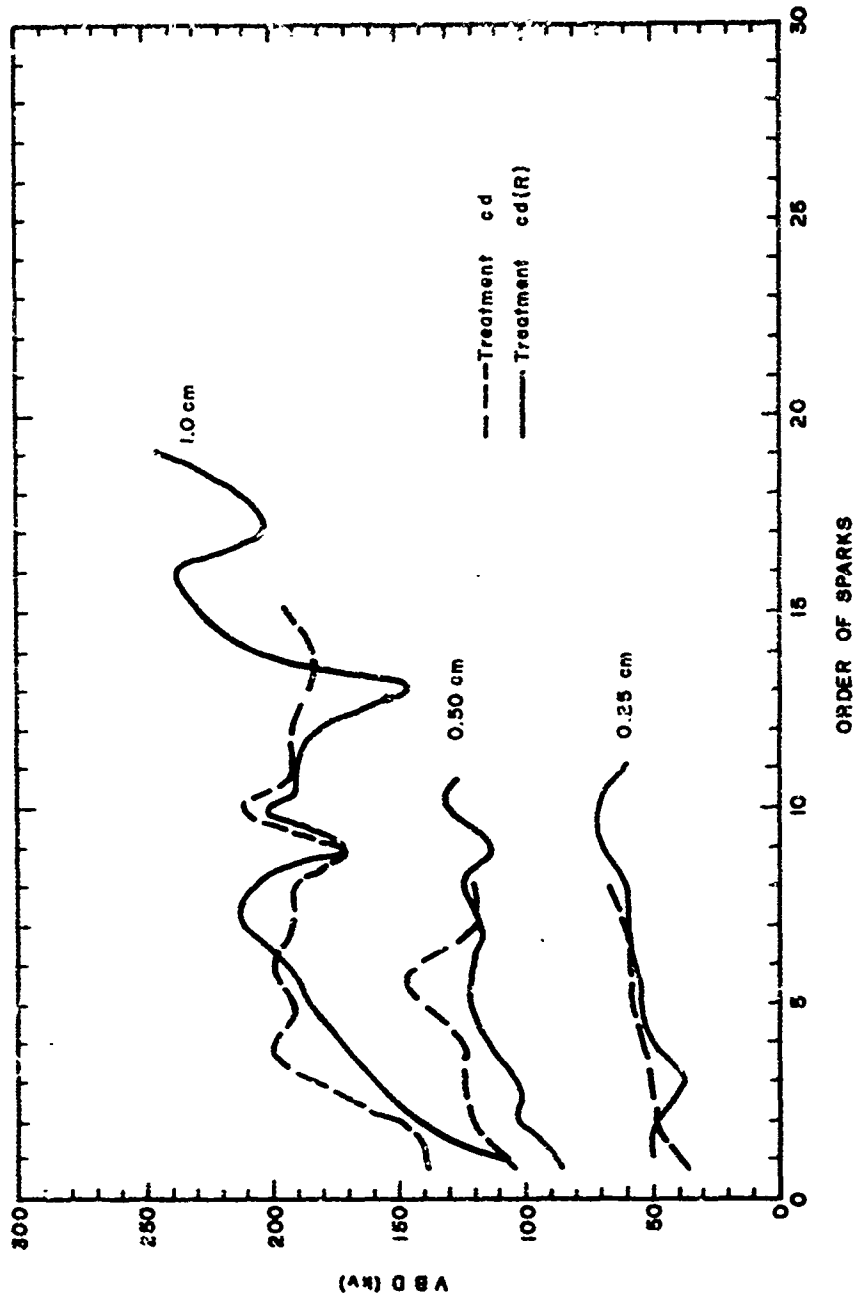
Figure 9-3. Reproducibility of Treatment cd

1-3306
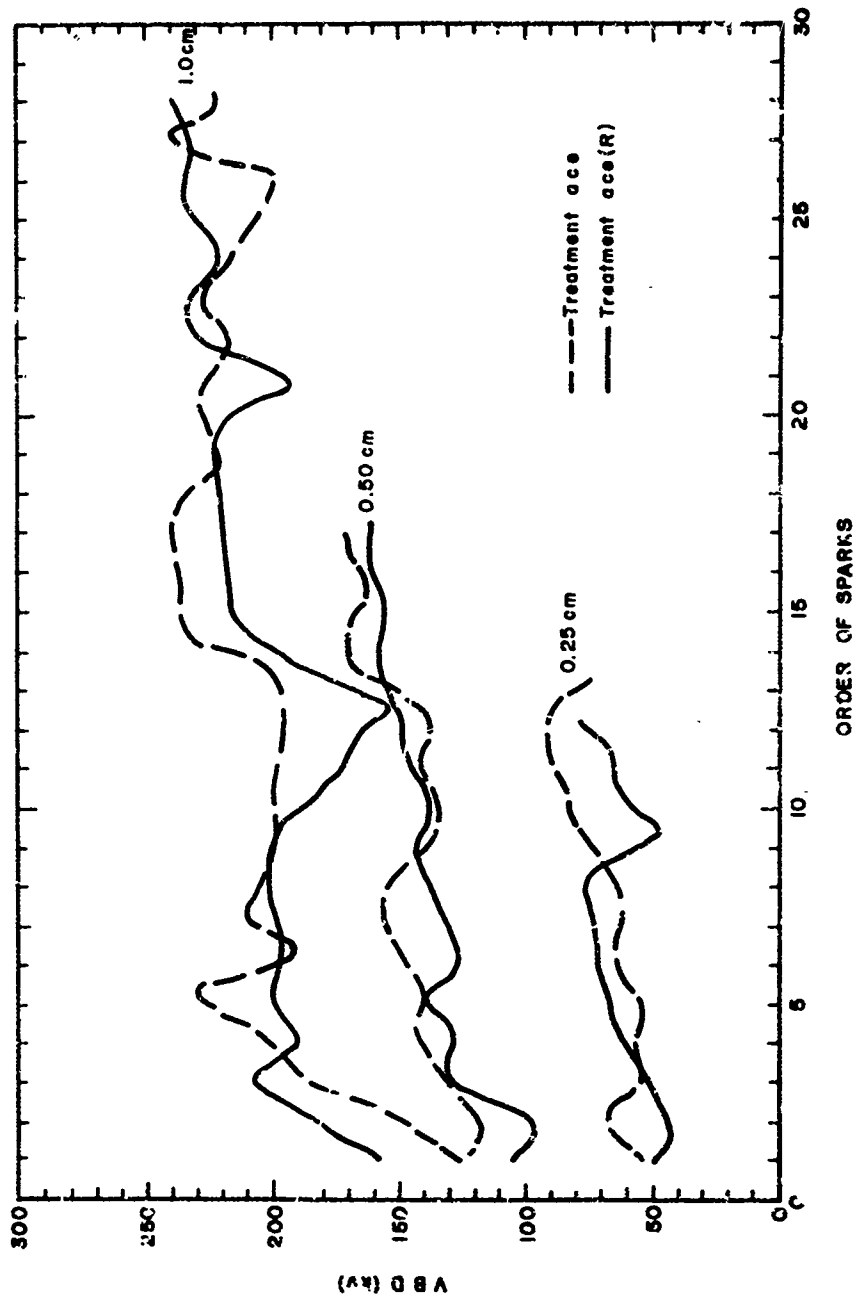
Figure 9-4. Reproducibility of Treatment ace

1-3307
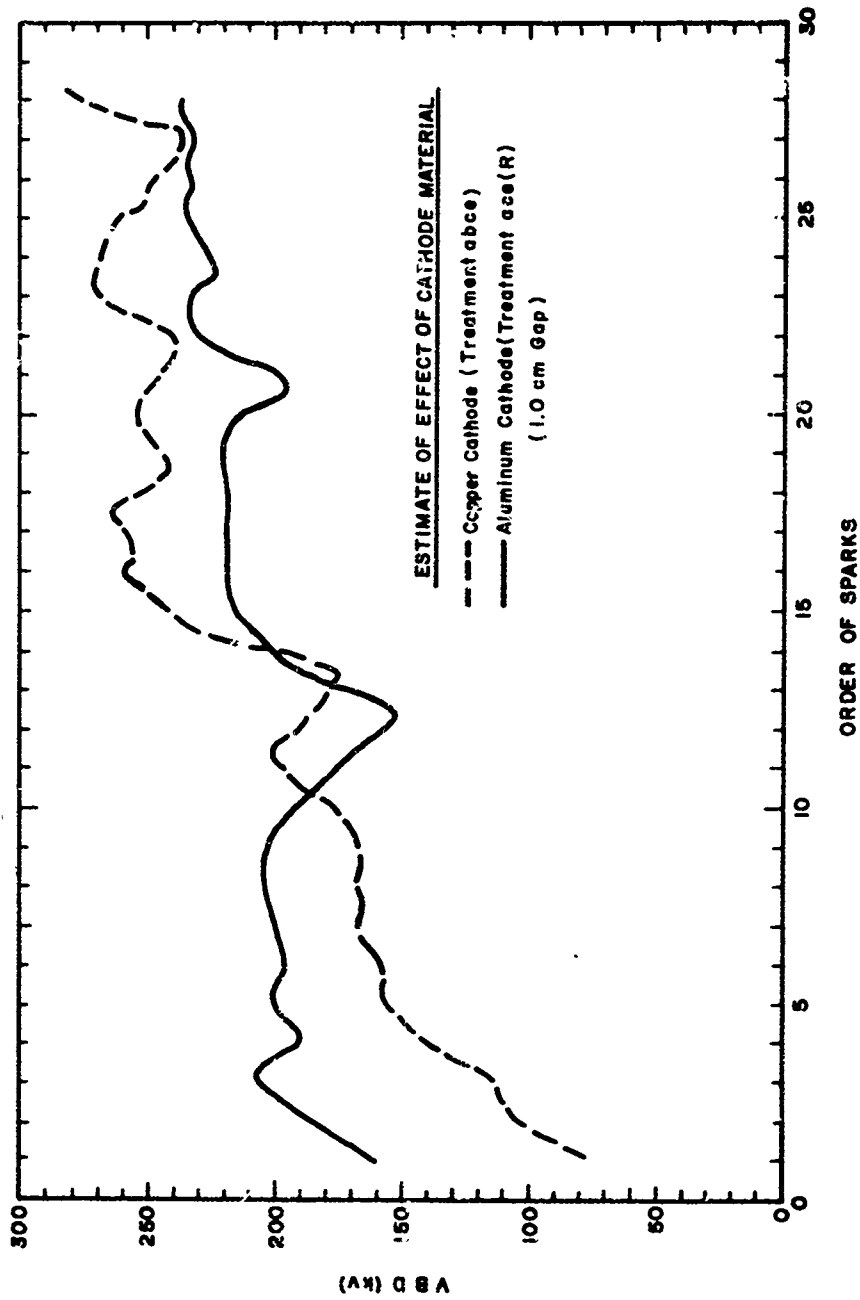
Figure 9.5. Comparison for Factorial Estimate
of Effect of Cathode Material

1-3308

of such conditioning the point-by-point factorial estimates may show little con-
sistency and much variation.

Averaging or selecting the optimum of several breakdown voltages
will usually compensate for immediate conditioning variation and has been
utilized in the preceding section. However, the results to date indicate that
sequences of breakdowns for fixed circuit parameters and gap separations may
be required to specify the long-term voltage conditioning curves for the various
combinations of experimental factors.

9.4   Breakdown Voltage as a Function of Gap
           and Transverse Magnetic Field

Breakdown voltage was found to vary as the square root of the gap
above ~ 0.75 cm and to vary linearly with gap below ~ 0.75 cm. The effect of
a transverse magnetic field of up to 400 gauss was also different in these two
gap ranges, apparently increasing the breakdown voltage below 0.75 cm and
decreasing it for gaps above 0.75 cm. The response of a single treatment to
changes in gap and magnetic field is given in Figures 9-6 and 9-7. The average
breakdown for all treatments with Bruce Profile anodes is given as a function
of the square root of the gap in Figure 9-8 and as a linear function of gap in Fig-
ure 9-9. The two regimes are clearly separated at about 0.75 cm. The aver-
age effect of a transverse magnetic field for treatments with Bruce Profile
anodes is evident in Figure 9-10, where the effect is consistent over the entire
three-day test sequence. Similar results were obtained for treatments with
spherical anodes and Figure 9-11 which uses optimum and average breakdown
voltages of the entire Block of Thirty-Two may be taken as a summary of the
effects of gap and transverse magnetic field.

9.5   Voltage Collapse

Breakdown is defined as the collapse of voltage across the vacuum
gap to near zero and involves a current buildup of six or more orders of mag-
nitude from 10^{-12} to 10^{-3} A just prior to breakdown to 10^2 to 10^3 A during

9-15
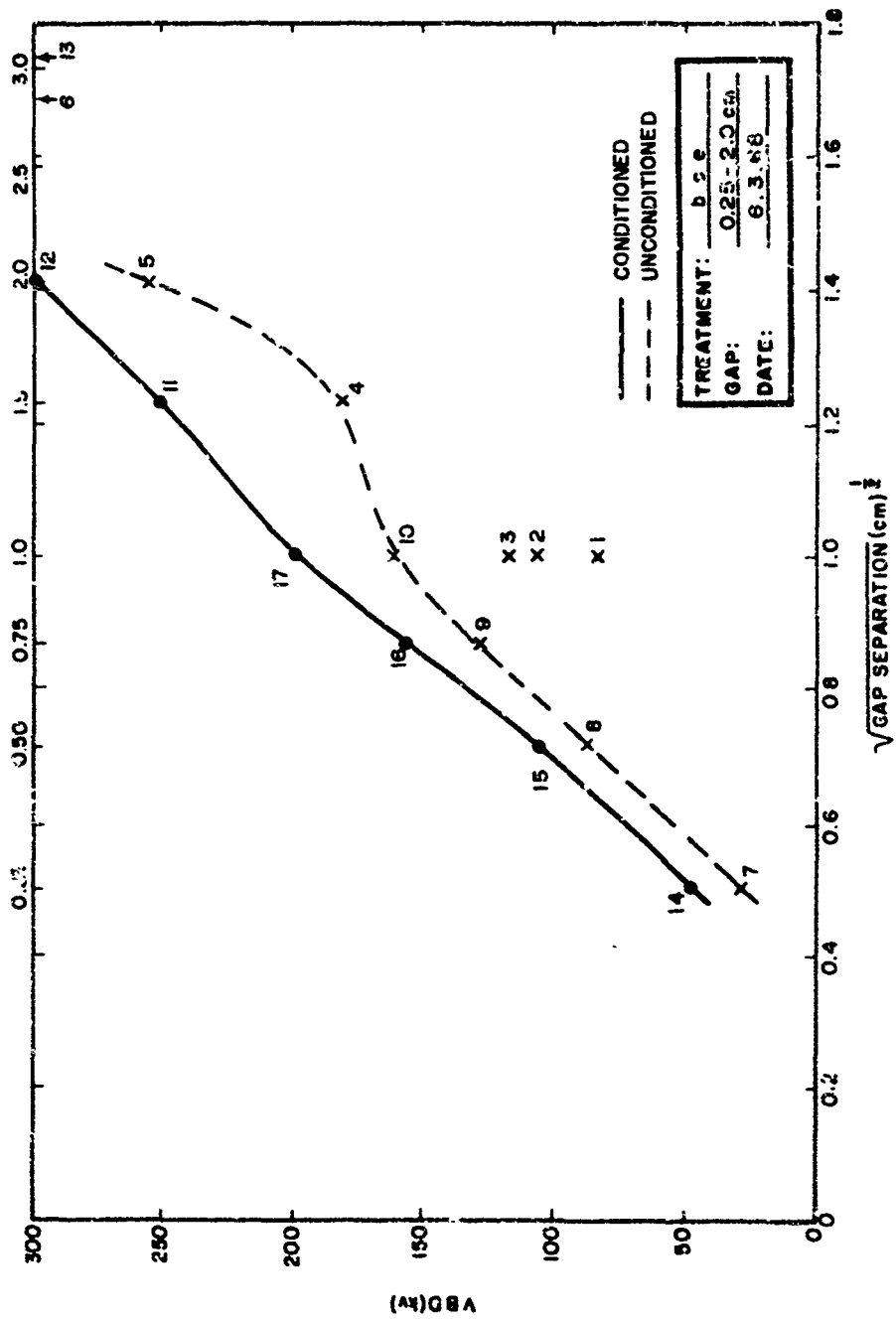
Figure 9-6. Plot Showing Sequence of Breakdowns
(Treatment bce) for Initial Test Series

1-2910
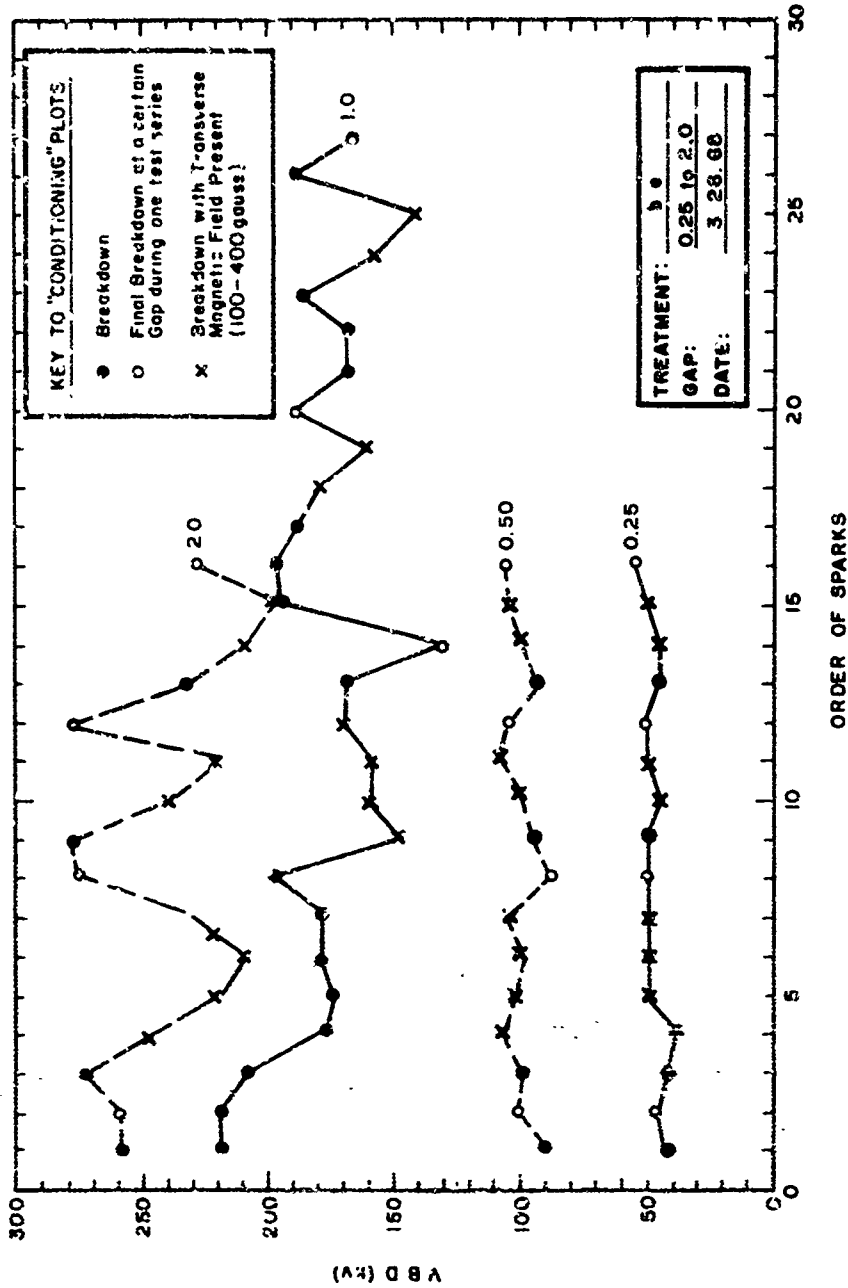
Figure 9-7.   Breakdown Voltage Conditioning Plot
for Treatment be

1-2939
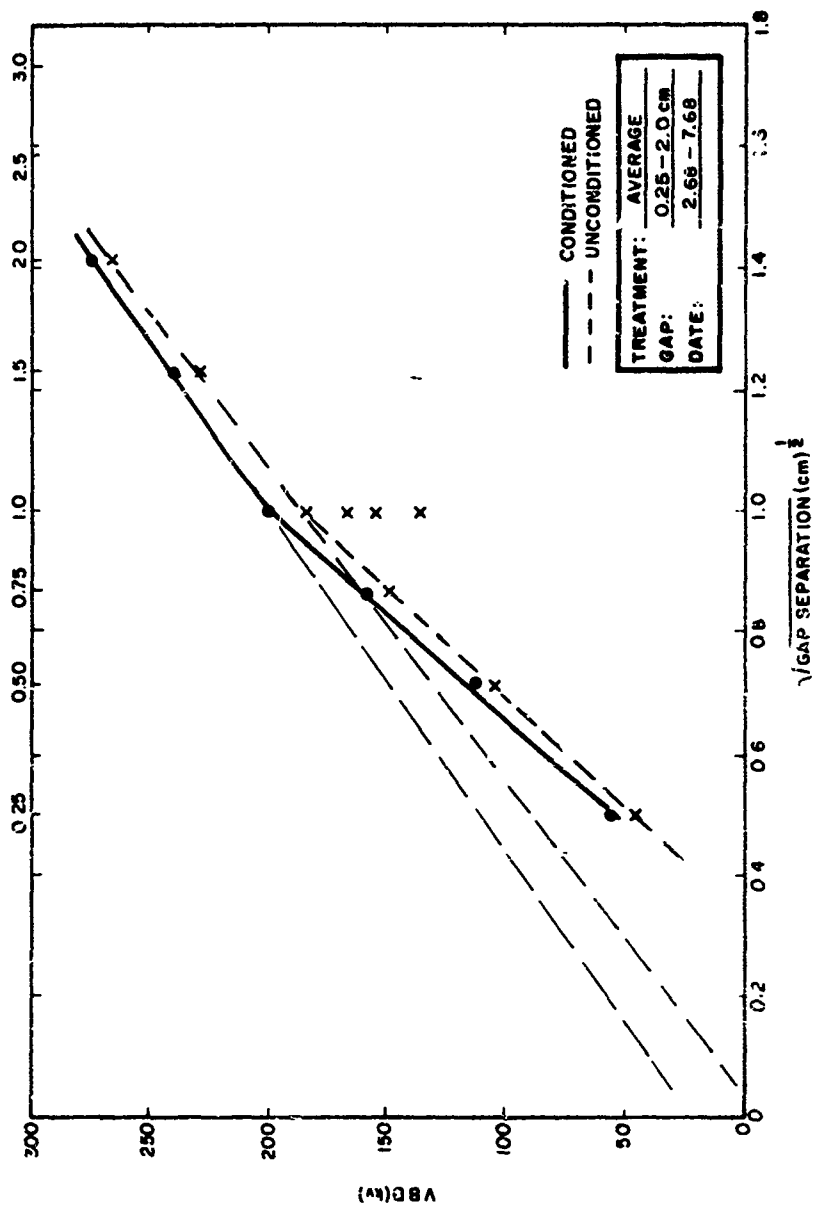
Figure 9-8. Breakdown Voltage vs $(Gap)^{1/2}$ for average of All Treatments with Bruce Profile Anodes-Initial Test Series
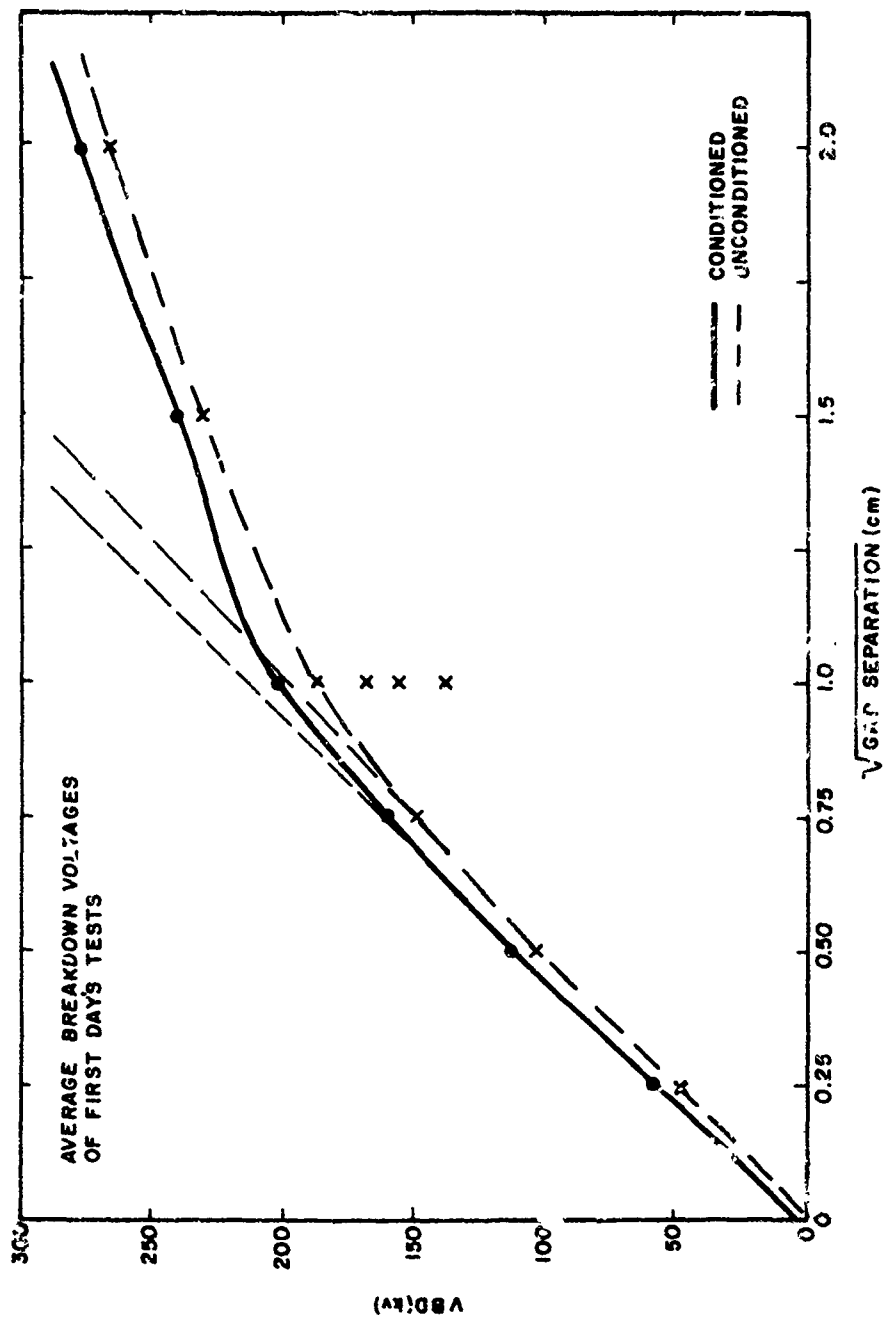
Figure 9-9. Linear Plot of Average Breakdown Voltage
vs Gap for All Treatments with Bruce Profile
Anode-Initial Test Series

1-2932
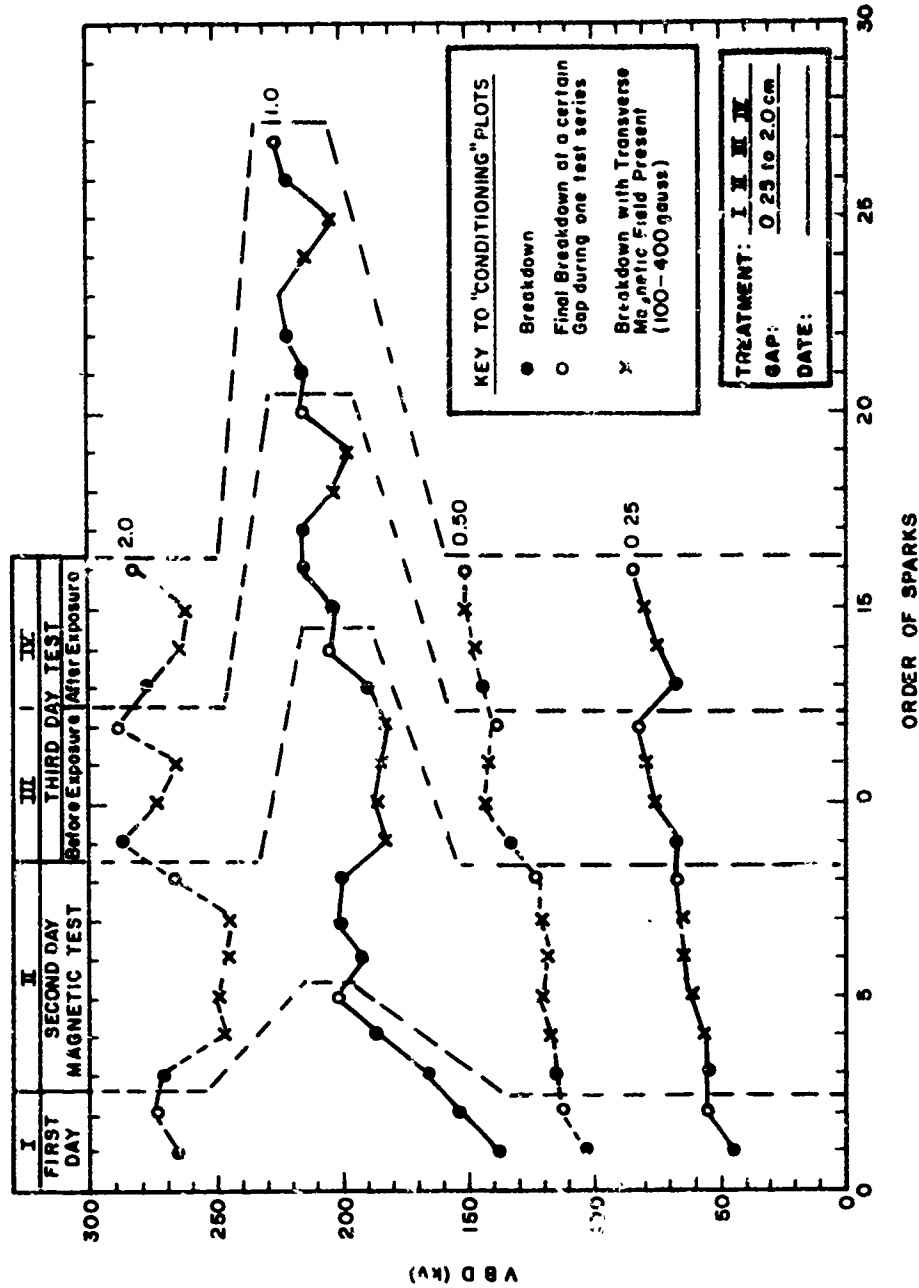
Figure 9-10. Conditioning Plot - Average Breakdown Voltages for Treatments with Bruce Profile Anodes

1-2936
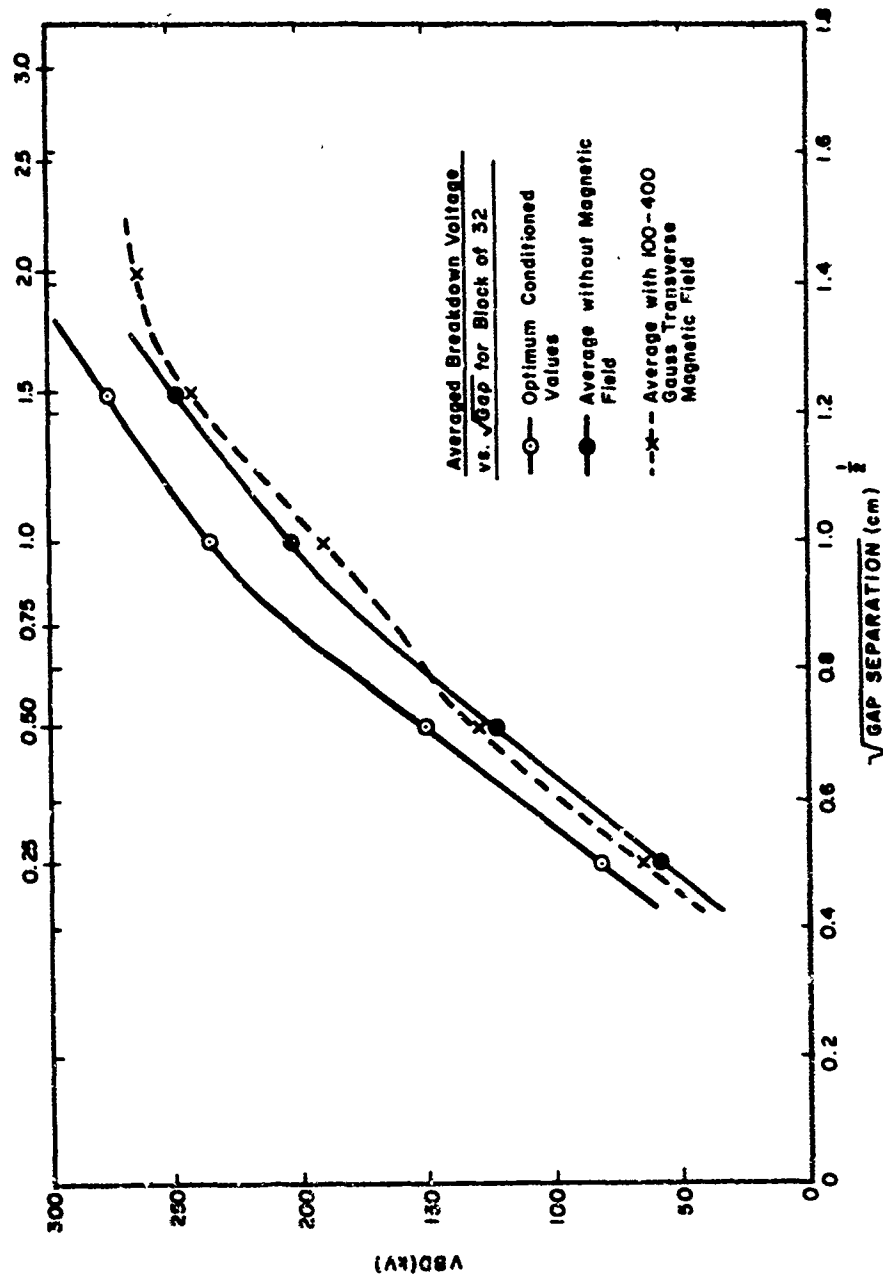
Figure 9-11. Averaged Breakdown Voltages vs $\sqrt{Gap}$ (for Block of Thirty-Two - Effect of Gap and Transverse Magnetic Field

1-3557

breakdown. The effect of this current is to discharge the immediate capacitance of the gap and associated structures. For the conditions of this experiment (series resistance of 80 ohms at the high voltage bushing) it has been observed with a capacitive divider that the voltage collapse has the following features:

(1) Time to total collapse is of the order of hundreds of nanoseconds and increases in an approximately linear manner with gap and in the range 0.25 to 2.0 cm is approximately 400 ns/cm.

(2) Frequently the collapse is interrupted by one or more recovery periods before total collapse.

(3) Variability in characteristic times as measured by standard deviation is over 50% in many cases.

(4) Current flow causing voltage collapse rises very quickly (< tens of nanoseconds) to a peak value of several hundred amperes and decays to zero in about 1.2 μs for R_s = 80 ohms.

Typical oscilloscope traces of voltage collapse are given in Figure 9-12. From many such measurements of 16 representative treatments overall average collapse and recovery times were computed. The distribution of individual times was apparently normal when histograms of the values were plotted. Thus the average is a meaningful parameter and its variation with gap is shown in Figure 9-13. In view of the large (frequently > 75%) variation in collapse times for each treatment a comparison between treatments is not warrented.

Interpretation of the dependence of voltage collapse time upon gap is difficult because little information exists concerning the initiation and transition mechanisms. The approximately linear dependence upon gap and the partial recovery strongly suggest some characteristics transit times for particle exchange (ions - electrons). Alternately the measured time may be a result of a time varying resistivity or equivalent impedance of the gap during

Gap		Treatment	Gap		Treatment
0.25 cm		ae - 100 ns/cm	1.0 cm		c - 200 ns/cm
		cd - 100 ns/cm			ad - 200 ns/cm
0.50 cm		ae - 200 ns/cm	1.5 cm		ac - 200 ns/cm
		a - 200 ns/cm			bd - 200 ns/cm
0.75 cm		b - 200 ns/cm	2.0 cm		c - 200 ns/cm
		ac - 100 ns/cm			ac - 200 ns/cm

Figure 9-12. Voltage Collapse -
Block-of-32

2-1244
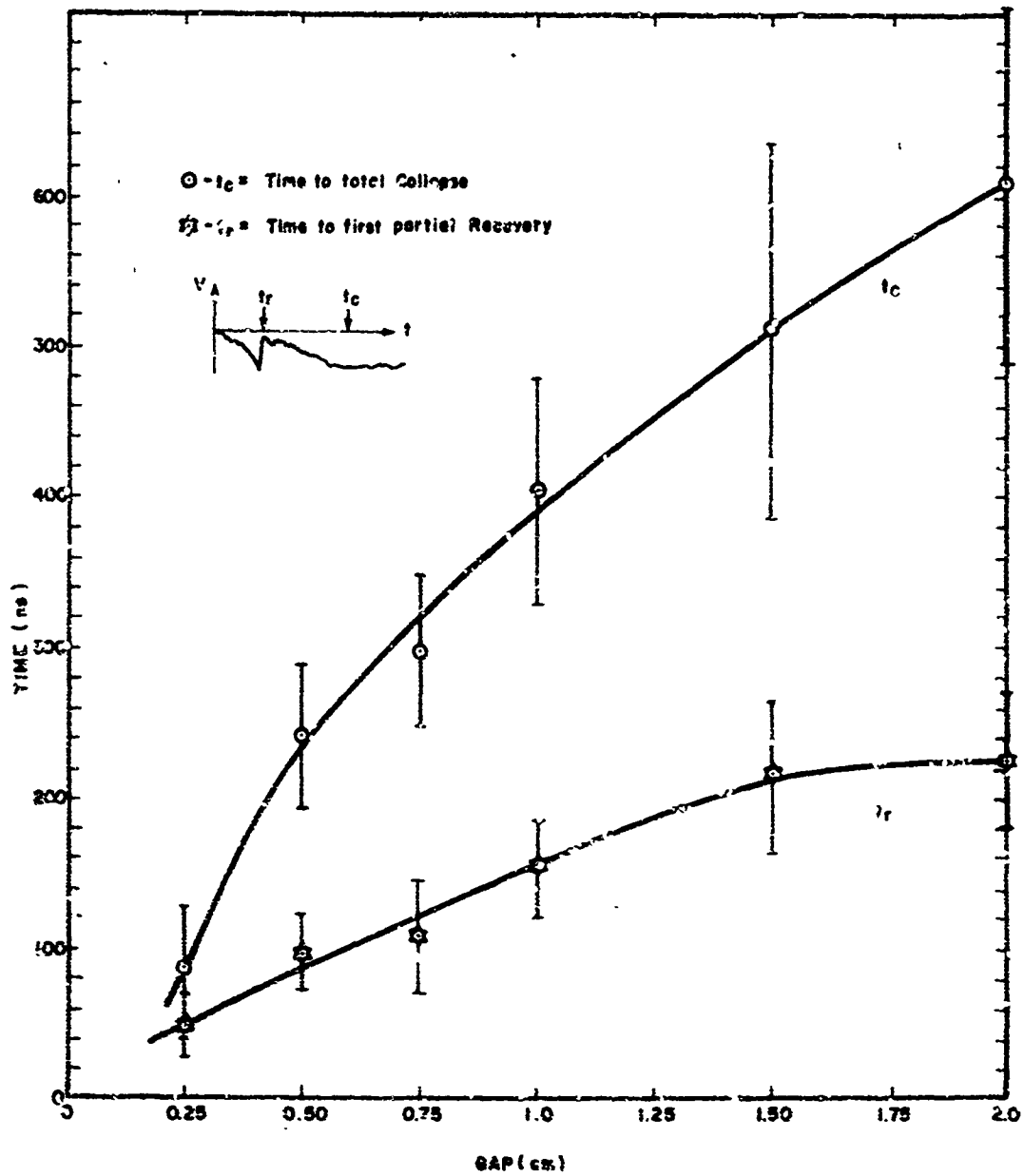
Figure 9-13. Average Time to Voltage Collapse for
Sixteen Treatments from Block-of-Thirty-Two

1-3561

9-24

the initial stages of arc formation. A later experiment, the Energy Conditioning Study, investigates voltage collapse in more detail (see Section 10.6).

9.6 . Effect of Gas Exposure Upon Breakdown Voltage

It is often observed that electrodes which have been suitably conditioned to a high breakdown voltage and subsequently left without stress in a clean high vacuum for periods of tens of hours will again require conditioning to reach the previous voltage level. The usual explanation of this effect stresses the adsorption of gas on the electrode surfaces. For instance a monolayer of nitrogen would be adsorbed in eight hours at 7.5×10^{-10} torr and a monolayer of water vapor at 4×10^{-10} torr. To investigate this effect in shorter times electrodes were deliberately exposed to various gas mixtures at pressures from 10^{-6} torr to atmosphere. This was done at the end of the normal test sequence and thus, with conditioned electrodes.

The lowest level of exposure was to a 20% O_2 - 80% N_2 high purity gas mixture at 10^{-6} torr for 1 minute and was done for treatments with Bruce Profile anodes. Average breakdown voltages taken before and after exposure showed that the effect of this low level exposure was negligible. At the 1.0 cm prime gap the average breakdown voltage before exposure was 217 kV and immediately after exposure was 214 kV.

A much more severe exposure to plant atmosphere at atmospheric pressure for several minutes produced an immediate lowering of breakdown voltage of up to 60%. This type of exposure was done with spherical anodes and averaged results are given in Table 9-6. The 0.25 cm gap, being the first tested after exposure, shows the greatest effect. A second similar exposure is tolerated somewhat better but the level is lower than that before exposure.

Intermediate levels of exposure to high purity N_2 and N_2-O_2 mixtures at atmospheric pressure indicated a slight initial lowering of breakdown voltage. However, conditioning to the original level was usually rapid and the effect of the second exposure was generally negligible in that there was no significant or consistent change in breakdown voltage from the conditioned exposed level (see Table 9-6).

Table 9-6. Average Breakdown Voltages for Exposure Tests - Treatments with Spherical Anodes

		0.25 cm Gap					0.50 cm Gap			1.0 cm Gap		
	Treatment	Before Exposure	After First Exposure	After Conditioning	After Second Exposure	After Conditioning	Before Exposure	After First Exposure	After Second Exposure	Before Exposure	After First Exposure	After Second Exposure
Exposure to Atmosphere (15 psi)	a	113	53	77	78	95	173	125	156	280	219	234
	ac	73	51	68	83	75	144	129	128	217	212	206
	d	68	41	53	54	67	140	121	135	240	224	230
	abd	107	84	--	80	--	179	154	138	275	227	206
	abcd	90	46	--	67	--	172	115	129	282	187	184
	acd	89	65	81	81	94	158	145	147	223	225	200
Exposure* to High Purity N₂ Then N₂ - 80% O₂ - 20% (15 psi)	(1)	101	63	84	66	67	141	138	134	222	223	221
	c	60	56	64	62	65	106	106	108	178	182	189
	bc	101	84	66	74	--	164	142	128	231	221	--
	ad	74	53	67	40	56	161	154	145	245	239	243
	bd	69	62	57	62	64	115	115	122	213	215	210
	acd(R)	61	54	71	67	74	120	121	128	201	196	212
	bcd	75	67	75	62	46	152	144	140	242	225	223
Number of Consecutive Breakdowns Used in Average		6	10	6	10	6	3	10	10	3	10	10

* For these tests, the first exposure was to N_2, the second exposure to the N_2-O_2 mixture.

In summary exposure to atmosphere resulted in significant reduction in breakdown voltage, a reduction that did not disappear with some conditioning. On the other hand, exposure to pure gases (15 psia) in general, had a much smaller effect and conditioning usually brought the breakdown voltage back up up to its original level. Exposure at low pressures (10^{-6} torr) to pure gases had a negligible effect. The difference is probably due to the presence of contamination - solid particles, organic vapors, or water vapor - in the atmosphere which would not be as prevalent in the high purity gases. The inevitable formation of adsorbed layers of gases does not of itself appear to be a seriously degrading factor.

9.7   Effect of Breakdowns on Electrode Surfaces

The electrodes tested in this experiment experienced 90 or more breakdowns distributed over gaps of from 0.25 cm to 3.0 cm. A number of breakdowns in several treatments occurred with an energy storage capacitor bank of 0.15 μF (or up to 6750 J at 300 kV). The initial surface was that produced by rotary polishing with 600 grit silicon carbide paper and consisted of uniform circular grooves approximately 0.01 mm wide. The majc. effects of breakdown were:

(1)   The anode surface directly opposite the cathode is severely burned, melted and eroded as shown in Figure 9-14.

(2)   The cathode surface opposite the anode is covered with deposits of anode material in the form of both discrete clumps and a fine continuous film. These deposits may or may not be accompanied by craters in the cathode material. With energy storage discharges, characteristic arc traces termed "fern-marks" are present. The more obvious features are evident in Figure 9-14.
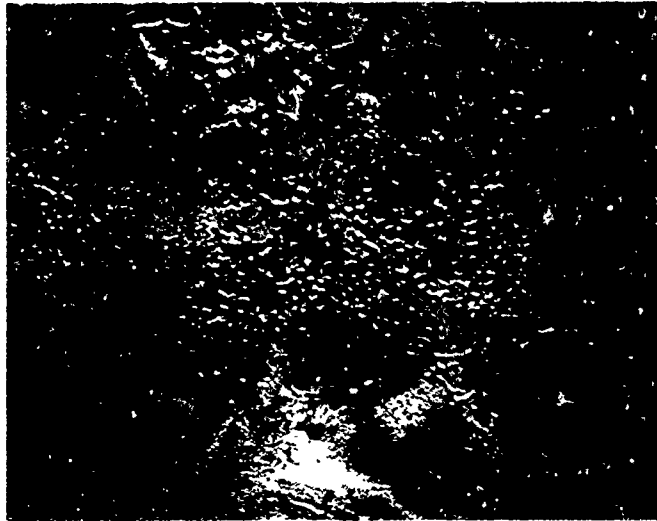
Anode - Treatment e - 10X
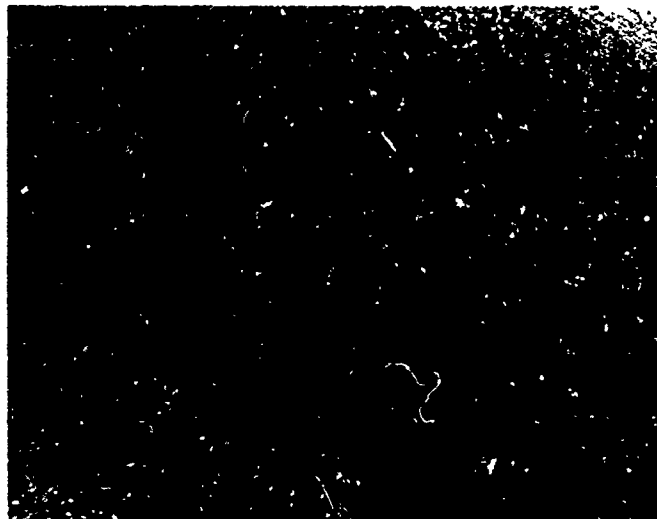
Cathode - Treatment c - 10X

Figure 9-14.Typical Anode and Cathode
Surface Change Features

2-1243

The effects noted above are easily visible and have relatively sharply defined boundaries. The areas involved were measured and found to range from 0.9 to 5.1 cm^2 for anode effects, and from 0.5 to 5.9 cm^2 for cathode effects. These areas may be expected to relate directly to conditioning and their perimeters occur where the electric field, extimated at the 1.0 cm prime gap, has fallen off by 15 to 30% relative to the field in the center. At smaller gaps the percentage change would be greater. The relavent geometries are given in cross-section view in Figure 9-15. On the average anode effects covered a roughly circular area of 1.4 cm^2 for the 1.28 inch spherical anode and 2.2 to 2.3 cm^2 for all other anode sizes and shapes; namely 4-inch Bruce and sphere and 1.28 inch Bruce. Thus, as might well be expected, the constant cathode geometry of a 2-inch diameter sphere confined conditioning to high field regions of the electrodes. Conditioning then appears as a benefical change of anode and cathode surfaces that tends to progressively spread out over the entire highly stressed area.

9.8   Conclusions

The complexity of the effects of factors such as electrode material, electrode size and shape, and final processing in terms of vacuum or hydrogen firing is evident in the results of the Block of 32 Experiment. Those factors which emerged from Factoral Analysis with clear trends were:

Anode Material:	Copper results in approximately 10 to 20% higher breakdown voltages than aluminum.
Cathode Material:	Copper results in approximately 10% higher breakdown voltages than aluminum.
Electrode Processing:	In general hydrogen firing results in higher breakdown voltages than vacuum firing. However the interactions of this factor with electrode material are high, and in some cases aluminum electrodes benefit from vacuum firing.

9-29
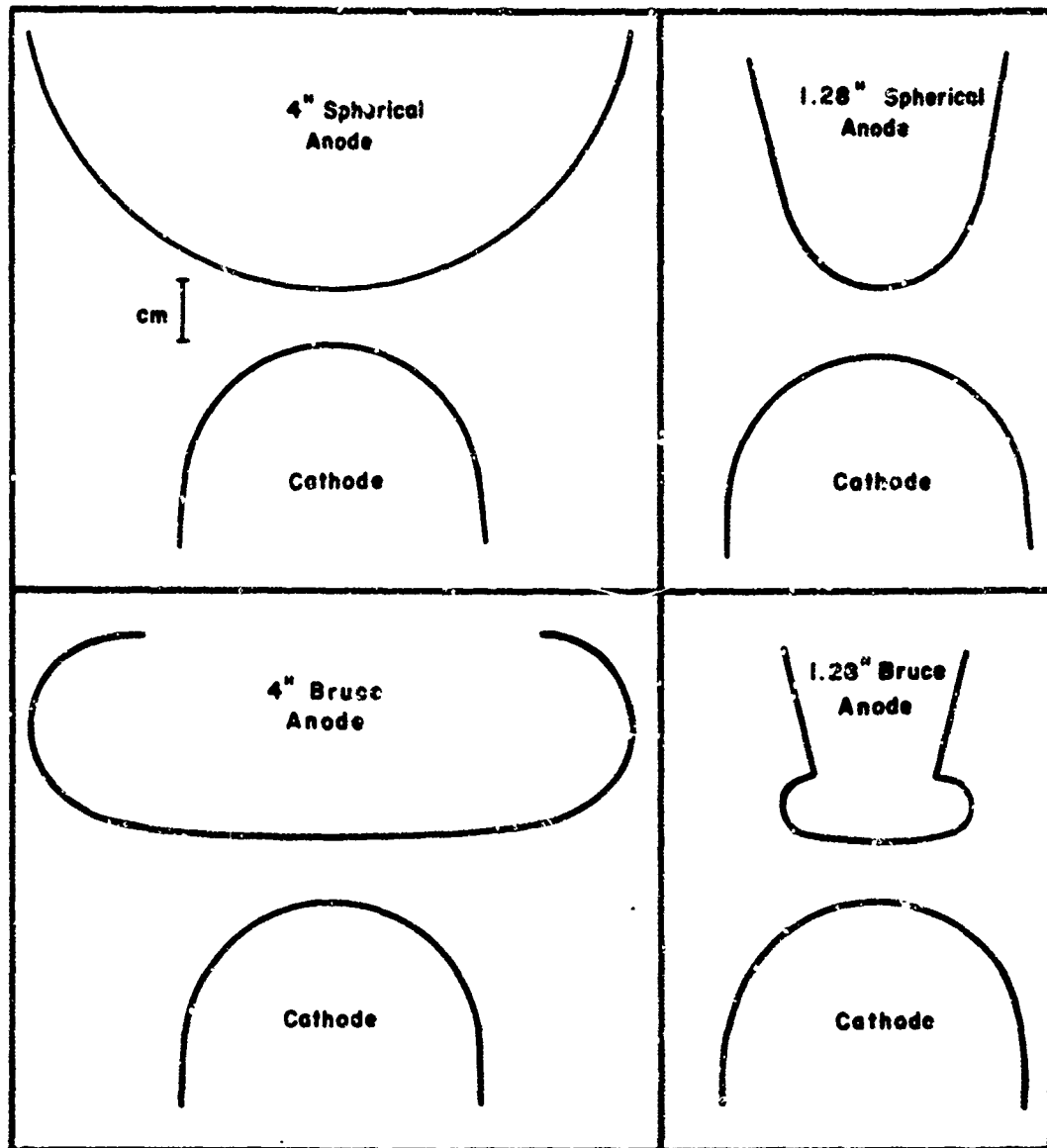
Figure 9-15. Geometrical Factors of Size and Shape for
Block-of-Thirty-Two Cross Section View of Electrode
Pairs at 1. 0 cm Gap

1-3558

9-30

The factors of anode size and shape exhibited no simple influence, and thus a short interpretation of their effects is not possible.

Breakdown voltage was found to depend linearly upon gap for small gaps (<.75 cm) and to follow a square root dependence for larger gaps (>.75 cm). Similarly a transverse magnetic field of up to 400 gaus: raised the breakdown voltage for small gaps and lowered it for large gaps.

Conditioning was identified as probably the most important consideration and the next experiment examines this in greater detail by including the energy available to each discharge as a factor (see Figure 9-16 for the result of a preliminary exploration). Gas exposure was found to have a severly degrading effect if it included contamination such as is present in the normal factory environment but not if it is restricted to pure gases such as oxygen and nitrogen, even up to atmospheric pressure.
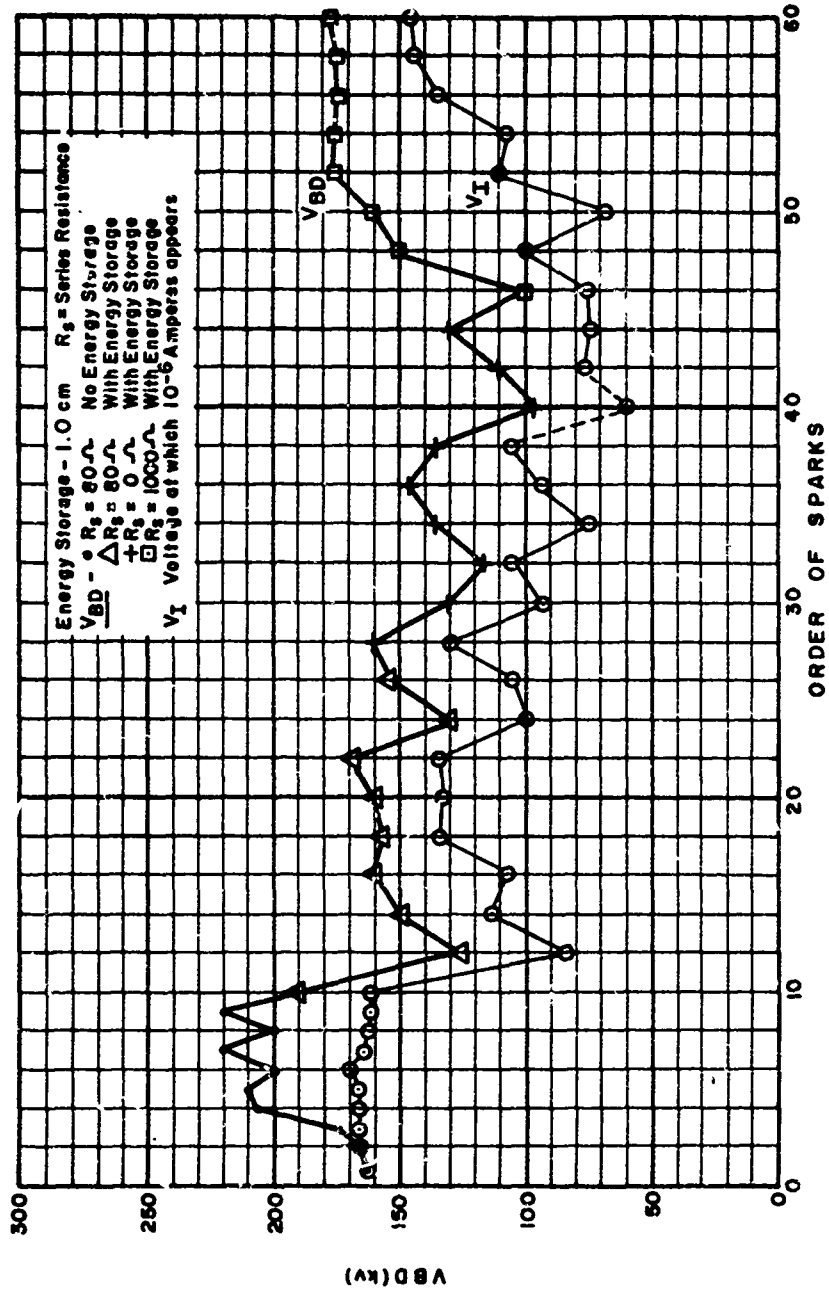
Figure 9-16. Preliminary Energy Conditioning Sequence at 1.0 cm Gap for Aluminum Electrodes (Treatment c)

1-3564a

SECTION 10

ENERGY CONDITIONING STUDY

10.1   Introduction

High voltage vacuum devices almost invariably require a series of conditioning discharges to reach operating voltage levels. Even after conditioning there will be infrequent breakdowns. Such spurious breakdowns are troublesome but not necessarily intolerable if there is no deterioration in subsequent performance. However, most high voltage, high power vacuum tubes operate with considerable energy available to any discharge. Then the effect of a spurious breakdown may be catastrophic, leading to low breakdown voltages, high prebreakdown currents, loss of vacuum, or mechanical damage.

The energy conditioning study investigated in detail conditioning with discharges having available energy levels of from ~ 50 joules to 6750 joules over a range of electrode materials and sizes for uniform field geometry. Further control of discharge characteristics was provided by series resistance variations (from 25 ohms to 30 kilohms) and a fast crowbar which could divert energy from the vacuum gap within 500 ns of the initiation of the discharge.

10.2   Experimental Design

The basic experimental series follows a three factor two level full factorial design as given in Table 10-1. Copper was chosen as an anode material since it is widely used for that purpose by the electron tube industry due to its excellent thermal properties. Refractory metals were used for cathode materials; nickel because it is already extensively used and titanium alloy because of its superior performance in the Pilot Experiment. The factorial design was later extended to include additional material combinations. Vacuum firing served as a controlled final processing for all electrode materials.

Table 10-1. Experimental Design - Energy Conditioning Study

Factorial Design

Factor	High Level	Low Level
A High Impedance Conditioning	With	Without
B Electrode Size	4 inch Diameter	1.28 inch Diameter
C Cathode Material	Ti-7 Al - 4 Mo	Nickel

Anode: OFHC Copper

Electrode Geometry: Bruce Profile for Uniform Field

Surface Finish: 600 Grit SiC

Final Processing: Vacuum Firing at 900°C for 6 hours.

Bakeout: Chamber at 375°C for 6 hours, Electrodes at 500° for 6 hours.

Initial Test Gap: .75 cm

Test Sequence: See Table 10-2

Specification of Treatments

Treatment	High Impedance Conditioning	Electrode Size	Cathode Material	Date Tested	Date Replicated
(1)	Without	1.28 Inches	Ni	2/3/69	3/3/69
a	With	1.28 Inches	Ni	2/18/69	-
b	Without	4 Inches	Ni	1/20/69	2/24/69
ab	With	4 Inches	Ni	1/27/69	6/2/69
c	Without	1.28 Inches	Ti	4/21/69	-
ac	With	1.28 Inches	Ti	3/24/69	3/31/69
bc	Without	4 Inches	Ti	3/17/69	-
abc	With	4 Inches	Ti	3/10/69	4/7/69
ab-Cu*	With	4 Inches	Cu	4/14/69	-
ab-Ti*	With	4 Inches	Ti	4/28/69	-
ab-Ni*	With	4 Inches	Ni	5/12/69	-

*These treatments are extensions of the basic factorial design in that the anode material was the same as the cathode material rather than being copper in all cases.

A fixed gap of 0 75 cm was chosen as the prime gap because conditioning at this gap at various energy levels produced breakdowns from 35 kV to 300 kV. Thus, a single gap setting covered the entire voltage range of the 300 kV apparatus.

The factor of high impedance conditioning was merely the first of five combinations of energy and series resistance. The sequence is specified in Table 10-2 where a brief motivation for each series is given.

Voltage was applied in either a slow ramp (about 5 kV/s) or in steps of 10 kV each minute. The circuit pertinent to this study has been given in Figure 3-5. Voltage, prebreakdown currents, pressure surges, voltage collapse waveforms, and breakdown current waveforms were observed. Before each day's testing the bushing was conditioned to 300 kV with the gap set at 5.0 cm.

10.3   Effect of Energy Conditioning on Breakdown Voltage

The extended sequence of breakdowns during which the available energy and series resistance was varied over a wide range provided information regarding the following:

(1)   Typical response of metal electrodes to many high energy discharges.

(2)   Role of high impedance conditioning as opposed to high energy conditioning in obtaining high breakdown voltage levels.

(3)   Effectiveness of fast crowbarring in maintaining high breakdown voltage levels during high energy discharges.

(4)   The critical levels of energy and/or series resistance, i.e. what is the maximum energy or current that an electrode system can tolerate without degradation?

Conditioning curves in which the breakdown voltage is plotted as a function of breakdown sequence provide a convenient way of reporting the response of an electrode system to energy conditioning discharges. Figures 10-1 through 10-3 give the results for representative treatments.

10-3

Table 10-2. Experimental Sequence for Energy Conditioning Study

Series	R_S	Energy Storage	Purpose	Number of Discharges
Initial	30 K ohm	Absent		
1	30 K ohm	Absent	**High Impedance Conditioning:** Limited energy discharges produce a smooth but significant (50% or more) increase in breakdown voltage level.	90
2	1000 ohm	Present	**Moderate Energy Conditioning:** Sufficient energy and rate of flow of energy produces significant changes in conditioning performance, but not so much that permanent damage occurs. This provides initial energy conditioning	90
3	25 ohm	Present	**Energy Discharge:** High Energy discharges with relatively little protective resistance damage the electrodes, this stage simulates failure of a high power tube under operating conditions.	9
4	1000 ohm	Present	**Moderate Energy Reconditioning:** Recovery characteristics of the damaged electrodes are determined with moderate energy discharges.	45
5	30 K ohm	Present	**High Impedance Conditioning with Energy:** Reconditioning and performance with energy available through a high impedance usually restores the breakdown voltage level to approximately the initial conditioned value or higher.	45
6	25 ohm	Present	**Energy Discharge:** A second damaging series of discharges simulate tube failure.	9
7	30 K ohm	Present	**High Impedance Reconditioning with Energy:** Recovery is again investigated and the electrodes are partially reconditioned.	45
8	125 ohm	Present	**High Energy Discharges with Crowbarring:** Energy storage discharges with little protective resistance would normally damage the electrodes. A fast high pressure gas crowbar (~ 500 ns) diverts energy to ground from the capacitor bank that would otherwise participate in the discharge. The objective is to determine the protection offered the electrodes by crowbarring.	90
9	125 ohm	Absent	**Limited Energy Investigations:** Various gap and transverse magnetic field levels are explored with low energy discharges.	--

Note: Treatments with High Impedance Conditioning (high level factor A) will follow above sequence, those without High Impedance Conditioning (low level factor A) will omit Step 1. As a means of establishing control 3 breakdowns under High Impedance Conditions precede Step 2 for low A treatments. Normally the tests are divided among the available days as follows:

Day 1 - Step 1   Day 3 - Steps 5, 6, 7, (8)

Day 2 - Steps 2, 3, 4   Day 4 - Steps (8), 9

Each day's testing begins with 9 breakdowns with the previous day's final circuit.
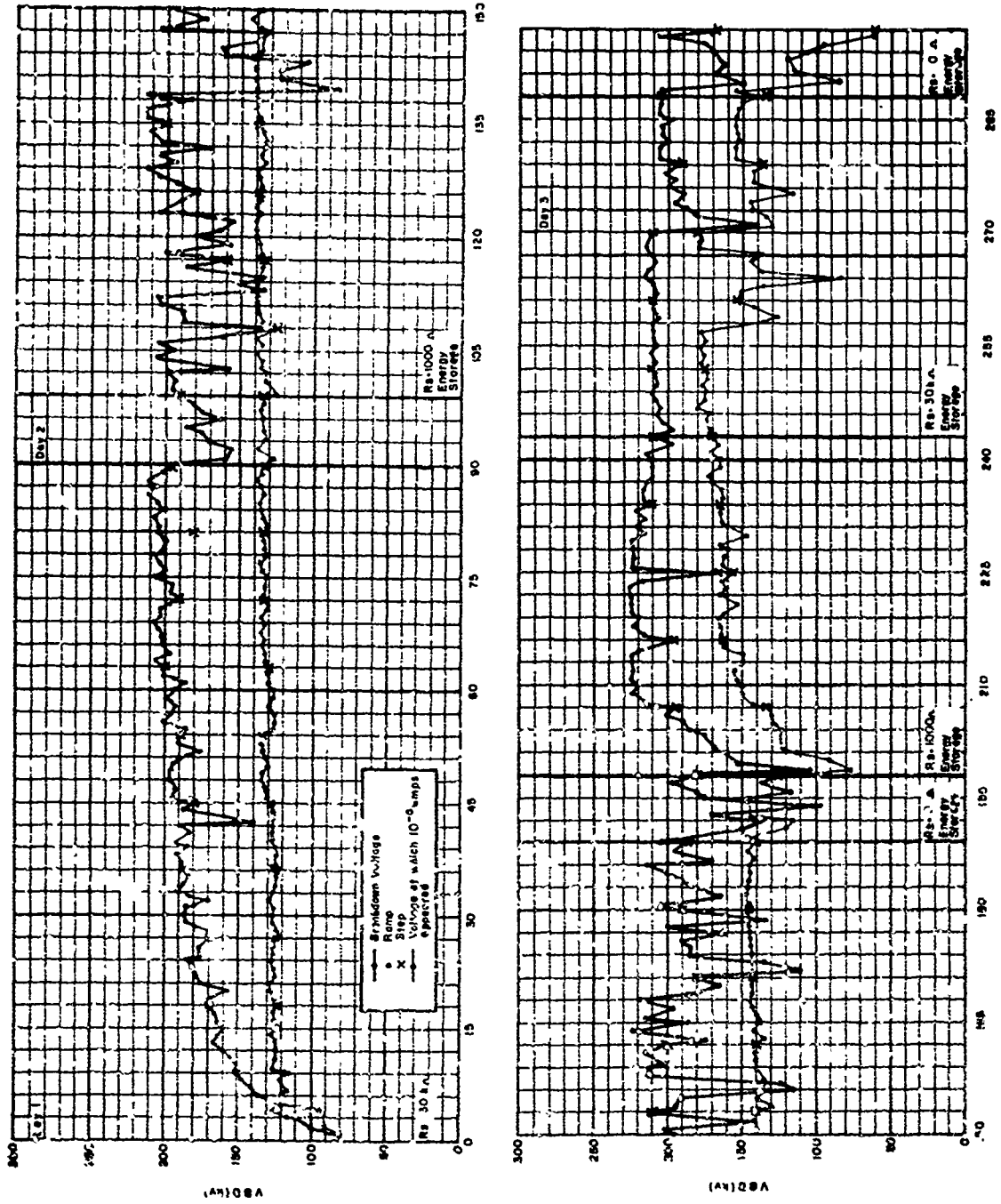
Figure 10-1. Energy Conditioning Curve for Treatment abc.
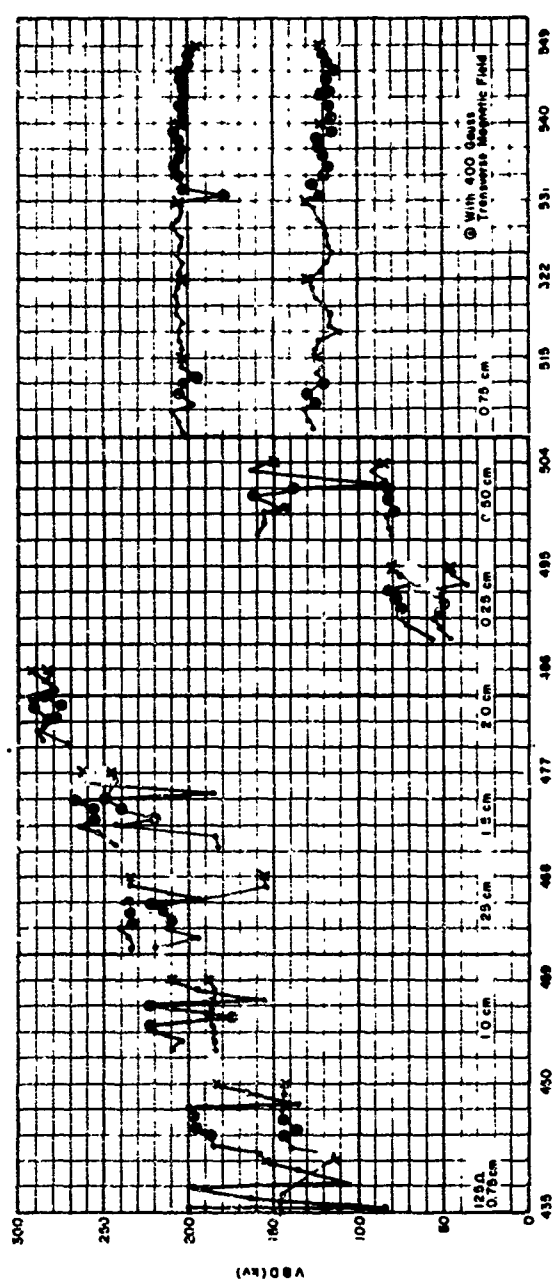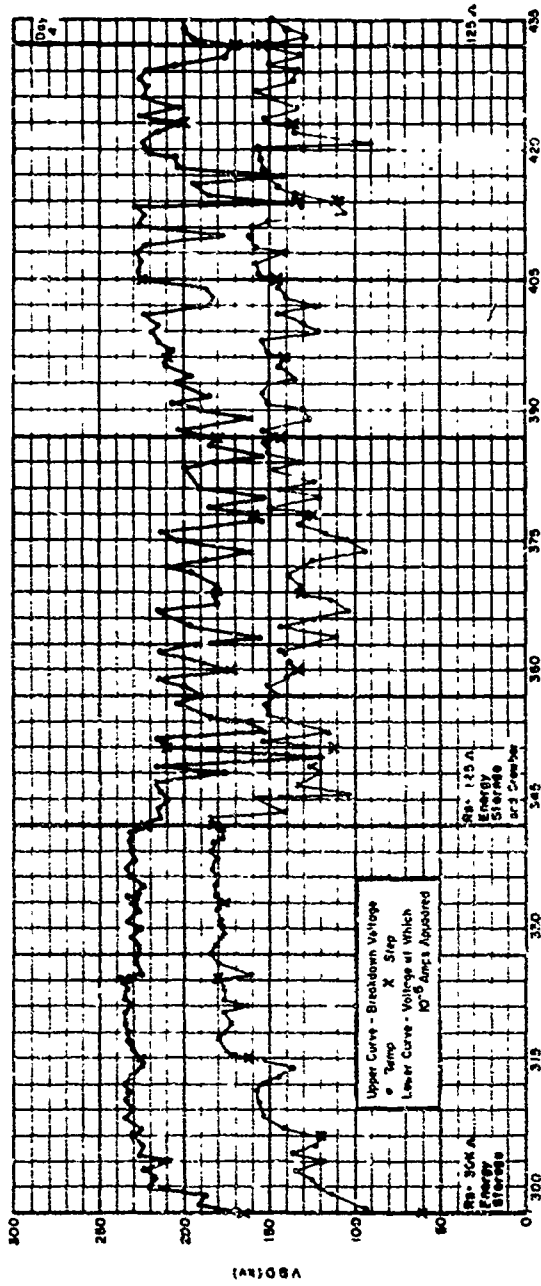
Figure 10-1. Energy Conditioning Curve for Treatment abc (continued)
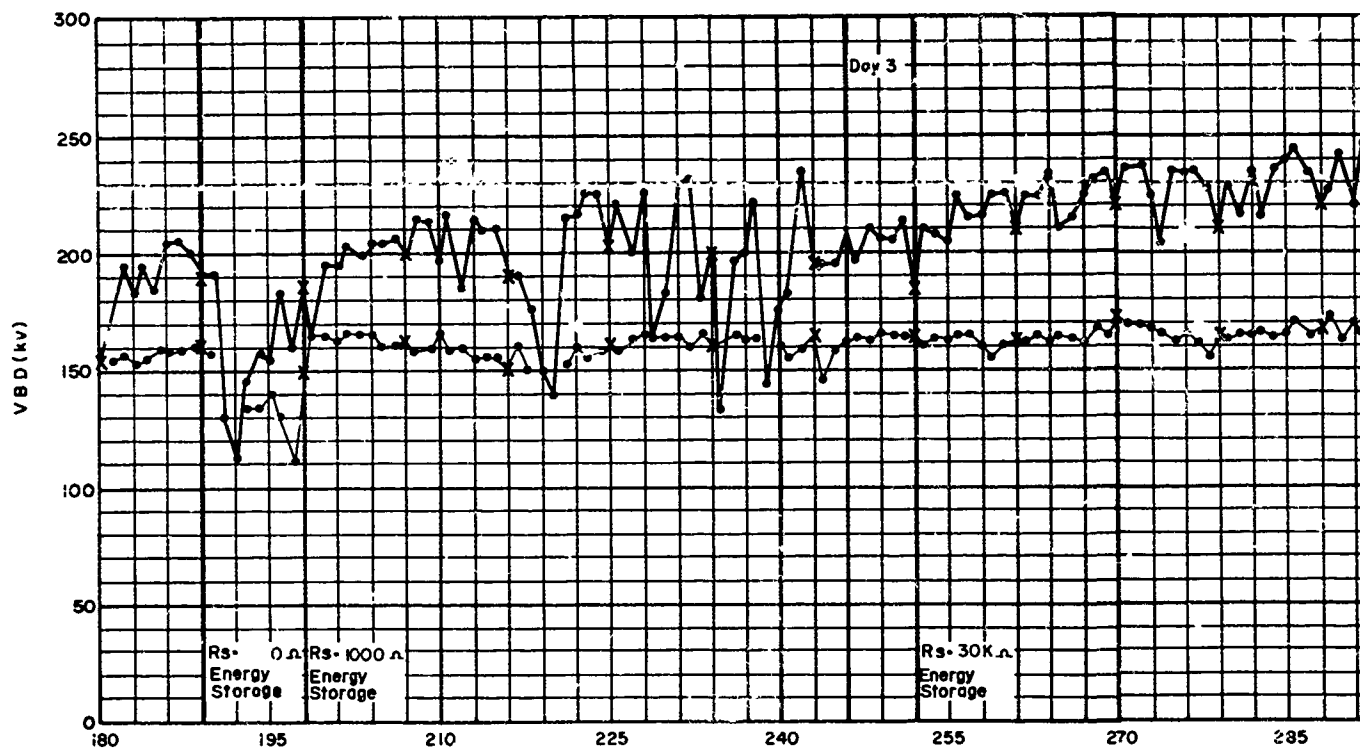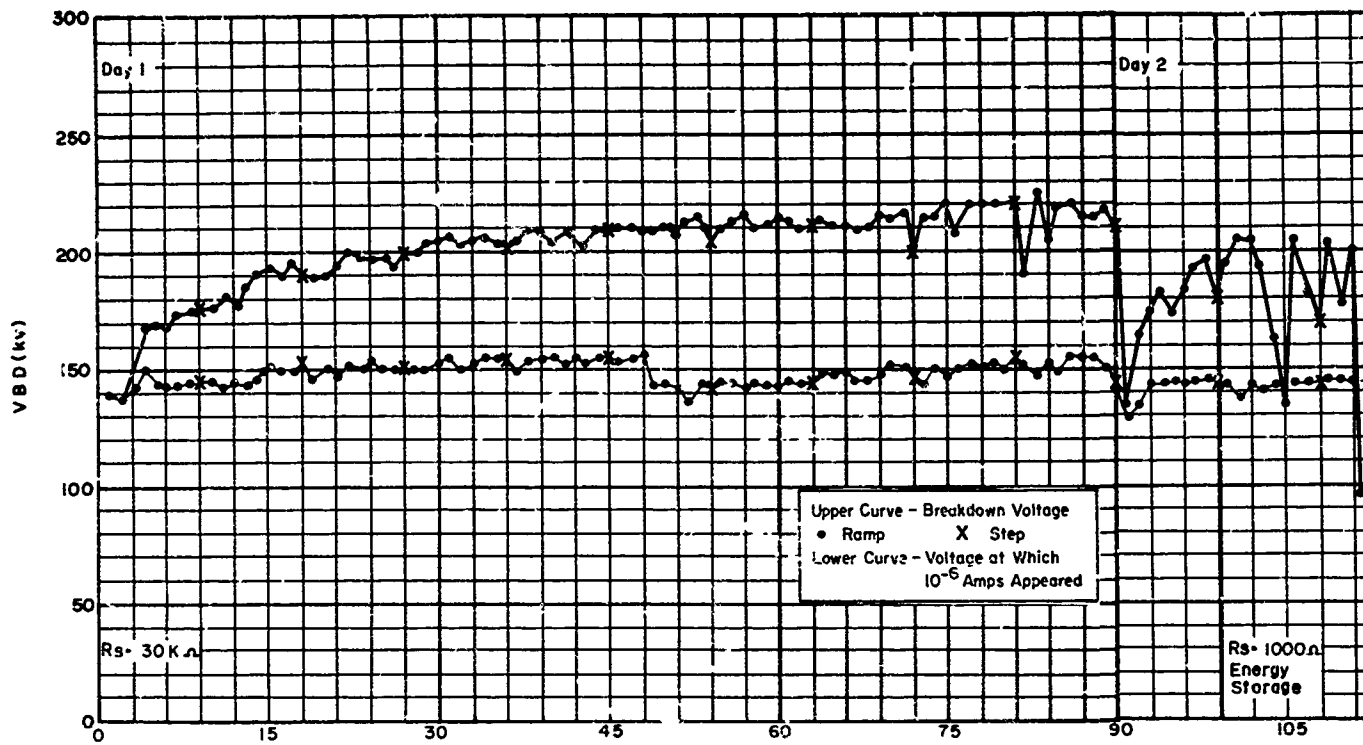
1-3827
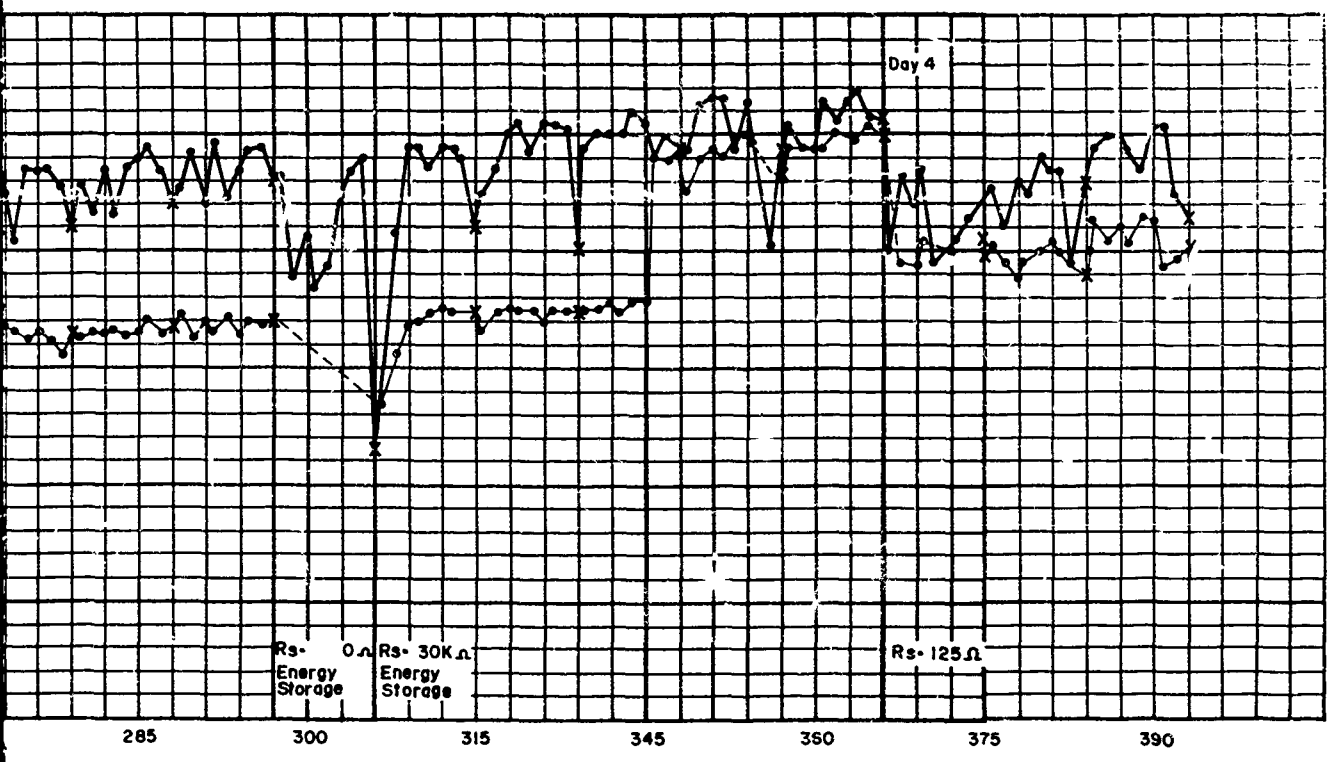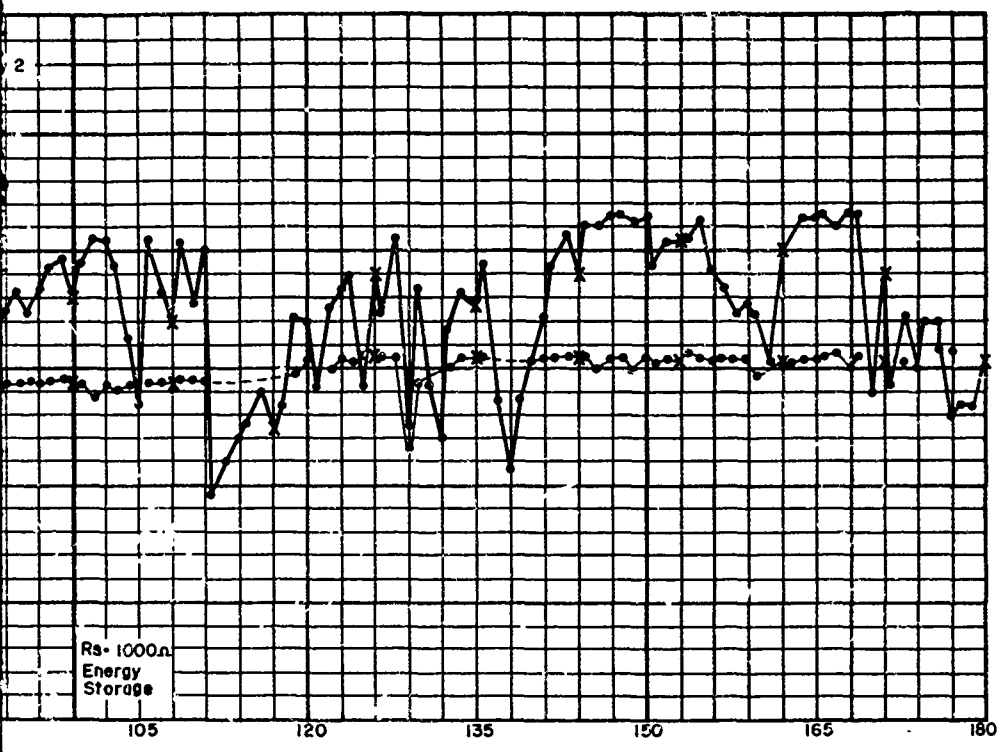
Figure 10-2. Energy Conditioning Curve
for Treatment ab-Ti

10-7
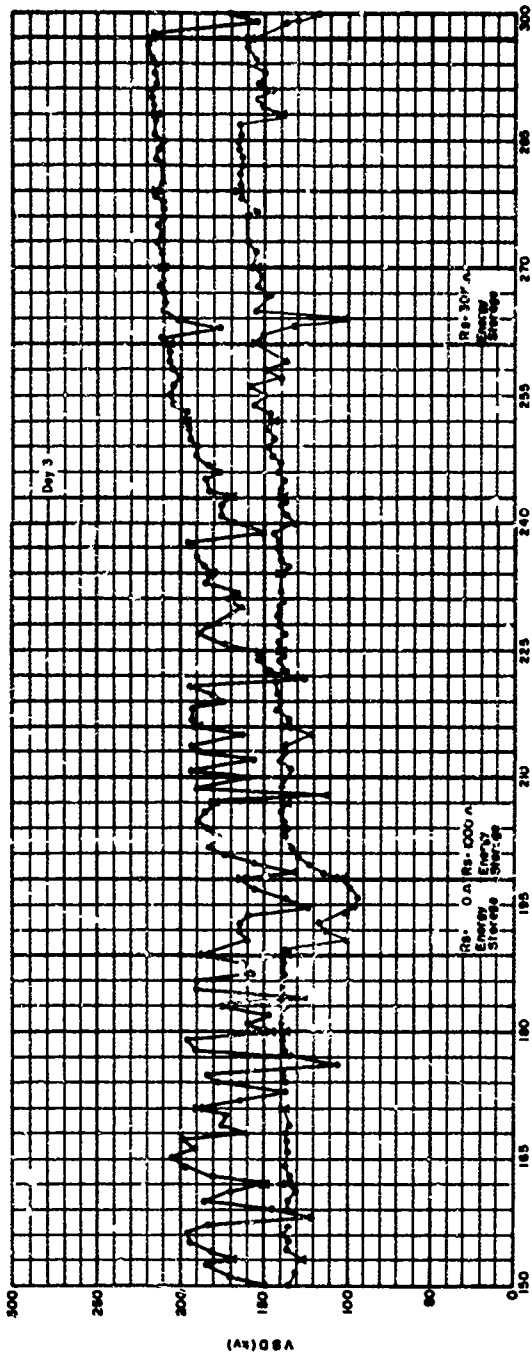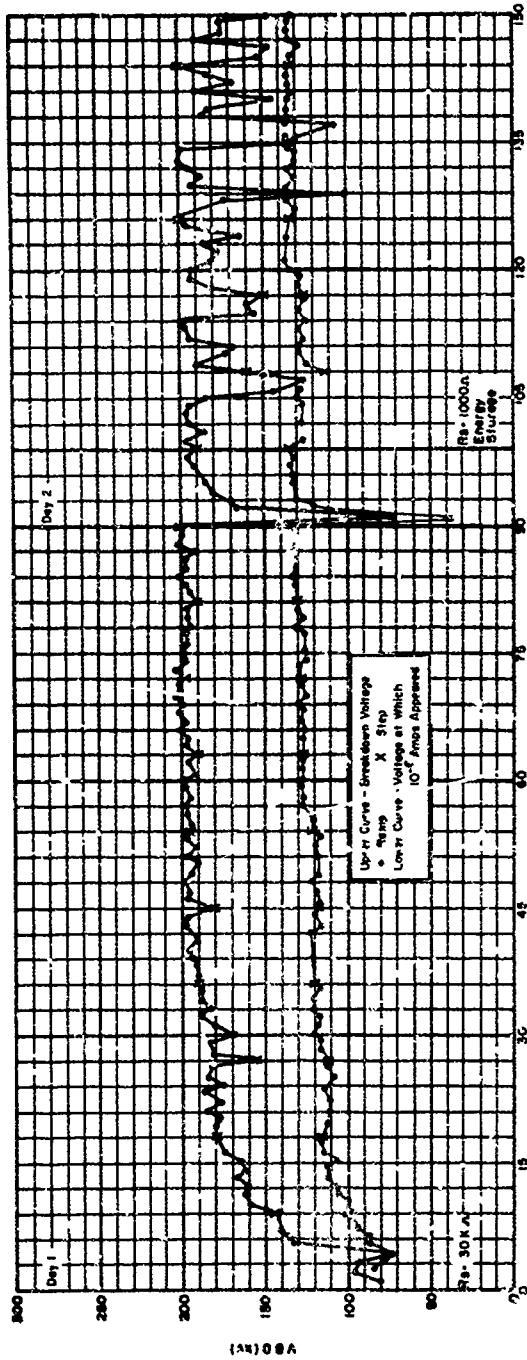
Figure 10-3. Energy Conditioning Curve for Treatment ab(R)
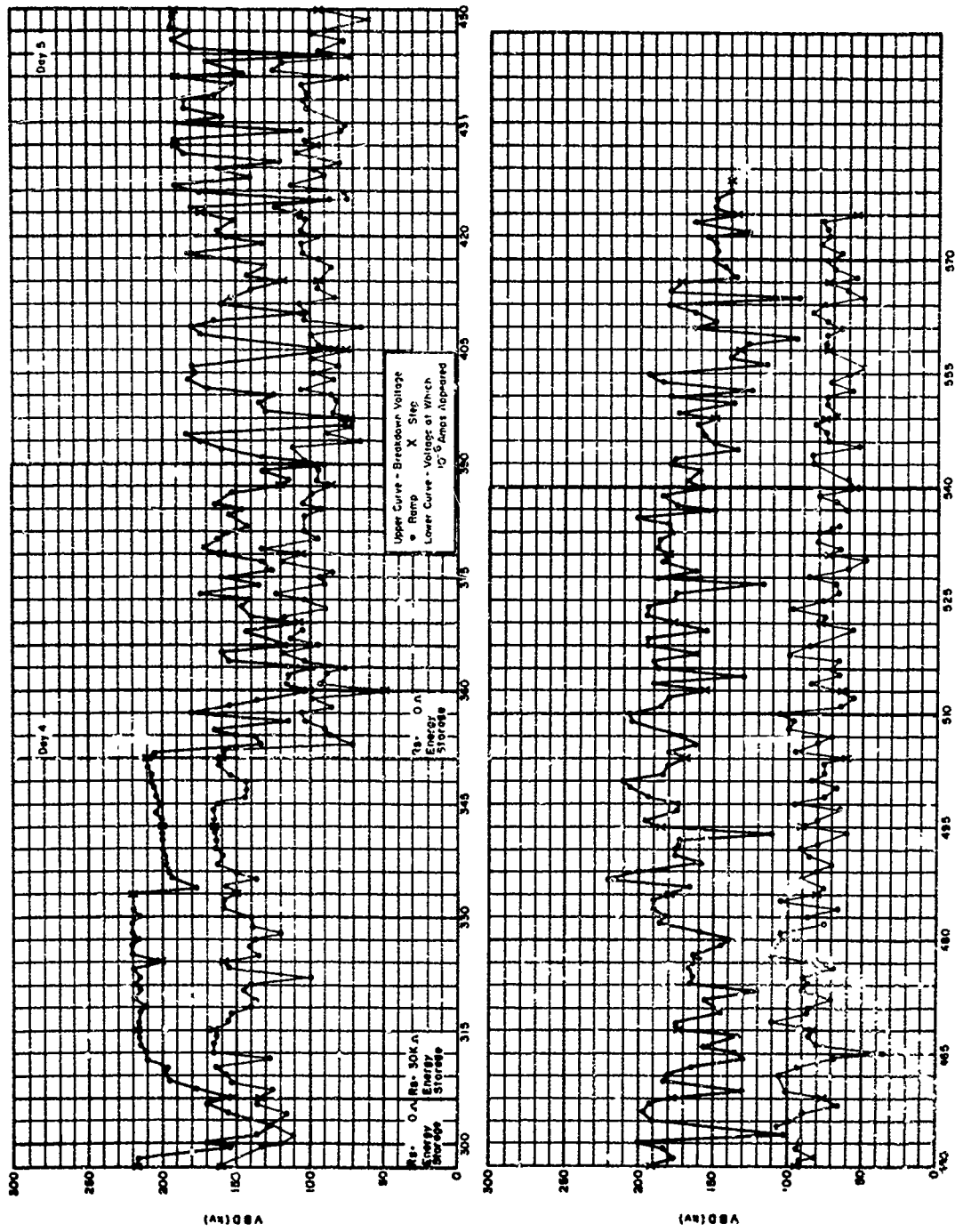
1-3817

Figure 10-3. Continued

Included is the voltage at which 10^{-6} amperes of prebreakdown current occurred as breakdown was approached. This gives a rough estimate of emission characteristics and is further discussed in Section 10.5

While individual treatments differ in their response to the conditioning sequence, the differences are concerned with level only and do not change the trends noted for energy conditioning. Thus, a reliable simplified description of energy conditioning phenomena can be obtained by averaging breakdown voltage levels from the eight basic factorial treatments. Figure 10-4 gives such a simplified conditioning curve in which breakdown voltage appears as a function of the electric circuit parameters of energy storage and series resistance.

The initial breakdown level for unconditioned electrodes was about 140 kV. High impedance conditioning (HIC), i.e., 90 discharges with 30 kilohms series resistance, raised the average breakdown voltage to 202 kV. However, the subsequent moderate energy conditioning (MEC), series of 90 discharges with 1 kilohm series resistance and 0.15 μF capacitive energy storage reduced this to 187 kV. The above procedure was followed for half of the treatments. For the remainder, the unconditioned electrodes were immediately subjected to the MEC series and yielded an average breakdown voltage of only 174 kV. The scatter as measured by the standard deviation was 4.5% for the HIC series and increased to about 14% for the MEC series, with or without previous HIC. The subsequent conditioning sequence was the same for all treatments.

At this point HIC had produced higher breakdown voltages but had not reduced scatter. The next series was one of high energy discharges intended to simulate failure of a high power vacuum tube under operating conditions. The overall average breakdown voltage dropped to 145 kV with occasional values as low as 35 kV. There was no apparent dependence of this minimum level on initial HIC.

Subsequent reconditioning under moderate energy discharge conditions (1 kilohm, Energy, Storage) brought the average breakdown voltage level to 197 kV for MEC electrodes and to 205 kV for HIC electrodes. This
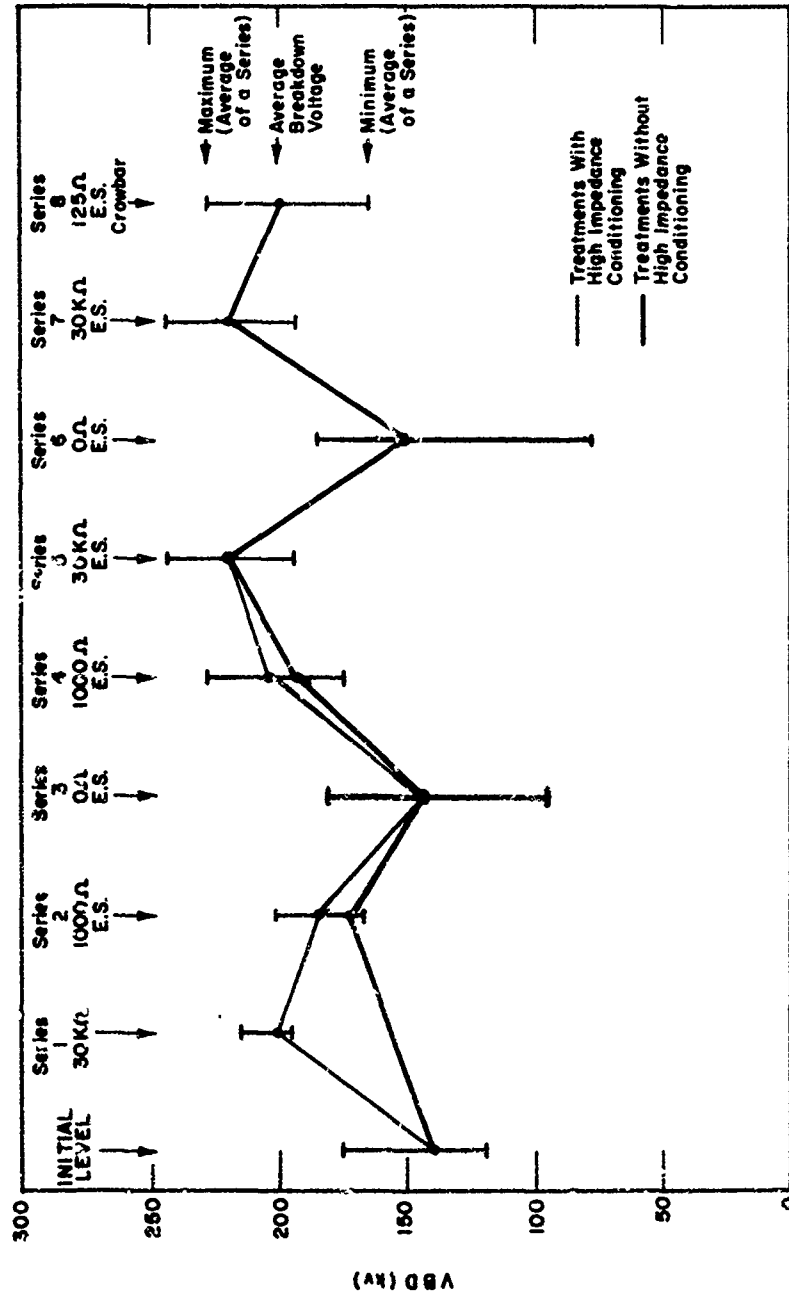
Figure 10-4. Typical Energy Conditioning Performance - Average Breakdown Voltage Level as a Function of Electric Circuit Parameters of Energy Storage and Series Resistance

1-3216

difference is only 4% and is, therefore, probably not significant. The scatter was a few percent less than in the previous case, and a more interesting result was the general increase in breakdown voltage after a "failure".

The next series of discharges investigated high impedance (30 kilohms) conditioning with energy storage. The sharply reduced scatter (< 4% on the average) and high average level of breakdown voltage (220 kV) indicates that this series impedance is sufficient to eliminate the usual degrading effects of energy storage. Other tests showed that the series resistance can be as low as 5 kilohms and still produce performance typical of high impedance conditioning .

A second high energy discharge series produced average breakdown voltages of 151 kV However, high impedance conditioning rapidly restored the average breakdown voltage level to the former level of 220 kV. Thus, it appears that no permanent damage was done and also that conditioning was complete in that the highest stable level of the sequence was attained.

The effect of fast crowbarring (diversion within 500 ns) was next studied with a series resistance of 125 ohms and energy storage. Under such conditions crowbarring seems to have been partially effective and the average breakdown voltage level dropped by only 10% to 201 kV. However, scatter increased to about 15% on the average.

This typical behavior outlined above indicates that many high energy discharges can be endured without permanent damage, that high impedance conditioning is helpful in quickly reaching high breakdown voltage levels, that crowbarring within 500 ns is partially but not totally effective in limiting damage due to high energy discharges and that a series resistance of ~ 5 kilohms is required to limit the damage due to energy storage to a negligible level.

The standard energy conditioning sequence purposely limited the number of highly damaging discharges to a small number so that the sequence necessary for factorial analysis could be completed. It is of interest, however, to know the long term response of electrodes to high energy discharges. For this purpose several treatments were subjected to an extended series of high

energy discharges (24 ohms, Energy Storage) at the end of the standard test sequence. One such series is given in Figure 10-3 for electrodes consisting of a copper anode and a nickel cathode. This resulted in low breakdown voltages and a high emission level. Similarly tested titanium alloy electrodes showed a much better tolerance of high energy discharges (see Figure 10-5). In this case there was, after an initial and severe decline in breakdown voltage, a stabilization in breakdown voltage level and a decrease in emission, as shown by the increasing voltage necessary to produce 10^{-6} amperes.

A tentative conclusion is that the titanium anode is responsible for vastly improved tolerance of high energy discharges. This is explored further in Section 10.9.

10.4   Factorial Influences on Breakdown Voltage

High impedance conditioning, cathode material, and electrode size were investigated at two levels each in the basic factorial experiment. Anode material was later included in an extended series.

High impedance conditioning, as noted in the previous section, was the initial conditioning series and was specified as present for only half of the treatments. The remaining treatments, after three initial control breakdowns were immediately subjected to moderate energy conditioning (1000 ohms, Energy storage). Thus the factorial estimate relating to high impedance conditioning deals with its effect on breakdown voltage level during the subsequent conditioning series No. 2 through No. 9. These series have been defined in Table 10-2.

Before a factorial analysis can be carried out reliable measures of the performance of each treatment must be obtained. Thus average breakdown voltages were computed for portions of the conditioning curves which exhibited no upward or downward trend. In this way the average levels represent the stable response of the electrodes to discharges of various energy and series resistance levels. A measure of scatter is derived by computing the standard deviation of the values used in the average. The results are given in

DAY I

Upper Curve - Breakdown Voltage
● Ramp   X Step
Lower Curve - Voltage at which
10^{-6} Amps Appeared

VBD(kv)

300
250
200
150
100
50
0

15   30   45   60   75   90

Rs = 30 k ohm

Withstand Te
Time and numb
of Breakdown
230 kV
220 kV
210 kV

5min 5min
10min 2 B/D   2 B/D
4 B/D
10min
0 B/D

VBD(kv)

300
250
200
150
100
50
0

190   205   220   235   250   265

Ramp

Withstand   Wit

BREAKDOWN ORDER

1-4263
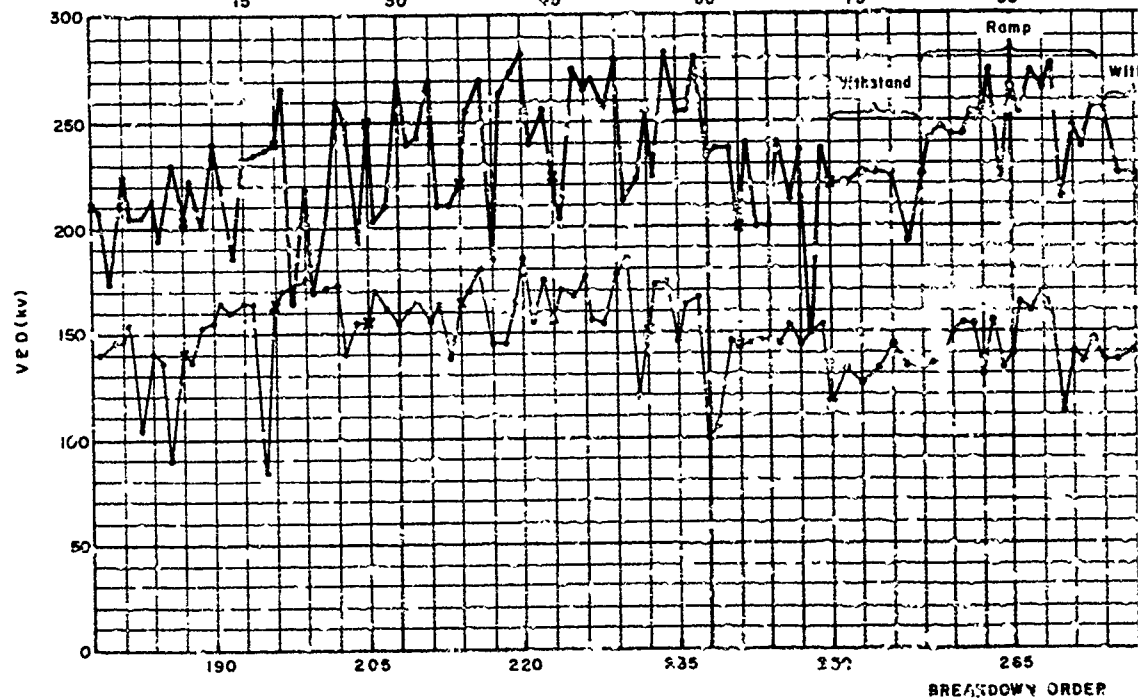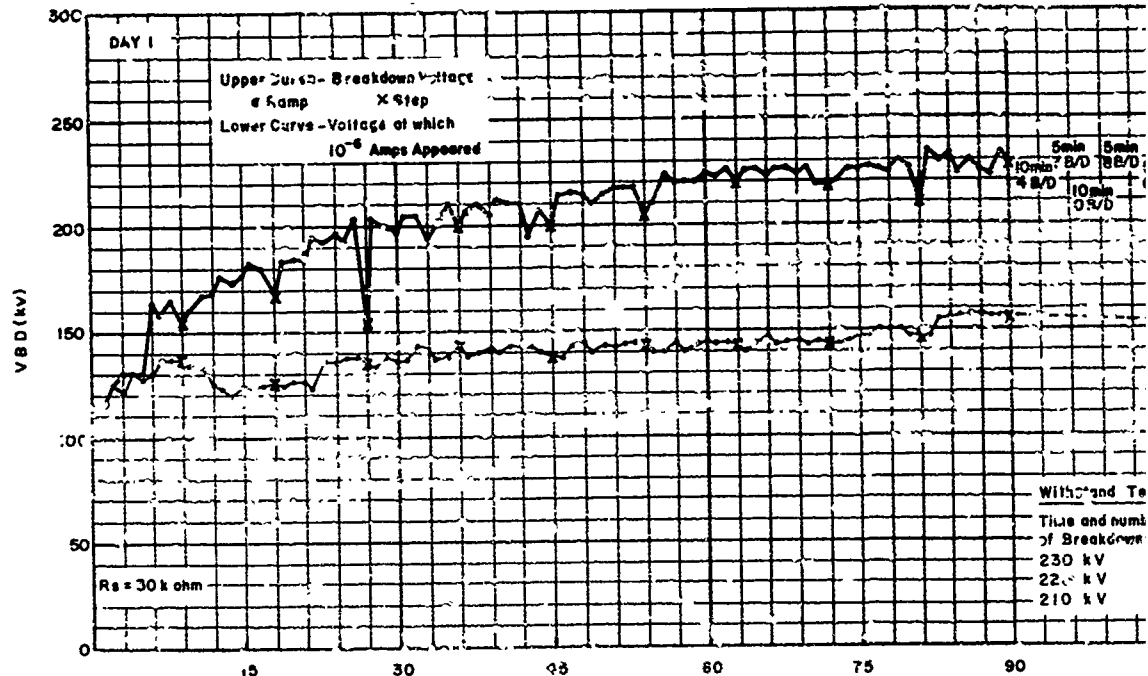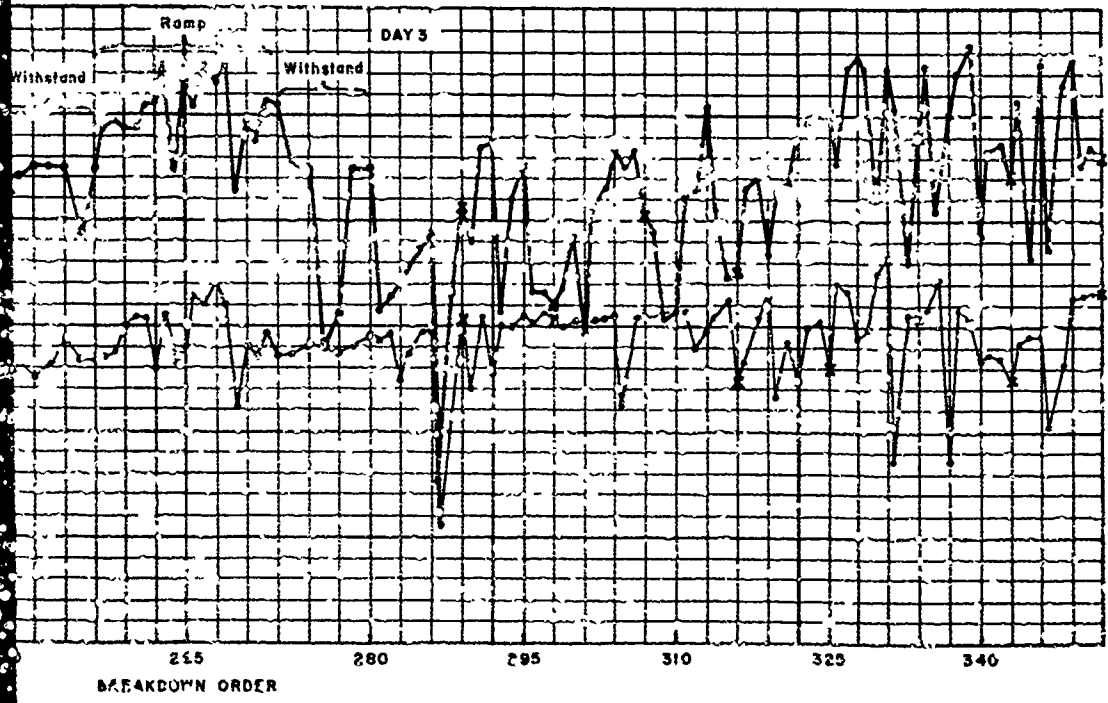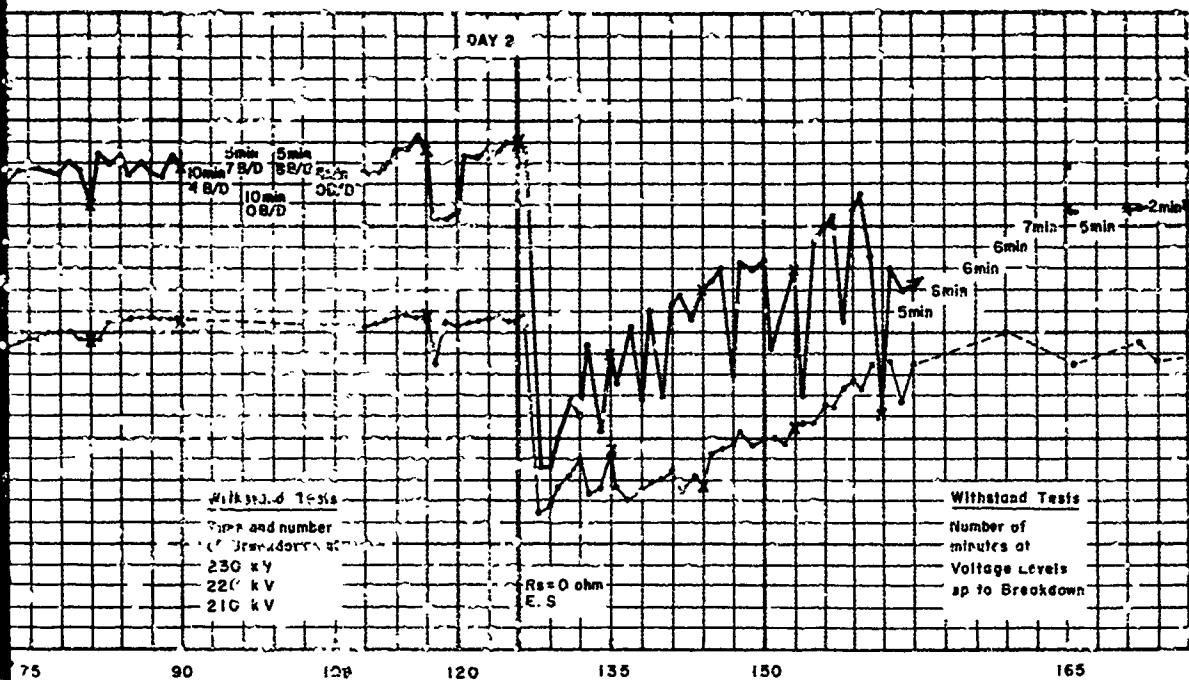
Figure 10-5. Conditioning Curve for Treatment a b: Ti2 - 4-Inch Diameter Bruce Profile Electrodes - Ti-7Al-4Mo Anode and Cathode with Extended Series of High Energy Discharges.

Upper Curve – Breakdown Voltage
● Ramp   X Step
Lower Curve – Voltage at which
        10^{-6} Amps Appeared

Rs = 30 k ohm

Withstand Tests
Number of
Breakdowns in
a certain
Time Period
Steady Currents
$280 - 5.4 \times 10^{-4}$ A
$270 - 3.8 \times 10^{-4}$ A
$260 - 3.1 \times 10^{-4}$ A
$250 - 2.6 \times 10^{-4}$ A
$240 - 1.7 \times 10^{-4}$ A

DAY 4

24 in 5 min
22 in 5 min
1 in 5 min
13 in 44 min
10 in 31 min

VBD(kv)

355   370   385   400   415   485   500

2 mo

DAY 5

1.0 cm

.75 cm

TP at end
3×10^{-6}

Rs = 30 k ohm

VBD(kv)

550   575   590   605   682

BREAKDOWN ORDER

1.0 cm Withstand Test

kV	Time (min)	Number B/D	Ipk (mA)	$\langle 10^{-6} \rangle$ kV
305	4	10	0.20	---
240		10	0.15	---
230	10	10	0.13	---
270	60	5	0.1	198
280	25	3	0.11	204
290	0	6	0.14	---
300	1	3	0.3	196

Day Number 5 (Electrodes Cool 14 Hours)

300	4	4	0.23	204
190	12	5	---	---
260	44	2	0.16	---
245	4	1	0.16	---
300	20	4	0.22	---
290	10	2	0.13	207

0.75 cm Withstand Test
at High Current Levels

Figure 10-5. Continued

Table 10-3. Included are the maximum and minimum values for the level portion of each series.

Yates' Algorithm was then used to obtain the estimates of the various factor effects and interactions shown in Table 10-4. It was found that the maximum breakdown voltages for each series was also a useful measure but that the minimum breakdown voltage was too variable to give reasonable factorial estimates.

Electrode size (B) stands out as the largest single effect, with smaller electrodes giving higher breakdown voltages. The factors of high impedance conditioning and cathode material do not show up as significant. High impedance conditioning raises the breakdown voltage slightly (~ 6%) in the immediately following conditioning series but the factorial estimates for the initial series show that treatments with high impedance conditioning had breakdown voltages ~ 5% higher than those without high impedance conditioning. The sign of the cathode material effect (C) varies with discharge series and only during series four is it large enough to be considered significant.

The factorial experiment was extended to include anode material in three treatments in which the cathode and anode were of the same material, either copper, nickel, or titanium alloy. The factors of size and high impedance conditioning were fixed at their high levels so comparisons as to effect of electrode material are made for 4-inch diameter vacuum fired Bruce Profile electrodes. Table 10-5 gives the pertinent comparisons. Introducing titanium alloy as an anode is seen to have the greatest effect, breakdown voltage levels are 10 to 20% higher when both electrodes are titanium alloy than for any other material combination tested. The difference between copper and nickel electrodes is not as great and varies with discharge series, copper was initially better but by series five nickel gave slightly high breakdown voltages.

In summary, conclusions of the factorial experiment are that smaller electrodes have higher breakdown voltages than large electrodes, that there is little difference between titanium and nickel when used as cathode materials opposite a copper anode, and that introducing a titanium anode leads to

10-16

Table 10-3 Average, Maximum, and Minimum Br
for Energy Conditioning St

Treatment	Initial Breakdown Voltage Level (3 B/D)	Series 1 High Impedance Conditioning R_a = 30 Kilohm/no Energy Storage				Series 2 High Impedance Conditioning R_b = 1 Kilohm/with Energy Storage				Series 3 Minimum Breakdown Voltage During Energy Discharge	Series 4 Energy Reconditioning R_a = 1 Kilohm/with Energy Storage				H R_a =
		Average Breakdown Voltage	σ	Maximum Breakdown Voltage	Minimum Breakdown Voltage	Average Breakdown Voltage	σ	Maximum Breakdown Voltage	Minimum Breakdown Voltage		Average Breakdown Voltage	σ	Maximum Breakdown Voltage	Minimum Breakdown Voltage	Average Breakdow Voltage
(1)	153	...	--	---	---	177	20	212	140	90	200	21	230	152	224
(1) R	140	...	--	---	---	174	17	203	119	85	175	20	210	120	238
a	148	217	11	235	185	202	30	232	123	35	196	31	234	130	230
b(R)	142	---	--	---	---	181	20	212	117	120	187	17	205	125	216
ab(R)	132	197	3	203	190	169	25	203	105	123	175	17	195	125	214
c	127	...	--	---	---	168	25	211	117	126	195	26	226	147	244
ac	176	210	5	217	198	192	26	221	131	120	229	12	250	185	240
ac(R)	165	217	6	227	205	204	20	233	152	156	217	23	244	135	256
bc	124	...	--	---	---	172	20	200	120	102	196	18	208	138	193
abc	120	199	17	212	175	183	37	225	85	96	218	7	225	165	209
abc(R)	120	198	7	206	175	146	21	179	92	130	182	13	195	138	204
ab - Cu	124	212	2	218	207	182	7	194	160	99	206	17	219	150	201
ab - T₁	150	213	6	220	208	188	27	217	130	112	194	31	235	132	232
ab - N₁	122	200	4	205	194	167	15	182	120	140	170	17	192	135	214

*Treatment (1) did not employ crowbarring

Note Average standard deviation, maximum and minimum breakdown voltage levels are computed for portions of the conditioning curves which exhibit no general upward or downward trend and are based on 20 to 40 ramp applications of voltage.

Series 4 reconditioning with Energy Storage		Series 5 High Impedance Conditioning With Energy R_s = 30 Kilohm/with Energy Storage				Series 6 Minimum Breakdown Voltage During Energy Discharge	Series 7 High Impedance Reconditioning R_L = 30 Kilohm/with Energy Storage				Series 8 High Energy With Crowbar R_s = 125 Ohm/with Crowbar and Energy Storage			
Maximum Breakdown Voltage	Minimum Breakdown Voltage	Average Breakdown Voltage	σ	Maximum Breakdown Voltage	Minimum Breakdown Voltage		Average Breakdown Voltage	σ	Maximum Breakdown Voltage	Minimum Breakdown Voltage	Average Breakdown Voltage	σ	Maximum Breakdown Voltage	Minimum Breakdown Voltage
230	152	224	8	245	213	125	246	24	268	170	*217	28	253	156
210	120	238	17	248	147	115	260	8	272	234	209	29	246	105
234	130	230	17	244	160	50	193	22	222	160	205	31	240	78
205	125	216	10	225	175	54	209	18	227	145	165	21	197	110
195	125	214	3	219	210	127	218	3	221	211	---	--	---	---
226	147	244	8	251	230	150	218	3	225	210	227	12	240	183
250	185	240	17	255	165	108	237	3	243	232	216	14	234	183
244	135	256	7	265	242	167	219	8	234	193	214	22	234	175
208	138	193	3	198	180	127	208	6	216	183	182	23	211	80
225	165	209	4	225	197	150	231	3	235	220	192	19	279	121
195	138	204	2	209	200	135	228	9	235	186	204	15	226	163
219	150	201	1	203	200	115	217	2	221	215	182	22	213	130
235	132	232	10	248	205	114	253	13	269	263	---	--	---	---
192	135	214	3	219	207	90	234	4	230	223	---	--	---	---

Table 10-4. Factorial Estimates for Energy Conditioning Study

Effect or Interaction	Average Breakdown Voltage						Maximum Breakdown Voltage				
	Initial Series	2	4	5	7	8	2	4	5	7	8
μ – Mean	140	180	199	221	220	201	214	221	232	232	229
A – Effect of High Impedance Conditioning	7	12	10	4	0	6	11	8	6	-3	9
B – Effect of Electrode Size	-21	-8	-11	-26	-7	-30	-9	-26	-32	-14	-24
AB – Interaction of High Impedance Conditioning and Electrode Size	-14	-12	-5	3	16	18	-3	-5	4	10	18
C – Effect of Cathode Material	-7	-3	20	0	7	6	0	11	-1	-4	-2
AC – Interaction of High Impedance Conditioning and Cathode Material	15	5	18	2	21	-7	6	11	9	22	-3
BC – Interaction of Electrode Size and Cathode Material	-8	6	6	-14	-1	-4	5	5	-9	6	7
ABC – Interaction of all Three Factors	-12	6	-1	7	-14	-7	11	1	7	-9	-6
Average Minimum Breakdown Voltage							117	145	191	191	130

Note: These results are based upon eight treatments: l, a, b(R), ab(R), c, ac, bc, abc

10-18

Table 10-5. Comparisons for Effect of Anode Material – Energy Conditioning Study

Compare to →	Anode-Cathode	Treatments (Series) Compared	Averaged Levels					Maximum Levels			
			Initial	2	4	5	7	2	4	5	7
Copper Electrodes	Ti / Ti	ab:Cu – ab:Ti	-26	-6	12	-31	-36	-23	-16	-45	-48
	Ni / Ni	ab:Cu – ab:Ni	2	15	36	-13	-17	12	27	-16	-17
	Cu / Ni	ab:Cu – ab(R)	-8	13	31	-13	-1	-9	24	-16	0
	Cu / Ti	ab:Cu – abc	4	-1	-12	-8	-14	-31	-6	-22	-14
	Cu / Ti	ab:Cu – abc(R)	4	36	24	-3	-11	15	24	-6	-14
Nickel Electrodes	Cu / Cu	ab:Ni – ab:Cu	-2	-15	-36	13	17	-12	-27	16	17
	Ti / Ti	ab:Ni – ab:Ti	-28	-21	-24	-18	-19	-35	-43	-29	-31
	Cu / Ni	ab:Ni – ab(R)	-10	-2	-5	0	16	-21	-3	0	17
	Cu / Ti	ab:Ni – abc	2	-16	-48	5	3	-43	-33	-6	3
	Cu / Ti	ab:Ni – abc(R)	2	21	-12	10	6	3	-3	10	3
Titanium Electrodes	Cu / Cu	ab:Ti – ab:Cu	26	6	-12	31	36	23	16	45	48
	Ni / Ni	ab:Ti – ab:Ni	28	21	24	18	19	35	43	29	31
	Cu / Ni	ab:Ti – ab(R)	18	19	19	18	35	14	40	29	48
	Cu / Ti	ab:Ti – abc	30	5	-24	23	22	-8	10	23	34
	Cu / Ti	ab:Ti – abc(R)	30	42	12	28	25	38	40	39	34

significantly higher breakdown voltages. High impedance conditioning appears helpful but not essential in reaching high voltage levels. These conclusions are valid over a wide range of energy and series resistance.

10.5   Prebreakdown Current

Interelectrode current preceeding breakdown was monitored with an electrometer and found to vary from less than 10^{-9} amperes to 2×10^{-3} amperes. Low current levels were usually unstable and were encountered during the early stages of conditioning and the moderate energy discharge series ($R_s = 1000$ ohms, Energy Storage $= .15 \mu f$). Currents of above 10^{-8} amperes were usually constant at a given voltage. During most of the conditioning sequence stable prebreakdown currents of from 10^{-6} to 10^{-3} amperes preceeded breakdown.

The dependence of prebreakdown current upon voltage was usually of an exponential nature and conformed roughly to the Fowler - Nordheim equation indicating field emission from cathode protrusions. Representative graphs of current versus voltage plotted on the usual Fowler - Nordheim coordinates are given in Figure 10-6. The relevant equation is:

$$I = A \left(\beta \frac{V}{d} \right)^2 \exp \frac{-Bd}{\beta V} \qquad \begin{aligned} V &= \text{Voltage} \\ d &= \text{Gap} \end{aligned}$$

Where A includes the emitting area and B is approximately a constant depending in part upon the work function ϕ. A Fowler - Nordheim plot of log I/V^2 versus I/V is then a straight line if the currents are of field emission origin and several emitting sites are dominant (i. e. there is an equivalent field enhancement factor β).
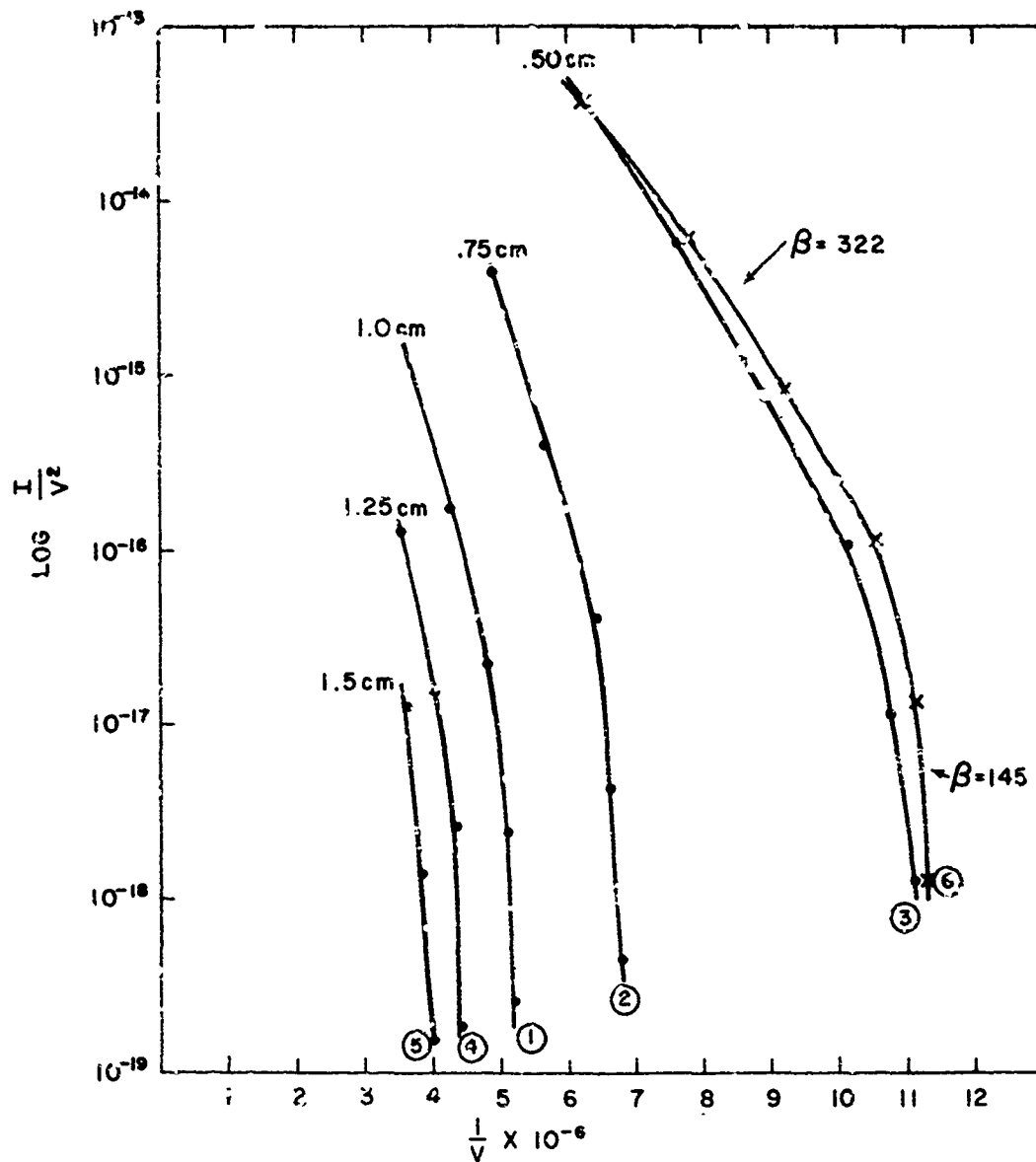
Figure 10-6. Fowler-Nordheim Plot - 4 Inch Diameter
Bruce Profile Electrodes After Conditioning
Anode and Cathode of Ti - 7 Al - 4 Mo

1-4044

A distinctive feature usually found for well conditioned electrodes in this experiment is the bend at about the 10^{-5} ampere current level. Below that current level the slope of the Fowler-Nordheim plot would gave an equivalent field enhancement factor β of 145 for the 0.50 cm gap of Figure 10-3. Above 10^{-5} amperes the slope changes and an increased β of 322 is calculated for the same gap. In this case a repeat run at 0.50 cm after a number of runs to breakdown at other gaps yields much the same slopes and thus this behavior of β is reproducible. The conclusion is that at some current level the field enhancement factor increases. The contribution of ionic space charge has been suggested by Watson as a possible explanation of this effect.

Another indication of field emission is that the voltage necessary for 10^{-6} amperes of emission was approximately a linear function of gap. This follows from the uniform field geometry in which the cathode field strength is a linear function of gap. Figure 10-7 gives this variation for seven representative treatments. The variation between treatments was not great and on the average a macroscopic cathode field of 195 kV/cm was required to produce 10^{-6} amperes of field emission current from well-conditioned electrodes.

The relationship between prebreakdown current and breakdown voltage is presently uncertain and may not be of causal nature. There is a strong correlation between <u>changes</u> in the 10^{-6} ampere voltage level and <u>changes</u> in breakdown voltage. However the lack of any consistent correlation between total prebreakdown current and breakdown voltage would imply that <u>total</u> prebreakdown current is not especially important, and that it is the current at an individual emitting site that determines the breakdown voltage. This site may not be a dominant contributor to the total current yet still produce a thermal instability initiating breakdown. Until decisive experiments have been carried out to clearly identify the mechanisms of vacuum breakdown, it is useful only to note that prebreakdown current is correlated in some way with the breakdown voltage level. The conditioning curves of Figure 10-8 give an idea of this correlation and include calculated field enhancement factors for each breakdown. In general, measurements of prebreakdown current cannot be used to predict breakdown voltage.
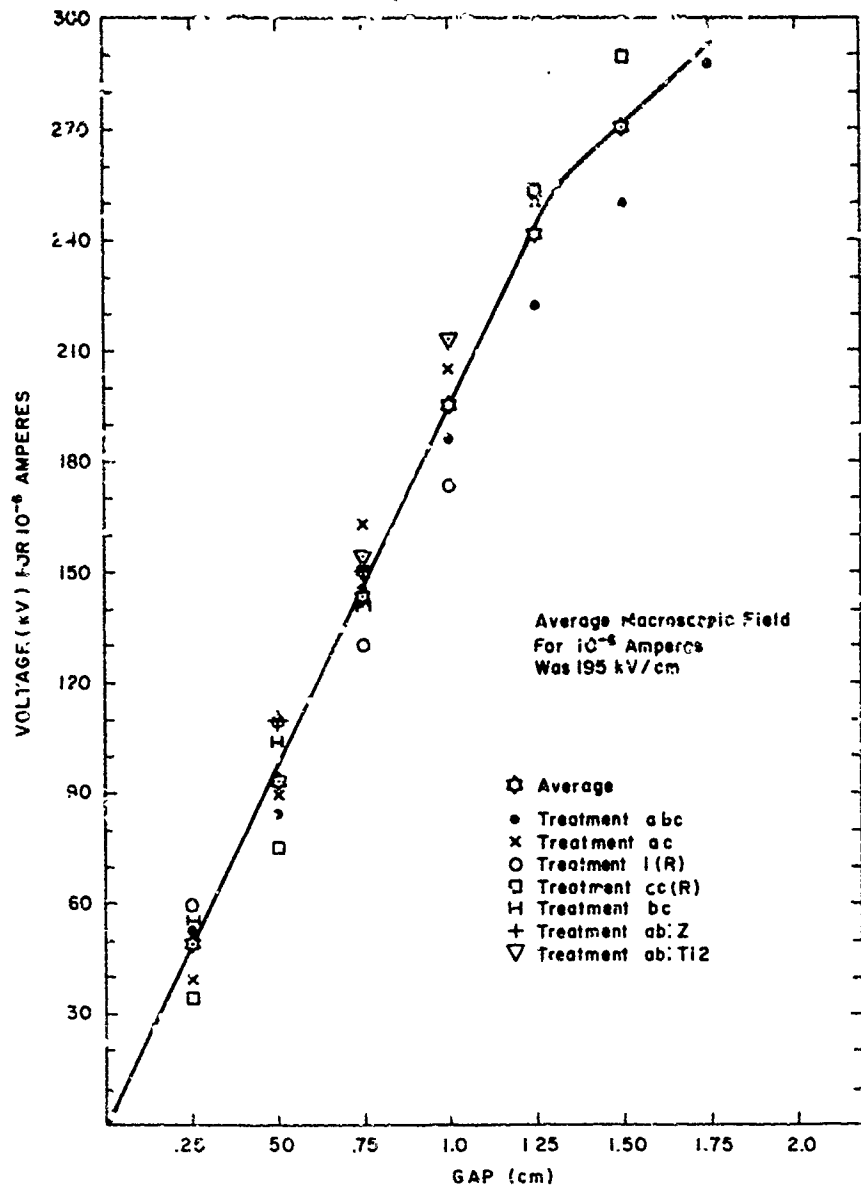
Figure 10-7. Dependence of Voltage for 10^{-6} Amperes of
Prebreakdown Current Upon Gap for Representative
Treatments - Measurements are for
Well-Conditioned Electrodes

1-4046
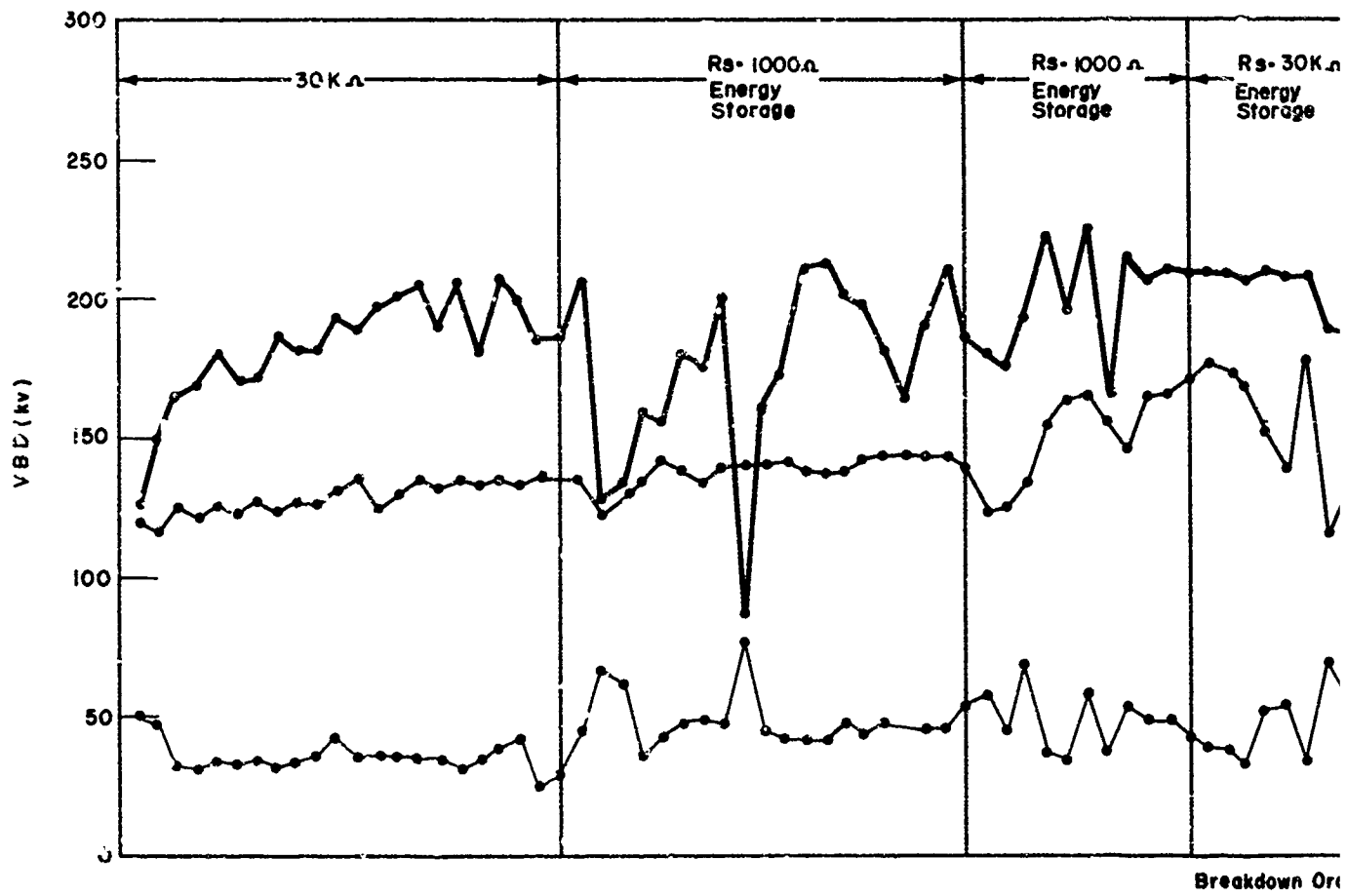
1-3826
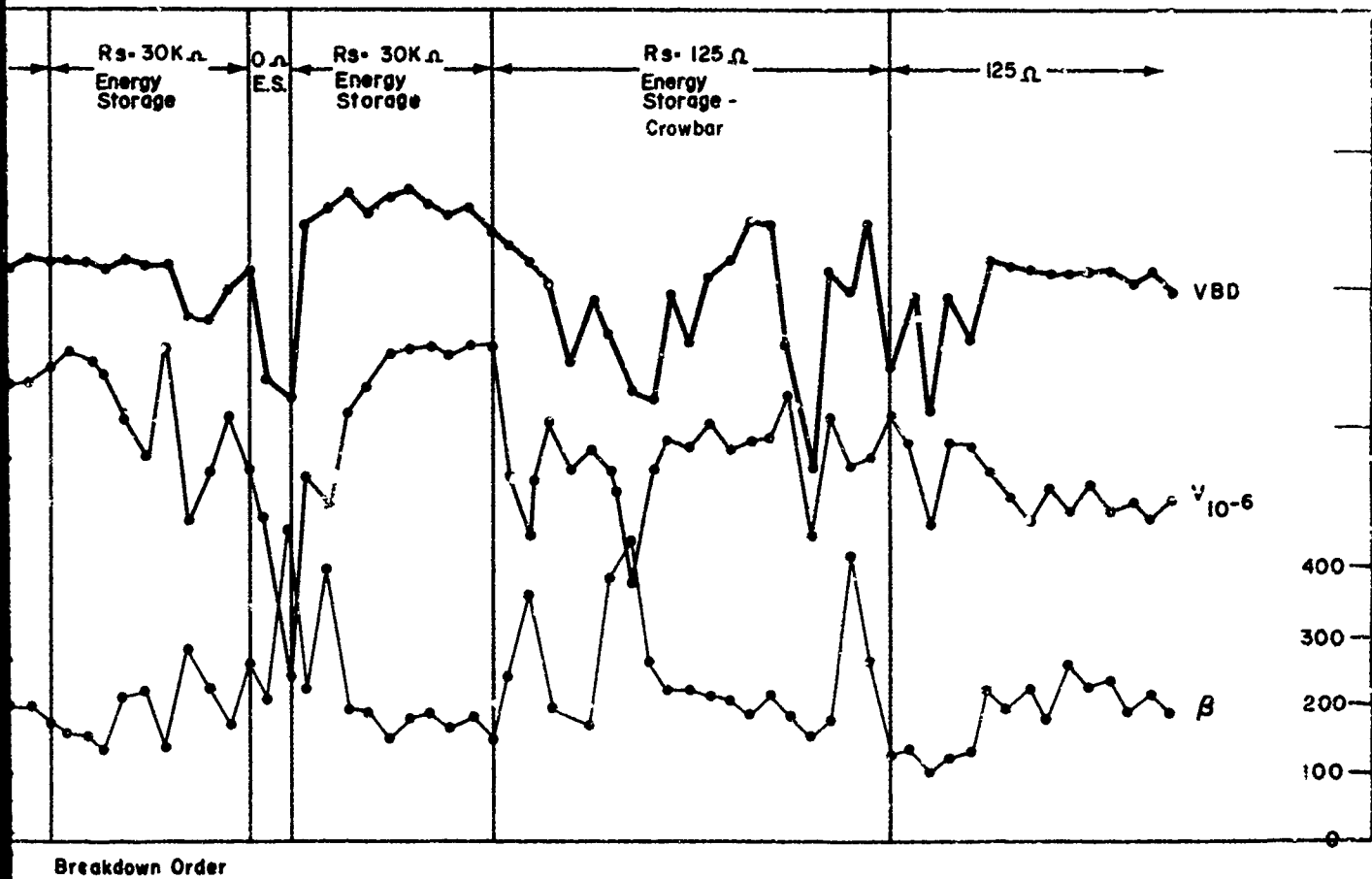
Figure 10-8 Correlation of Curves
for Breakdown Voltage, 10^{-6} A
Voltage Level, and Computed Field
Enhancement Factor β for
Treatment abc - Energy
Conditioning Study

The variation in prebreakdown current with conditioning is primarily a function of the type of discharge. Low energy discharges generally produce low emission levels (i.e. the voltage for 10^{-6} amperes is high and the last measureable current prior to breakdown is low, usually 10^{-5} to 10^{-4} amperes). Moderate energy discharges (R_s = 1000 ohms with 0.15 μF of energy storage) do not significantly change prebreakdown current levels from what they were during a low energy discharge conditioning sequence (R_s = 30 kilohms). High energy discharges (R_s = 0 ohms with 0.15 μF of energy storage) substantially increase the prebreakdown current level in that the voltage necessary for 10^{-6} amperes drops by as much as 50% and often the current just prior to breakdown exceeds 2×10^{-3} amperes. These effects are evident in Figure 10-8.

10.6   Discharge Characteristics

10.6.1   Introduction

DC vacuum breakdown is defined as the collapse of the gap voltage to near zero. This occurs as capacitive energy is discharged to ground by currents of the order of hundreds of amperes. The rate at which the voltage collapses (or alternately the current flow) depends on two major factors:

(1)   Amount and availiability of capacitive energy--i.e., the external electric circuit.

(2)   Effective instantaneous impedance of the developing vacuum discharge.

Since the material which eventually constitutes the plasma generated upon breakdown must come from the electrodes in vacuum breakdown, the vacuum discharge, relative to breakdown in other media, has a rather slow development, passing throuhg two distinct phases in times of the order of hundreds of nanoseconds. These can conveniently be classified as:

(1) **Initial High Impedance Spark Phase**

During the initial 100 to 500 ns considerable current flow (hundreds of amperes) occurs while significant voltage is still across the gap. Thus power input to both the discharge and the electrode surfaces is very high, reaching values of 10^7 joules/second. However since the duration of this phase is short (5×10^{-7} seconds) the total energy dissapated is of the order 1 to 10 joules. The effective impedance of the vacuum gap during this phase is ~ 1000 ohms.

(2) **Low Impedance Arc Phase**

Once the required plasma has been generated by the spark phase, an arc discharge characterized by high currents (hundreds or thousands of amperes) at low voltages occurs. The magnitude and duration of this arc are determined only by the external electric circuit. If sufficient charge is not available it may never develop. In vacuum the arc extinguishes very rapidly if the current drops below 5 to 0.5 amperes, the exact value depending on electrode material and gap.

The complex physical mechanisms active during these initial phases have so far received little attention--expecially at high voltages. One pertinent study by Epstein, et. al[1] of plasma processes in a 60 kV vacuum spark found the following sequence. The total current rises monotonically to thousands of amperes. During the early stages of the discharge a large fraction of this consist of electrons which are accelerated to the full gap voltage. A plasma which neutralizes the space charge develops, allowing the current to rise to high values. Plasma oscillation and intense microwave radiation appear as a result of the interaction of the fast electron streams with the plasma. The

electrons lose energy during this stage and eventually a quiescent plasma occurs until a new fast electron stream appears. This alternation of fast electron stream, interaction with plasma, energy loss, quiescent plasma, new fast electron stream continues for about 500 ns. Then the impedance of the discharge collapses. This collapse is brought about when a dense plasma vaporized from the anode by incident electron streams arrives at the cathode. These mechanisms are capable of explaining the major features of the discharges observed in the present experiment.

10.6.2   Experimental Observations

Voltage collapse was monitored with a capacitive voltage divider and an oscilloscope. It was coupled to the high voltage bushing on the gas side and isolated from the electrodes only by about 20-inches of large diameter conductor. Thus the voltage collapse waveform is an accurate representation of voltage across the gap, with transit time isolation of not more than 2 to 5 ns.

The breakdown current pulse is observed on the cathode side with a low inductance resistive monitor of 0.1 ohms or 0.03 ohms, depending on the maximum current expected.

Typical voltage collapse and breakdown current waveforms are given in Figure 10-9. The pertinent circuit is given in Figure 10-10.

10.6.3   Discharge with 30 Kilohm Series Resistance

With a series resistance of 30 kilohms the typical discharge consists of a rapid buildup of current to about 160 amperes in less than 10 ns. This is followed by a decay of current to near zero in about 500 ns. At the same time the gap voltage has collapsed to a low value during the first 40 to 100 ns. This behavior is independent of whether or not the energy storage capacitor bank is connected. Thus 30 kilohms of series resistance effectively isolates the gap and associated bushing capacitance from the rest of the external circuit.
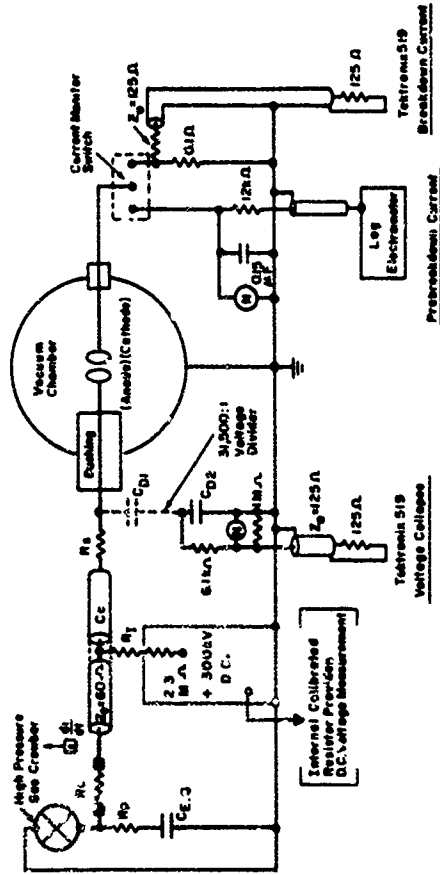
Series Resistance	Voltage Collapse-100ns/cm	Current	Time Scale
1. $R_S = 30$ k ohm without energy storage			100 ns/cm 100 ns/cm
2. $R_S = 30$ k ohm with energy storage			100 ns/cm 100 ns/cm
3. $R_S = 1000$ ohm without energy storage			200 ns/cm 100 ns/cm
4. $R_S = 1000$ ohm with energy storage			100 ns/cm 1 μs/cm
5. $R_S = 0$ ohm without energy storage			500 ns/cm
6. $R_S = 0$ ohm with energy storage			1 μs/cm 1 μs/cm
7. $R_S = 125$ ohm with energy storage and crowbar			200 ns/cm Crowbarring at 500 ns
8. $R_S = 30$ k ohm without energy storage			
9. $R_S = 0$ ohm with energy storage	without crowbar with crowbar		500 ns/cm 500 ns/cm

(Amplitudes are not to a single scale)

├──┤cm   ├─┤ cm

Figure 10-9. Typical Discharge Waveforms

2-1416

Figure 10-10. Schematic of Electrical Test and Instrumentation Circuits

R_s = Series Resistance

R_c = Crowbarring Resistance (20 ohm) (Removeable)

R_p = Protective Resistance (4 ohm)

$C_{E.S.}$ = Energy Storage Capacitance (0.15 μf)

C_{D1} = Voltage Divider Capacitance (1.9 pF)

C_{D2} = Voltage Divider Capacitance (1200 pF)

R_I = Power Supply Isolation Resistance (2.3 Mohm)

C_c = Cable Capacitance (~900 pF)

1-3556a

10-29

The limited peak current and subsequent shape of the current decay waveform suggest that the vacuum spark, during the initial 500 ns, has a fairly high impedance. Since the voltage is initially around 200 kV and the peak current is 160 amperes, the initial impedance is around $Z = V/I = 1250$ ohms. Subsequently the decay of current is similar to that of a capacitor through a resistor. In this case the bushing capacitance and the spark impedance, if considered to be resistive, form an R-C circuit whose decay time constant is approximately 200 ns. If the bushing capacitance is assumed to be 150 pf, the equivalent resistance is $R = \tau/c = 1300$ ohms. Measurement of typical integrated currents (charge) supports the assumption that a capacitance of around 150 pf is being discharged from 200 kV to a very low voltage.

Thus a consistent description of the high impedance discharge is that it is equivalent to the discharge of a small capacitance through a spark resistance of the order of 1000 ohms. This occurs in a time of ~ 500 ns. The energy dissipated in the gap and on the electrode surfaces during this discharge is of the order of 10 joules or less.

Conditioning with discharges typical of a 30 kilohm series resistance produces high stable breakdown voltages. Reasonably low prebreakdown current levels are also found. This type of discharge can be referred to as a low energy vacuum spark.

10.6.4   Discharge with 1 Kilohm Series Resistance

When the series resistance is 1 kilohm the high voltage cable can now supply significant currents to the discharge. If the initial voltage is 200 kV, 200 amperes can be delivered if the gap voltage drops to a low value. In this case the energy storage capacitor bank becomes a critical element if connected.

Voltage collapse time increases due to the necessity of discharging both cable and bushing capacitance. However, collapse times are approximately the same whether or not the energy storage capacitor bank is connected. This indicates that by the time the current is being drawn from the energy storage capacitor bank, the gap impedance is very low so that currents of around 200 amperes can be passed with a low voltage drop in the gap. In other words, after about 300 ns the discharge is in the arc phase. This phase will continue for several times constants of the RC circuit formed by the 0.15 μF capacitor bank and the 1 kilohm series resistance, that is, for times of the order of 300 μs. During this lengthly arc, power dissipation in the gap and on the electrode surfaces is expected to be at a low level.

The effect of this form of discharge (R_s = 1 kilohm with energy storage) is to produce erratic and often low breakdown voltages. However, the average prebreakdown current level is not changed significantly. Although the energy dissipated in the gap cannot in this case be calculated, it seems reasonable to refer to this as a moderate energy discharge.

10.6.5   Discharge with 25 Ohms of Series Resistance

When the series resistor at the high voltage gas-to-vacuum bushing is replaced by a conductor the only remaining resistance in the discharge circuit is located at the energy storage capacitor bank. There a total resistance of 24 ohms provides for protection of the capacitor bank and effective crowbar operation. The discharge without energy storage is then the discharge of cable capacitance and, as shown in Figure 10-9, it exhibits a fairly long discharge with minor oscillations. With energy storage the voltage collapse waveform is complicated by reflections in the unterminated cable, but appears to have settled to a lower level after about 300 ns, indicating that at this time the gap impedance is low. The current, after an initial peak due to bushing capacitance discharge, builds up to a second peak in 1 to 2 μs. The current then decays with a time constant of 3.6 μs.

The effects of this discharge on breakdown voltage and prebreakdown current levels are severe. The breakdown voltage is initially reduced by as much as a factor of between 2 and 5, and the prebreakdown current at a certain voltage increases significantly. With some electrode materials it can be expected to reach 2 ma or more, before breakdown. Materials such as nickel and titanium, when included as the anode material, have demonstrated great tolerance for such high energy discharges. After the initial drop in performance, a series of 40 to 60 discharges appears to lead to performance that is as good or better than that found with only low energy discharges (high impedance conditioning - R_s = 30 Kilohms).

10.6.6   Crowbarring - Effect on Discharge

The high pressure gas crowbar is capable of diversion within 200 ns. When applied in the system shown in Figure 10-10 the effects of diversion become apparent in the current waveform after about 400 to 500 ns. as shown in Figure 10-9. This is for a series resistance of 125 ohms which, with energy storage, is normally a damaging discharge in the sense that breakdown voltage levels drop and prebreakdown current levels increase. Crowbarring was not entirely effective in eliminating this damage.

The conclusion is that electrode damage due to high energy discharges, measured as a deterioration in vacuum gap insulation performance, occurs during the first stages of the discharge - certainly within several microseconds. Crowbarring that cuts off the energy supply at 500-1500 ns does not maintain high breakdown voltages. The solution is to add resistance or inductance to the system so that the energy (current) cannot reach the gap during the initial stages of the discharge. Then crowbarring will most likely be effective.

It is again important to note that the above conclusions are based upon treatments in which the anode was copper. Treatments in which the anode is a refractory metal such as titanium alloy or nickel have shown a much greater tolerance of high energy discharges and will be discussed in Section 10-?.

10.7   Effect of Time in DC Vacuum Breakdown

Breakdown voltage is usually defined as the last measurable voltage across the gap just prior to breakdown. This convention has been followed throughout the present experimental program. In other experiments, breakdown voltage has sometimes been taken as the maximum steady voltage that could be held for a specified time period. In vacuum breakdown these definitions do not yield the same results, since for a given vacuum gap the breakdown voltage is apparently a strong function of the time for which the voltage is applied. This section reports measurements of this dependence of breakdown voltage on time at voltage or rate of voltage application.

The withstand tests were carried out for the four inch diameter Bruce Profile nickel electrodes after completion of the normal energy conditioning sequence. A series impedance of 30 kilohms limited the intensity and duration of each discharge to such a low energy (< 10 joules) that it could be assumed that the well-conditioned electrode surfaces did not change during the test. The gap was set to 0.75 cm and the voltage stadily increased (at a rate of ~ 5 kV/s) to breakdown after which a series of step withstand tests were carried out at lower voltage levels down to a level at which no breakdown would occur over a period of several hours. Steps of 5 kV were used and the voltage was held at each level (except for the momentary drop to zero during each discharge) for a time of either 1 hour or until 10 to 20 breakdowns had occurred. The voltage levels were tested in a random sequence and periodically the ramp breakdown voltage (5 kV/s) was determined to verify that the electrodes had not changed appreciably. Each level was investigated at least twice, and the times between breakdown were apparently random at any one level.

Results are given in Figure 10-11. The breakdown voltage level is plotted as a function of the log of the mean time to breakdown at each voltage level. The mean time to breakdown increases rapidly as the stress is reduced, leading to an exponential withstand characteristic.
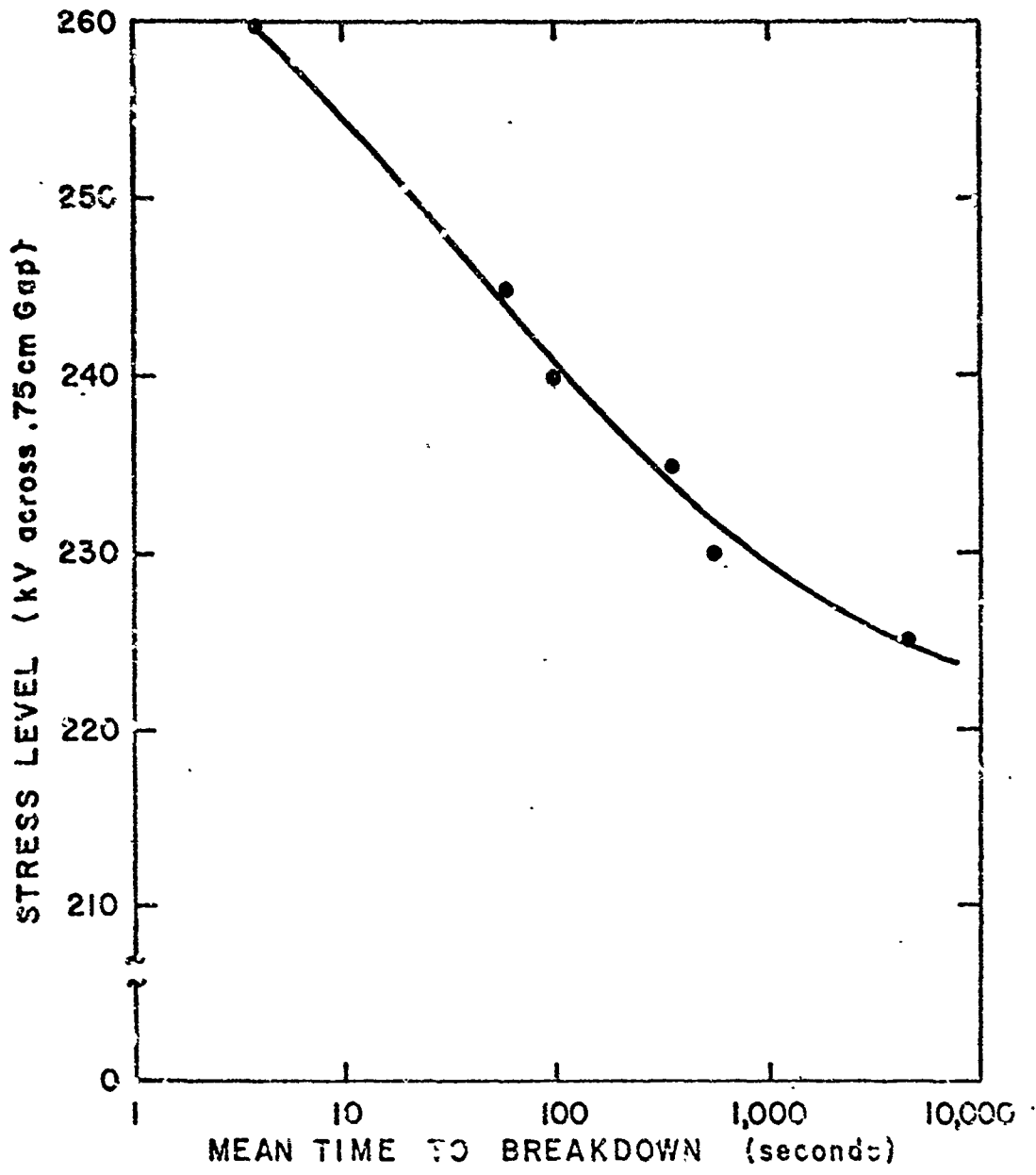
Figure 10-11. Typical Withstand Properties of High Impedance
Conditioned Vacuum Gap - 4-Inch Diameter
Uniform Field Nickel Electrodes.(20)

The steady prebreakdown current prior to breakdown was, even at the highest stress levels, less than 4×10^{-5} amperes. Thus, assuming as a worst case that this is due to a single field emission beam, localized power input to the anode is less than $P = VI = (2.45)(10^5)(4)(10^{-5}) = 9.8$ watts. While this would not lead to significant general heating of the anode in the time periods involved, it does suggest that a possible cause of long time dc breakdown is localized thermally generated instabilities of the anode surface. Thus, at lower stress levels, the prebreakdown current and power flow is less and the mean time to breakdown is longer. Since the prebreakdown current depends exponentially on voltage due to its field emission origin (see Section 10.5), it is reasonable that if the current is a precursor to breakdown through heating of the anode surface, then the mean time to breakdown will be exponentially dependent upon voltage level. This could occur at lower and lower stress levels until the conduction of heat away from local anode hot spots is sufficiently rapid to prevent instabilities. The instability mechanism has been suggested by Watson[2] to be evolution of gas from the hot spot and by Davies[3] to be the electrostatic pulling away of a thermally softened blob of anode material.

10.8   Surface Changes Due to Breakdown

Conditioning is produced by the discharge of electrical energy in the vacuum gap and on the electrode surfaces. The changes brought about on the electrode surfaces are easily visible and differ according to the amount of energy discharged, the electrode material, and the gap spacing. In this section the more prominent features of surface changes due to high energy discharges are examined. Possible mechanisms and implications regarding the nature of conditioning are considered.

High energy discharges produce distinctively different changes on the anode and cathode--the dominant features are:

(1)   Anode: Melted and eroded regions cover the anode surface subject to high energy discharges. Near the edges of the electrodes the surface is cleaned and partially

etched. Numerous melt patterns with a distinct struc-
ture are visible, usually with a circular outline and a cen-
tral crater. There is often evidence of the ejection of
molten particles in a direction nearly tangential to the
surface.

(2) Cathode: The cathode surface is usually covered by a
deposit of material from the anode. This surface layer
is generally highly adherant and consists of a continuous
film (as if condensed from a metal vapor) and discrete
impacted particles. Often, regions of this coating can be
linked to corresponding areas of the anode by distinguish-
ing patterns. Craters are sometimes found in the under-
lying cathode material. Traces of arcs (descriptively
called "fern-marks") over extensive areas are often
visible.

These features are shown in Figures 10-12 to 10-14. Two of these
figures provide a comparison with the 600 grit SiC finish which was the final sur-
face finish prior to testing. In most cases this finish is completely obliterated
by high energy conditioning. However it should be noted that areas of extreme
change can frequently be adjoined by areas in which the original 600 grit SiC fin-
ish is apparently untouched. Thus it cannot be concluded that the 600 grit finish
is of itself incapable of enduring the high stresses achieved after conditioning.
Rather, conditioning produces changes in surface structure such that initial sur-
face finish is not an important factor for electrodes that are to be conditioned.
Indeed, this was one of the conclusions of the Pilot Experiment (See Section 7).

The shape of melt patterns on the anode suggests localized and gen-
eral heating of the anode surface by field emission electron beams. These
heated regions will then flow more easily when the spark occurs. The character-
istic circular ring of metal projecting from the surface with regularly spaced
protrusions can be explained as a result of melting and mechanical forces
accompanying the diffusion of magnetic flux into the surface. In effect the
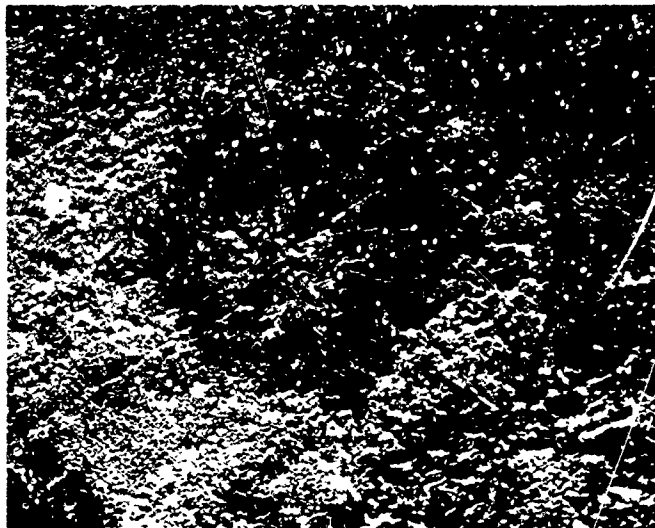
(a) Aluminum Anode - Note Melted and Eroded
Areas Around Crater (~ 10 X)
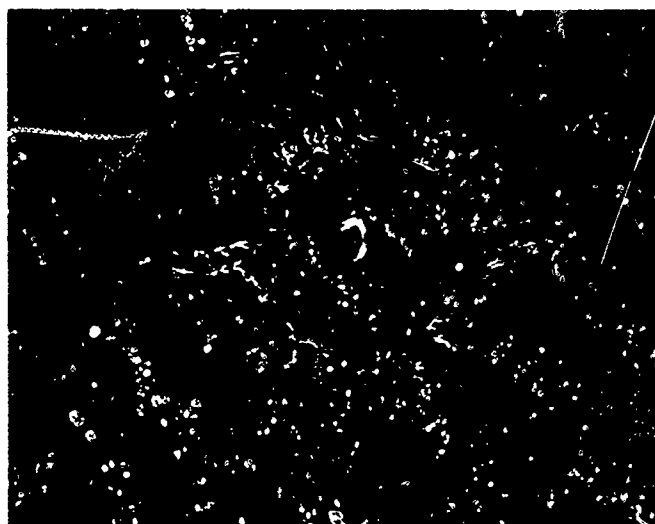
(b) Stainless Steel Anode - Note Central Crater
and Pattern of Ejected Material (~ 10 X)

Figure 10-12. Surface Changes on Aluminum and Stainless Steel
Anodes Due to High Energy Discharge Conditioning

2-1412
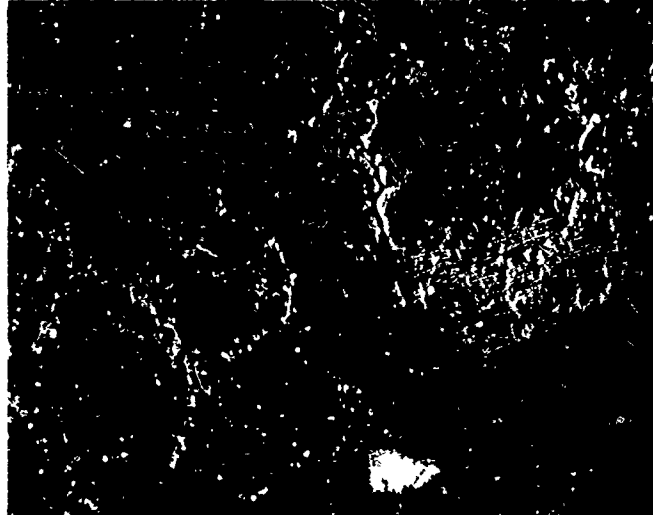
(a) General View - Note Lower Central Area in Which
Original 600 Grit Finish Is Undisturbed (~ 5 X)
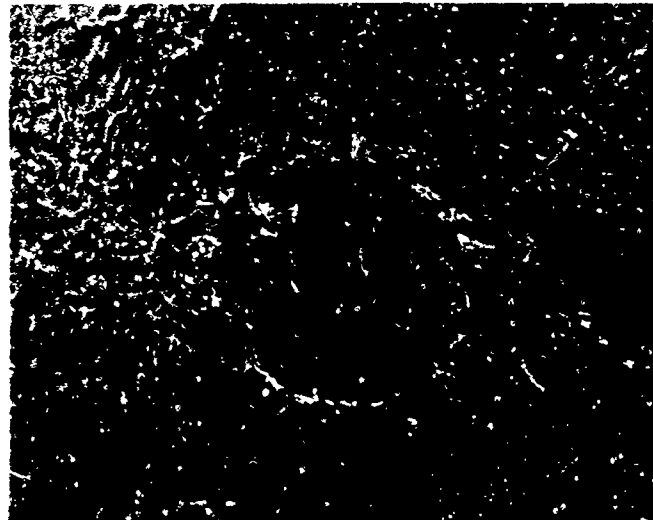
(b) Detail of Characteristic Ring Pattern (~ 10 X)

Figure 10-13. Surface Changes or Ti-7Al-4Mo Anode Due
to High Energy Discharge Conditioning

2-1413

(a) Cathode Subject to Heavy Deposit of Anode Material
in Form of Spattered Droplets and Condensed Vapor (~ 10X)

(b) Traces of Long Duration Arcs on Surface of Cathode (~ 10X)
Note Original 600 Grit Finish in Upper Right Corner

Figure   10-14. Surface Changes on Copper Cathodes
Due to High Energy Discharge Conditioning

2-1414

current flow in the spark channel produces a magnetic field which interacts in a complex manner with the nearby electrode surface. This phenomemon has been described by Watson[4] in some detail. During the discharge, in addition to surface disruption, particles of molten anode material are ejected. This, any material evaporated from the anode before breakdown, and vapor produced by the breakdown, are sufficient to explain the film of anode material which coats the cathode.

The cathode surface, as a result of localized spark effects and the impact or condensation of anode material, appears to be considerably rougher when compared to the intial surface finish. However, the microscopic structure revealed in Figure 10-14 shows that the projections are roughly hemispherical with melted surfaces. Thus, as far as field emission projections or whiskers are concerned (which have dimensions of the order of microns), the surface is not rougher in terms of producing regions of higher electric field. This of course depends upon the excellent adhesion and smooth shape of impacted particles. In some cases the result of high energy discharges is a surface with high emission levels. A copper anode was particularly likely to give a highly emissive surface when subjected to high energy discharges; while an electrode pair with a titanium alloy anode would, when conditioned by high energy discharges, tend to a less emissive state. In both of these cases the initial cathode material was titanium alloy.

In one test with 4-inch Diameter Bruce Profile stainless steel (Type 304) electrodes the anode particles impacted and flattened out on the cathode in the usual manner. When the voltage was reapplied many of these platters were pulled erect by the electric field, but remained attached at one end. This produced sharp projections (see Figure 10-15) with high field enhancement factors (>100). The net result was very high prebreakdown currents and low breakdown voltages. The projections could not be removed by conditioning. The lack of adhesion in this case was probably due to contamination of the cathode surface by a heated thermionic cathode (see Section 11).
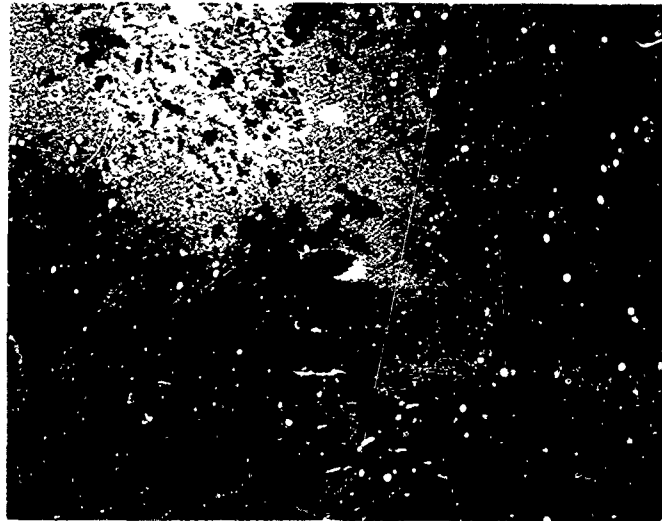
(a) General View - Highest Projection is in
Center of Photograph (~ 10X) (Projection is ~ 0.5 mm high)

(b) Detail of Sharpest Projection
Showing Area From Which
It Was Lifted (~ 12 X)
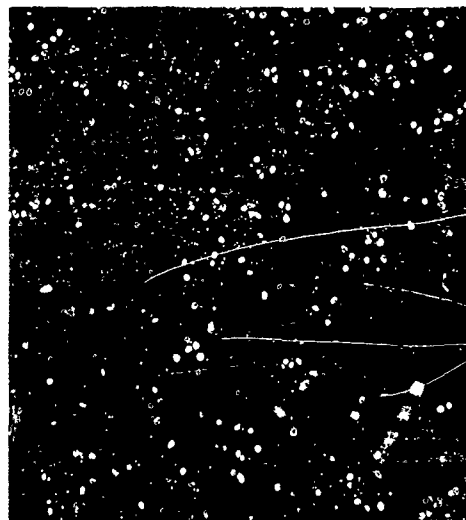
(c) Detail of Tip of
Sharpest Projection (~ 15 X)

Figure 10-15. Anomalous Damage Due to Partial Adhesion of
Anode Material on Cathode Surface Stainless Steel Electrodes

2-141b

High energy discharge conditioning, based on these observations of electrode surface changes, involves the melting and disruption of the anode surface. This is accomplished by prebreakdown electron beams and the discharge itself. Evaporation and ejection of anode material leads to a more or less complete coating of the opposite cathode surface. This process tends to spread out over the entire highly stressed surface area unless severe damage confines breakdown to one area.

10.9   Anode Material

Anode material was found in the basic factorial Energy Conditioning Study to be an important factor. The extensive transfer of anode material to the cathode typical of high energy discharge conditioning (see Section 10-8) would make this strong dependence almost inevitable. However, in the Energy Conditioning study the range of anode materials was limited, and the number of high energy discharges was low. Therefore, in parallel with the following experiment, a series of treatments were carried out to investigate the anode material effect in vacuum breakdown. The cathode material was usually Ti-7Al-4Mo and the anode materials included aluminum, copper, stainless steel Type 304, nickel, lead, tungsten, and Ti-7Al-4Mo. For all treatments a large number of high energy discharges were used in conditioning.

The usual experimental procedures were followed and consisted of machining of the electrodes to a Bruce Profile, 600 grit SiC finish, ultrasonic cleaning, and vacuum firing at a temperature near the melting point for 6 hours at 375° C with concurrent electrode bake at 400° C. The electrodes were first conditioned with a series resistance of 30 kilohms at a 0.75 cm gap. This was followed by a long series of high energy discharges with a total series resistance of 25 ohms and an energy storage capacitor bank of 0.15 μF (or 6750 joules at 300 kV). These procedures were standard except that lead had to be fired and baked at 200° C because of its low melting point. In some of the treatments Barium Contamination was present.

Typical experimental results are given in Figures 10-16 and 10-17. The usual smooth rise in breakdown voltage with high impedance conditioning is followed by a sharp drop in breakdown voltage level when high energy discharges are introduced. The breakdown voltage level slowly conditions up, reaching for some anode materials a higher level than before. There is considerable scatter with high energy discharges and it was found that the maximum breakdown voltage of an extended series was the most reliable measure of performance, although mean values are also of interest. The minimum value was so variable as to be of little use, but is interesting as an indication of the possible effects of a single high energy discharge.

The dominant role of <u>anode</u> material is well illustrated by the results of a treatment in which the anode was Ti-7Al-4Mo and the cathode was copper. As shown in Figure 10-18, the response of this combination to high energy discharges was excellent, just as if the cathode and anode were Ti-7Al-4Mo. This may be compared to the case of a copper anode opposite a titanium or nickel cathode - combinations which deteriorate in performance as a result of high energy discharges (see Figure 10-3).

Experimental results are given in Table 10-6 which also contains the physical parameters used in the correlation analysis. It was found that with high energy discharges there is a strong correlation between physical properties of the anode material and the breakdown voltage level. Melting point temperature, specific heat, and density were found to give the most reasonable fit in an equation of the form:

$$V_{BD} = A \, T_m^a \, C_p^b \, D_m^c$$

where:

A = 1.56   at a 0.75 cm gap for 4-inch Diameter

a = 0.77   Bruce Profile Electrodes.

b = 0.53

c = 0.29

10-43
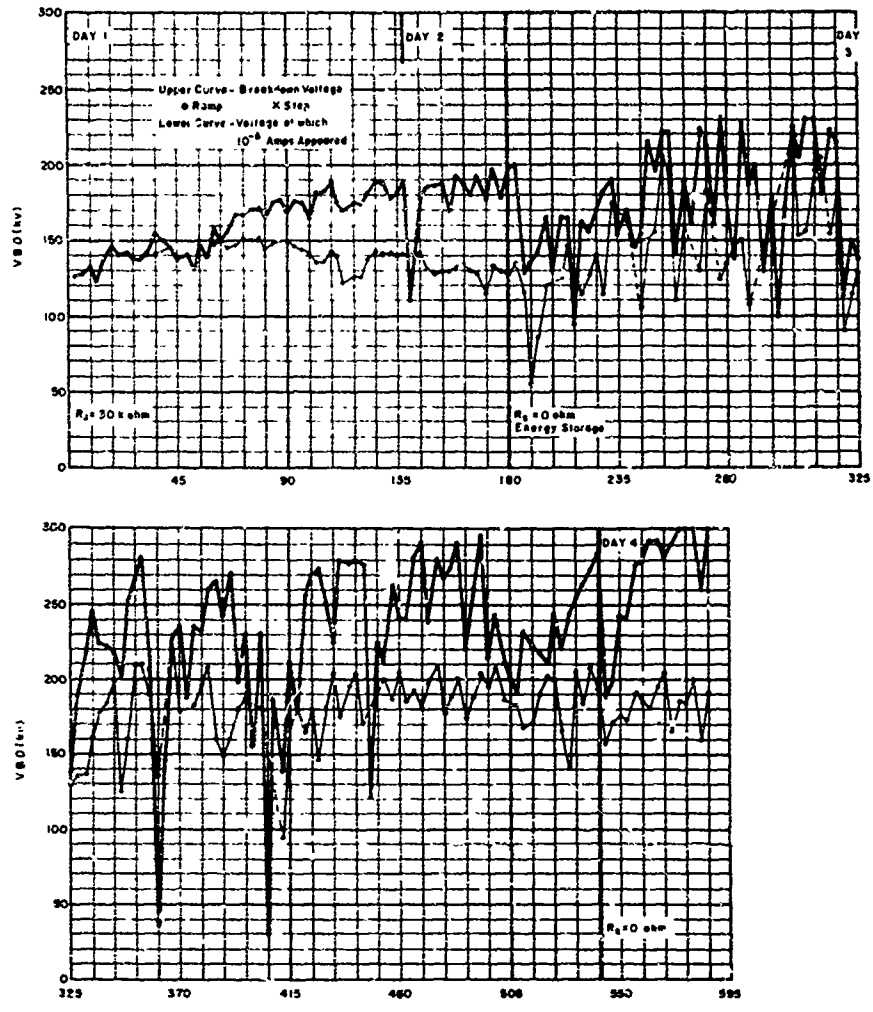
Figure 10-16. Conditioning Curve, 4-Inch Diameter Bruce Profile
Electrodes Stainless Steel 304 Anode and Cathode at 0.75 cm Gap
(Every Third Breakdown Has Been Plotted)

1-4264

10-44
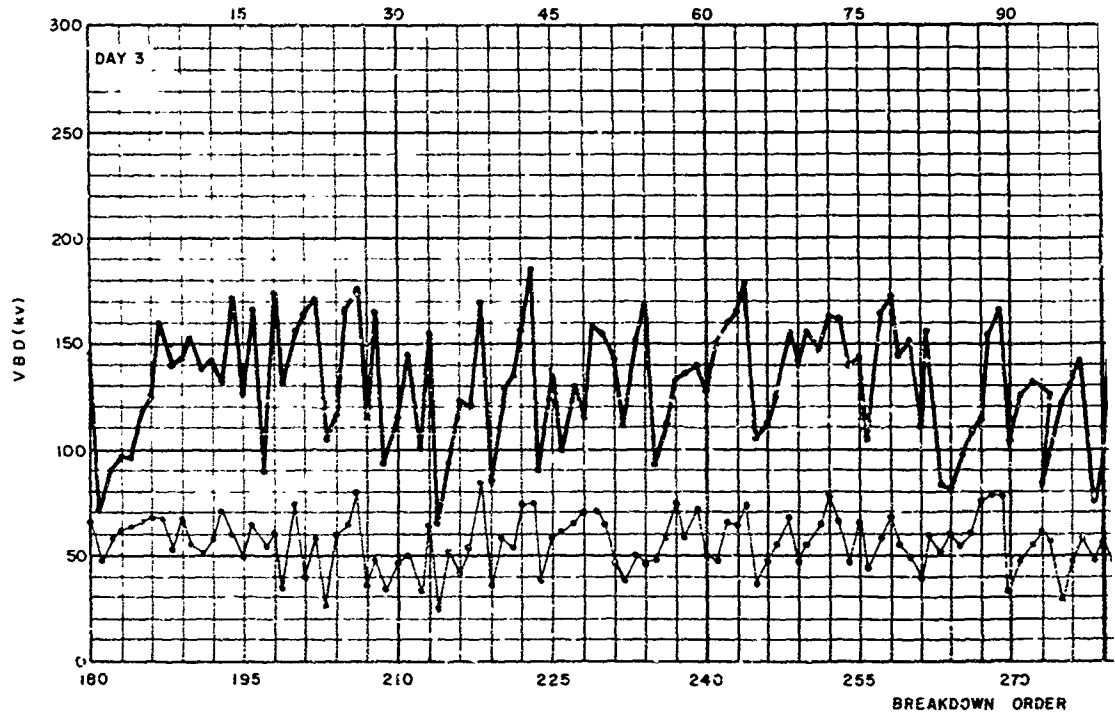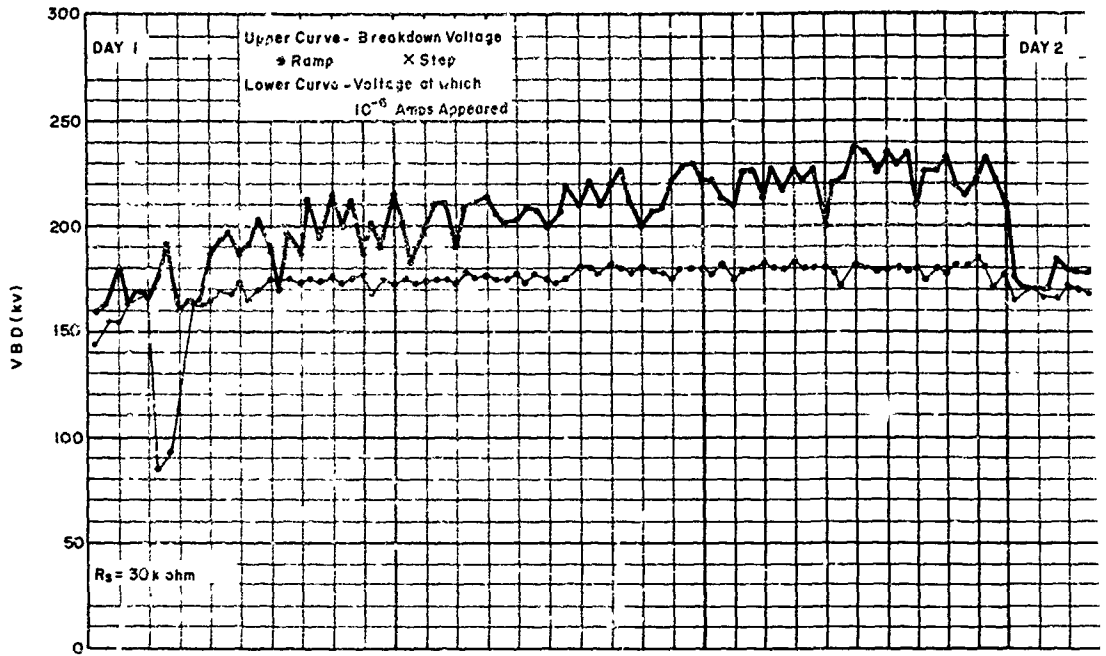
1-4265
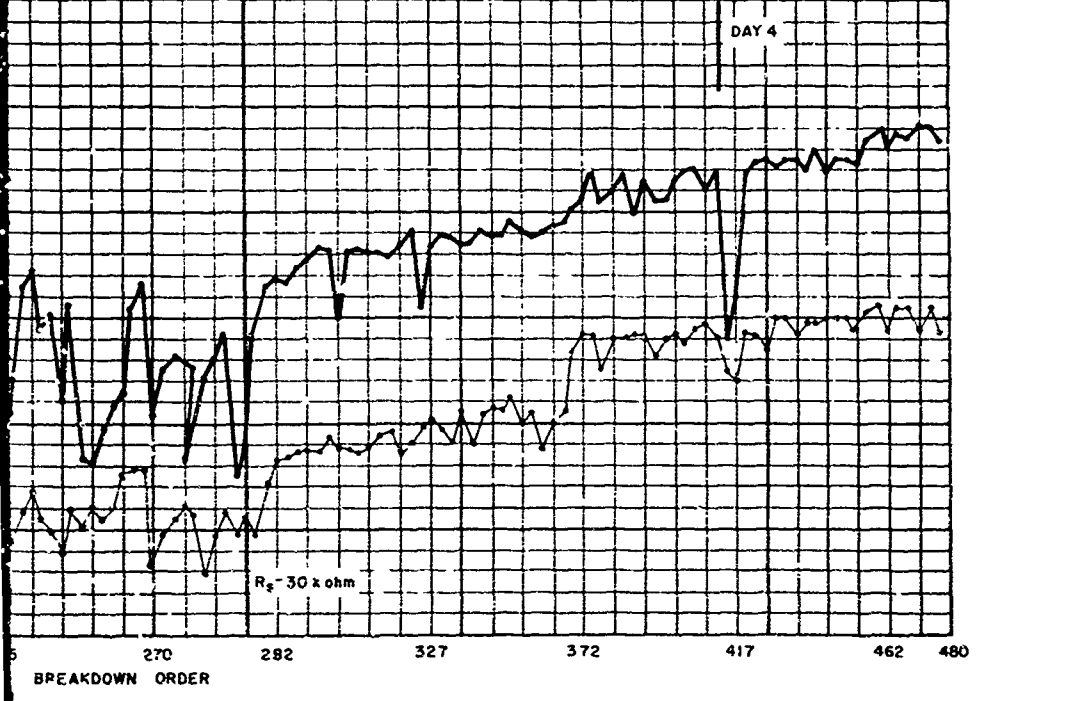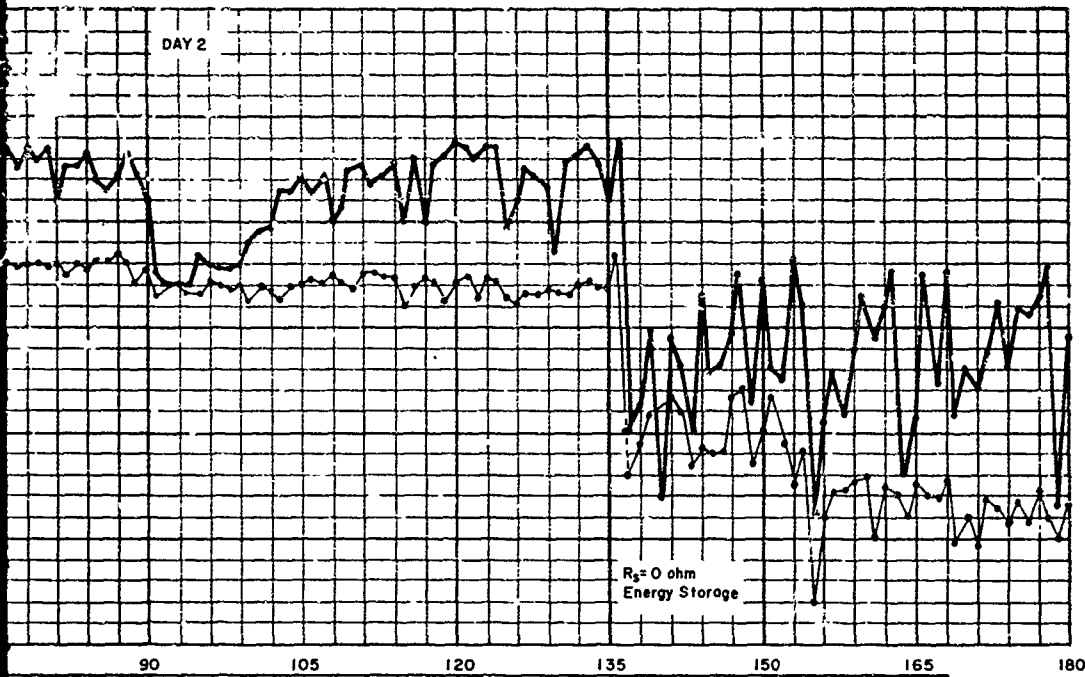
Figure 10-17 Conditioning Curve,
4-Inch Diameter Bruce Profile
Electrodes Aluminum Anode and
Ti-7Al-4Mo Cathode at 0.75 cm Gap

10-45
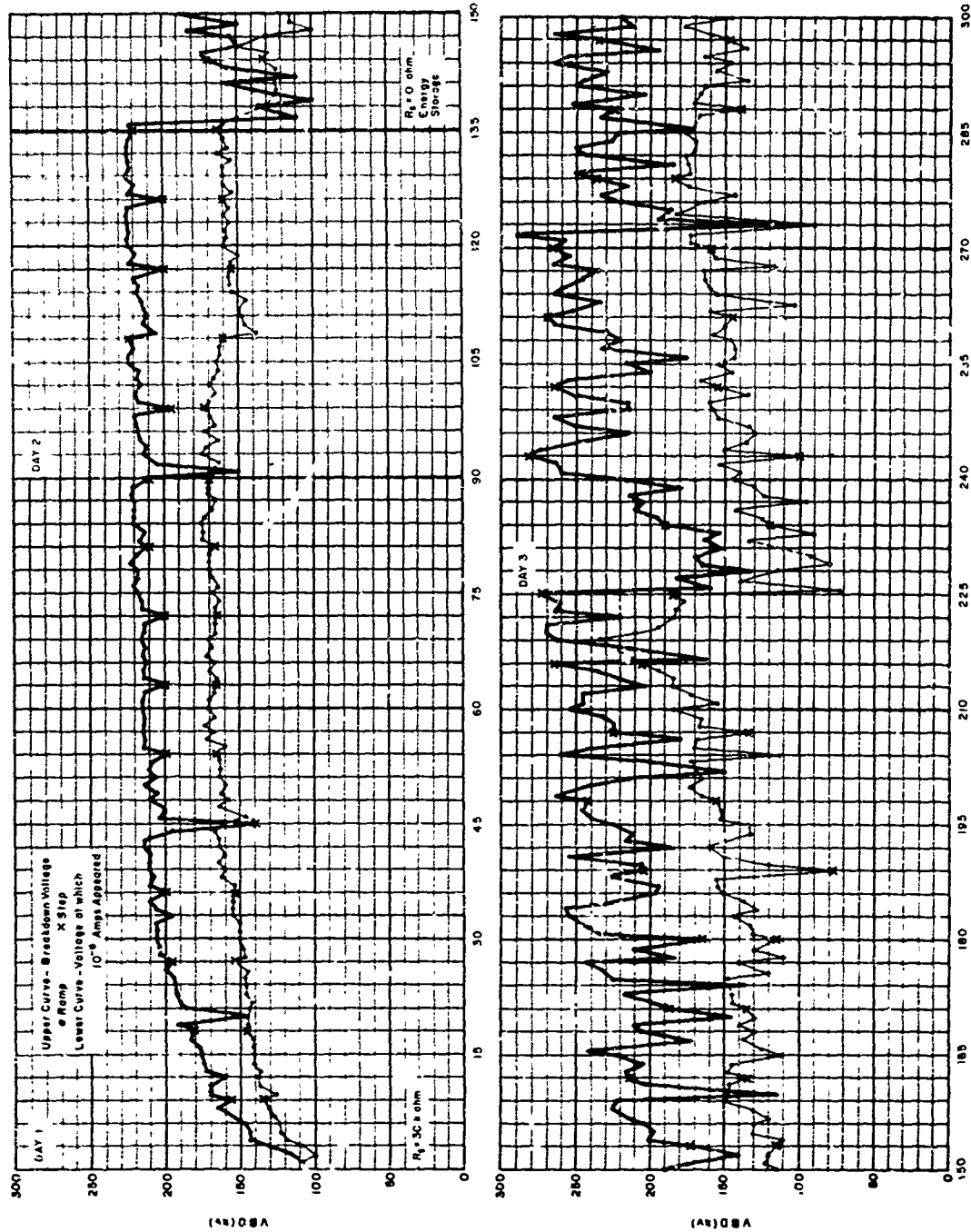
Figure 10-18. Conditioning Curve, 4-Inch Diar.ster Bruce Profile
Electrodes Ti-7Al-4Mo Anode and OFHC Copper Cathode
Low and High Energy Discharges - 0.75 cm Gap

1-4266
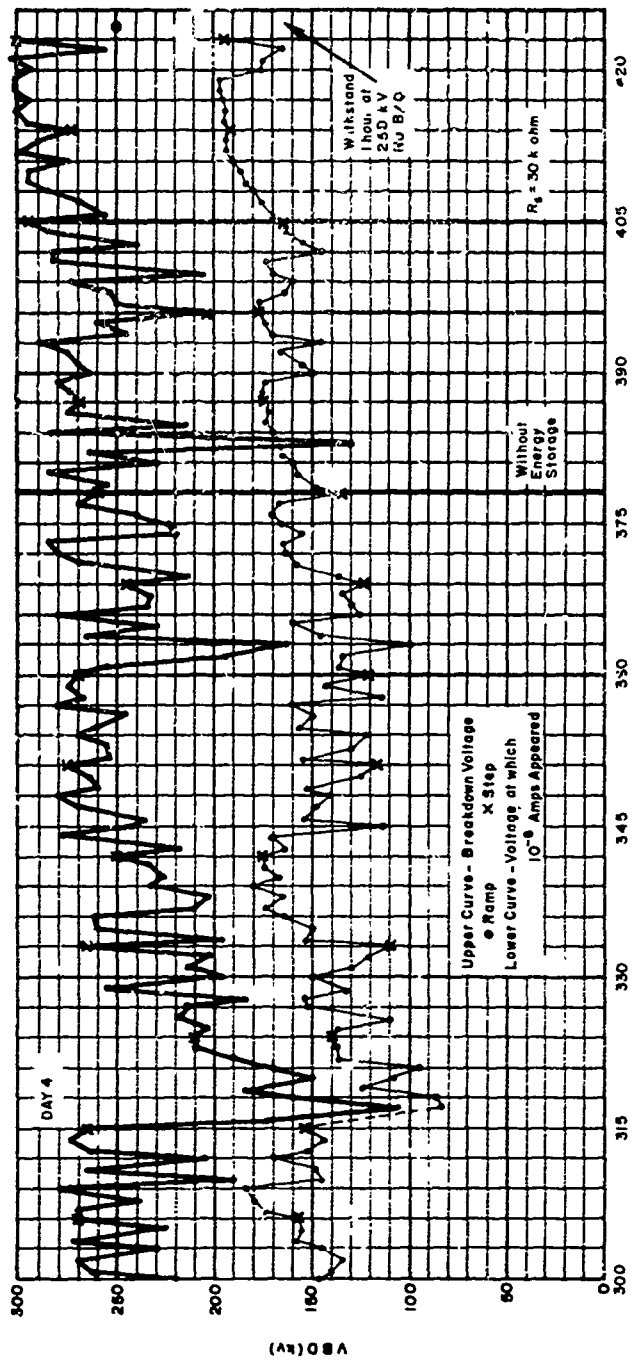
Figure 10-18. Continued

1-4266

Table 10-6. Effect of Anode Material on Breakdown Voltage and Physical Constants of Anode Materials.

	Electrode Material		Breakdown Voltage Levels for High Energy Discharges			Final Low Energy Discharges
Treatment Code	Anode Material	Cathode Material	Maximum	Minimum	Average (Approximate)	
ab:Ti2	Ti	Ti	285	170	240	285
Ba:Ti	Ti	Ti	280	100	230	280
ab(R)	Cu	Ni	220	95	150-175	190
AM 1	Ti	Cu	290	105	260	300
AM 2	Al	Ti	185	62	140	240
AM 3	SS	SS	293	30	250-270	297
Ba:Ni	Ni	Ni	300	170	270	300
AM 4	Pb	Ti	76	32		115

Physical Constants of Anode Materials

Material	Tm (°K)	$Cp \left(\frac{cal}{gm}\right)$	$Dm \left(\frac{gm}{cc}\right)$
Al	933	.215	2.7
Cu	1356	.092	8.9
Ni	1726	.106	8.75
Ti (alloy)	1971	.123	4.48
SS 304	1749	.120	8.0
Pb	601	.0305	11.34
W	3683	.0322	18.8

The relationship $V_{BD} = A \, T_m^a \, C_p^b \, D_m^c$ was expressed in log form and a linear multiple regression analysis using a time-shared computer was carried out for several different sets of experimental results. In all cases the least squares fit was excellent with an index of determination of above 0.95.

Figure 10-19 plots this dependence for several anode materials and indicates the measurements used in its derivation. It can be seen that the breakdown level of a lead anode was predicted to be 72 kV and experimentally found to be about 76 kV.

The physical mechanisms responsible for the correlation found here are presently uncertain. Zinn, et al.[6] have found a similar correlation of breakdown voltage level with anode specific heat and the temperature necessary for a vapor pressure of 10^{-5} torr. The data used in their analysis was obtained at gaps of 0.5 mm and it was suggested that anode heating by field emission electron beams was the cause of breakdown. Rosanova and Granovski[6] investigated Al, Cu, Fe, Ni, Mo, W and graphite as anode materials (no dependence on cathode material was found) and obtained the same ranking as the present experiment. They rejected a correlation of thermal properties and breakdown voltage on the grounds that graphite had a low breakdown voltage while its thermal properties would predict a high breakdown voltage. It is suggested that the breakdown voltage increases as the Young's modulus of the anode material, thus indicating a clump breakdown mechanism.

In practice it appears that the actual mechanism could depend on experimental technique or the degree of conditioning. Thus gas evolution from an anode hot spot might precipitate breakdown at first, but later the electrostatic extraction of a particle from a thermally weakened area would lead to breakdown. In any case, the empirical correlation presented here provides a practical means of ranking anode materials and estimating the breakdown voltages expected of various material combinations under high energy discharge conditions. Further experimentation is necessary to positively identify the exact mechanisms of breakdown.
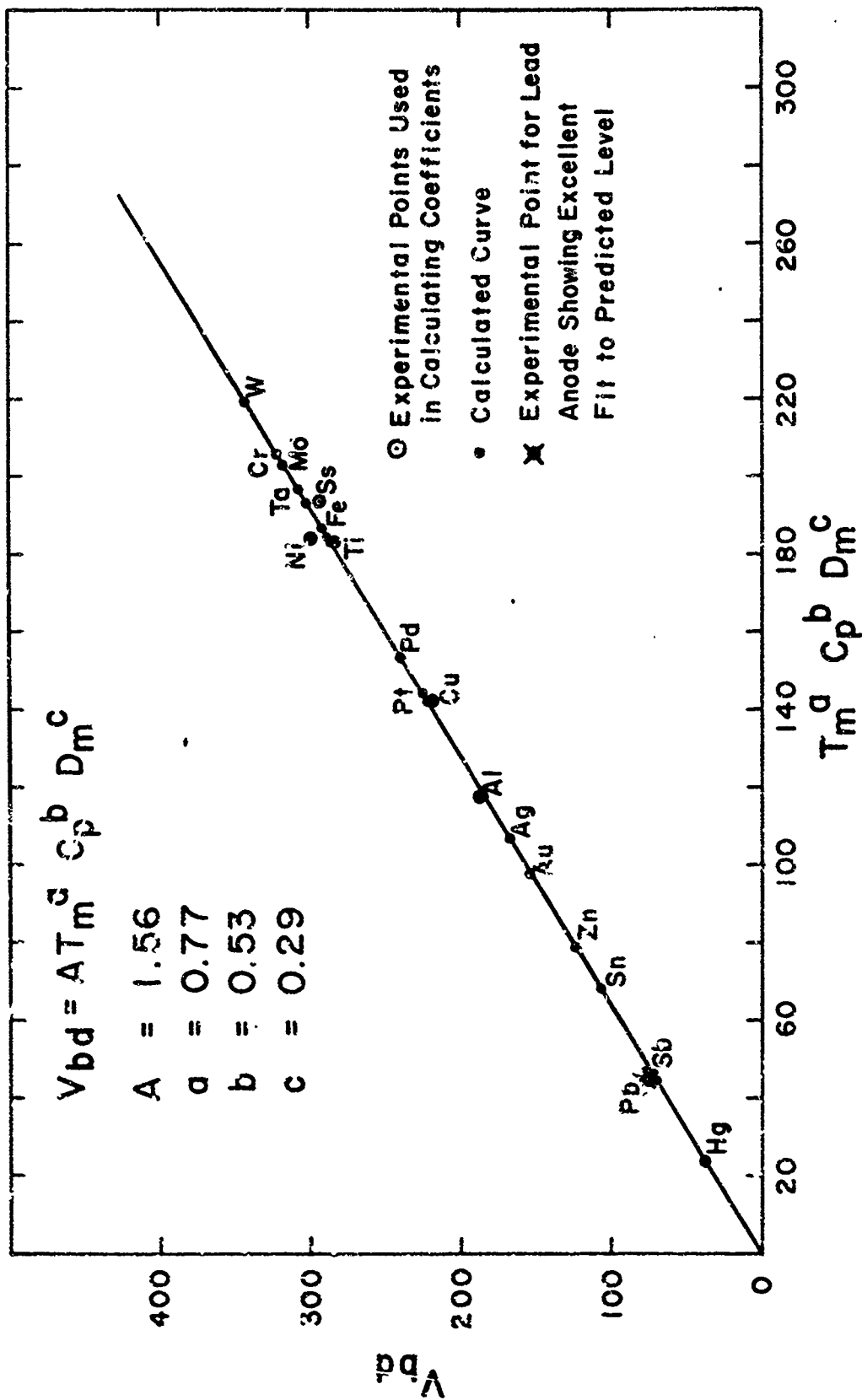
Figure 10-19. Correlation Between Anode Material Physical Properties and Breakdown Voltage During High Energy Discharge Conditioning

10.10   Conclusions

In this experiment conditioning has emerged as one of the most important factors in vacuum insulation. For a given set of electrodes the breakdown voltage was strongly dependent upon the number and nature of conditioning discharges. The energy of each discharge was critical, with the beneficial or damaging effects being produced in the first microsecond if energy was available.

It was found that a series resistance of around 30 kilohms, which limited the current from the energy storage bank to a maximum of 10 amperes at 300 kV, provided isolation of the gap. This high impedance conditioning in which each discharge dissipates less than 10 joules, produced a steady and smooth increase in breakdown voltage without any increase in prebreakdown current.

When the series resistance was 1 kilohm and a 0.15 μF capacitive energy storage bank was connected (for up to 6,750 J at 300 kV), the breakdown voltage often dropped to low levels. There was, however, no marked change in prebreakdown current level for these moderate energy discharges.

High energy discharges, produced with 24 ohms of series resistance and the 0.15 μF energy storage bank, were initially damaging. The breakdown voltage often dropped by more than 50%. Electrode materials such as copper, lead, and aluminum continued to degrade, reaching low average breakdown voltages with high prebreakdown currents (> 2 mA in some cases).

However, high energy discharge conditioning was discovered to have a critical dependence on anode material. The cathode became covered with an adherant and continuous coating of anode material in the form of a condensed vapor and discrete particles. For some anode materials such as titanium, nickel, and stainless steel the breakdown voltages achieved by high energy conditioning was actually higher than that obtained with high impedance (low energy) conditioning.

The breakdown voltage was then found to correlate extremely well with physical and thermal properties of the anode material. An equation of the form:

$$V_{BD} = A T_m{}^a C_p{}^b D_m{}^c$$

was found to give the best fit where T_m is the melting temperature, C_p is the specific heat, and D_m is the density. The coefficients were approximately: $a = 0.77$, $b = 0.53$, and $c = 0.29$. These results have been related to breakdown models in which the thermal interaction of field emission beams with the anode surface plays the initiating role.

Withstand tests with voltage maintained at fixed levels for varying lengths of time showed that the mean time to breakdown increases exponentially as the stress level is decreased from the ramp voltage (5 kV/s) breakdown level. Prebreakdown currents were found to behave as would be expected for field emission if it was assumed that the field enhancement factor β increased as the total current increased.

The vacuum discharge was found to rise rapidly in current (> 2 x 10^{10} A/s) with a relatively slow collaspe of voltage across the gap. The time to total voltage collapse for the 0.75 cm gap was about 100 ns. The initial phase of the discharge appeared to have a high impedance (~ 1000 ohms), accounting for the observation that most of the discharge damage occurs during the first microsecond.

Finally, it was found that proper choice of electrode material (especially the anode) and conditioning technique makes possible stress levels of up to 400 kV/cm across large gaps for broad area electrodes.

SECTION 11

BARIUM CONTAMINATION STUDY

11.1   Introduction

High voltage vacuum tubes which use a thermionic cathode of the
Barium Oxide type to supply the necessary electrons are usually found [1] to be
limited to lower electric stresses than tubes not subject to the decomposition
and evaporation products from this heated cathode. The most probable explana-
tion for this lowering of operating stress is the reduction of work function of the
metal surfaces when barium and/or barium oxide is deposited. This would lead
to higher prebreakdown currents and lower breakdown voltages than for the
uncontaminated case.

Thus barium contamination is an important factor in high voltage
vacuum tube performance. Accordingly, an experimental series investigating
the effects of controlled barium contamination of copper, nickel, titanium alloy,
and stainless steel electrodes has been carried out. The contamination was
produced by a typical high power tube Barium Oxide Cathode heated in the vicin-
ity of the gap and directed at either the cathode or anode. In addition, the energy
available to the discharge was varied over a wide range (10 J to 6750 J) so as to
make possible a comprehensive study of energy conditioning of contaminated
electrodes.

The effects of barium contamination were found to depend both on
electrode material and the method of conditioning. These effects will be de-
scribed in detail. In general, barium contamination reduced the breakdown voltage,
but conditioning returned it to the uncontaminated level. Also there was no
permanent increase in prebreakdown current after contamination. Thus, it
appears that the degrading effects of barium contamination may be alleviated by
proper conditioning. However, in some cases high energy discharges and barium
contamination of the cathode resulted in permanent damage to the electrode
system due to poor adhesion of impacted anode particles on the contaminated
cathode.

11-1

11.2   Experimental Procedure

The techniques of materials processing, prefiring and baking developed in previous experiments were used to obtain repeatable results. The electrodes were machined to Bruce Profile for a uniform field geometry and were four inches in diameter. After rotary polishing to a 600 grit SiC finish, they were ultrasonically cleaned and fired in vacuum at 900°C for six hours. The electrodes were then allowed to cool, removed from the firing furnace, and installed in the test chamber. The entire system was pumped overnight, baked at 400°C for six hours, and cooled for over 48 hours before testing.

The barium contamination was introduced by moving a heated Barium Oxide Cathode into the vicinity of the gap by means of the rod and bellows assembly has been shown in Figure 3-12. This mechanism is attached to the loading port and can be withdrawn from the gap to beyond the surface of the port - a distance of about 18 inches. The Barium Oxide cathodes were obtained from Machlett Laboratories and are typical of those used in high voltage vacuum tubes. The hot emitting surface (~ 1 cm^2) was directed at either the cathode or anode electrode of the vacuum gap. A metal shield protected the other electrode from direct contamination. A fresh barium oxide cathode was used for each treatment.

The usual contamination cycle placed the barium oxide cathode within approximately 3 cm of the electrode surface to be contaminated and about 3 cm from the center of the electrodes. The angle between the hot surface of the barium cathode and the electrode surface was about 45°. This orientation was chosen to provide even coverage of the 4 inch diameter surface from the 1 cm diameter source. In a later experiment with 1.28 inch diameter electrodes the barium oxide cathode was placed directly in front of the electrode surface at a spacing of 2 to 3 mm. This, of course. produced more contamination in a given time and it was found that periods of less than one hour were sufficient. For the larger electrodes tens of hours were required to produce significant effects.

Before use the Barium Oxide cathode had to be "activated". The activation procedure converts the barium and strontium carbonates of the unused cathode to oxides and free barium in such a way that a stable adherent layer is produced on the nickel substrate. This is accomplished by gradual heating under
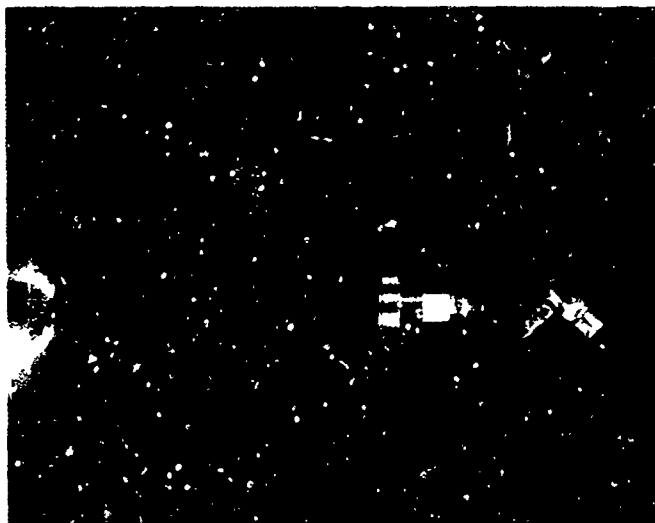
Figure 11-1. Mechanism for Introducing Barium
Contamination Source into Vacuum Gap

2-1315

vacuum. The filament current is set to 0.5 and 0.6 amps for one minute each, then increased in 0.1 amp steps every two minutes up to 1.0 amp. This level is held for 15 minutes and corresponds to the normal operating temperature of about 800°C. The current is then increased to 1.1 amps for three minutes before resuming the normal level of 1.0 amperes.

The activation sequence was performed with the barium oxide cathode near the vacuum gap. Subsequent running was either at normal operating temperature (1.0 ampere filament current) or at higher levels (up to 1.3 amperes). Exposure times as long as several days, with elevated temperatures to increase the amount of contamination evolved were used. The barium oxide cathode was withdrawn during high voltage testing.

The usual test sequence was to condition the 0.75 cm vacuum gap with high impedance (R_S = 30 kilohms) discharges of low energy, expose the cathode or anode electrode to the heated barium oxide cathode, and then recondition the vacuum gap. A comparison of breakdown voltage and prebreakdown current levels before and after exposure then gave the effect of the barium contamination. This cycle of condition - contaminate - recondition was repeated several times with various degrees of contamination, which were produced by varying the temperature or running time of the barium oxide cathode. After this high impedance - low energy series, high energy discharges (R_S = 25 ohms with 0.15 μF of energy storage) were used in the same cycle of condition - contaminate - recondition.

11.3   Experimental Results

11.3.1   General

The experimental results are conveniently reported in the form of conditioning curves in which the breakdown voltage and the voltage to produce 10^{-6} amperes of prebreakdown current are plotted as a function of the breakdown order. Most results were obtained with contamination of the cathode of electrode pairs of copper, nickel, stainless steel (Type 304), or titanium alloy (Ti-7Al-4 Mo). In most of the curves every third breakdown has been plotted so as to

11-4

keep the overall curve to a reasonable length. Any breakdown which was significantly different from adjacent breakdowns in terms of breakdown voltage or prebreakdown current level has also been included.

11.3.2   Copper Electrodes

Copper electrodes subjected to barium contamination of the cathode (see Figure 11-2) showed several unexpected effects. Initially, there was only a slight change in breakdown voltage after exposure, and the electrodes rapidly reconditioned to a higher level than before contamination. Prebreakdown current was increased, with breakdown occurring at lower current levels, but this too, quickly conditioned to its former level, and in fact, after contamination and conditioning the emission currents were lower. Finally upon exposure for 16 hours to the barium oxide cathode run at elevated temperature (1.2 amps filament current) the gap, after exposure, showed a progressive decrease in breakdown voltage as conditioning proceeded. The prebreakdown current levels prior to breakdown were extremely erratic, with breakdown usually occurring before 10^{-6} amperes was reached.

At this point, in order to condition rapidly, a technique of repeated sparking was introduced. This was possible with the 30 kilohms series resistance because each breakdown discharged mainly the gap and immediate bushing capacitance with the current from the high voltage cable being limited to around 5 amperes. Thus the high voltage cable dropped in voltage by only a few percent, the vacuum gap recovered, and the 2 mA power supply rapidly recharged the cable until breakdown again occurred. This sequence was repeated several times a second to give hundreds of conditioning breakdowns in a short time.

With repeated sparking, the gap soon conditioned to higher breakdown voltages and lower prebreakdown currents than before contamination. This sequence of condition - contaminate - condition with single breakdowns - condition with repeated sparking - was repeated several times with similar results. At one point an extended series of single breakdowns (breakdown number 1760 through 2170) proved ineffective in reconditioning after barium contamination, while repeated sparking reconditioned the gap in a short time. Thus, the close

11-5

Upper Curve - Breakdown Voltage
  ● Ramp   X Step
Lower Curve - Voltage at which
        10⁻⁶ Amps Appeared
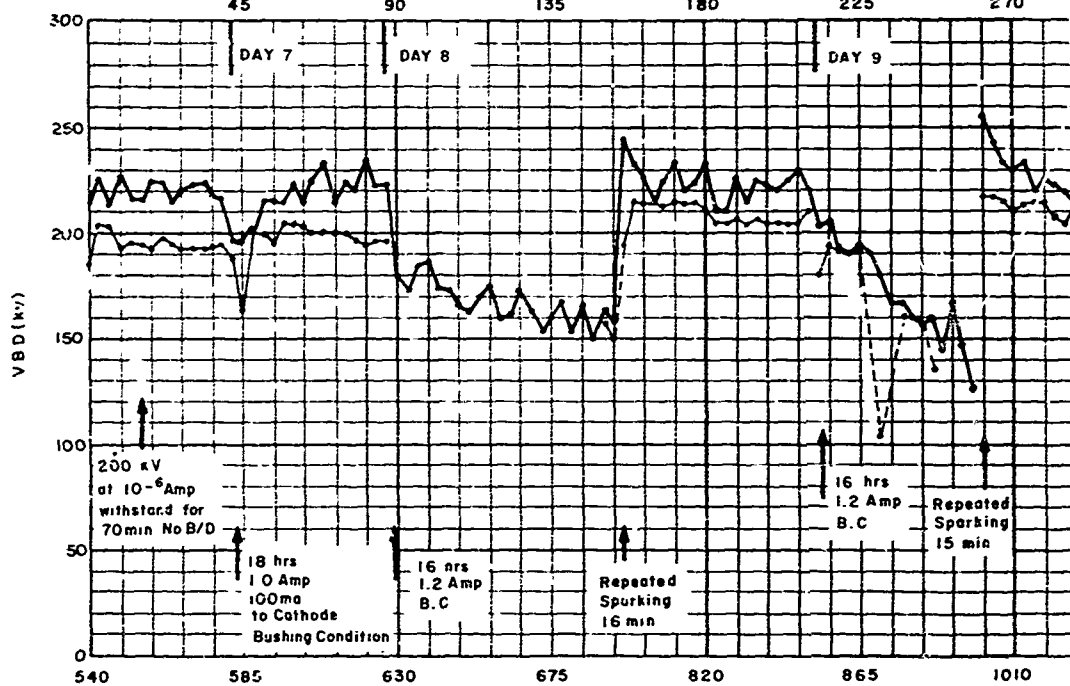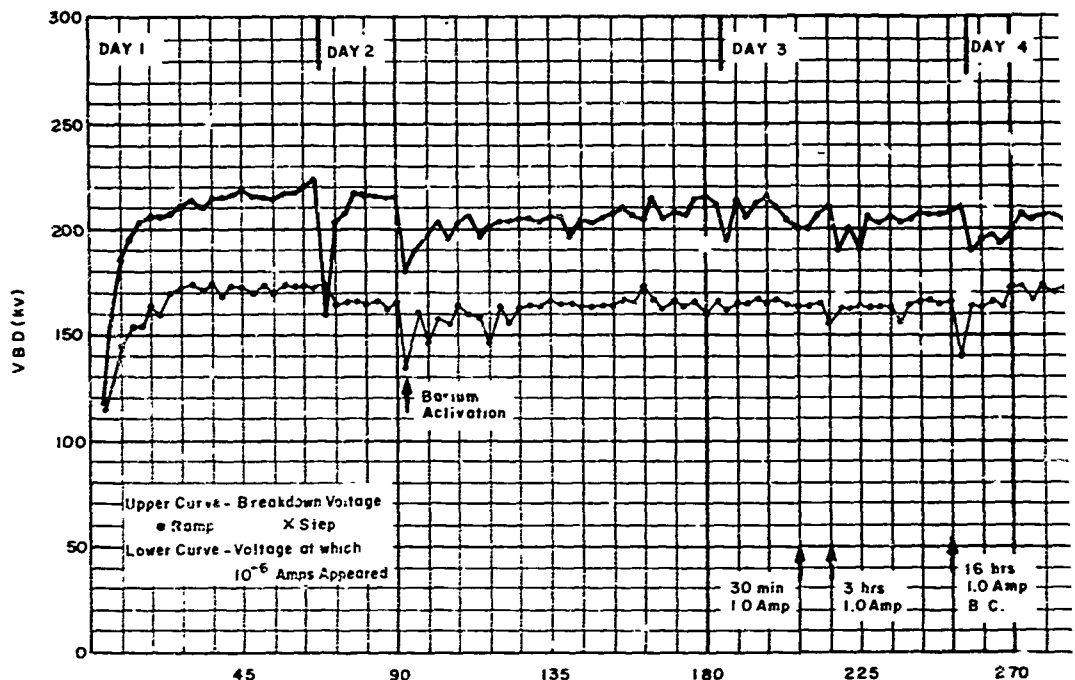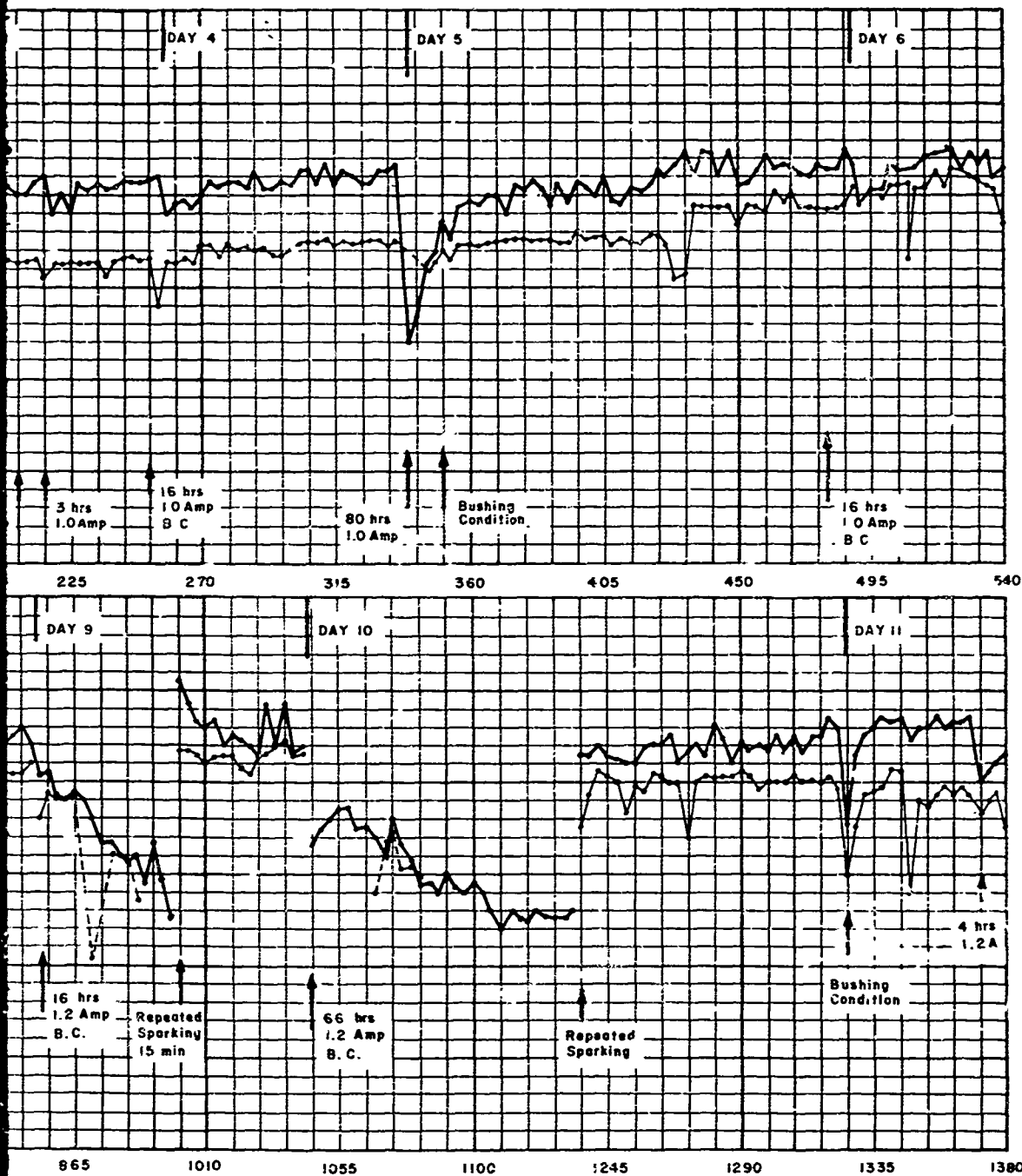
1-4272

Figure 11-2 Conditioning Curve for
Barium Contamination Treatment 1 -
4-Inch Diameter Bruce Profile Vacuum
Fired OFHC Copper Electrodes at 0.73
cm Gap - R_s = 30 Kilohms
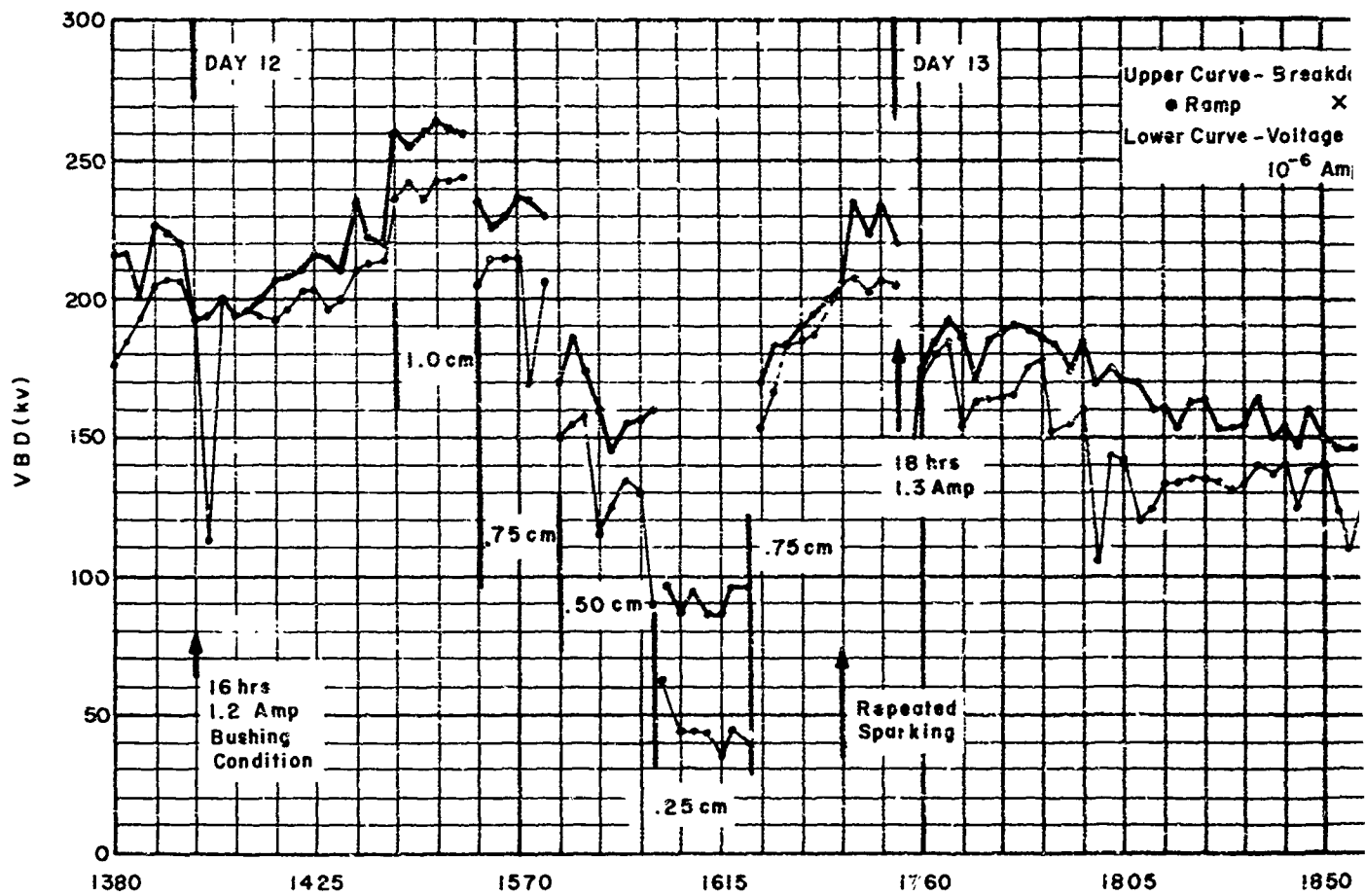
1-4272
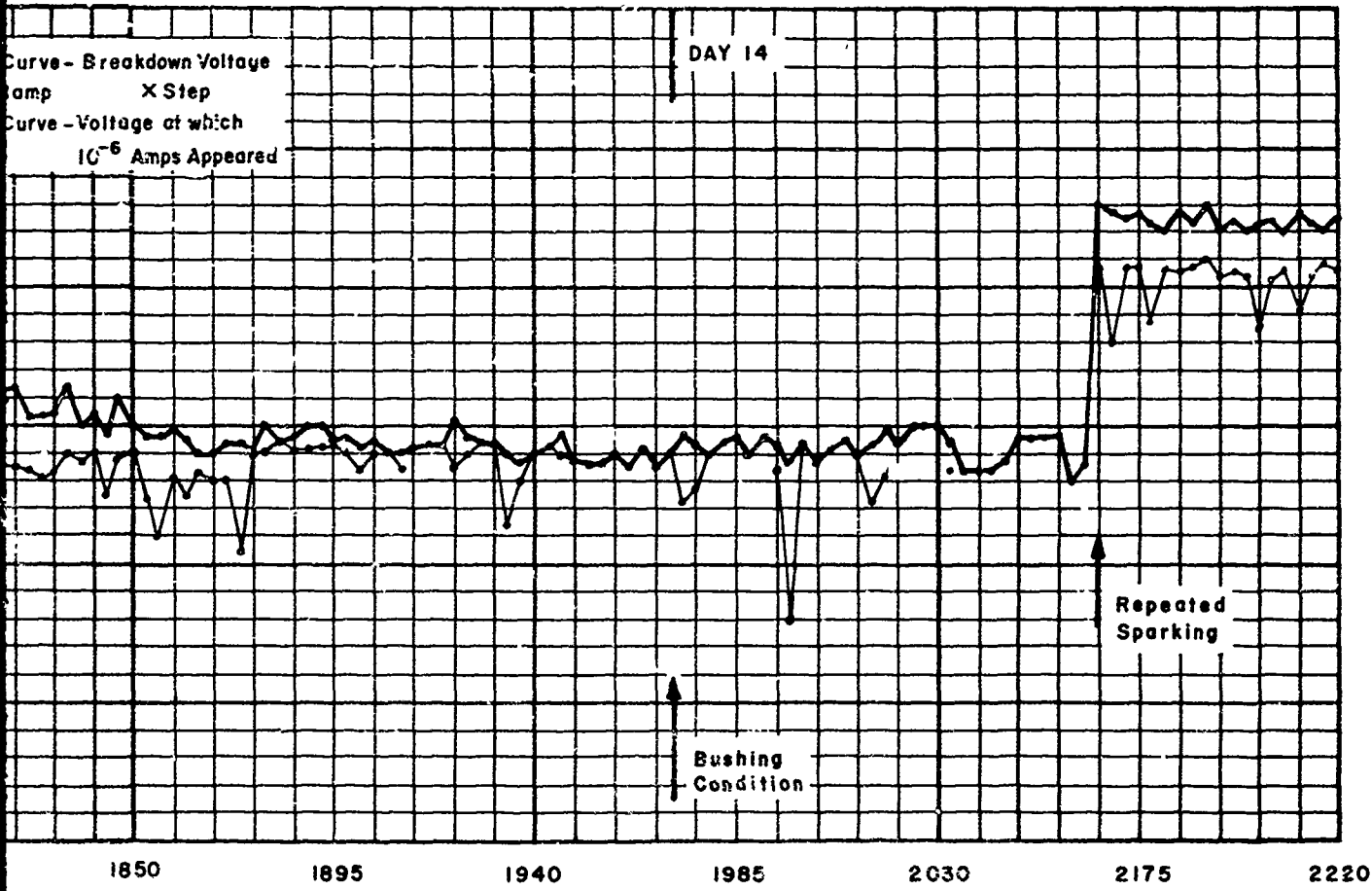
Figure 11-2. Continued

11-7

spacing in time of the repeated sparking conditioning appears to be important, and not just because more breakdowns are obtained.

After 13 exposures to various levels of barium contamination, these OFHC copper electrodes had a breakdown voltage of 225 kV for a 0.75 cm gap, with 10^{-6} amperes of prebreakdown current at 205 kV. The dependence of these levels on gap was approximately linear up to 0.75 cm, with an apparent square root dependence above 0.75 cm as shown in Figure 11-3.

The electrode surfaces were examined at the end of the experiment and several interesting features not usually found were observed. Unlike almost all other electrode pairs in this program, there was no general transfer of anode material to the cathode. This can be attributed to the very limited discharge energy (R_S = 30 kilohms, no energy storage).

Indeed, it was found that in general these low energy discharges produced little anode surface damage. When, in other experiments, the series resistance was 100 ohms the energy stored in the high voltage cable (1000 μF capacitance and thus 45 joules at 300 kV) was able to flow into the gap at such a rate that considerable anode material was transferred to the cathode, leaving behind a severely eroded and melted surface. (see Figures 10-13 and 9-14). The principal effect of thousands of low energy discharges was to reveal the grain structure of the anode as shown in Figure 11-4a. This etching, or preferential removal of surface material, was most likely the result of electron bombardment. That electron bombardment is capable of such an effect has been demonstrated for electron beam pulses of 10 μs duration[2]. In the present experiment the electron beam energy could be delivered during both the prebreakdown field emission phases and the early stages of the breakdown before a low impedance arc has formed.

Other changes on the anode surface for low energy high series resistance discharge include several severely eroded regions. A typical region is shown in Figure 11-5b. This is thought to be the result of a concentration or repeated application of electron beams. In addition several craters were noted which are typical of a localized spark. A representative crater is shown in Figures 11-4c and 11-4d.

11-8
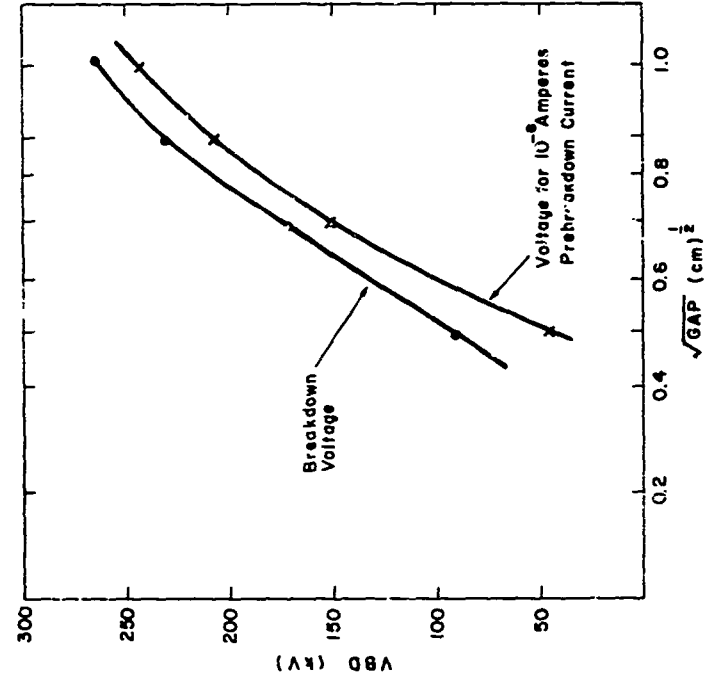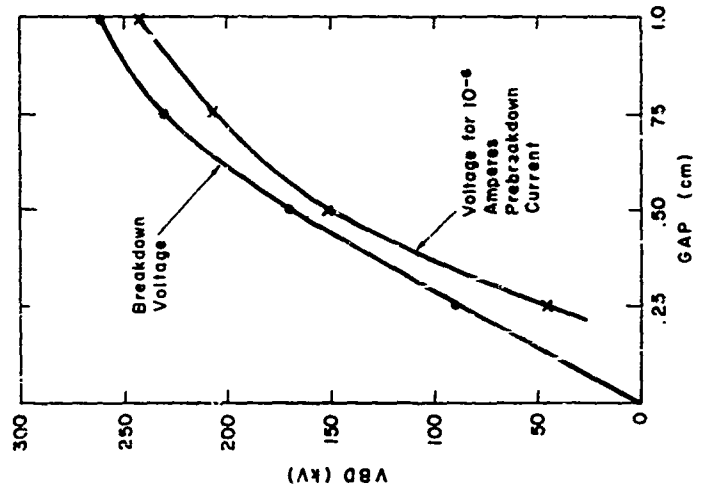
Figure 11-3. Dependence of Breakdown Voltage and Voltage for 10^{-6} Amperes of Prebreakdown Current on Gap and $\sqrt{\text{Gap}}$ for 4-Inch Diameter Bruce Profile OFHC Electrodes

1-4111
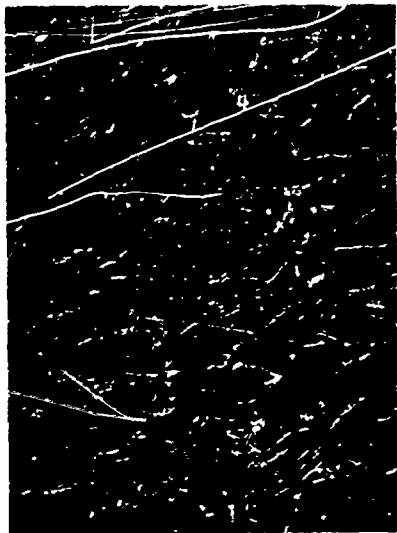
(a) Grain Structure Revealed by
Electron Bombardment (~ 49 X)

(b) Severely Eroded
Region (~ 40 X)
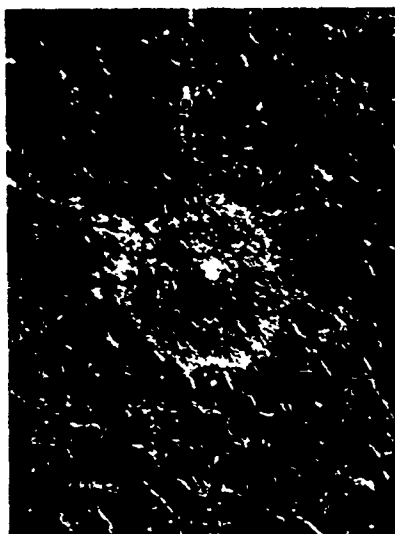
(c) General View of
Crater (~ 20 X)
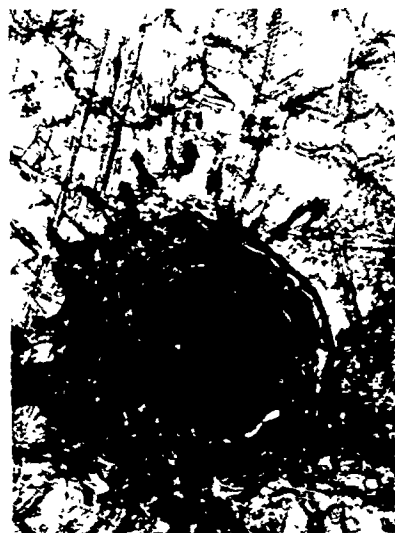
(d) Detail of Crater (~ 75 X)

Figure 11-4. Surface Changes on Copper Anode Due to
Many Low Energy Discharges

2-1457
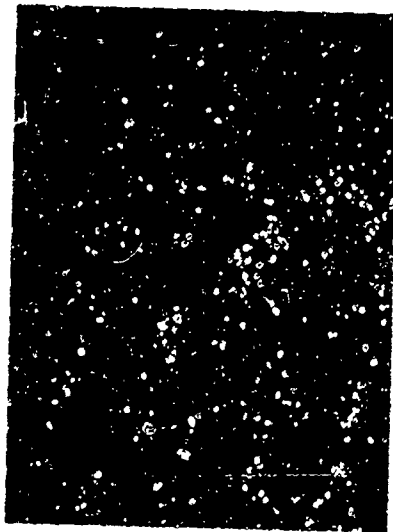
(a) General View of Cathode
Surface (~10 X)
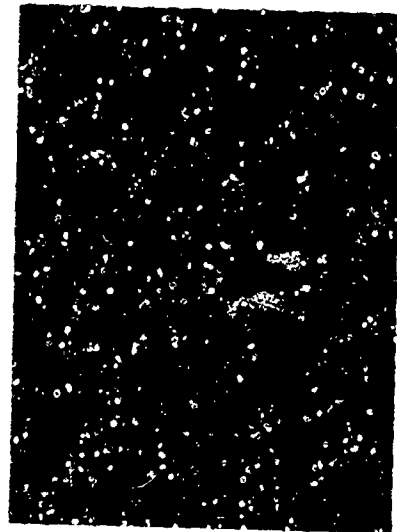
(b) Detail of Cathode Surface
Showing Crater and
Protrusions (100 X)

(c) Detail View with Tips of
Protrusions in Focus (100 X)
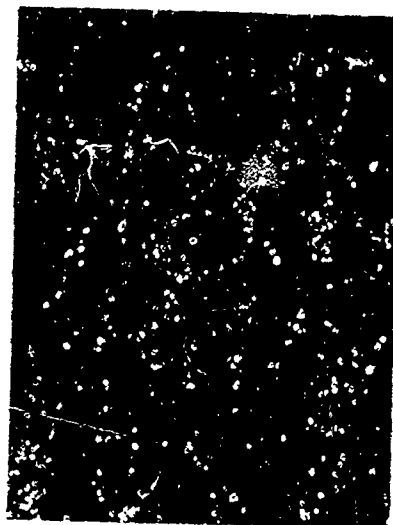
(d) Detail View with Surface in
Focus - Note 600 Grit Polishing
Marks (100 X)

Figure 11-5. Surface Changes on Copper Cathode Due
to Many Low Energy Discharges[20]

2-1464

The cathode surface was covered in the central regions of the electrode by small protrusions and craters as shown in Figure 11-3. The underlying 600 Grit polishing marks are generally undisturbed. It is reasonable to attribute the protrusions to the impact of anode material.

In one early treatment the barium contamination source was directed at the anode of a pair of copper electrodes. There was no measurable or consistent change. This result compared with the effects found with cathode contamination, however mild and transient, led to conducting the balance of the treatments with cathode contamination.

Copper electrodes were also tested for the effects of barium contamination of the cathode at a smaller gap of 0.25 cm. It was found that there was little effect of contamination on breakdown voltage and almost no effect on prebreakdown current levels. High energy discharges produced the usual wide scatter and frequent low breakdown voltages accompanied by a general increase in prebreakdown current. The dependence of breakdown voltage and voltage for 10^{-6} amperes of prebreakdown current on gap up to 0.75 cm was near linear as shown in Figure 11-6.

11.3.3   Ti-7Al-4 Mo Electrodes

Titanium alloy electrodes were subjected to barium contamination of the cathode at gaps of 0.50 cm and 0.75 cm. There was only a small drop in breakdown voltage at the 0.50 cm gap even after 66 hours of exposure to a barium oxide cathode which was heated at 1.3 A filament current (normal operating temperature is achieved with 1.0 A) (Figure 7). This decrease was quickly removed by conditioning. At the 0.75 cm gap repeated sparking was used for fast conditioning and a breakdown voltage level of 230 kV with 10^{-6} amperes of prebreakdown current at 172 kV was reached. After exposure to the heated barium oxide cathode the breakdown voltage dropped by 100 kV and breakdown occurred before the 10^{-6} amperes of prebreakdown current was reached. This decrease was conditioned away in a short time. High energy discharges were then intro-
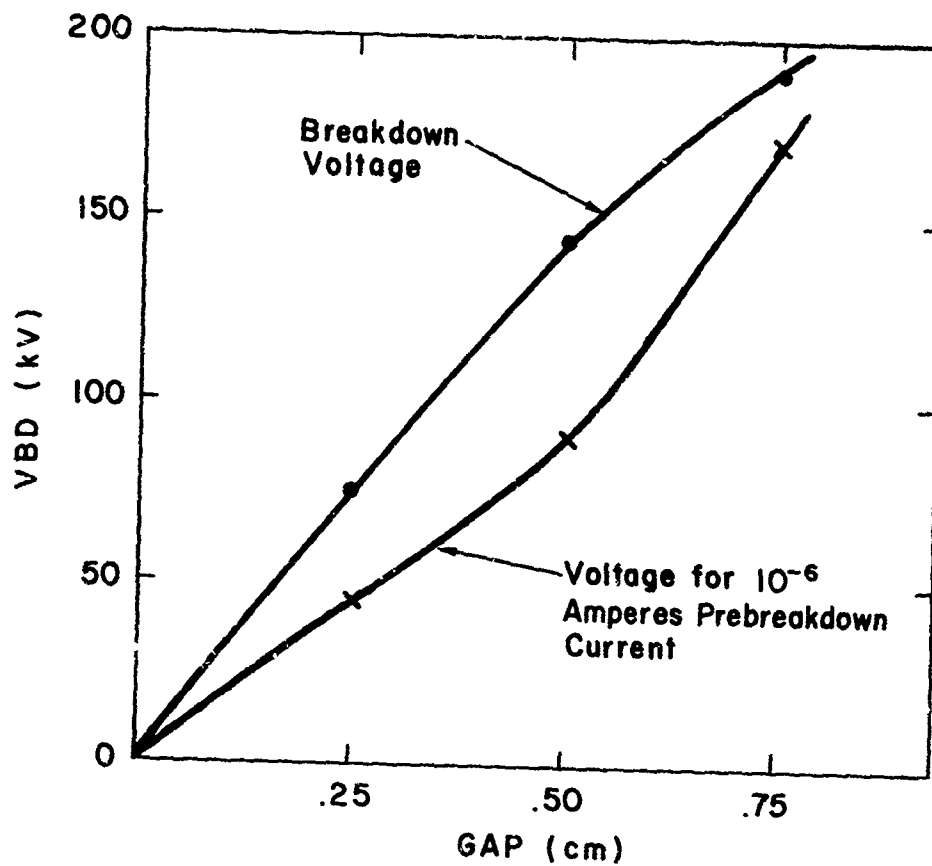
Figure 11-6. Dependence of Breakdown Voltage on Gap
for 4 inch Diameter Bruce Profile Copper Electrodes Before
Barium Contamination

1-4112
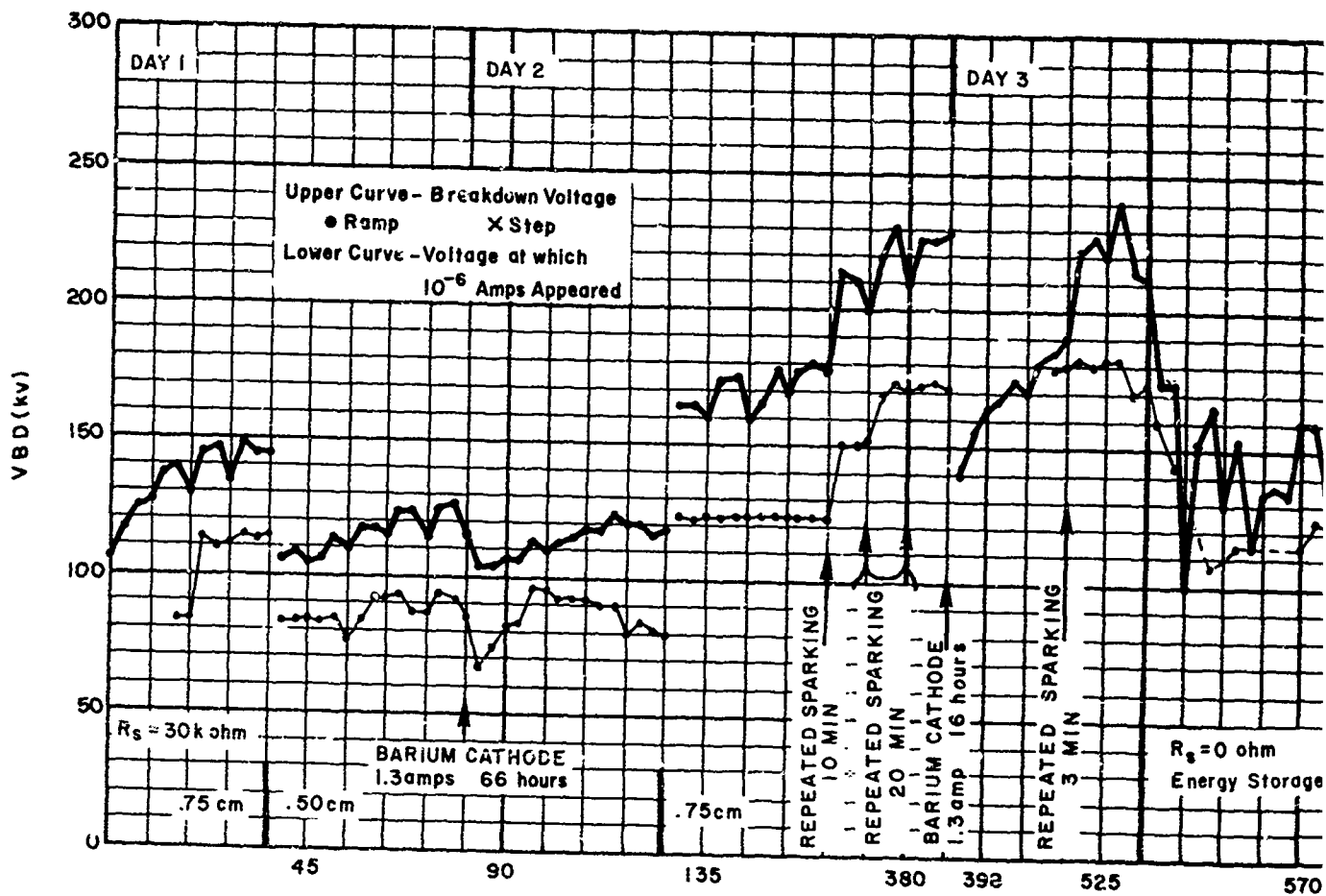
1-4271
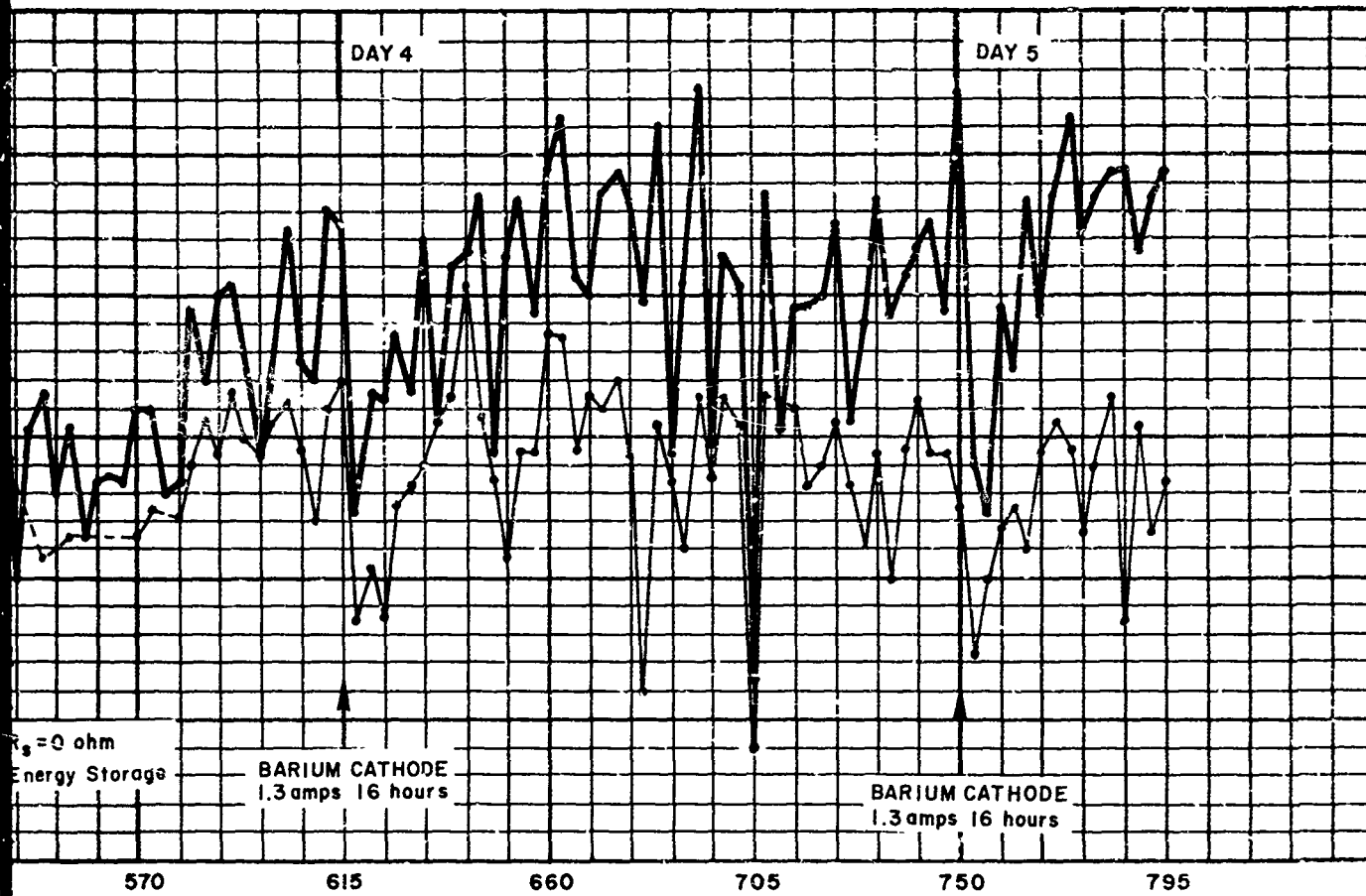
Figure 11-7 Conditioning Curve
for 4-Inch Diameter Bruce Profile
Electrodes - Ti-7Al-4Mo Anode and
Cathode - Barium Contamination

11-14

duced and again the effects of barium contamination could not be distinguished
from the usual scatter encountered with high energy discharges. A maximum
breakdown voltage of 272 kV was reached with a 10^{-6} ampere prebreakdown cur-
rent level of 145 kV.

11.3.4   Nickel Electrodes

Nickel electrodes subjected to barium contamination of the cathode
responded much the same as copper, except that no progressive decrease in
breakdown voltage with conditioning was noted. Again repeated sparking was used
for rapid conditioning. High energy discharges were introduced and the usual
immediate drop in breakdown voltage was followed by a slow but steady recondi-
tioning to higher breakdown voltages than had been reached with low energy dis-
charges. With high energy discharges the effects of barium contamination were
hardly distinguishable from the normal scatter and occasional drops in break-
down voltage. At the end of these tests the breakdown voltage for a 0.75 cm gap
was 300 kV with 10^{-6} amperes of prebreakdown current at 170 kV.

A pair of 1.28 inch diameter Bruce Profile nickel electrodes were
severely contaminated by placing the barium oxide cathode directly in front of the
cathode electrode at a distance of 2 mm. In this case only one hour at a slightly
elevated temperature (filament current 1.1 amps) was required to produce signi-
ficant contamination (see Figure 11-8). The effect of contamination was to drop
the breakdown voltage from 250 kV to 125 kV for the 0.75 cm gap. This decrease
was conditioned away in ~ 50 discharges (low energy) and then reappeared. Low
energy discharges (R_S = 30 kohm) were not effective in raising the breakdown
voltage, and high energy discharges (R_S = 0 ohm, $C_{E.S.}$ = 0.15 μF) were intro-
duced. Under these conditions a maximum breakdown voltage of 290 kV was
reached with the 10^{-6} ampere voltage level stable at ~ 175 kV, which is higher
than it was initially with low energy discharges. Thus, for nickel electrodes
subjected to severe barium contamination, high energy conditioning resulted in
better performance than was found with low energy discharges in the uncontami-
nated case.
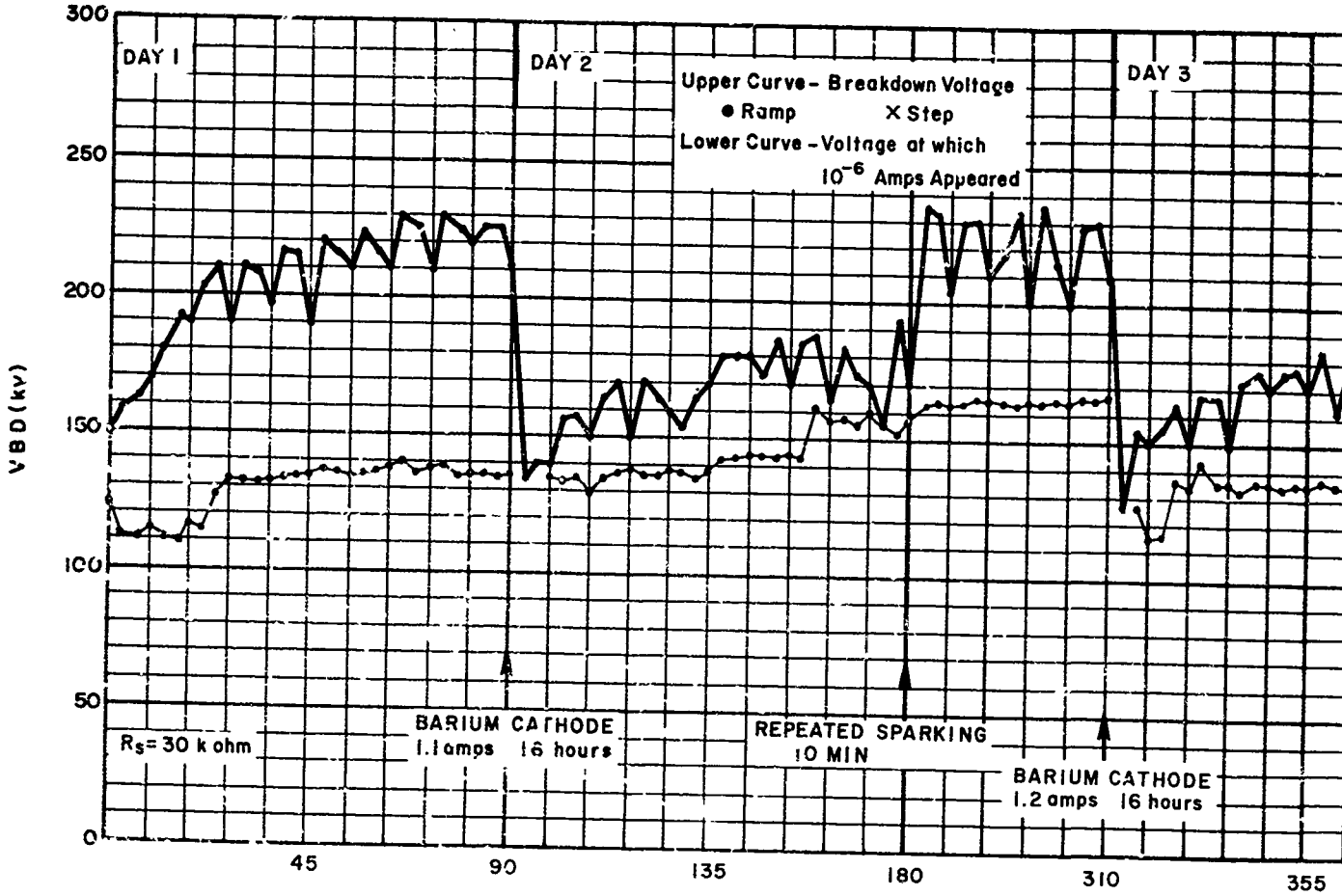
1-4273
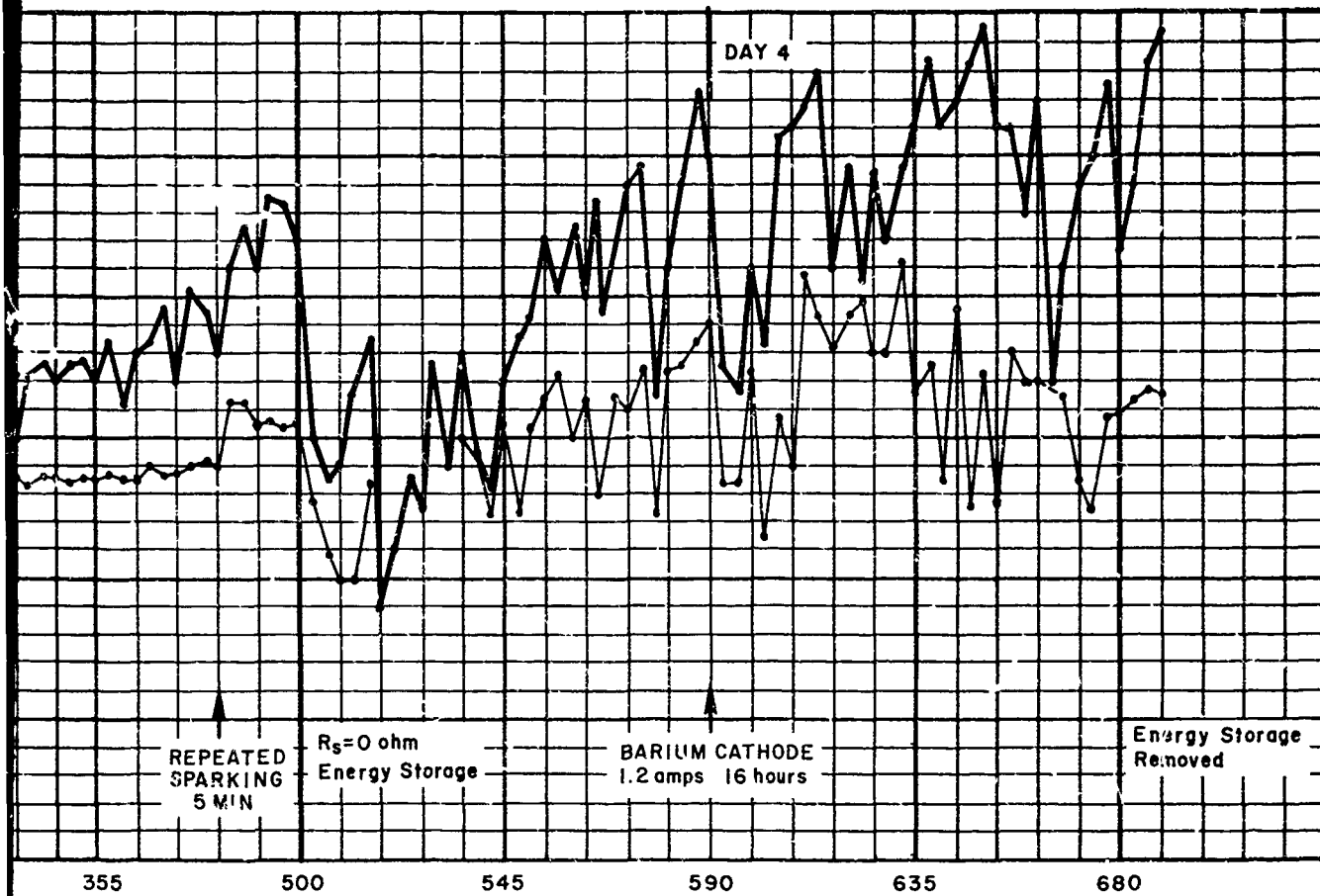
Figure 11-8 Conditioning Curve for
4-Inch Diameter Bruce Profile
Electrodes Nickel Anode and Cathode at
0.75 cm Gap - Barium Contamination
of Cathode

11-16

Subsequently barium contamination was repeated (see spark number 435, Figure 11-8) and a drop in breakdown voltage was followed by some reconditioning and then a permanent decline in insulating performance. Visual observation of the electrodes revealed that the layer of anode material which had been deposited on the cathode by high energy discharges had been fractured and was partly pulled off, forming large (~ 1 mm) and sharp projections. These are shown in Figure 11-9. It was not possible to eliminate these by conditioning and the breakdown voltage at a 3.0 cm gap was ~ 250 kV, with the 0.75 cm gap breaking down as low as 40 kV. This damage is similar to that encountered with particles on stainless steel electrodes which had been contaminated. It is reasonable to attribute the poor adhesion of the surface layer to contamination from the barium oxide cathode. The thickness of the layer was ~ 0.05 mm. This gives a total volume of approximately 0.015 cubic centimeters of anode material transferred to the cathode. Analysis of a central portion of the surface layer revealed that is was mostly nickel but with a significant percentage of Barium (0.03 to 0.3%). There were also traces of Fe, Mn, Si, Ti, and Cu.

11.3.5   Stainless Steel Electrodes

When stainless steel electrodes were used the 0.75 cm gap initially conditioned to 205 kV with low energy discharges (see Figure 11-10). Upon exposure of the cathode to barium contamination the breakdown voltage dropped to 120 kV with breakdown occurring before the 10^{-6} ampere prebreakdown current level was reached. After reconditioning to 210 kV the 10^{-6} ampere breakdown current level was sometimes reached at 190 to 200 kV. High energy discharges introduced after high impedance reconditioning but before the scheduled exposure to barium contamination, produced the anomolous damage which has been described in Section 10.8. Particles of anode material ejected during breakdown impacted on the cathode and flattened out in the usual manner, then upon reapplication of voltage some of these flattened particles were pulled erect by electrostatic forces. The result was a number of very sharp projections of up to 0.5 mm
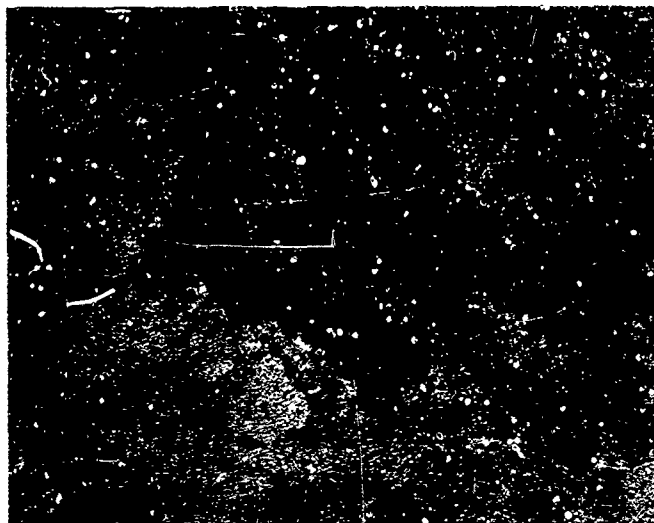
(a) General View of Broken and Pulled Away Coating
of Anode Material on Cathode (~ 5X)
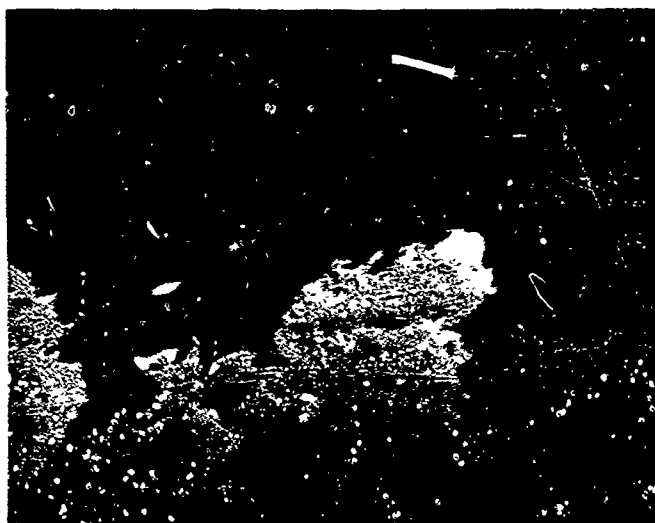
(b) Detail of the Edges of Fractured Coating (~ 10X)

Figure 11-9. Damage on Nickel Cathode due to Fracture of
Coating of Anode Material (Nickel) - Lack of
Adhesion is due to Barium Contamination

2-1426
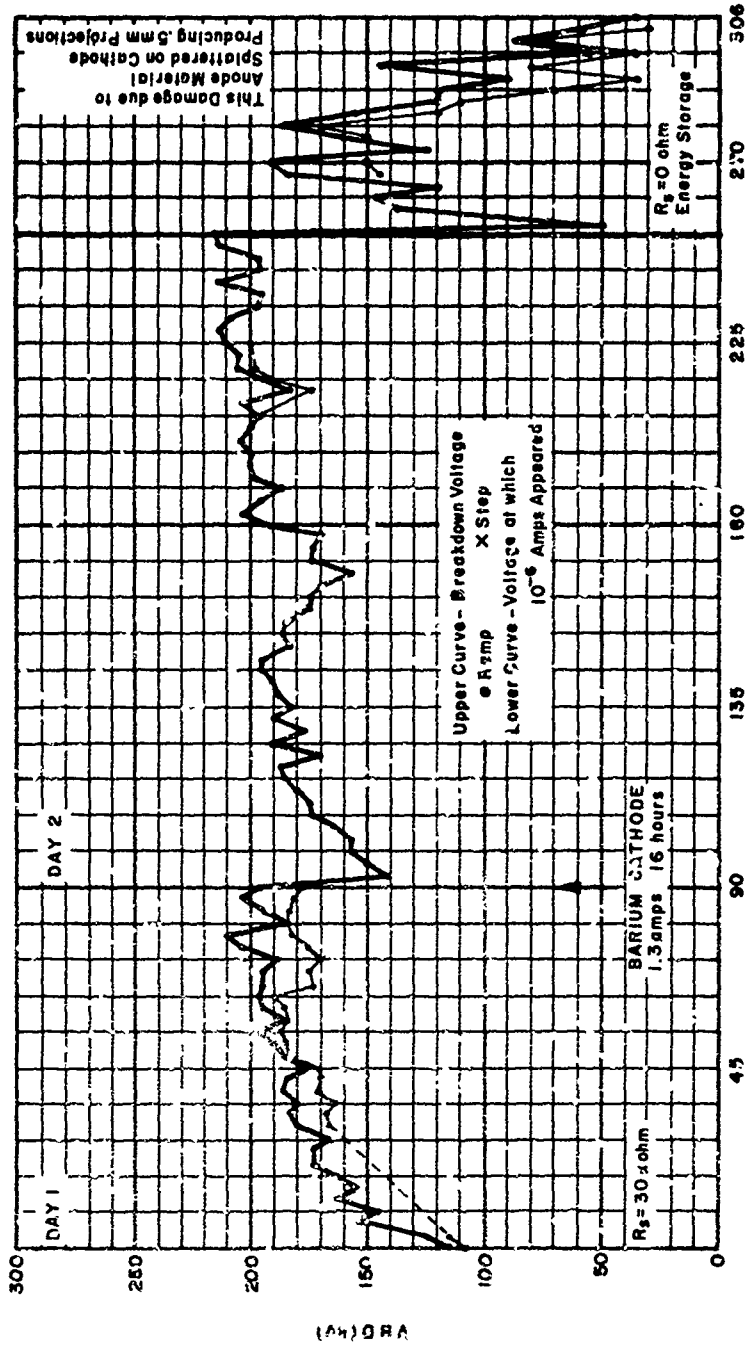
Figure 11-10. Conditioning Curve for 4-Inch Diameter Bruce Profile
Electrodes Stainless Steel Anode and Cathode - with Barium Contamination

1-4270

in length. These have been shown in Figure 10-15. Since this and the contaminated nickel cathode are the only cases in which impacted particles were partially pulled loose, it is reasonable to attribute the poor adhesion to the presence of contamination. Once present, the projections produced very high prebreakdown currents and low breakdown voltages. Conditioning was not effective in reducing the effect of the projections. A test with uncontaminated stainless steel electrodes (see Section 10.9) and high energy discharges did not show this effect.

11.4   Interpretation of Results

In an earlier experiment, Brodie[3] found that exposure of small nickel electrodes to a heated barium oxide cathode reduced the breakdown field from 4.4×10^5 V/cm to a significantly lower value and increased prebreakdown field emission current by several orders of magnitude. The electrodes could be conditioned back to a field of 4.4×10^5 V/cm by low energy discharges at a 0.5 mm gap, but the emission current was greater by a factor of over 15. These effects were conclusively related to the deposition of barium on the tips of whiskers in an experiment with a cylindrical projection tube. The barium decreased the work function of the emitting tips and thus increased field emission currents. Conditioning then destroyed the emitting sites which had been rendered unstable by increased emission. This explanation is supported by considerable experimental evidence[4, 5] that vacuum breakdown at a small gap (0.5 mm) is usually due to the explosive vaporization of field emitting protrusions on the cathode when the current density exceeds a certain critical value.

At the larger gaps (0.75 cm) and higher voltages of the present study the mechanisms of breakdown have not been clearly identified. Indeed, it appears that several mechanisms are possible. Thus the complex and variable effects of barium contamination described in the previous section are not entirely unexpected. The most significant difference noted for large gaps as compared to the small gap of Brodie is that the prebreakdown current was not permanently increased as a result of barium contamination followed by low energy discharge conditioning. Therefore it appears that conditioning at large gaps (high voltages) is capable of removing barium contamination from emitting sites on the cathode.

11-20

The initial effect of contamination was to increase emission and cause breakdown to occur at lower total prebreakdown currents than before contamination. That is, before contamination many microamperes of field emission current could be drawn without breakdown, while after contamination breakdown often occurred before 1 µA of prebreakdown current appeared. The opposite was usually the case in Brodie's work -- breakdown occurred at currents of the order of 10 µA before contamination, while after contamination prebreakdown currents of up to 500 µA are reported.

When the discharge energy was increased from the ~ 10 joules available with the 30 kilohms series resistance to the 6750 joules available with the energy storage capacitor bank, large quantities of anode material were transferred to the cathode. This of course covers any barium contamination which has not been removed by the discharge. At this point in two experiments (nickel or stainless steel electrodes) some of the anode material deposited on the cathode was partially pulled loose to form large (~ 1 mm) and sharp projections. The breakdown voltage was subsequently extremely low. This poor adhesion is most likely due to the prior barium contamination.

Finally, while the response to barium contamination of the materials tested (Cu, SS, Ni and Ti-7Al-4Mo) varied from material to material, in general these variations were not found to be significant. No pattern was discernable and the variation in response for a single material was considerable.

11.5   Conclusions

At large gaps (~ 0.75 cm) and high voltages (up to 300 kV) the effects of barium contamination are complex.

Immediately after exposure a decrease in breakdown voltage was found with breakdown occurring at lower prebreakdown current levels. Conditioning with either low or high energy discharges would usually restore the breakdown voltage to its initial level. There was no permanent increase in prebreakdown current as a result of barium contamination. When high energy discharges were used in conditioning after barium contamination, the transferred

particles of anode material in some cases did not adhere well. The result was large (~ 1 mm) projections which caused low breakdown voltages. This second order effect of contamination could not be eliminated by conditioning.

SECTION 12
CONCLUSIONS

SECTION 12
CONCLUSIONS

12.1   General

In this section, the major results of each experimental block are summarized, and the factors studied are discussed in terms of significance, interactions, range, and effect on breakdown voltage. The complete list of factors for all experiments is given in Table 12-1. Finally, the most important factors — anode material and energy conditioning — are discussed in relation to practical applications and some promising areas for future work are given.

12.2   Preliminary Experiment

When voltage was applied across unbaked electrodes the first observable activity in the vacuum gap was the appearance of microdischarges. These were conditioned out in time and with increase in voltage, viz., when all the gas close to the surface of the electrode had been removed. Prior to this, however, they produced surface roughening and field enhancement at the cathode, and so lead to field emission. Higher breakdown voltages were achieved with slow conditioning by controlled gas evolution than with spark conditioning. X-rays were produced by microdischarges and field emission electrode beams. Visible radiation was identified with anode hot spots due to these field emission beams. At high potentials the field enhancement factor grew at constant voltage and runaway to breakdown sometimes resulted. Indication of runaway was given by both x-radiation, visible radiation and gap current, but none was a reliable non-destructive prebreakdown indicator of incipient breakdown. Breakdown was associated with release of gas from the anode and the breakdown voltage was approximately proportional to the square root of the gap separation.

12.3   Seven Factor Pilot Experiment

A seven factor partial factorial experiment showed that the titanium alloy Ti-7Al-4Mo was superior to copper as an electrode material. Surface

12-1

Table 12-1. Sequence of Experiments - High Voltage Breakdown Study

I	II	III	IV	V	VI
Preliminary Experiment	Pilot Experiment	Block of Eight	Block on Thirty-Two	Energy Conditioning Study	Barium Contamination Study
Uniform Field Stainless Steel To 160 kV Prebreakdown Phenomena Field Emission Microdischarges X-Radiation Visible Radiation Pressure Surges Conditioning Techniques Sparking Gas Evolution (Performed with Existing Apparatus while 300 kV Apparatus was Constructed)	To 300 kV Factors Anode Material) Ti-7Al-4Mo OFHC Cu Cathode Material Ti-7Al-4Mo OFHC Cu Anode Finish Fine Coarse Cathode Finish Fine Coarse Anode Geometry Bruce Profile Sphere Cathode Geometry Bruce Profile Sphere Bakeout Complete System Electrodes Only	To 300 kV Uniform Field Factors Anode Processing Vacuum Firing Hydrogen Firing Cathode Processing Vacuum Firing Hydrogen Firing Electrode Size 4 Inch Diameter 1.28 Inch Diameter Transverse Magnetic Field to 500 Gauss	To 300 kV 2 Inch Diameter Spherical Cathode Factors Anode Material OFHC Cu Aluminum Cathode Material OFHC Cu Aluminum Electrode Processing Vacuum Firing Hydrogen Firing Anode Size 4 Inch Diameter 1.28 Inch Diameter Anode Shape Bruce Profile Sphere Transverse Magnetic Field 0 to 400 Gauss Energy Storage 100 to 6750 Joules Gas Exposure Conditioning Time to Voltage Collapse	To 300 kV Initial Gap = 0.75 cm Uniform Field Factors High Impedance Conditioning With Without Cathode Material Ti-7Al-4Mo Nickel Electrode Size 4 Inch Diameter 1.28 Inch Diameter Anode OFHC Copper Also tests with: Aluminum, Ti-7Al-4Mo Nickel, Stainless Steel Lead, Molybdenum Tungsten Energy Conditioning Level Series Resistance from 25 Ohms to 10 kilohms Energy Storage from 50 J to 6750 J with 0.15 µF Capacitor Bank Prebreakdown Current Breakdown Voltage Collapse and Current Pulse	To 300 kV Initial Gap = 0.75 cm Uniform Field Factors Electrode Material Ti-7Al-4Mo Nickel OFHC Cu 304 Stainless Steel Barium Contamination Level Without Cathode Only Anode Only Both Electrodes Energy Conditioning Prebreakdown Current

finish was not important, in as much as there was no significant difference between the performance yielded by 600 grit or 1 micron finishes. Spherical or curved electrodes which reduce the highly stressed area were superior to plane electrodes. Greater reliability and consistency of breakdown values were achieved when the entire system rather than the electrodes only were subjected to a bake-out cycle. Breakdown voltage was proportional to the square root of the gap, and,with repetitive spark conditioning,the log of the maximum prebreakdown current was a linearly decreasing function of the square root of the gap. Transfer of anode material to the cathode was observed. Gas released prior to breakdown suggested a breakdown mechanism in which gas released from the anode by heating, due to a field emission electron beam, collects and ionizes in the beam and enhances the emission at the cathode site until an unstable feedback results in breakdown. Most of the scatter or error was related to the lack of control of the gas content of the electrodes and this led to the design of the next experiment.

12.4   Block of Eight Experiment

A four factor full factorial experiment confirmed the significant but complex role that electrode gas content plays in determining the breakdown voltage of a vacuum gap. Electrode size was the most important factor overall, with smaller electrodes yielding better performance. Breakdown voltage was proportional to the square root of gap separation above 0.75 cm. Conditioning with sparks increased the breakdown voltage, for example, by as much as a factor of 2.3 with 26 sparks. The application of a transverse magnetic field of 250 gauss lowered the breakdown voltage for gaps greater than 0.75 cm and raised the breakdown voltage for smaller gaps. Interactions between factors were large. Thus adding gas (hydrogen firing) was beneficial for small electrodes, with anode gas content more decisive than cathode gas content. Voltage collapse time was found to vary linearly with gap separation up to approximately 1.5 cm, beyond which it was constant at about 550 ns. The average rate was 300×10^{-9} sec/cm.

12.5   Block of Thirty-Two Experiment

A five factor full factorial experiment showed again that interactions between factors were important. While the complexity of the results militates against simple conclusions, the following emerged: Copper was a better electrode material than aluminum, especially for the anode. Small electrodes had higher breakdown voltages than large electrodes and the effects of gas content depended strongly on electrode material, with hydrogen firing for copper and vacuum firing for aluminum yielding better results. Breakdown voltage varied linearly with gap up to 0.75 cm and as the square root of the gap above 0.75cm. Similarly, a transverse magnetic field of up to 400 gauss raised the breakdown voltage slightly for small gaps (< 0.75 cm) and lowered it for large gaps (> 0.75 cm). Time to voltage collapse was again found to be an approximately linear function of gap. Exposure of conditioned electrodes to pure gases (C_2 and N_2) did not seriously affect the breakdown voltage, but exposure to the plant atmosphere with its contaminants significantly lowered the breakdown voltage. An extensive transfer of anode material to the cathode was observed and preliminary experiments showed that the discharge energy had a major effect on breakdown voltage. Indeed, conditioning was recognized as probably the most important consideration and the next experiment examined this in greater detail by including the energy available to each discharge and the isolating or series resistence as factors.

12.6   Energy Conditioning Study

Conditioning emerged clearly as one of the most important factors in vacuum insulation. The breakdown voltage was strongly dependent upon the number and nature of conditioning discharges. The energy level of each discharge was critical with the beneficial or damaging effects being produced in the first microsecond. Low energy discharges (< 10 joules with a series resistance of 30 kilohms) produced a smooth increase in breakdown voltage with low pre-breakdown current levels. Moderate energy discharges (0.15μF 1000 ohms series resistance - 6750 joules at 300 kV) resulted in erratic and low breakdown voltages but little change in prebreakdown current levels. High energy

discharges, produced with 24 ohms of series resistance and the 0.15μF energy
storage bank, were initially damaging. The breakdown voltage often dropped by
more than 50%. However, high energy conditioning was discovered to have a
critical dependence on anode material. Anode materials such as copper, lead
and aluminum continued to degrade reaching low average breakdown voltages
with high prebreakdown currents (> 2 mA in some cases). However, when the
anode was a refractory metal such as titanium, nickel or stainless steel a con-
tinuation of the high energy conditioning series produced, initially, a recovery of
the gap insulation characteristics and ultimately led to a higher breakdown level
(e.g., 300 kV for a 0.75 gap) than that achieved with high impedance, low energy
conditioning. Cathode material was not important and the cathode was gradually
covered with a film of transferred anode material. Prebreakdown current was of
field emission origin and at high levels became an important factor due to gen-
eral heating of the anode. The vacuum discharge was found to require times of
about 300 ns to reach a low voltage arc phase with currents of hundreds of
amperes produced within 10 ns. Thus, damage occurred within 1 μs if sufficient
energy was available and crowbarring at 500 ns was only partially effective in
limiting electrode damage. The excellent correllation of breakdown voltage with
physical properties of the anode material (melting point temperature, specific
heat, and density) suggested that breakdown under high energy conditions might
occur when field emission electron beams heat a region of the anode until it be-
comes mechanically weak, at which stage a clump is extracted by the electro-
static field and accelerated across the gap, causing breakdown upon impact with
the opposite electrode. Long term withstand tests with voltage maintained at
fixed levels for varying lengths of time showed that the mean time to breakdown
increased exponentially as the stress level was decreased.

12.7   Barium Contamination Study

Contamination of the cathode electrode, with decomposition and
evaporation products from a heated barium oxide thermonic cathode, reduced
the breakdown voltage. In general, however, conditioning by sequences of sparks
restored this to a higher level than before contamination. Also, the prebreakdown

12-5

current levels were lower for contaminated cathodes than for clean electrodes. Anode contamination had a negligible effect both on the breakdown voltage and prebreakdown current levels. Exposure times of the order of days were required for significant effects with the barium oxide cathode at normal operating temperature. With many high energy discharges, contamination of the cathode generally resulted in permanent damage, and consequent lowering of the breakdown voltage level, due to poor adhesion of the impacted anode particles on the contaminated cathode.

12.8   Summary

Table 12-2 summarizes the effects, interactions and recommendations for the factors studied in the complete experiment. Many have been shown to have significant and complex effects on high voltage insulation in vacuum and, thus, for reliable and consistent performance, rigorous control of materials and processes is required. For a number of important factors, the existence of large interactions makes prediction or their combined effects difficult. Several factors, however, merit special consideration in high voltage electron tubes. Conditioning, properly applied, will more than double the breakdown voltage level in most cases. When the available discharge energy during operation and fault conditions is high, it is essential to condition with discharges of sufficient but not excessive energy. This depends critically on anode material; hence proper choice of electrode materials is crucial. Geometry is also important, and, in general, smaller areas yield better performance, even though the peak electric stress may be higher. It is, therefore, recommended that the design of each tube be given separate and individual consideration as far as selection and optimization of the various factors and parameters, particularly the electrode materials, processes and geometries. This should be followed by a thorough evaluation of conditioning as a function of the available discharge energy.

Table 12-2. Factors and Effects in Vacuum Insulation

FACTOR	EFFECT ON BREAKDOWN VOLTAGE	INTERACTS WITH	RANGE STUDIED	RECOMMENDATIONS	For Details Refer To:
CONDITIONING	Increases B.D.V. by more than a factor of 2 in most cases.	Discharge Energy, Anode Material	< 10 Joules to 6750 Joules < 10 sparks to 10^3 sparks	Conditioning technique is very important. If high energy discharges are possible, conditioning should use high energy, discharges and a good anode material.	6-4, 9-3, 10-3, 11-3
ANODE MATERIAL	Refractory metals have higher B.D.V.'s than non-refractory metals.	Conditioning, Discharge Energy, Gas Content	Ti, Ni, SS, Cu, Al, Pt	Use refractory metals, especially when high energy discharges are to be endured.	7-3, 8-2, 9-2, 10-9
CATHODE MATERIAL	Cu better than Al. No significant difference between Ni, Ti, SS.	Gas Content, Anode Material - with many moderate or high energy discharges the cathode becomes covered with a layer of anode material.	Ti, Ni, SS, Cu, Al	Some improvement can be obtained with high strength cathode material.	7-3, 8-2, 9-2, 10-4
GEOMETRY OF ELECTRODES	Spherical or curved surfaces better than flat surfaces. Small areas better than large areas.	Gas Content, Polarity	Plane to Spherical. Active areas from .5 cm^2 to 80 cm^2	Use geometries which minimize highly stressed area, even if this increases the maximum electric field.	7-3, 8-2, 9-2, 10-4
GAP	B.D.V. is proportional, to Gap below .75 cm, to $\sqrt{Gap}$ above .75 cm	Gas Content, Geometry	.25 cm to 4.0 cm	------	7-3, 7-4, 8-2, 9-2, 9-4, 11-3-2
PROCESSING BAKEOUT	Bakeout increases B.D.V., and improves consistency.	Electrode Material and Geometry	Hydrogen firing to 900°C. Vacuum firing to 900°C. Electrode only and complete system bakeout at 400-500°C.	Hydrogen or vacuum firing of electrodes can be beneficial. Complete system bakeout is useful.	7-3, 8-2, 9-3

Table 12-2. Continued

Table 12-2. Continued

FACTOR	EFFECT ON BREAKDOWN VOLTAGE	INTERACTS WITH	RANGE STUDIED	RECOMMENDATIONS	For Details Refer To:
SURFACE FINISH	Not significant if surface is reasonably smooth and clean.	------	1 μ Polish to 600 grit SiC paper finish	Do not expend effort beyond that which produces a clean and reasonably smooth surface.	7-3, 7-6, 7-7
GAS CONTAMINATION	Pure gases have a negligible effect, but gases with dust and organic contamination reduce the B.D.V.	Degree of Conditioning; exposure seldom reduces B.D.V. to below unconditioned level.	$N_2 - O_2$ at 10^{-5} torr and 15 psia, also plant gas.	Avoid exposure to contaminated gases.	9-6
BARIUM CONTAMINATION	Temporary reduction in B.D.V. that can be conditioned away.	Cathode (lowered B.D.V. only when on Cathode), Conditioning, High Energy Discharge.	Normal operating to higher temperatures were used for the contaminating barium oxide cathode.	Proper conditioning techniques can minimize degrading effects.	11-1, 11-2, 11-3, 11-4, 11-5
MAGNETIC FIELD	Lowers B.D.V. for gaps < 15 cm - raises B.D.V. for gaps > 75 cm.	Gap	0 to 400 gauss transverse to electric field.	Avoid magnetic field in highly stressed regions.	8-2, 8-3, 9-2, 9-4
PREBREAKDOWN CURRENT	High prebreakdown currents can heat anode and lead to breakdown...	Gap, Magnetic Field, Conditioning, Electrode Material.	< 10^{-12} amperes to 2×10^{-3} amperes.	When possible, condition to produce low prebreakdown currents.	6-4, 6-5, 7-4, 8-3, 10-5, 11-3-2

12-8

12.9   Future Work

The most promising areas for future work are:

(1) Application of refractory anode materials in realistic tube configurations. Perhaps this would require the use of composite anodes (e.g., Ti backed with Cu) to handle thermal problems.

(2) External cooling of the anode to reduce detrimental electron beam heating due to high prebreakdown currents — cooling to liquid nitrogen temperatures is especially attractive.

(3) Further investigation and standardization of conditioning techniques for a range of tube types.

(4) Use of pulse conditioning for rapid improvement in breakdown voltage (possibly without even removing tubes from operation for more than several milliseconds), and precise control of discharge energy.

(5) Long term withstand tests — especially when gradual contamination is likely (from a barium oxide cathode, etc.).

(6) Alternatives to spark conditioning should be investigated — for example, controlled melting of anode and cathode surfaces under vacuum by pulsed or continuous electron or laser beams.

IDENTIFICATION OF PERSONNEL

The following personnel were active on the Program:

Dr. M. J. Mulcahy	Program Manager
P. C. Bolin	Project Engineer
Dr. A. S. Denholm	Director, Electro Physics Division
Dr. S. V. Nablo	Director, Particle Physics Division
W. R. Bell	Senior Electrical Engineer
F. Y. Tse	Senior Electrical Engineer
G. K. Simcox	Senior Electrical Engineer
A. Watson	Senior Physicist
M. M. Thayer	Metallurgist
Y. J. McCoy	Electrical Engineer
S. C. Zanen	Electrical Engineer
R. White	Electrical Engineer
A. C. Stewart	Engineering Manager
D. J. Maynard	Senior Mechanical Engineer
S. K. Wiley	Senior Mechanical Engineer
J. E. Lavelle	Design Engineer
R. Benoit	Design Engineer
R. M. Heinonen	Design Engineer
L. Silvo	Design Engineer
R. M. Parsons	Engineering Aide
C. Boudreau	Engineering Aide
D. A. Bryant	Senior Technician
R. T. Merchant	Technician
L. Indingaro	Technician
F. Battistello	Technician
R. Comeau	Technician

Prof. H. Freeman   Consultant
M. I. T. - Dept. of
Economics and Social
Science

Prof. A. Argon   Consultant
M. I. T. - Dept. of
Mechanical Engineering

Dr. N. E. Woldman   Consultant
Metallurgy

SECTION 13
REFERENCES

__Section 4__

(1) Charbonnier, F. M., "A Brief Review of Vacuum Breakdown Initiation Processes,"Proceedings of the IIIrd International Symposium on Discharges and Electrical Insulation in Vacuum, Paris, p. 15 (September 1968).

(2) Hawley, R. et. al., Proc. IEE 114?, 1237 (June 1967).

(3) Germain, C. and Rohrbach, F., "High Voltage Breakdown in Vacuum", Conference on Spark Discharges, Liverpool, England in Vacuum, V18, No. 7, p. 371 (5-7 April 1967).

(4) "Power Sources for Directed Energy Weapons (U)", (S) Final Report Under Contract AF08(635)-2166, Ion Physics Corporation, Burlington, Massachusetts (1964).

(5) Tomaschke, H.E., "A Study of Projections on Electrodes and Their Effect on Electrical Breakdown in Vacuum", University of Illinois, Coordinated Science Laboratory, Report R-192 (1964).

(6) "Electrostatic Power Generator", Quartely Report No. 1 Under Contract AF33(615)-1168, Ion Physics Corporation, Burlington, Massachusetts (1964).

(7) Chodorow, M., et al, "Design and Performance of a High-Power Pulsed Klystron", Proc. IRE 41, 1584 (1953).

(8) Mansfield, W.K., "Prebreakdown Conduction Between Electrodes in Continuously Pumped Vacuum Systems", Brit. J. Appl. Phys. 8, 73 (1957).

(9) Silvkov, I. N., "The Influence of the Electrode Temperature on the Electrical Breakdown Strength of a Vacuum Gap", Sov. Phys.-Tech. Phys. 3, No. 4, 708 (1958).

(10)   Little, R. P. and Whitney, W. T., "Studies of the Initiation of
        Electrical Breakdown in Vacuum", Naval Research Laboratories
        Report 5944 (1963).

(11)   Maitland, A., "Influence of the Anode Temperature on the Break-
        down Voltage and Conditioning Characteristics of a Vacuum Gap",
        Brit. J. Appl. Phys. 13, 122 (1962).

(12)   Donaldson, E. E. and Rabinowitz, M., "Effects of Glass Contamina-
        tion and Electrode Curvature on Electrical Breakdown in Vacuum",
        J. Appl. Phys. 34, No. 2, 319 (1963).

(13)   Srivastava, K. D., Preceedings of the Eighth Electrical Insulation
        Conference, 68C6-EI-28, p. 14-20, Los Angeles, California
        (December 1968).

(14)   Pivovar, L. I., et al, "The Effect of the Electron Current Component
        on Development of Electrical Breakdown in High Vacuum", Sov.
        Phys. -Tech. Phys. 2, No. 5, 909 (1957).

(15)   Sanford, J., Brookhaven National Laboratory, Private Communica-
        tion (June 1964).

(16)   Brodie, I., "Vacuum Breakdown in the Presence of Thermionic
        Cathodes", J. Vacuum Sci. Technol. V2, p. 249 (1965).

(17)   Germain, C., Jeannerot, Rohrbach, F., Simon, D. and Tinguely,
        R., Proceedings of the Second International Symposium on
        Insulation of High Voltages in Vacuum, p. 279, Boston (October
        1964).

(18)   Jedynak, L., J. Appl. Phys., 35, No. 6, 1727-1733 (June 1964).

(19)   Cranberg, L. C., "The Initiation of Electrical Breakdown in
        Vacuum", J. Appl. Phys. 23, 518 (1952).

(20) Arnold, K. W., et al, "Electrical Breakdown Between a Sphere and a Plane in Vacuum", Proceedings of Sixth International Conference on Ionization Phenomena in Gases, Paris (1963).

(21) Slivkov, I. N., "Mechanism for Electrical Discharge in Vacuum", Sov. Phys.-Tech. Phys. 2, 1928 (1957).

(22) Bennette, C.J., Swanson, L. W. and Charbonnier, F. M., Proceedings of Second International Symposium on Insulation of High Voltages in Vacuum (1966). p. 11 and 21

(23) Coenraads, C.N., "Field Emission and Its Influence on Electrical Breakdown in Vacuum", Proceedings of Twenty-Fourth Annual Conference on Physical Electronics, Massachusetts Institute of Technology (1964).

(24) Hadden, R.J.B., "The Effect of Surface Treatment on the Electrical Breakdown Between Copper Electrodes at 50 Cycles at Very Low Pressure", Atomic Energy Research Establishment, England, G/M92 (1951).

(25) Gumbel, E. J., "Statistical Theory of Extreme Values and Some Practical Applications", National Bureau of Standards Applied Mathematics Series, No. 33, U.S. Government Printing Office, Washington, D.C. (1954).

(26) Hill, L. R. and Schmidt, P. L., "Insulation Breakdown as a Function of Area", AIEE Trans. 67, 442 (1948).

(27) Germain, C. and Rohrback, F., "Mechanisme des Decharge dans le Vide", Proceedings of Sixth International Conference on Ionization Phenomena in Gases, Paris (1963).

(28) Rosanova, N. B. and Granovskii, V. L., "On the Initiation of Electrical Breakdown of a High Vacuum Gap", Sov. Phys.-Tech. Phys. 1, No. 3, 471 (1957).

(29)   Schneider, S., et al, " A Versatile Electronic Crowbar System",
         Proceedings of Seventh Symposium on Hydrogen Thyratrons and
         Modulators, 436 (1962).

(30)   Britton, R.B., "Transition in the Electrical Conduction Mechanism
         in Vacuum", Proceedings of Twenty-Fourth Annual Conference on
         Physical Electronics, Massachusetts Institute of Technology (1964).

(31)   Denholm, A.S., "The Electrical Breakdown of Small Gaps in
         Vacuum", Can. J. Phys. $\underline{36}$, 476 (1958).

Section 5
(1)   Davies, O.L., Editor, The Design and Analysis of Industrial
         Experiments, (2nd Edition) Hafner Publ. Co., New York (1963).

(2)   Yates, F., "Design and Analysis of Factorial Experiments",
         Imperial Bureau of Soil Science, London (1937).

(3)   Daniel, C., "Use of Half-Normal Plots in Interpreting Factorial
         Two-Level Experiments", Technometrics $\underline{1}$ 311 (1959).

Section 6
(1)   Britton, R.B., "Transition in the Electrical Conduction Mechanism
         in Vacuum", Proceedings of Twenty-Fourth Annual Conference on
         Physical Electronics, Massachusetts Institute of Technology (1964).

(2)   Arnal, R., "On the Initiation of Electric Discharges in Vacuum",
         C.R. Acad. Sci. (Paris), $\underline{238}$, 2061 (1954); "Electric Microdis-
         charges in Dynamic Vacuum", Ann. Phys. (Paris, $\underline{19}$, 830;
         Available as Translation USAEC-TR-2837 (1955).

(3)   Mansfield, W.K., "Prebreakdown Conduction in Continuously
         Pumped Vacuum Systems", Brit. J. Appl. Phys. $\underline{11}$, 454 (1960).

(4)   Pivovar, L.I. and Gordienko, V.I., "Microdischarges and Predis-
         charges Between Metal Electrodes in High Vacuum", Sov. Phys.-
         Tech. Phys. $\underline{28}$, 2101 (1958); "Prebreakdown Conduction Between
         Electrodes in Ultrahigh and High Vacuum", Sov. Phys.-Tech.
         Phys. $\underline{7}$, 908 (1963).

(5)   Evans, R.D., "The Atomic Nucleus", Chapt. 20, 21, McGraw-Hill
        (1955).

Section 7
(1)   Holland, L., "Vacuum Deposition of Thin Films, "Chapman and
        Hall, Ltd.

(2)   Watson, A. "Theory of Vacuum Breakdown-Ionic Field Enhancement
        and the Instability Mechanisms" -Addendum to this report.

Section 8
(1)   Watson, A. "Magnetic Influences in Vacuum Breakdown" -Addendum
        to this report.

(2)   Watson, A. "Theory of Vacuum Breakdown-Ionic Field Enhancement
        and the Instability Mechanisms", Addendum to this report.

Section 9
(1)   Mulcahy, M.J. and Watson, A., High Voltage Breakdown Study
        Eighth Quarterly Progress Report - Appendix A-3, "The Pumping
        Conductance of Plane Parallel Discs" - Report No. ECOM-00394-7,
        (November 1966).

Section 10
(1)   Epstein, H.M., Gallagher, W.J., Mallozzi, P.J., and Stratton,
        T.F., "Plasma Processes in a Vacuum Spark", 1968 Annual Meeting
        of the Division of Plasma Physics, American Physical Society,
        Miami Beach, Paper 3E6 (November 1968).

(2)   Watson, A. "Theory of Vacuum Breakdown" -Addendum to this
        Report.

(3)   Davies, D.K. and Biondi, M.A., Journal of Applied Physics, 39
        No. 7, p. 2979 (June 1968).

(4)   Watson, A., Bell, W.R., Mulcahy, M.J. "High Voltage Vacuum
        Breakdown Study - Twelfth Quarterly Progress Report", Ion Physics
        Corp., ECOM-00394-12 - Appendix A-Electrode Damage From
        Transient Heavy Current Sparks (March 1968).

(5)   Zinn, M.H., Taylor, G.W. and Chrepta, M.M., "Influence of
       Electrode Material on High Voltage Vacuum Breakdown", IEEE
       International Electron Devices Meeting, Washington, D.C. (1967)

(6)   Rosanova, N.B. and Granovskii, V.L., Soviet Physics, Technical
       Physics,1, No. 3 p. 471 (English Translation).

Section 11

(1)   Doolittle, H.D., "Vacuum Power Tubes for Pulse Modulation",
       Machlett Cathode Press, 21, No. 1, p. 2-15 (1964)

(2)   "High Power Tube Program", Final Report Contract Air Force
       19(628)-500, MIT Lincoln Laboratory, p. 14-17 (November 1963)

(3)   Brodie, I.J. Vacuum Science Technology, 2, p. 249 (1965)

(4)   Alpert, D., Lee, D.A., Lyman, E.M. and Tomaschke, H.E.,
       Proceedings of the International Symposium on Insulation of High
       Voltages in Vacuum, Massachusetts Institute of Technology, p. 1,
       (1964)

(5)   Utsumi, T.J., Applied Physics, 33, No. 7, p. 2989, (1967)